

Université des Sciences et Technologies de LILLE
Ecole Doctorale Biologie Santé

THÈSE

Pour l'obtention du grade de
DOCTEUR DE L'UNIVERSITE DE LILLE1

Discipline Biochimie

Présentée et soutenue publiquement par

Haoling QI

Interactions de la phospho-protéine neuronale Tau avec des protéines partenaires comme cibles thérapeutiques dans la maladie d'Alzheimer.

Sous la direction du Dr. Isabelle LANDRIEU

Soutenance prévue le 20 Novembre 2015 devant le jury composé de :

Rapporteur :	Mme le Docteur May C. MORRIS Directeur de recherche (CNRS-IBMM, Université de Montpellier1)
Rapporteur :	Mr le Docteur Nicolas WOLFF Directeur de recherche (Institut Pasteur Paris)
Examineur:	Mme le Docteur Isabelle CALLEBAUT Directeur de recherche (CNRS-IMPIC, Université Pierre et Marie Curie)
Directrice de thèse :	Mme le Docteur Isabelle LANDRIEU Directeur de recherche (CNRS-UGSF, Université de Lille1)

Remerciements

Le travail de thèse présenté dans ce manuscrit a été effectué au sein de l'équipe « RMN et Interactions Moléculaires » de l'Unité de Glycobiologie Structurale et Fonctionnelle (UGSF) – UMR8576 à l'université de Lille 1. Je tiens à remercier le laboratoire d'excellence « DISTALZ » (Développement de stratégies innovantes pour une approche transdisciplinaire de la maladie d'Alzheimer) et l'université de Lille1 pour avoir subventionné ce travail de thèse.

Je souhaite tout d'abord remercier l'ensemble des membres du jury qui ont accepté d'évaluer mon travail de thèse : Dr. May C. Morris et Dr. Nicolas Wolff en leur qualité de rapporteurs ainsi que le Dr. Isabelle Callebaut en sa qualité d'examinatrice.

Je souhaite exprimer mes sincères remerciements au Dr. Isabelle Landrieu, directrice de thèse, qui m'a fait découvrir la RMN des biomolécules et m'a transmis ses connaissances de biochimie pendant mon stage de Master et mon travail de thèse. J'aimerais souligner sa patience, son soutien, sa disponibilité ainsi que sa grande contribution à cette thèse. Ses conseils avisés ont permis de faire avancer mon travail de thèse dans la bonne direction.

Je tiens également à adresser mes remerciements au Dr Guy Lippens pour son accueil au sein du laboratoire et de m'avoir encouragé au cours de mon stage et la thèse.

Merci au Dr. François-Xavier Cantrelle pour l'organisation et la réalisation des expériences de la spectroscopie RMN aussi que sa grande patience pour ma formation au principe et à l'acquisition des spectres RMN. Grace à son soutien technique, j'ai pu obtenir et analyser les spectres RMN présentés dans ce manuscrit.

Je remercie aussi le Dr. Caroline Smet-Nocca pour ses intéressants cours de RMN pendant mon Master et également pour ses précieux conseils dans mon comité suivi de thèse.

Merci au Dr. Xavier Hanouille pour sa disponibilité, sa sympathie et son expérience transmise dans le laboratoire.

Mes remerciements sont également adressés au Dr. Prakash Rucktooa et Mr. Julien Schelpe, qui m'ont donné des conseils très utiles dans mes expériences et m'ont aidé à résoudre des problèmes techniques.

Je voudrais adresser mes remerciements aux personnes qui m'ont accompagnées et supportées dans le bureau. Dr. Morkos Henen et Dr. Riccardo Perruzzini qui m'ont donné un grand soutien amical et m'ont permis d'améliorer mon anglais pendant mes deux premières années de thèse. Egalement au Dr. Marie Dujardin, Mme Luiza Bessa et Dr. Amina Kamah, qui ont partagé leurs connaissances aussi bien du point de vue des expériences que de la rédaction du manuscrit.

Un merci au Dr. Isabelle Huvent, Dr. Juan Lopez, Dr. Amina Kamah et Mr. Clément Despres, pour nos discussions sur la protéine Tau et les conditions d'agrégation, qui m'ont inspiré énormément dans mon travail.

Un merci au Dr. Idir Malki, Mme. Pauline Bellanger et Dr. Robert Schneider pour leur gentillesse et encouragements pendant la rédaction de ce manuscrit.

J'adresse aussi mes remerciements aux personnels de l'IRI que j'ai pu côtoyer pendant ces années d'étude. Notamment, Dr. Zoé Lens, Mme. Elisabeth Ferreira, Mme Marie-André Fleurbaix, Dr. Stéphanie Baelen, Dr. Didier Monté et Mme. Frédérique Dewitte pour leurs conseils avisés dans le laboratoire pendant ces trois années.

Je remercie le Dr. Loïc Brunet et le Dr. Nicolas Barois pour leurs accompagnements lors de l'apprentissage technique et théorique de la microscopie électronique en transmission.

Je remercie le Dr. Béatrice Chambrud (INSERM, UMR788, Kremlin Bicêtre) pour le support dans la préparation des extraits de cerveau du rat utilisés dans les expériences de phosphorylation, ainsi que les Dr. Jeremy Gunawardena et Dr. Sudhakaran Prabakaran, (*Department of Systems Biology, Harvard Medical School, USA*), pour leurs contributions dans le travail de 'Characterization of the neuronal Tau protein as a target of the ERK kinase'.

Egalement, un grand merci au Dr. Marie-Christine Galas (JPArC, UMR1172, Lille) pour son soutien et ses conseils avisés dans le travail de 'Nuclear Magnetic Resonance Spectroscopy characterization of Tau interaction with DNA and its regulation by phosphorylation'.

Je remercie l'ensemble du personnel de l'UGSF, car je ne peux pas citer chacun, pour ces trois années que j'ai passé en votre compagnie.

Et enfin, un spécial et grand merci à mes parents, Tao et mes amis pour leur soutien pendant ces années passées.

Table of Contents

Résumé	3
Description des travaux de thèse	5
Abstract	23
Abbreviations	25
Publications	27
Communications:	27
Introduction	29
Part 1. Alzheimer's disease.....	31
1. Pathway hypothesis in the physiopathology of AD.....	34
1.1 Amyloid cascade hypothesis	34
1.2 Tau cascade hypothesis	37
1.3 β -Amyloid and Tau.....	40
1.4 Genetic risk factors in AD	41
2. Tau and its multiple physiological functions	42
2.1 Tau gene and isoforms.....	42
2.2 Multiple binding functions	44
Part 2. The aggregation of neuronal Tau protein	47
1. Aggregation nuclei	48
2. Aggregation cofactors.....	52
3. Mutation modulated aggregation.....	54
4. 'Hyperphosphorylation' model in the <i>in vitro</i> and <i>in vivo</i> studies.....	57
5. Impact of hyper-phosphorylation on aggregation	58
Part 3. Deregulation of kinases and phosphatases in AD	61
1. AD-related kinases.....	62
2. AD-related phosphatases	65
3. A brief history of ERK kinase and MAPK cascades.....	68
4. MAP kinase Erk1/2 in Alzheimer's disease	71
Part 4. Docking interactions	73
1. Strategies of modular interactions in protein kinases and phosphatase networks.....	73
2. Conserved docking sites in MAP kinases	76
3. ERK1/2 and other MAP kinases recruitment grooves	77
4. F-docking sites and F-docking domain	81

Objectives	85
Results	89
Part 1	91
ERK-mediated Tau phosphorylation and the recognition of multiple docking sites by ERK kinase	91
Analysis of kinase activity in rat brain extract	97
1. Inhibition of kinases of rat-brain-extract in Tau phosphorylation assays	97
2. Inhibition ERK activity by PEA-15 <i>in vitro</i>	99
3. Inhibition ERK activity by anti-pTEpY ERK antibodies in rat brain extract.....	103
4. Conclusion:	104
<i>manuscript in preparation:</i>	105
Characterization of the neuronal Tau protein as a target of the ERK kinase	105
Part 2	131
Analysis of the kinase activity of the activated isoforms of ERK kinase	131
1. Comparison of ERK phospho-isoform enzymatic activity with Tau	135
2. Site-specific rate of phosphorylation	140
Part 3	143
NMR characterization of Tau interaction with DNA and its regulation by Tau phosphorylation.....	143
<i>paper (published on January 27, 2015)</i>	147
Nuclear Magnetic Resonance Spectroscopy characterization of Tau interaction with DNA and its regulation by phosphorylation	147
Discussion	163
1. Analytical characterization of Tau phosphorylation by ERK and by brain extracts	165
2. Kinase activity in rat brain.....	168
3. Pathological aspects of Tau phosphorylation	168
4. Interaction of Tau with ERK kinase and other binding partners.....	171
5. The regulation of Tau/DNA interaction by phosphorylation	175
Perspectives	177
Materials and Methods	185
<i>manuscript in preparation:</i>	187
The study of posttranslational modifications of Tau protein by Nuclear Magnetic Resonance spectroscopy: phosphorylation of Tau protein by ERK2 recombinant kinase and rat brain extract and acetylation by recombinant Creb-binding protein.	187
References	243

Résumé

Dans la maladie d'Alzheimer (MA), la protéine Tau est le composant principal des dégénérescences neurofibrillaires (NeuroFibrillary Tangles, NFTs) observées dans le cerveau des patients. Dans des conditions pathologiques, la phosphorylation anormale a été observée sur la protéine Tau, qui pourrait perturber les fonctions biologiques de Tau et sont associées à une forme agrégée de Tau. Dans le but d'apporter des éléments de compréhension à ces mécanismes de phosphorylation de Tau et d'en comprendre les effets sur les fonctions de Tau et son agrégation, la spectroscopie de résonance magnétique nucléaire (RMN) a été utilisée. La RMN a tout d'abord permis une caractérisation analytique de la protéine Tau phosphorylée. D'autre part, la RMN a également permis d'étudier les interactions de Tau avec des partenaires moléculaires. La kinase ERK (Extracellular signal-regulated Kinase) est une des kinases impliquées dans l'hyperphosphorylation associée à la dégénérescence neuronale. Dans ma thèse, je me suis concentrée sur la caractérisation *in vitro* de la kinase ERK2 avec la protéine Tau comme substrat. En utilisant la spectroscopie RMN, les résidus sérine et thréonine de Tau modifiés par ERK2 ont été identifiés. Parmi de 17 motifs S/T-P présents dans la séquence de Tau, il y a 14 sites phosphorylés par ERK2. Ce profil de phosphorylation est très semblable à celui obtenu avec un extrait de cerveau de rat, en présence d'acide okadaïque pour inhiber les phosphatases. La protéine Tau phosphorylée par un extrait de cerveau de rat est utilisée depuis de nombreuses années comme modèle de Tau hyperphosphorylée dans des études biochimiques. Cette protéine hautement phosphorylée a une capacité à agréger supérieure à Tau non modifiée. Nous avons montré que la protéine Tau phosphorylée uniquement par la kinase ERK2 présente des propriétés d'agrégation semblables à la protéine Tau phosphorylée par les extraits de cerveaux de rat.

D'autre part, l'interaction de Tau avec ERK2 recombinante a été étudiée *in vitro* en utilisant la RMN. Nous avons mis en évidence de multiples peptides d'ancrage situés dans les domaines de liaison aux microtubules (MTBDs) de Tau. Les séquences des peptides sont compatibles avec les séquences consensus décrites reconnues par ERK1/2. La constante de dissociation (Kd) caractérisant cette interaction a été définie par RMN du fluor. A notre connaissance, il s'agit d'un premier exemple d'un substrat de ERK2 reconnu par des sites multiples d'ancrage.

Par ailleurs, ces études ont été poursuivies sur les conséquences fonctionnelles des phosphorylations par ERK2. Des oligonucléotides interagissent avec Tau au niveau des séquences Tau[209-246] et Tau[267-289] de Tau. Nous avons démontré que cette interaction est abolie par la phosphorylation de Tau par la kinase ERK2.

En conclusion, la phosphorylation de Tau par la kinase ERK2 de motifs Sérine/Thréonine-Proline, localisés tout le long de sa séquence mais particulièrement dans le domaine régulateur riche en proline a un impact sur les capacités d'agrégation de la protéine modifiée et sur ses propriétés d'interaction avec un partenaire moléculaire physiologique, l'ADN. Ces résultats concordent avec les études réalisées dans des contextes cellulaires qui identifient ERK comme une kinase activée dans des conditions de stress du neurone qui pourrait conduire à une phosphorylation pathologique de Tau.

Description des travaux de thèse

J'ai étudié au cours de mes travaux de thèse trois aspects principaux de la phosphorylation de Tau.

1. **La phosphorylation de Tau par la kinase ERK2, et la reconnaissance par ERK2 de sites d'ancrage dans la séquence de Tau.** Les sites multiples de phosphorylation de Tau par la kinase ERK2 sont identifiés par la spectroscopie de RMN. Nous avons observé que le profil de phosphorylation de Tau par ERK2 est très semblable à celui obtenu avec l'activité kinase d'un extrait cerveau du rat, en présence d'acide okadaïque pour inhiber les phosphatases. De plus, nous avons montré que la protéine Tau phosphorylée uniquement par la kinase ERK2 présente des propriétés d'agrégation semblables à celles de la protéine Tau phosphorylée par l'activité kinase des extraits de cerveau de rat *in vitro*. La capacité d'agrégation de ces formes phosphorylées de Tau est plus importante que celle de la protéine non phosphorylée. Nous avons observé des fibres de la protéine Tau phosphorylée par ERK2 par microscopie électronique. En outre, nous avons montré que la kinase ERK2 peut interagir avec Tau par l'intermédiaire de sites multiples d'ancrage dont les séquences sont compatibles avec les séquences consensus décrites dans la littérature comme site de reconnaissance de ERK1/2.

2. **La caractérisation d'activité des phospho-isoformes d'activation de ERK2 envers Tau.** La kinase ERK2 doit être activée dans sa boucle d'activation pour présenter une activité kinase. Il y a 2 résidus phosphorylables dans cette boucle, un résidu Tyrosine Y et un résidu Thréonine T. La phospho-isoforme qui présente une double phosphorylation est décrite comme active (ERK2 pTEpY). Les activités de différents phospho-isoformes de la kinase ERK2 recombinante envers Tau ont été étudiées en utilisant la RMN pour caractériser les phosphorylations. ERK2 pTEY présente une activité enzymatique tout comme l'isoforme décrite comme active, ERK2 pTEpY. L'isoforme qui présente une simple phosphorylation de la Tyrosine ERK2 TEpY n'est pas active. Notre étude par RMN suggère une efficacité et spécificité similaires de l'isoforme ERK2 pTEY avec ERK2 pTEpY pour la phosphorylation de Tau *in vitro*.

3. **La caractérisation de l'interaction de Tau avec l'ADN et sa régulation par la phosphorylation de Tau.** L'interaction de Tau avec des oligonucléotides double-brin d'ADN

in vitro est démontrée au niveau moléculaire. Deux sites d'interaction principaux qui se trouvent dans le domaine riche en proline (PRD) et dans le MTBDs ont été identifiés par une étude RMN (Qi et al. 2015). La phosphorylation de Tau par ERK2 est capable de modifier ses propriétés d'interaction avec l'ADN, un partenaire moléculaire physiologique.

Méthodologie: La spectroscopie de RMN est utilisée beaucoup comme un outil analytique dans mes études. La RMN nous a permis d'identifier les résidus de Tau qui sont phosphorylés dans nos échantillons, ainsi que d'estimer leur niveau de modification. Ceci nous a permis de définir les profils de phosphorylation de Tau obtenus *in vitro* par la kinase ERK2 recombinante ou par les extraits de cerveau du rat. Ces échantillons caractérisés sont ensuite utilisés pour analyser les conséquences fonctionnelles d'un profil spécifique de phosphorylation sur la capacité d'agrégation de Tau ou sa fonction physiologique de liaison à l'ADN. D'autre part, cette méthodologie nous permet également d'étudier des mécanismes de régulation des kinases, comme l'étude des différences forme d'activation de ERK2 ou sa capacité de reconnaissance de Tau comme substrat par l'intermédiaire de sites d'ancrage spécifiques.

Partie 1: La phosphorylation de Tau induite par la kinase ERK2, et la reconnaissance d'ERK2 vers le substrat Tau.

1. Identification des sites phosphorylés de la protéine Tau par kinase ERK2

En vue d'identifier les phospho-sites de la protéine Tau par ERK2, l'échantillon de phospho-Tau est préparé et analysé en suivant un protocole que nous avons décrit en détail dans 'The study of posttranslational modifications of Tau protein by Nuclear Magnetic Resonance spectroscopy: phosphorylation of Tau protein by ERK2 recombinant kinase and rat brain extract and acetylation by recombinant Creb-binding protein.', chapitre de livre destiné à être publié dans *Protocols in Molecular Biology*, Springer. Le schéma ci-dessous montre le principe de l'attribution des résonances correspondant à des phospho-sites. Ces résonances sont bien visibles et se trouvent dans une zone spécifique du spectre qui ne contient aucune résonance dans le spectre 2D ^1H , ^{15}N HSQC spectre de Tau non phosphorylée. L'attribution des phospho-sites est basée sur les données de 3D [^1H , ^{15}N , ^{13}C] HNCACB spectre qui nous permet d'identifier les résidus pS/pT-P et aussi les résidus en

position 'i-1'. En cas de deux résidus identiques en position 'i-1', il est nécessaire d'acquérir un second spectre 3D tel que 3D [^1H , ^{15}N , ^{15}N] HNCANN spectre donnant le déplacement chimique de NH du résidu 'i-1'. Ce second spectre donne une information supplémentaire pour discriminer 2 dipeptide de séquences identiques telles que X-pS/pT-P (Figure 1). De cette manière, 15 phospho-sites sont identifiés en utilisant la RMN pour un échantillon de Tau phosphorylé *in vitro* par la kinase ERK2 (Figure 3, A, spectre en rouge).

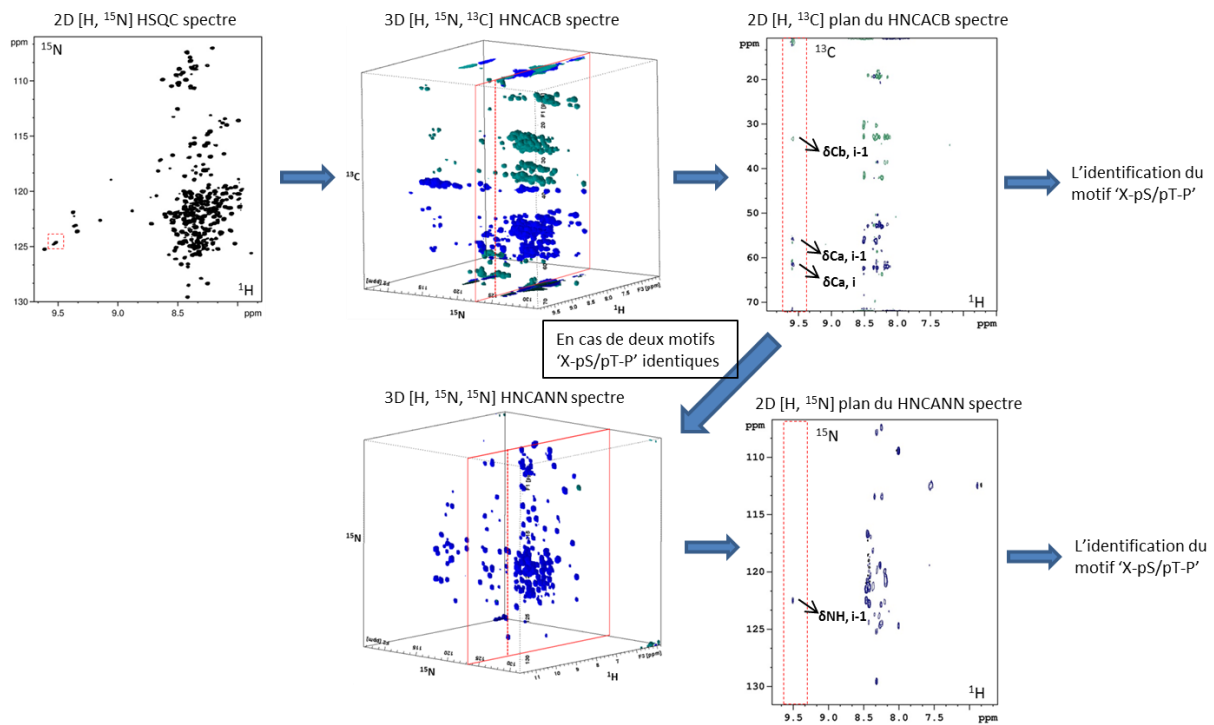


Figure 1 : Principe de l'attribution des résonances de spectre HSQC 2D qui correspondent aux sites phosphorylés dans les motifs 'X-pS/pT-P' dans la séquence de Tau.

2. Cinétique des sites spécifiques de phosphorylation

Les sites phosphorylés par kinase ERK2 sont annotés dans le spectre HSQC de ^{15}N Tau (Figure 3, spectre en rouge). Afin de définir plus précisément les sites préférentiels phosphorylés par ERK2 au long de la séquence de Tau, une évolution dans le temps de phosphorylation est réalisée avec ERK2 activée, dans laquelle le spectre HSQC 2D est acquis à chaque point à l'échelle du temps de réaction (Figure 2).

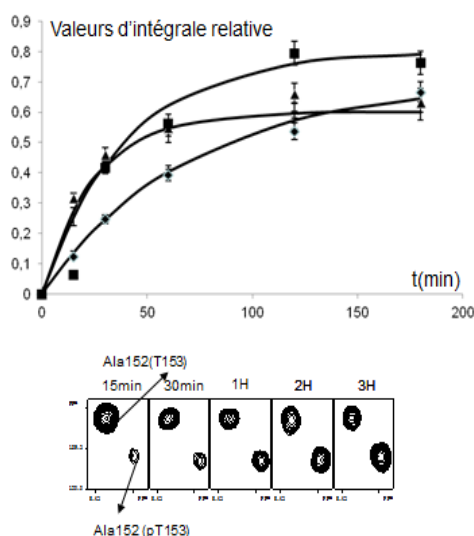


Figure 2: Cinétique de phosphorylation de Tau par ERK2. L'intégrale du volume de pic correspondant aux résidus pS/pT augmente avec la période d'incubation. Chaque point de donnée dans le graphique correspond à l'intégrale d'une résonance dans le spectre 2D de la protéine Tau incubée avec ERK2 activée pendant une certaine durée de temps indiqué sur l'axe des abscisses. Les triangles correspondent aux résonances de pS²³⁵, les diamants aux résonances de A¹⁵² (mesure indirecte de pT¹⁵³), et les carrés indiquent les résonances G²⁰⁷ à côté de pT²⁰⁵. Les données sont modélisées par une équation mono-exponentielle $1 - (e^{-t/T})$. Les barres d'erreur rendent compte de la variabilité des données correspondant au rapport signal sur bruit.

Les volumes des résonances identifiées sont utilisés pour évaluer le niveau de modification de phosphorylation sur un site phosphorylé spécifique à chaque point de temps. Donc une cinétique site-dépendant de phosphorylation est obtenue (Figure 2). Les cinétiques de phosphorylation les plus rapides sont observées pour pS²³⁵, pS⁴⁰⁴ et pS⁴²², dont les résonances sont déjà détectées dans le spectre HSQC après 15 minutes de l'incubation avec ERK2.

3. *In vitro* phosphorylation de Tau par ERK2 recombinante ou par un extrait de cerveau de rat

L'activité catalytique de ERK2 vis-à-vis de Tau comme substrat conduit à obtenir une protéine avec des sites multiples phosphorylés. De façon similaire, la modification de 12 à 15 sites par molécule de Tau est rapportée lors de son incubation avec un extrait de cerveau de rat (M Goedert et al. 1993; Biernat et al. 1992; Alonso et al. 2001). Nous avons utilisé l'activité kinase d'un tel extrait pour phosphoryler la protéine recombinante ^{15}N , ^{13}C Tau *in vitro* pour déterminer la part de ERK2 dans ce mélange de kinases. La majorité des résonances correspondants aux phospho-sites (en noir, Figure 3, A) sont déjà observés dans le spectre de Tau phosphorylée par kinase ERK2 recombinante (en rouge, Figure 3, A) sauf les résonances identifiées comme pS²⁰⁸, pS²¹⁰, pS²⁶² et pS³⁵⁶ correspondant aux résidus qui ne se trouvent pas dans des motifs S/T-P (Figure 3, A). Le niveau de phosphorylation pour chaque pS/pT est mesuré par l'intégrale de volume des pics correspondant (Figure 3, B). On voit que pS⁴⁶ est phosphorylée beaucoup plus efficacement par l'extrait de cerveau du rat que par ERK2 recombinante, mais généralement, pour les sites pT⁵⁰, pT¹⁵³, pT¹⁷⁵, pT¹⁸¹, pS²⁰², pT²⁰⁵, pT²³¹, pS²³⁵, pS³⁶⁹, pS⁴⁰⁴ et pS⁴²², les niveaux de phosphorylation sont très similaires et élevés (plus que 50%) dans ces deux conditions. La protéine Tau phosphorylée par un extrait de cerveau de rat en présence d'acide okadaïque est un modèle qui est utilisé depuis longtemps pour générer une protéine Tau hyperphosphorylée pour des études biochimiques. Nos résultats représentent néanmoins la première caractérisation détaillée du profil de phosphorylation correspondant à cette « hyperphosphorylation ».

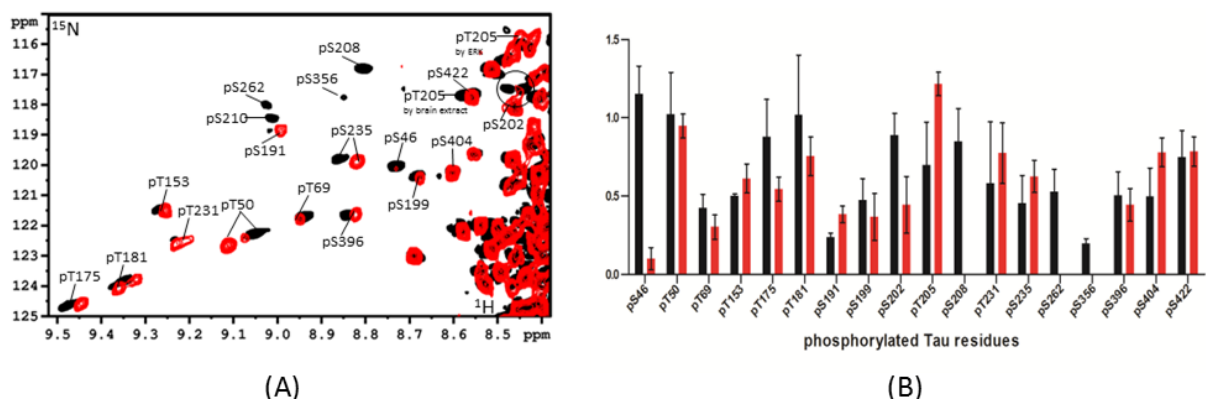


Figure 3 : Comparaison des phosphorylations de la protéine Tau par la kinase ERK2 et l'extrait de cerveau du rat. (A) superposition des spectres HSQC 2D de Tau phosphorylée par ERK2 recombinante activée par MEK1 *in vitro* (en rouge) et par l'extrait de cerveau du

rat (en noir). Les résonances correspondant aux phospho-residus sont annotées dans les spectres. (B) Les intégrales relatives des résonances des résidus pS/pT sont montrées avec les barres noires représentant toutes les phosphorylations par l'extrait de cerveau du rat et avec les barres rouges, les phosphorylations par ERK recombinante. Les intégrales relatives sont obtenues de trois expériences et les valeurs moyennes sont représentées sur le graphique avec les barres d'erreur.

4. L'activité de la kinase ERK2 dans l'extrait de cerveau du rat

Nous avons donc montré que la kinase ERK2 recombinante a une capacité à phosphoryler la protéine Tau en générant un profil de phosphorylation similaire à celui par un extrait de cerveau du rat. Pour démontrer que ce dernier provient majoritairement de l'activité kinase de ERK2 dans l'extrait, nous avons tout d'abord confirmé la présence de ERK2 activée dans ces extraits. Trois extraits de cerveau de souris ont été évalué par immunodétection avec un anticorps contre la kinase ERK2 active, doublement phosphorylée (dp ERK ou ERKpTpY). On détecte effectivement une bande dans les extraits à la taille attendue d'environ 42kDa, qui correspondant à la bande détectée avec la kinase recombinante activée utilisée comme contrôle positif (Figure 4, A). Selon de l'intensité des bands immunodétectés, la quantité de kinase ERK2 acitivée est estimée à 6ng/ μ l, donc environ 0.1 μ M de ERK2 active dans un extrait de cerveau du rat.

Pour confirmer la part de l'activité kinase de ERK dans ces extraits, l'anticorps contre dp ERK1/2 est utilisé pour bloquer l'activité de la kinase ERK1/2 activée dans l'extrait de cerveau du rat. La phosphorylation de Tau cause un retard de migration sur le gel SDS-PAGE, la protéine Tau hyperphosphorylée migrant à une masse apparente d'environ 70kDa. L'ajout d'anticorps anti-dpERK1/2 à l'extrait de cerveau du rat avant l'incubation avec Tau conduit à obtenir une protéine Tau qui présente un retard nettement moins important à la migration. L'anticorps contre ERK1/2 activée parvient à bloquer la majorité de l'activité kinasique dans l'extrait de cerveau du rat (Figure 4, B).

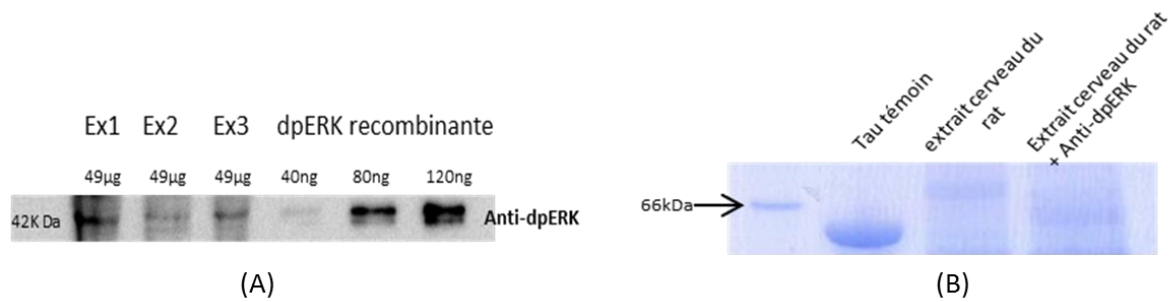


Figure 4: Analyse de l'activité de la kinase ERK dans les extraits de cerveau du souris ou rat. (A) ERK2 pTEpY est immuno-détectée par l'anticorps anti-dpERK1/2 dans les extraits de cerveau de trois souris (1^{ère} à 3^{ème} piste) et la préparation de ERK recombinante activée par MEK (4^{ème} à 6^{ème} piste). 7µl de l'extrait de cerveau à 7µg/µl de protéine sont déposés pour chaque souris et 40ng, 80ng et 120ng de ERK2 recombinante activée. (B) La bande correspondant à Tau phosphorylée par un extrait de cerveau, détectée vers 70kDa (3^{ème} piste), présente un retard de migration comparé à la Tau non phosphorylée (1^{ère} piste). En présence de l'anticorps anti-dpERK1/2, le retard de migration de Tau est moindre (4^{ème} piste comparée à 3^{ème}) et la migration est proche de celle de Tau non phosphorylée (1^{ère} piste).

Nous avons de plus utilisé la protéine PEA-15 (phosphoprotein enriched in astrocytes 15) comme inhibiteur spécifique de l'activité kinase d'ERK2 dans ces extraits. PEA-15 est une protéine qui peut spécifiquement lier la kinase ERK2 au niveau de la boucle d'activation (phosphorylée ou non) et inhiber son activité de phosphorylation (Mace et al. 2013). Après l'ajout de PEA-15 en excès à l'extrait, la bande de migration de Tau phosphorylée migre vers la position de Tau témoin à 52kDa sur le gel de SDS-PAGE (Figure 5). Dans le spectre HSQC 2D de cette protéine Tau phosphorylée en présence de PEA-15, les résonances correspondant aux résidus qui pourraient être phosphorylés par ERK2 sont absentes à l'exception de la détection de résonances résiduelles correspondant aux pS²³⁵ et pS⁴⁰⁴. Ces résidus pourraient être phosphorylés par une kinase additionnelle (Figure 5). Sur base de ces données, nous avons conclu que l'activité kinase de ERK2 représente une partie importante de l'activité kinase dans l'extrait de cerveau du rat lorsqu'on phosphoryle la protéine Tau *in vitro*. Les conséquences fonctionnelles de la phosphorylation de Tau par ERK2 ont ensuite été étudiées.

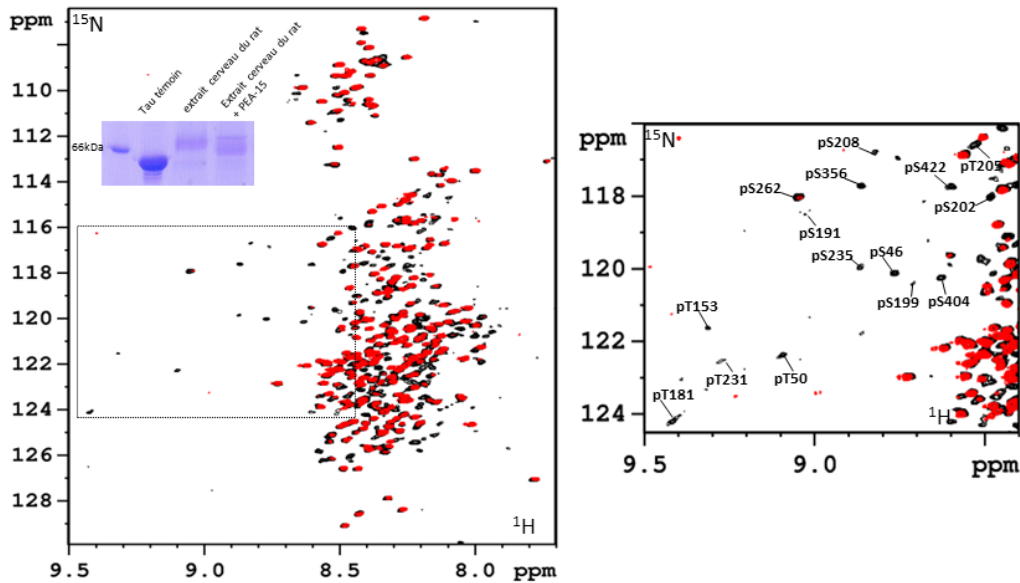


Figure 5: Superposition des spectres de ^{15}N Tau phosphorylée par un extrait de cerveau du rat sans PEA-15 (en noir) et en présence de PEA-15 (en rouge). Le zoom indiqué par le carré dans le spectre à gauche est représenté à droite, et les résonances des résidus phosphorylés sont annotés. L'analyse SDS-PAGE des échantillons de Tau non phosphorylée, Tau phosphorylée par un extrait de cerveau du rat et phosphorylée par un extrait en présence de PEA-15 est présentée dans l'insertion du spectre.

5. L'agrégation de phospho-Tau *in vitro*

Les essais d'agrégation de phospho-Tau ont été effectués *in vitro* avec 2 périodes d'incubation à 35°C, 2H et 4H. Les échantillons incubés à une concentration de 10 μM sont : phospho-Tau obtenu par incubation *in vitro* avec la kinase ERK2 recombinante, phospho-Tau obtenu par incubation *in vitro* avec l'extrait de cerveau de rat et Tau non-phosphorylé incubé en absence d'ATP ou de kinase comme contrôle. Les culots obtenus par centrifugation à 16000xg en 1H des échantillons incubés ont ensuite été déposés sur une grille et contrastés à l'uranyl avant d'être observés par microscopie électronique de transmission. Les images obtenues montrent que la phospho-Tau obtenue soit par incubation avec ERK2 recombinante, soit par incubation avec un extrait de cerveau forme des agrégats de morphologie similaire *in vitro*. On observe que les agrégats de phospho-Tau s'assemblent latéralement et se connectent en réseau. Des fibres de quelques μm de longueur sont également observées avec un aspect torsadé caractéristique. Ces objets sont spécifiquement observés dans les échantillons phosphorylés de Tau et pas dans la protéine Tau non phosphorylée (Figure 6).

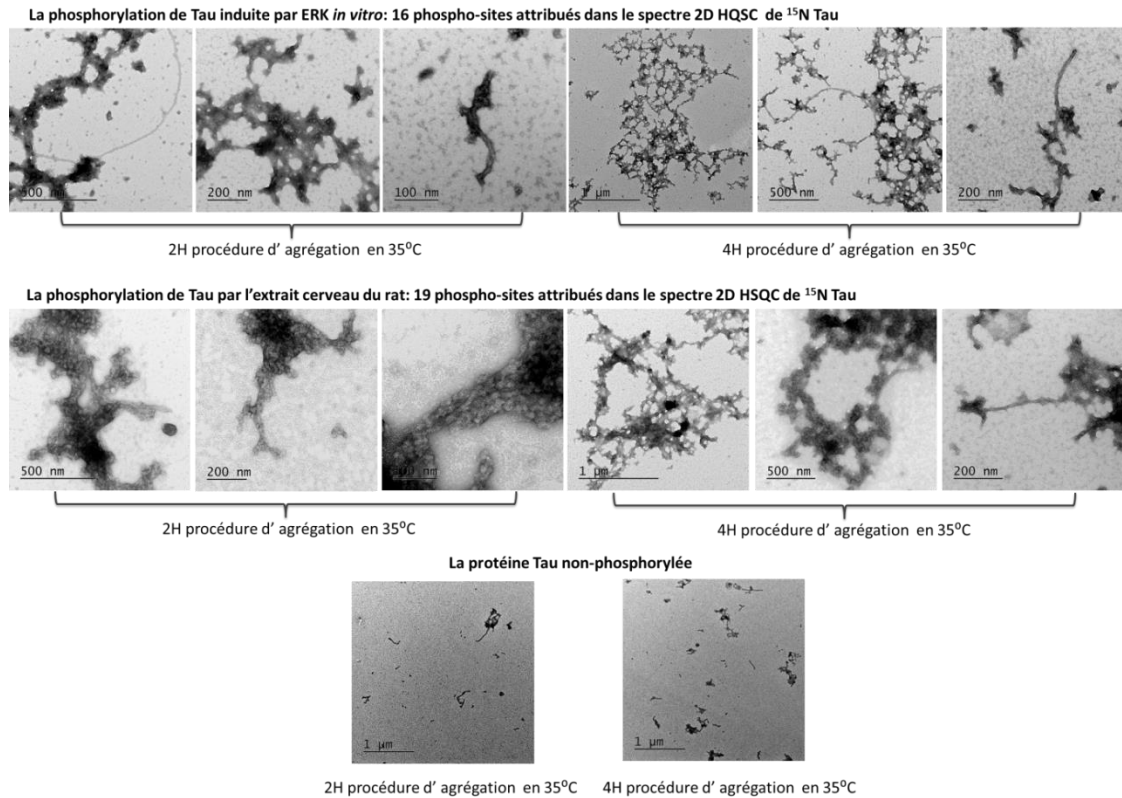


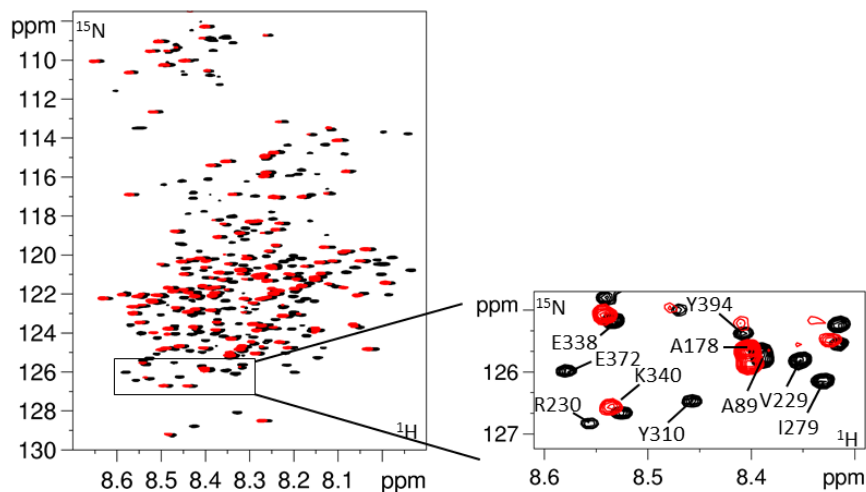
Figure 6: L'observation des agrégations de phospho-Tau phosphorylée par ERK2 recombinante ou par les extraits de cerveau du rat par la microscopie électronique en transmission.

6. Les sites d'ancrage (docking sites) de la kinase ERK2 dans la séquence de Tau

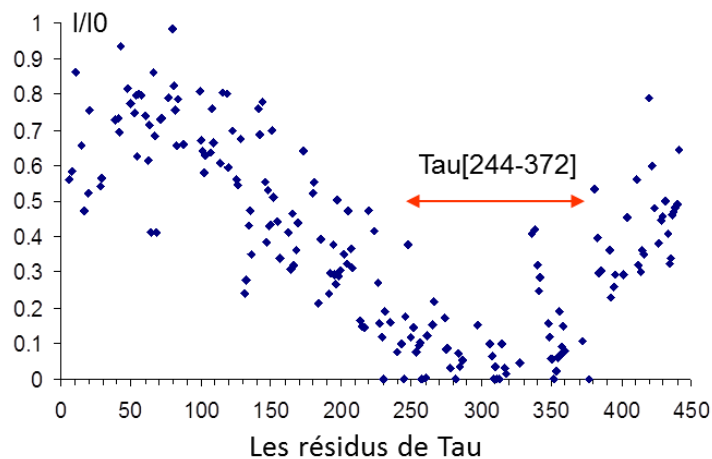
Des séquences de type « docking domain » (Domaine D) représentent des sites d'interaction des MAP kinases avec les enzymes en amont ou les substrats en aval dans la cascade des MAP kinases. La séquence de docking dans les protéines partenaires de ERK2 est en accord avec le consensus : $\psi_{1-3}\chi_{3-7}\phi\chi\phi$ ou $\phi\chi\phi\chi_{3-7}\psi_{1-3}$, dont ψ , ϕ , et χ correspondent à un résidu chargé positivement, un résidu hydrophobe et des résidus intervenants, respectivement (Whisenant et al. 2010; Garai et al. 2013). Pour mieux comprendre le mécanisme de modification de protéine Tau par la kinase ERK2 *in vitro*, nous nous sommes intéressés à l'interaction de ERK2 avec Tau, qui n'a jusqu'ici jamais été décrite.

Afin de définir des sites D potentiels de la kinase ERK2 dans la séquence de la protéine Tau, nous avons utilisé la RMN. Les spectres 2D ¹H, ¹⁵N de ¹⁵N Tau en présence ou absence de la kinase ont été comparés. Les intensités des résonances équivalentes dans les 2 spectres sont mesurées. Lors d'une interaction, les résonances des résidus affectés par cette

interaction présentent des perturbations, modifications de leur déplacement chimique et/ou diminution de leur intensité (Figure 7, A). Dans le cas de l'interaction de ERK2 avec Tau, nous avons calculé le rapport des intensités I/I0 pour de nombreux résidus le long de la séquence de Tau, correspondant aux données du spectre de Tau en interaction (I) par rapport au spectre contrôle de Tau libre (I0). Nous avons observé une décroissance du rapport des intensités vers MTBDs ou F[244-372] (K18) au long de la séquence (Figure 7, B).



(A)



(B)

Figure 7 : L'interaction de Tau avec ERK2. (A) La superposition des spectres HSQC 2D [^1H , ^{15}N] de ^{15}N Tau libre (en noir) avec ^{15}N Tau en présence kinase ERK2 avec ratio molaire 1 sur 5. Les spectres sont obtenus par RMN spectroscopie en 900MHz. Les résonances encadrées dans les spectres sont annotées à droite. (B) Graphique des intensités relatives des résonances dans le spectre de Tau/ERK2 (ratio molaire 1 sur 5) comparé avec les résonances correspondantes dans le spectre de référence de protéine Tau libre. Une décroissance des intensités relatives est observée sur la séquence de K18 correspondant

aux MTBDs de protéine Tau. 187 résonances plus intenses et isolées sont analysées, qui correspondent aux résidus dispersés au long de la séquence de Tau.

Le K18 est ensuite utilisé pour détailler les sites de l'interaction avec ERK2 en utilisant la même stratégie d'étude de RMN. Comparé les intensités des résonances correspondant aux spectres de ^{15}N Tau K18 libre et lié à la kinase ERK2, nous avons observé deux principaux sites d'interaction et un site moins fort avec ERK2, qui sont identifiés par les décroissances des intensités relatives dans la graphique en indiquant par les flèches oranges au long de K18 (Figure 8, A). Identifiant dans la séquence de K18, nous avons obtenu les deux principaux sites d'interaction correspondant aux F[274-288] et F[306-318], qui contient les séquences compatibles à la séquence de docking, $\psi_{1-3}\chi_{3-7}\phi\chi\phi$ ou $\phi\chi\phi\chi_{3-7}\psi_{1-3}$, pour kinase ERK1/2 (Figure 8, B).

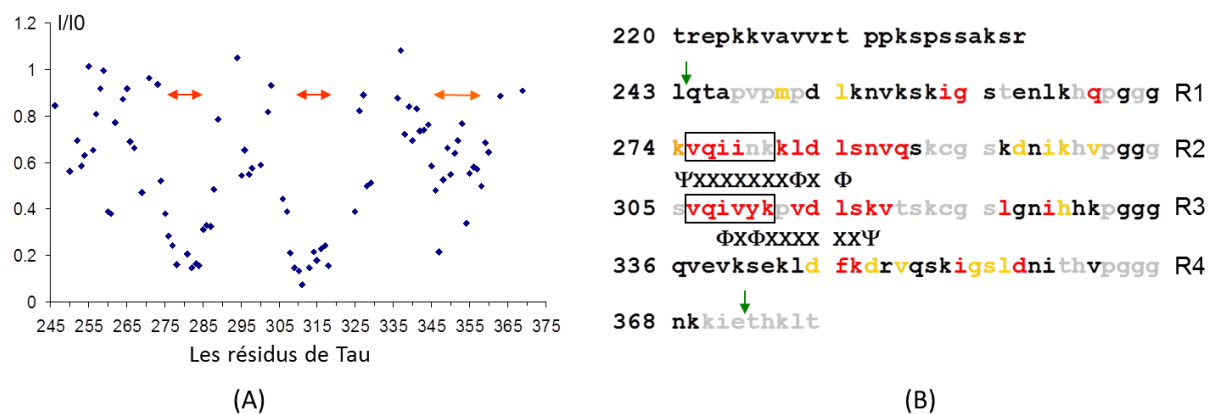


Figure 8 : L'interaction de Tau K18 avec ERK2. (A) Graphique des intensités relatives des résonances dans le spectre de Tau K18 lié avec ERK2 (ratio molaire 1 sur 2) comparé avec les résonances correspondantes dans le spectre de référence de Tau K18 seul. (B) La séquence de F[220-377] de Tau. Les résidus Q²⁴⁴ et E³⁷² de séquence de K18 sont indiqués par les flèches vertes. La décroissance des intensités relatives est représentée en couleur sur les résidus correspondants. Les résidus en rouge représentent ses intensités dans les spectres diminuant plus de 50% lors qu'ils interagissent avec ERK2. Les résidus dont I/I0 est moins de 0.6 sont en jaunes. Pour les résidus ne sont pas attribués, ils sont mis en gris dans la séquence. Les F[275-280] et F[306-311], montrés dans la boîte, correspondent aux peptides PHF6 et PHF6* (von Bergen et al. 2000).

7. L'interaction des peptides de Tau avec ERK2

Pour mieux confirmer l'interaction de ERK2 avec ces sites d'ancrage dans la séquence de Tau, nous avons choisi deux peptides qui possèdent une séquence peptidique correspondant au consensus de docking reconnu par ERK1/2 (Figure 8). F[220-240] et F[271-294] Tau ont été clonés et exprimés en fusion N-terminale avec His-Sumo. La fusion aide à solubiliser et stabiliser les peptides (Figure 9, A). ^{15}N His-SUMO F[220-240] Tau et ^{15}N His-SUMO F[271-294] Tau sont mélangés avec ERK2 avec le ratio 1 :2 dans les tubes RMN. Les perturbations des spectres HSQC 2D révèlent que ^{15}N His-SUMO F[271-294] Tau a la capacité d'interagir avec ERK2 mais pas le peptide F[220-240] Tau (Figure 9, B et C). Les résidus du peptide F[271-294] Tau dont l'intensité de résonance diminue en présence d'ERK2 correspondent bien à ceux observés dans la séquence Tau entière, tels de K²⁷⁴, L²⁸² et L²⁸⁴ indiqués en vert et rouge respectivement dans la séquence (Figure 9, A). Les résonances des résidus de His-SUMO ne sont pas affectées par la présence d'ERK2.

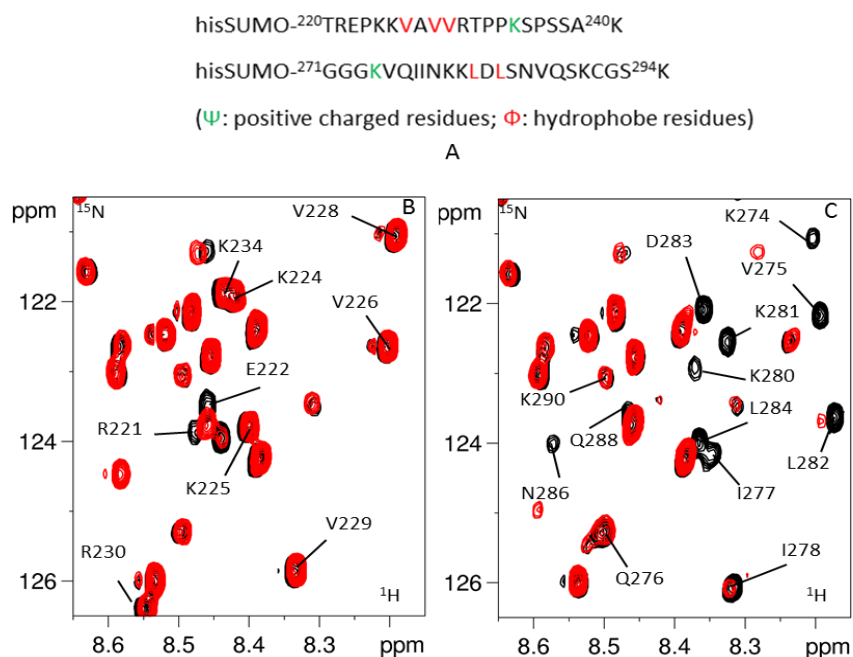


Figure 9: L'interaction des His-Sumo peptides avec ERK2. (A) La séquence des deux peptides de Tau, F[220-240] Tau et F[274-291] Tau, qui sont exprimés en fusion de His-SUMO. Les séquences contiennent un consensus $\Psi_{1-3}\text{x}_{3-7}\Phi\text{x}\Phi$ ou $\Phi\text{x}\Phi\text{x}_{3-7}\Psi_{1-3}$: les résidus chargés positivement sont indiqués en vert (Ψ) et les résidus hydrophobes (Φ) sont en rouge. (B) Détail de la superposition des spectres HSQC 2D de ^{15}N His-SUMO F[220-240] Tau avec ERK2, en rouge et de ^{15}N His-SUMO F[220-240] en noir. (C) Détail de la superposition des spectres HSQC 2D de ^{15}N His-SUMO F[274-294] Tau avec ERK2, en rouge et de ^{15}N His-SUMO F[274-294] Tau en noir.

8. Détermination de Kd par ^{19}F -RMN

Nous avons ensuite quantifié l'interaction de ERK2 avec Tau, ou le fragment K18, en utilisant la RMN du Fluor (^{19}F -RMN) pour estimer une valeur de Kd.

^{15}N K18 et ^{15}N Tau sont marqués *in vitro* par le groupe trifluorométhyl (CF₃) sur les résidus C²⁹¹ et C³²² qui se trouvent à proximité aux peptides d'ancrage. La kinase ERK2 est titrée de 12,5 μM jusqu'à 220 μM en mélangeant avec 50 μM [^{19}F , ^{15}N] Tau ou 50 μM [^{19}F , ^{15}N] K18 à volume constant. D'après les spectres de 1D Fluor, deux pics correspondant au ^{19}F du groupe trifluorométhyl se trouvent aux déplacements chimiques -71,97 et -71,98ppm dans le spectre contrôle de [^{19}F , ^{15}N] Tau et [^{19}F , ^{15}N] K18 (Figure 10, A, les spectres 1D en noir). Avec l'augmentation de la concentration de ERK2, les déplacements chimiques des deux pics sont graduellement perturbés et élargissent, des spectres rouges aux spectres violets (Figure 10, A). Le déplacement chimique du pic à -71,97ppm dans le spectre contrôle, que l'on peut détecter pour tous les points de titration, est utilisé pour calculer la valeur de Kd. La valeur de Kd pour l'interaction K18 et ERK2 est estimée à 173 μM et 79 μM pour l'interaction Tau et ERK2 (Figure 10, B). En plus, la polarisation de fluorescence (FP) a aussi été utilisée comme un autre moyen d'étudier l'interaction par le marquage de K18 avec un fluorophore. L'étude de l'interaction par FP a permis de calculer une valeur de Kd similaire pour l'interaction de K18 et ERK2, qui confirmant les résultats de ^{19}F -RMN.

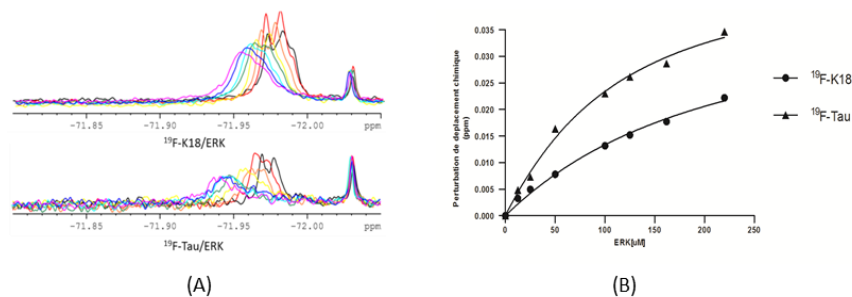


Figure 10 : Détermination de la valeur de la constante de dissociation Kd par ^{19}F -RMN. (A, B) Superposition des spectres 1D de 50 μM [^{19}F , ^{15}N] K18 ou Tau isolés (en noir) et après ajouts de différentes concentrations de ERK2 : en rouge 12,5 μM , orange 25 μM , jaune 50 μM , vert 100 μM , cyan 125 μM , bleu 162 μM et violet 220 μM . (B) La valeur du déplacement chimique pour chaque point de titration permet d'obtenir une courbe de saturation et de calculer un Kd. Pour [^{19}F , ^{15}N] K18/ERK2, le Kd est de 173 μM , pour [^{19}F , ^{15}N] Tau/ERK2, le Kd est de 79 μM . Ces Kd sont une estimation parce qu'on ne parvient pas à saturer la protéine Tau dans ces expériences.

Partie 2: Caractérisation de l'activité kinase des phospho-isoformes d'activation de ERK2 envers Tau.

Le spectre HSQC 2D [^1H , ^{15}N] de Tau phosphorylé par ERK2 pTEpY présente plusieurs résonances supplémentaires qui sont situées dans la région du spectre typique pour les résonances d'amide H-N de pT et pS (Figure 11).

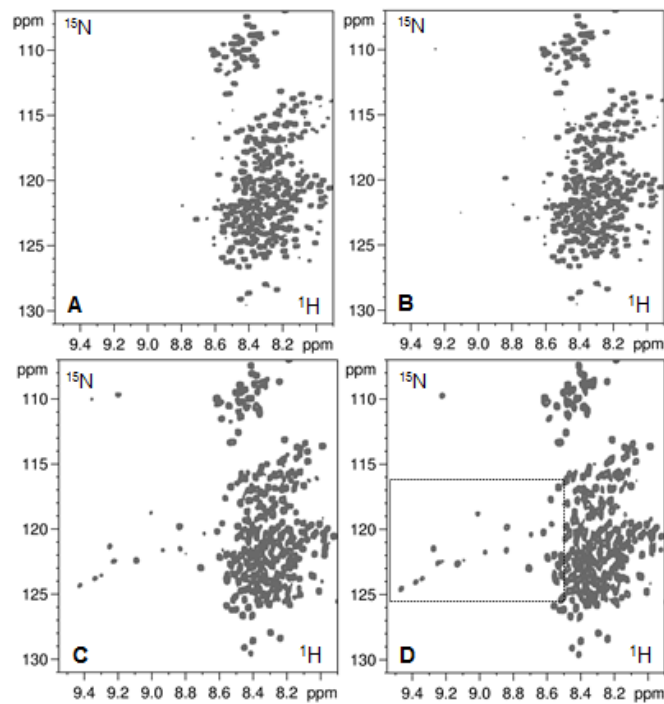


Figure 11 : La phosphorylation de Tau par différentes isoformes de ERK2. Comparaison du spectre HSQC 2D [^1H , ^{15}N] de ^{15}N Tau incubé pendant 3H à 37°C avec les différents phospho-isoformes de ERK2 (A) ERK2 TEY, (B) ERK2 TEpY, (C) ERK2 pTEY, (D) ERK2 pTEpY. Des résonances supplémentaires sont observées, comparé avec A, dans la région au-dessus de 8,6ppm sur l'échelle du proton de la protéine Tau modifiée par deux isoformes de ERK2 : ERK2 pTEY (C), et ERK2 pTEpY (D).

Les phospho-isoformes d'ERK2 pTEY et ERK2 TEpY ont été reçues de l'équipe du Prof. J. Gunawardena (Harvard Medical School, Etats-Unis), et obtenues par déphosphorylation de ERK2 pTEpY avec les phosphatases PP2A et PTP, respectivement (Sudhakaran Prabakaran et al. 2011). La distribution de phospho-isoformes est estimée par la spectroscopie de masse pour assurer que la phospho-isoforme ERK2 pTEpY est résiduelle dans chacune des préparations de kinases pTEY et TEpY. La comparaison des spectres HSQC 2D [^1H , ^{15}N] Tau phosphorylé par les différentes isoformes indique que l'incubation avec ERK2 non

phosphorylé conduit à aucune phosphorylation envers le substrat Tau (Figure 11, A). De même, dans le spectre 2D [^1H , ^{15}N] de Tau phosphorylé avec l'isoforme ERK2 TEpY, on voit quelques résonances de faible intensité qui pourraient correspondre à une phosphorylation résiduelle de T⁵⁰, T²⁰⁵ et S²³⁵. Il est possible que cette phosphorylation soit due au 20% résiduel de l'isoforme ERK2 pTEpY dans la préparation d'ERK2 TEpY, définis par la méthode MALDI-TOF quantitative (Prabakaran et al. 2011). Par contre, sur base des spectres HSQC de Tau phosphorylée par les ERK2 pTEY et ERK2 pTEpY, on peut conclure que ces isoformes phosphorylent de nombreux résidus S/T de Tau (Figure 11, C et D). La comparaison des résonances correspondant aux résidus phosphorylés confirme la spécificité similaire de phosphorylation envers Tau de ces deux isoformes (Figure 12). Par ailleurs, l'analyse quantitative de spectroscopie de masse atteste qu'il n'y a pas de contamination réciproque dans les préparations d'ERK2 pTEY et ERK2 pTEpY, bien que l'isoforme ERK2 pTEY contient un peu plus d'ERK2 non phosphorylé et donc proportionnellement moins de forme active. Ceci peut expliquer le niveau un peu plus faible de phosphorylation de Tau par la préparation d'ERK2 pTEY (Figure 12). Cela pourrait aussi être dû à une activité enzymatique moins efficace de l'isoforme pTEY mais on ne peut pas conclure.

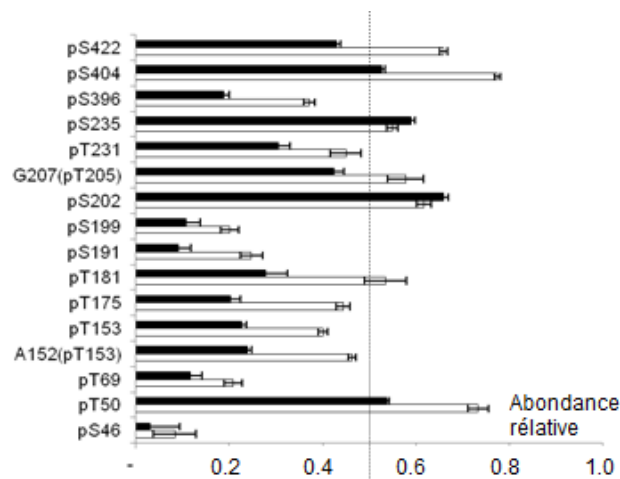


Figure 12 : Le schéma montre l'intégrale relative des résonances correspondant aux phospho-résidus de Tau. La valeur '1', c'est la moyenne de l'intégrale de trois pics isolés qui correspondent à trois résidus dispersés dans la séquence primaire de Tau. Les barres noires correspondent à la phosphorylation de Tau par ERK2 pTEY, et les blanches indiquent la phosphorylation par ERK2 pTEpY. Les barres d'erreur rendent compte de la variabilité des données correspondant au rapport signal sur bruit.

Partie 3: La caractérisation de l'interaction de Tau avec l'ADN et sa régulation par la phosphorylation de Tau par la spectroscopie RMN.

1. L'interaction de Tau441 avec double-brin des oligonucléotides

Les études de l'interaction de Tau avec l'ADN sont principalement effectuées par la RMN. On observe dans la séquence de Tau entière deux segments qui sont affectés par l'interaction avec l'ADN, qu'ils correspondent à la séquence de R²⁰⁹ à A²⁴⁶ qui se trouve dans le PRD jusqu'à N-terminal de MTDB, de K²⁶⁷ à S²⁸⁹ qui est situé dans le R2 du MTBD de protéine Tau (Figure 13). Les fragments de Tau, F[165-245] et F[244-372], qui correspondent respectivement aux PRD et MTBD isolés sont également capables d'interagir avec l'ADN, avec affinités similaires. La définition des sites d'interaction obtenus avec la protéine entière est confirmée avec les domaines isolés.

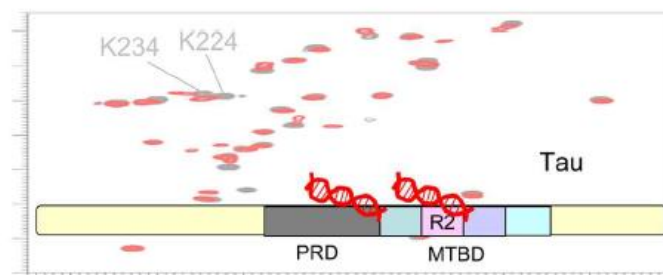


Figure 13 : Résumé de l'interaction de Tau avec les oligonucléotides d'ADN dans les domaines PRD et la région répétée R2 du MTBD de Tau.

2. L'interaction des peptides de Tau avec l'ADN

Deux peptides de Tau, ¹⁵N His-SUMO F[220-240] et ¹⁵N His-SUMO F[271-294], sont utilisés pour vérifier les sites d'interaction avec l'ADN. Ces peptides sont inclus dans les régions d'interaction de Tau avec des séquences oligonucléotidiques d'ADN Tau[209-246] et Tau[267-289]. Dans les spectres de ces peptides (Figure 14, A et B) en présence des oligonucléotides, on observe peu de perturbations des déplacements chimiques comparés aux perturbations observées pour ces mêmes expériences avec Tau entière ou les domaines PRD et MTBD isolés. Nous en avons conclu que la longueur des peptides, environ 20 acide aminés, n'est pas suffisante pour de lier les oligonucléotides avec 22 pair des bases.

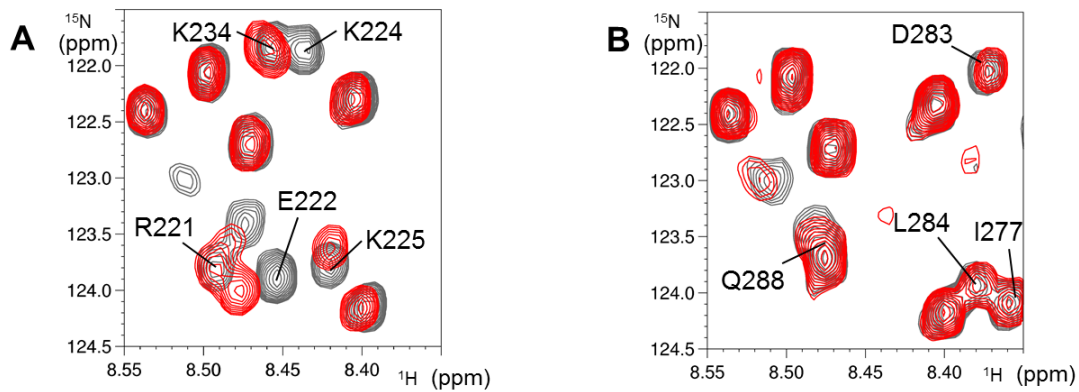


Figure 14 : Superpositions des spectres des peptides de Tau, ^{15}N His-SUMO F[220-240] (A) et ^{15}N His-SUMO F[271-294] (B), sans (en gris) ou avec (en rouge) les oligonucléotides d'ADN avec le rapport molaire 1 :1.

3. La régulation de l'interaction de Tau avec l'ADN par la phosphorylation

Nous avons utilisés 2 échantillons phosphorylés et caractérisés de Tau pour évaluer l'impact de la phosphorylation de Tau avec l'ADN. Un premier échantillon de Tau est phosphorylé par un extrait de cerveau de rat. Sur base des données de RMN, on observe que l'interaction de Tau avec l'ADN est abolie lorsque Tau présente ce profil de phosphorylation. Il y a de nombreuses phosphorylations dans le domaine PRD avec ce profil de phosphorylation. On peut comprendre que l'effet électrostatique empêche l'interaction dans cette région. Par contre il y a peu de phosphorylations proches du R2, à l'exception de la pS²⁶². C'est donc plus difficile d'expliquer pourquoi on perd l'interaction dans le domaine MTBD. Pour vérifier, nous avons utilisé cette fois un échantillon de Tau phosphorylé *in vitro* par la kinase CDK2/CycA3 (Laziza Amniai et al. 2009). Il y a moins de phosphorylation dans cet échantillon et aucune n'est localisée dans le MTBD. Néanmoins, on observe à nouveau aucune interaction avec les oligonucléotides, ni dans la région du PRD, ni dans le domaine répété R2. On doit conclure que la phosphorylation dans le domaine PRD a un effet global sur l'interaction de Tau avec l'ADN.

Abstract

Tau has a central role in neurodegeneration and is implicated in Alzheimer's disease (AD) development. Dysregulation of Tau in pathological conditions is correlated with abnormal phosphorylation that impairs its interaction with other proteins. Tau is found aggregated in neurons affected by the disease, typically in paired helical filaments (PHFs) constituted of hyper-phosphorylated Tau. Molecular mechanisms leading to pathological Tau are unknown. To better understand the mechanisms of Tau abnormal modifications and its impact on Tau functions and aggregation propensity, we have used Nuclear Magnetic Resonance (NMR) Spectroscopy. Given the number and proximity of the phosphorylation sites, a resolving method is necessary to characterize Tau phosphorylation pattern. An analytical characterization of Tau phosphorylation was performed in a first step using NMR spectroscopy. Additionally, NMR was used to study Tau interactions with molecular partners, and the impact of this phosphorylation on the interaction.

During my thesis I have characterized Tau phosphorylation by Extracellular signal-regulated kinase2 (ERK2), a mitogen-activated protein kinases (MAPKs) that responds to extracellular signals. ERK1/2 kinase activation in AD brain is well documented and previous studies propose that ERK1/2 is able to transform Tau into an AD-like state, although mainly documented by the detection of the AT8 epitope. Analysis of *in vitro* phosphorylated Tau by activated recombinant ERK2 with NMR spectroscopy revealed phosphorylation of 14 S/T-P sites among 17 such motifs. *In vitro* phosphorylation of Tau using rat brain extract and subsequent NMR analysis identified the same sites. Phosphorylation with rat brain extract is used as a model of Tau hyperphosphorylation in biochemical studies and result in an increased propensity of Tau to aggregate into fibres. Our results indicated that phosphorylation of Tau by ERK2 kinase alone was sufficient to produce the same phospho-Tau filaments. We then investigated the mechanism of ERK2 phosphorylation of Tau. Kinases are known to recognize their protein substrates not only by their specificity for a targeted S/T phosphorylation site but also by binding to peptidic linear motifs located outside of the phosphorylated motif, called docking sites. We identified two main docking sites along the Tau sequence using NMR spectroscopy, located in the microtubule binding domain (MTBDs) of Tau. These peptides match the described consensus for ERK1/2 docking sites called D-

sites. Tau is to our knowledge the first ERK2 substrate to present multiple docking sites instead of one high affinity single D-site motif. This may have implication in the regulation of signaling specificity in MAPK pathways in a cellular context.

Additionally, I have investigated the functional consequences of Tau phosphorylation by ERK2. We have shown that oligonucleotidic DNA fragments interact mainly with two binding sites in Tau sequence, Tau[209-246] and Tau[267-289] regions. These binding sites are respectively located in the proline rich domain (PRD) and MTBDs of Tau. I have shown that this interaction is abolished by Tau phosphorylation by ERK2.

ERK1/2 phosphorylation of Tau can take place in cells upon stress-signalling or once the phosphorylation fails to be counteracted by an efficient dephosphorylation. The ERK2 kinase is considered, based on a number of studies in cellular context, as a Tau kinase that could be involved in AD patho-physiology. We here reinforce this view by showing that the ERK2 kinase has the capacity by itself to phosphorylate Tau on many sites and that the resulting phosphorylation pattern increases phospho-Tau aggregation propensity. Additionally, ERK2 phosphorylation of Tau can lead to a loss of physiological function, such as its capacity to bind DNA. These results support the hypothesis that ERK2 activation under stress conditions might have a detrimental effect for Tau function and participate in AD physio-pathology.

Abbreviations

A β	β -amyloid
AD	Alzheimer's disease
APP	amyloid precursor protein
ATP	adenosine triphosphate
CaMKII	Ca ²⁺ /calmodulin-dependent protein kinase
CD	circular dichroism
CDKs	cyclin-dependent kinases
CNS	central nervous system
DRS	D-recruitment site
DYRK1A	dual-specificity tyrosine phosphorylated and regulated kinase 1A
ERK	extracellular signal-regulated kinase
FKBP52	FK506-binding protein
FRS	F-recruitment site
FTDP	frontotemporal degeneration linked with Parkinsonism
FTIR	Fourier transform infrared spectroscopy
GSK3 β	glycogen synthase kinase 3 β
GST	glutathione S-transferase
HPLC	high performance liquid chromatography
HSPGs	heparin sulfate proteoglycans
HSQC	heteronuclear single quantum coherence
IDP	intrinsically disordered protein
K _D	dissociation constant
MALDI-TOF	matrix-assisted laser desorption/ionization-time of flight
MAPs	microtubule-associated proteins
MAPKs	mitogen-activated protein kinases
MARKs	microtubule affinity-regulating kinases
MTBDs	microtubule-binding domains
MS	mass spectroscopy
NFTs	neurofibrillary tangles
NMR	nuclear magnetic resonance
PEA-15	15kDa phosphoprotein enriched in astrocytes
PHFs	paired helical filaments
PKA	cAMP-dependent protein kinase A
PMT	posttranslational modifications
PNS	peripheral nervous system
PP2A	protein phosphatase 2A
PPIase	peptidyl-prolyl cis/trans isomerase
p.p.m.	parts per million
PRD	proline-rich domain
PTPs	protein tyrosine phosphatases
SDS-PAGE	sodium dodecyl sulfate polyacrylamide gel electrophoresis
SP	senile plaques
SUMO	Small Ubiquitin-like Modifier proteins

Publications

1. **Qi, H.** Cantrelle, F.X. Benhelli-Mokrani, H. Smet-Nocca, C. Buée, L. Lippens, G. Bonnefoy, E. Galas, M-C. Landrieu, I. Nuclear Magnetic Resonance characterization of Tau interaction with DNA and its regulation by phosphorylation. *Biochemistry*. 2015 Feb 24;54(7):1525-33.
2. Kamah, A. Huvent, I. Cantrelle, F.X. **Qi, H.** Lippens, G. Landrieu, I. Smet-Nocca, C. Nuclear magnetic resonance analysis of the acetylation pattern of the neuronal Tau protein. *Biochemistry*. 2014 May 13;53(18):3020-32
3. Manuscript under preparation: *Methods in Molecular Biology*, Springer
Qi, H. Despres, C., Prabakaran, S., Cantrelle, F.X., Chambraud, B., Gunawardena, J., Lippens, G., Smet-Nocca, C., Landrieu, I. The study of posttranslational modifications of Tau protein by Nuclear Magnetic Resonance spectroscopy: phosphorylation of Tau protein by ERK2 recombinant kinase and rat brain extract and acetylation by recombinant Creb-binding protein. *Protocols in Molecular Biology*, Springer, Edited by Dr Caroline Smet-Nocca.
4. Manuscript under preparation:
Qi, H. Prabakaran, S. Cantrelle, F.X. Chambraud, B. Gunawardena, J. Lippens, G. Landrieu, I. Characterization of the neuronal Tau protein as a target of the ERK kinase.

Communications:

- (Poster) **Qi, H.** Cantrelle, F.X. Prabakaran, S. Gunawardena, J. Lippens, G. Landrieu, I. (2014) Docking peptides of the stress-related ERK kinase for the neuronal Tau protein. The 2014 Belgian Peptide Group Meeting. Ghent, Belgium, 10-11 Feb
- (Short talk) **Qi, H.** Interaction de la phospho-protéine neuronale Tau avec des protéines partenaires comme cibles thérapeutiques dans la maladie d'Alzheimer. Journées Scientifiques DISTALZ (2014) Lille, France, 12-13 Nov
- (Poster) **Qi, H.** Cantrelle, F.X. Prabakaran, S. Gunawardena, J. Lippens, G. Landrieu, I. (2014) Docking peptides of the stress-related ERK kinase for the neuronal Tau protein. *Advances in protein-protein interaction analysis and modulation*, EMBO Workshop (2014) Marseille, France, 9-12 Sep
- (Poster) **Qi, H.** Cantrelle, F.X. Prabakaran, S. Gunawardena, J. Lippens, G. Landrieu, I. (2015) NMR study of ERK-mediated hyperphosphorylation of the neuronal Tau. *Computational Aspects-Biomolecular NMR*, Gordon Research Conference, Il Ciocco, Italy, 7-12 Jun
- (Poster) **Qi, H.** Cantrelle, F.X. Kamah, A. Despres, C. Prabakaran, S. Gunawardena, J. Lippens, G. Landrieu, I. (2015) NMR study of ERK-mediated hyperphosphorylation of the neuronal Tau. 29th Annual Symposium of Protein Society, Barcelona, Spain, 22-25 July

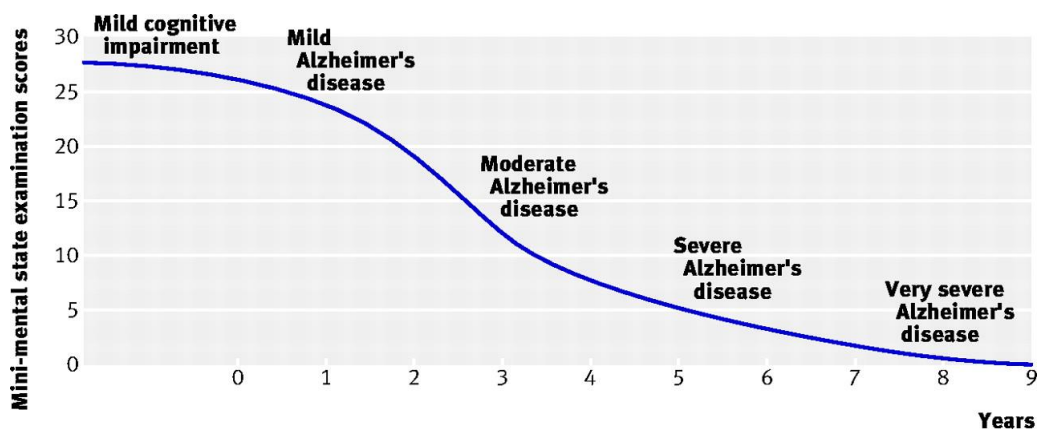
Introduction

Part 1. Alzheimer's disease

Alzheimer's disease (AD) was first described and reported by a German psychiatrist and neuropathologist Alois Alzheimer (1864-1915). He first described clinical and histological characters of cerebral lesions from his patient Auguste D, a woman who died at 56 years-old after 5 years of suffering from a progressive dementia at the 37th annual conference of German psychiatrists. AD is today affecting about 6% of the population aged over 65 with an increasing incidence with age. From the report of the World Health Organization (WHO) in 2015, about 47.5 million people worldwide are suffering from dementia with 7.7 million new cases appearing every year. Over half (58%) of the affected persons are living in low and middle-income countries. In 2030, the total number with dementia is expected to rise to 75.6 million and almost double in the following twenty years, reaching an estimated 135.5 million by 2050. AD is thus now a major public health problem linked to the increasing life span and the population expansion.

AD is a chronic neurodegenerative disease, which accounts for about 60-70% of all dementia cases. Symptoms of the disease include cognitive impairment like memory loss and dysfunctions in speaking and thinking. In addition, psychiatric symptoms and behavioral disturbances are also observed such as depression hallucination or delusions.

AD presents a progressive development from mild cognitive impairment to very severe AD spanning about a 9 year period (Figure 15). The early and mild cognitive impairment, like memory loss, can be observed several years before the diagnosis of AD is made. This kind of cognitive dysfunction is probably not distinct from what is expected in normal ageing. This early stage may remain relatively stable for several years, but it ends with a detectable deterioration in cognitive function, progressing two to five years. As the disease develops into moderate stages, the symptoms become clearer and more restricting and include cognitive deficits and behavioral changes. A near total dependence and inactivity of the patients characterizes the last severe stages of AD (Feldman & Woodward 2005).



Mild cognitive impairment: Complaints of memory loss, intact activities of daily living, no evidence of Alzheimer's disease

Mild Alzheimer's disease: Forgetfulness, short term memory loss, repetitive questions, hobbies, interests lost, impaired activities of daily living

Moderate Alzheimer's disease: Progression of cognitive deficits, dysexecutive syndrome, further impaired activities of daily living, transitions in care, emergence of behavioural and psychological symptoms of dementia

Severe Alzheimer's disease: Agitation, altered sleep patterns, assistance required in dressing, feeding, bathing, established behavioural and psychological symptoms of dementia

Very severe Alzheimer's disease: Bedbound, no speech, incontinent, basic psychomotor skills lost

Figure 15 : The progression of symptoms in the course of Alzheimer's disease (Feldman & Woodward 2005; Burns & Liffie 2009)

So far, causes of AD onset remain unclear. The risk to develop AD is considered multi-factorial from genetic causes to environmental impacts. It includes generally four aspects (Burns & Liffie 2009):

I. Sociodemographic:

Age: increasing age;

Sex: no consistent evidence;

National and ethnic profile: some evidence of regional variations;

II. Familial and genetic factors:

Family history: 3.5-fold increase in risk when a first degree relative is affected;

Diseases causing mutations: on chromosomes 1, 14, and 21(Nistor et al. 2007; Lott & Head 2005)

ApoE genotype;

Down's syndrome: everyone eventually develops the neuropathological features of AD (Lott & Head 2005);

Premorbid cognitive reserves: longer education and higher intelligence are protective;

III. Medical history and treatments:

Head injuries: anti-inflammatory drugs are associated with a reduction in risk;

Vascular risk factors: hypertension, diabetes, homocysteine, and cholesterol are all implicated;

Depression: associated with AD;

Herpes simplex: a risk factor, possibly mediated by the presence of ApoE e4;

IV. Habits:

Alcohol: drinking wine is protective;

Smoking: no consistent evidence;

1. Pathway hypothesis in the physiopathology of AD

In *post-mortem* AD diagnosis, senile plaques (SP) and neurofibrillary tangles (NFTs) have been considered for a long time as two pathological ‘hallmarks’ of AD, which are generated respectively via two major pathways: the Amyloid pathway and the Tau pathway. These pathways are still considered as two major hypotheses in the physiopathology of AD (Grundke-Iqba et al. 1986; Hardy & Higgins 1992). As the levels of SP and NFTs in AD brain are higher than that in normal cerebral system, the build-up of these two lesions remains the important target in AD research work. The senile plaques are extracellular deposits which are predominantly constituted by a small peptide (4kDa) with 38 to 42 amino acids, called amyloid peptide or beta amyloid ($A\beta$), while NFTs are the intracellular deposits mostly composed by the hyperphosphorylated and insoluble filamentous Tau protein (Figure 16).

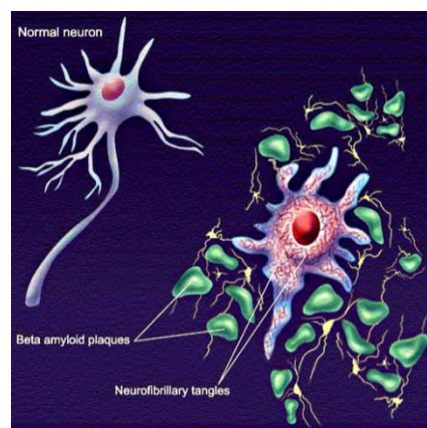


Figure 16 : Comparison of healthy neuron and Alzheimer’s neuron. Beta amyloid plaques are extracellular deposits while neurofibrillary tangles are generated inside the neuron. (http://userwww.sfsu.edu/art511_h/511final/alzheimerproposal/plaques.html)

1.1 Amyloid cascade hypothesis

The major issue in the amyloid cascade hypothesis is the excessive formation and/or defective clearance of $A\beta$ produced by altered amyloid precursor protein (APP) processing. The processing can be affected by multiple factors, such as alteration in signal transduction, genetic alterations or cellular degeneration (Armstrong 2009). Among them, genetic mutations have been demonstrated to associate with familial types of AD. The discovery of genetic mutations in three major genes, APP, PSEN1 and PSEN2, which encode the amyloid

precursor transmembrane protein and presenilin 1 and 2 (components of γ -secretase catalytic core), respectively, have provided a basic understanding of the amyloid pathway (Lalonde et al. 2002). Transgenic mouse models further suggest that the genetic mutation found in human APP are sufficient to develop extracellular A β deposit and exhibit Alzheimer's-like brain with neuropathology in mice (Games et al. 1995; Lalonde et al. 2002). The proteins implicated in the amyloid cascade (Figure 17) are therefore targeted in several clinical trials (Goldgaber et al. 1987; Sherrington et al. 1995; Levy-Lahad et al. 1995). The appearance of extracellular A β deposits was postulated in 1991 as the fundamental cause of the AD disease (Hardy & Allsop 1991). A β deposits are developed by A β oligomers predominantly constituted by A β 40 and A β 42 (40 and 42 amino acids Amyloid peptide) which are obtained through a sequential truncation from APP. The processing of APP can be divided into non-amyloidogenic and amyloidogenic pathway (Figure 17) (Zhang 2012). In these processes, APP protein can be first cleaved by α -secretase or β -secretase (BACE1) in extracellular domain, generating a soluble N-terminal ectodomain of secreted APP, sAPP α and sAPP β respectively, and the membrane-bound C-terminal fragments called C83 and C99, respectively. C83 and C99 can be further cleaved by γ -secretase, releasing respectively a 3-kDa peptide (p3) and 4-kDa A β 40/A β 42 peptides in the extracellular domain and the APP intracellular C-terminal domain (AICD). Secreted A β 40/A β 42 peptides have a tendency to polymerize into insoluble fibrils with β -sheet structure which are toxic for the neurons (Zhang 2012). A β oligomers, considered as the most toxic species, have been suggested as the prion protein (PrP) in Creutzfeldt-Jacob disease to be able to propagate the disease in the brain (Laurén et al. 2009). Intracerebral injection experiments suggest that the A β deposit will be developed much earlier and in larger amount in mice brains after the exogenous injection of brain extract from either AD patients or from transgenic mice APP23 and APP-PS1 (Kane et al. 2000; Meyer-Luehmann et al. 2006).

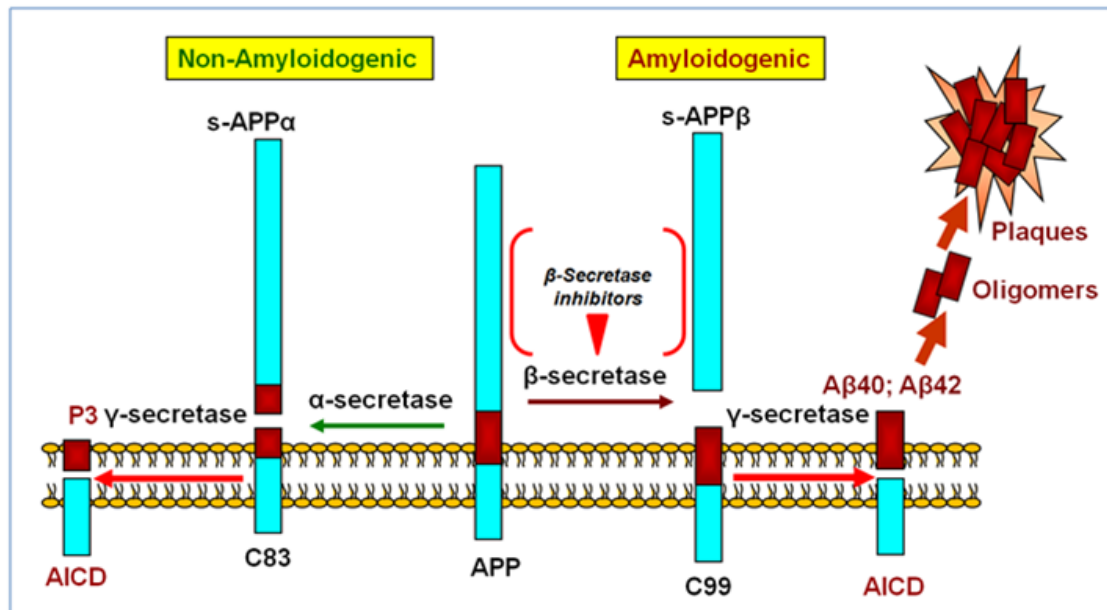


Figure 17: The processing of APP can be divided into non-amyloidogenic and amyloidogenic pathway (Zhang 2012). APP protein is cleaved by the α -secretase protease into soluble s-APP α and C-terminal fragment C83 in the non-amyloidogenic pathway. C83 will further be cleaved by the γ -secretase to release P3 and the intracellular domain AICD. On the other hand, APP can be processed in an amyloidogenic pathway, first by the β -secretase that releases a soluble s-APP β fragment and the intracellular C99 fragment. C99 will further be cleaved by the γ -secretase to release the amyloidogenic A β 40 and A β 42 peptides, and the intracellular domain AICD.

In amyloidogenic pathway, as the formation of A β 40 or A β 42 is dependent on the activity of β -secretase, it plays an essential role in amyloidogenic processing and pathogenesis of AD. Certain APP mutation in familial AD, for example, might substantially increase β -secretase-involved amyloidogenic processing and raise AD risks (Citron et al. 1992). The expression level and/or the activity of β -secretase is found increased in AD brains (Fukumoto et al. 2002; Holsinger et al. 2002), and also raises up with aging in human and animals' brain (Fukumoto et al. 2004). In addition, the activity of β -secretase is also revealed elevated in circumstances related to AD risk factors, like traumatic brain injury, stroke and cardiovascular events (Cole & Vassar 2008). Therefore, the inhibition of β -secretase activity is suggested as a very promising pharmaceutical approach to reduce A β generation by amyloid cascade in AD or AD risk factor cases.

1.2 Tau cascade hypothesis

Several neurodegenerative diseases have been shown to be related to the lesions of Tau protein and are referred to as 'Tauopathies' (Lee et al. 2001), including AD. Mutations in Tau gene can be found at the origin of frontotemporal degeneration linked with Parkinsonism with Tau inclusions (FTDP-Tau), as well as Pick's disease, progressive supranuclear palsy, and corticobasal degeneration where Tauopathies display specific forms of Tau deposits in the brain, such as pick bodies in the case of pick disease (Lee et al. 2001; Omalu et al. 2011; Rajput et al. 2006; Santpere & Ferrer 2009).

Tau protein is able to polymerize under certain conditions and its aggregated forms might be assembled into NFTs which would induce the neuronal death (Bandyopadhyay et al. 2007). The aggregation of Tau protein is suggested to be induced by one or multiple events, such as hyperphosphorylation or other posttranslational modifications and/or Tau gene mutations (Mietelska-Porowska et al. 2014). This might lead Tau to lose its physiological function(s), such as microtubule stabilization, and/or gain toxicity due to the formation of various aggregated species like oligomers, PHFs (Paired helical filaments) and NFTs (Figure 18) (Mietelska-Porowska et al. 2014). A hypothesis of Tau aggregation pathway is illustrated in Figure 18. The increasing misfolded Tau monomers in the cytoplasm might polymerize into insoluble granular oligomers (GTOs) or successively multimerize via dimer/trimer and small soluble oligomer formation. PHFs are then constituted by Tau oligomers where β -sheet structure is proposed as the primary molecular organization (Medina & Avila 2014). PHFs are further assembled into NFTs which are thought to be responsible for neuronal death (Figure 18, A).

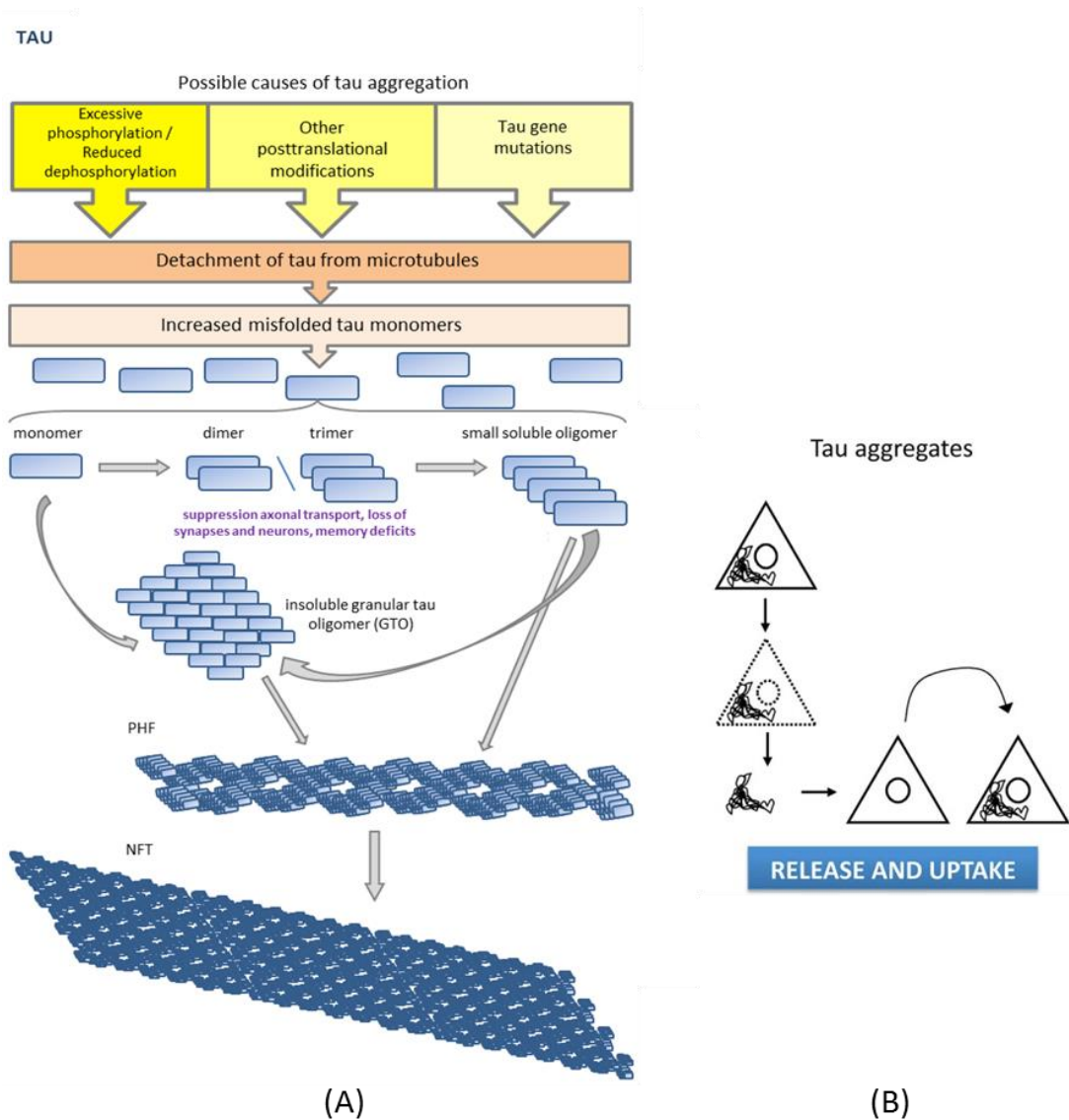


Figure 18 : The process of Tau aggregation and its intercellular infection. (A) The process of Tau aggregation in cells (Mietelska-Porowska et al. 2014). (B) The releasing and uptake of Tau aggregates. The neuron (illustrated by solid-line triangle) is dying due to the toxicity of Tau aggregates such as NFTs and various aggregated forms are released into ectodomain after the lysis of neurons (illustrated by dot-line triangle). These Tau aggregated species are infectious and capable to internalize into surrounding neurons, propagating dysfunctions and aggregation process of Tau protein (Medina & Avila 2014).

Detection of aggregated Tau in *post-mortem* brain has been used as diagnostic for AD. Stages linked to the disease progression have been defined based on the staining by Tau antibodies. A progression through the various brain regions appears to be conserved during the disease evolution, from the hippocampus (Figure 19, Stage II-III) to finally extend to broader neocortex area (Figure 19, Stage IV-VI) (Braak et al. 1993). More recently, an

immunodetection with the AT8 antibody that recognizes Tau protein aberrantly phosphorylated replaces the initial detection of the aggregates by silver staining, showing that abnormal phosphorylation is linked to the disease progression (Braak et al. 2006).

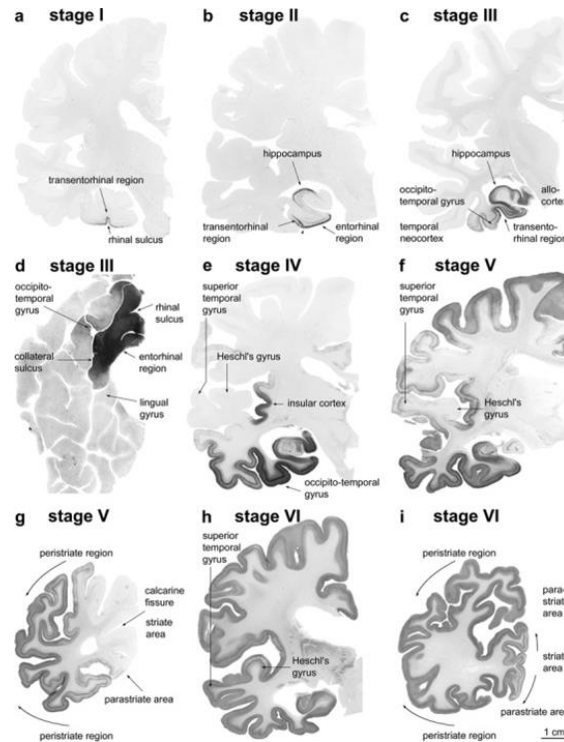


Figure 19: Staging of Alzheimer's disease-associated neurofibrillary pathology using immunocytochemistry. The evolution of neurofibrillary pathology is represented by immunostained hyperphosphorylated Tau protein by monoclonal antibodies AT8 recognizing Tau phosphorylation at Ser202 and Thr205 (Braak et al. 2006).

This stepwise propagation in the various brain areas is now proposed to be due to Tau propagation through the brain, in a prion-like manner (Hyman 2014; Sanders et al. 2014). Studies *in vivo* have indicated that the injection of synthetic Tau fibrils can, in a time-dependent manner, induce a pathological propagation of NFT-like inclusions in transgenic mice's brain overexpressing mutant human Tau (P301S) (Iba et al. 2013). Other interesting studies recently show that Tau filaments can be generated by the injections of brain extract from either P301S transgenic mouse or post-mortem AD patients into the brain of transgenic mice expressing wild-type human Tau (line ALZ17), and the spreading of Tauopathies is observed from injection sites to connected brain regions (Clavaguera et al. 2013). Therefore, these findings strongly suggest a neuron-to-neuron way of Tauopathies propagation. It is not

known yet which kind of composition and morphology of Tau aggregates enables to initialize such intracerebral pathological spreading (Clavaguera et al. 2014).

Once the neuron dies, the intra-NFTs as well as other misfolded Tau species could be released into the extracellular space. They are suggested to be up-taken by the surrounding neurons, seeding abnormal conformations of Tau protein and mediating the disease progression in the brain (Figure 18, B) (Medina & Avila 2014). Physiologically, Tau protein can be also secreted and transferred between synaptic connected neurons, as an elevated level of secreted Tau is also found in AD cases, in a process independent of neuron death (Pooler et al. 2013). A monoclonal antibody against Tau protein is shown to trap extracellular Tau species, preventing internalization in cells and blocking thus the aggregates propagation (Kfoury et al. 2012). The mechanisms of Tau aggregate propagation might thus provide new therapeutic strategies for AD and Tauopathies.

One of the downstream effects in amyloid cascade, due to the extracellular deposition of A β , is signal transduction to initiate the Tau pathway leading to NFTs formation (Armstrong 2009). As the most important component in NFTs, intracellular Tau protein and its pathological cascade are then important to elucidate in the development of neuronal pathogenesis in AD.

1.3 β -Amyloid and Tau

Although two AD hallmarks, extracellular amyloid plaques and intracellular neurofibrillary tangles, are generated in distinct way, there are considerable debates about the neurotoxicity of A β and Tau aggregated species. Their synergistic roles on pathological impacts get also more attention these years. So far, increasing evidence show that small soluble oligomers of A β can exert its neurotoxicity via Tau-dependent Fyn pathway at post-synaptic dendrites (Ittner et al. 2010). Despite Tau protein being predominantly located along neuronal axons, there is small amount of Tau physiologically located in somato-dendritic compartment where Fyn kinase anchored by Tau would phosphorylate NMDA receptor (NR), and then stabilize the interaction of NR with postsynaptic protein PSD-95 in order to induce neurotransmitter signaling (Haass & Mandelkow 2010). In addition, Tau

might have significant redistribution under pathological conditions into soma and dendrites due to more hyperphosphorylated Tau detaching from Microtubules (MTs). Therefore, more Fyn/Tau complex moving into dendritic spin, more upregulation of NR phosphorylation occurring to strengthen excitotoxic signaling from neurotransmitter glutamate which dramatically enhances A β toxicity to neurons (Ittner et al. 2010). Transgenic mouse assays prove that truncated Tau might be excluded from dendrites and sequester Fyn kinase in soma, mitigating the induction of A β toxicity (Ittner et al. 2010). In addition, the absence of Tau in tau^{-/-} mice disrupts the targeting of Fyn in dendrites, and finally prevents memory loss and improves survival in A β -forming transgenic mouse model (Ittner et al. 2010).

Therefore, Tau might play an essential role for A β -induced synaptotoxicity in neurodegeneration. Recently, immunization therapy for A β oligomers and/or abnormal phosphorylated Tau protein is proposed as a promising therapeutic strategies to reduce Tau pathology and A β -induced neuronal toxicity (Nisbet et al. 2014).

1.4 Genetic risk factors in AD

In addition to investigate the mechanism of A β and/or Tau aggregation pathways, amount of efforts have been devoted on the identification of genetic causes and risk factors of AD. In 2005, a genome-wide association study (GWAS) was initiated to screen and to discover new genes which were not previously suspected (The Wellcome Trust Case Control Consortium 2007). Variants of Apolipoprotein E (APOE ϵ) were found to be significant genetic risk factors for late-onset AD (LOAD). In additional studies, over 20 loci were found to associate with LOAD, including BIN1, CR1, CLU, phosphatidylinositol-binding clathrin assembly protein (PICALM), CD33, EPHA1, MS4A4/MS4A6, ABCA7, CD2AP, SORL1, HLA-DRB5/DRB1, PTK2B, SLC24A4-RIN3, INPP5D, MEF2C, NME8, ZCWPW1, CELF1, FERMT2, CASS4 and TRIP4 (Chouraki & Seshadri 2014). The ongoing research work, devoted to the less frequent and rare variants, allow to discover two novel genes, TREM2 and Phospholipase D3 (PLD3) which were then identified for their roles for APP process in LOAD (Jin et al. 2014; Cruchaga et al. 2014). The relationships between these genes and the current AD pathophysiology hypothesis are not obvious, nevertheless, further research on their roles in AD development could offer new hypothesis on the physiopathology of AD.

These results provide us a larger scale of view on AD-related genes that were never found or even previously thought of being involved in biological pathways of AD pathophysiology. This may offer in the future new possibilities to design drugs in AD treatments.

2. Tau and its multiple physiological functions

Tau protein was first described by Weingarten et al and Witman et al in mid-1970s as an important factor involved in the assembly of the MTs as it has been demonstrated that Tau protein, a heat stable protein, is able to promote *in vitro* the assembly of tubulins into MTs and be incorporated throughout its length (Witman et al. 1976; Weingarten et al. 1975). An essential function of Tau protein is thus to initialize and stabilize the MTs under the physiological conditions. However, more and more evidence suggest that Tau might exert multiple functions in various physiological cellular regulations and in potential pathogenesis mechanism.

2.1 Tau gene and isoforms

Tau protein is encoded by a single gene *MAPT*, composed by 16 exons and located on the chromosome 17q21 (Neve et al. 1986; Andreadis et al. 1992; Andreadis et al. 1995). Tau is mainly expressed in the central nervous system (CNS), and also found at a lower level in the peripheral nervous system (PNS).

In adult human brain, there are 6 isoforms of Tau protein, each isoform being generated by an alternative splicing of exons. The isoforms of Tau range from 352 to 441 amino acids corresponding to 45 to 65 kDa molecular weight. These 6 isoforms differ by the presence or absence of the exon2 (E2) and E3 which are related to the number of N-terminal insertions, and E10 corresponding to a segment in the Microtubule Binding Domain (MTBD) in Tau sequence (Goedert et al. 1989). Alternatively, the splicing of E2 and/or E3 leads to the isoforms without N-terminal insert (0N) or with either 29 (1N) or 58 (2N) amino acids supplementary in the N-terminal of Tau. The inclusion or exclusion of E10 distinguishes the Tau isoforms containing 4 repeated motifs (4R) or 3 repeated motifs (3R) in Tau sequence (Figure 20, A, B). Therefore, the longest full-length Tau isoform in human brain is referred as

2N4R. Certain isoforms are specifically expressed during the development, for instance, the isoform ON3R is the only Tau isoform present during fetal stages whereas other isoforms are produced during adulthood (Goedert & Jakes 1990; Kosik et al. 1989). The isoforms 1N3R and 1N4R are mostly present in adult human Tau, and the 3R and 4R isoforms are approximately equally represented (Goedert & Jakes 1990). Therefore, it seems that each Tau isoform has its own biological role(s) and the encoding of E2, E3, and E10 is suggested relevant to the function(s) of Tau in the cellular process. Moreover, the stoichiometry of human Tau isoforms expression and their biochemical properties might be altered due to different pathological Tau mutations in hereditary FTDP-17 (Hong et al. 1998).

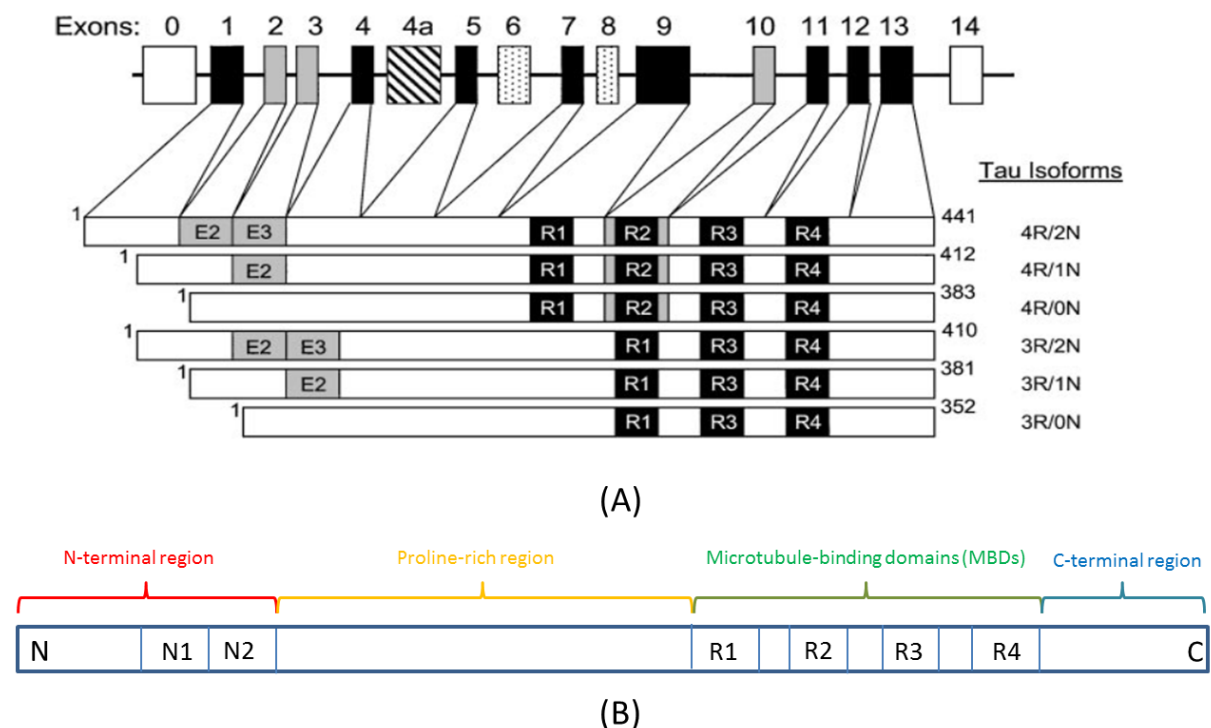


Figure 20 : Illustration of human Tau gene and the 6 translated Tau isoforms obtained by alternative mRNA splicing in the Central Nervous System. (A) Tau protein is expressed by a single gene which contains 16 exons. The exon0 (E0) works as part of the promoter sequence. The alternative splicing of E2, E3, and E10 in grey boxes generates finally different sequence length of Tau isoforms, including the full-length isoform 2N4R and the other composed by 3 or 4 repeated microtubule-binding motifs (3R or 4R) and different number of N-terminal inserts (0N, 1N, or 2N). E6 and E8 in stippled boxes and E4a in striped box are not transcribed in human CNS but are expressed in the peripheral nervous system, producing higher molecule weight Tau isoforms termed as big Tau (Lee et al. 2001). (B) Schematic representation of full-length human Tau isoform. It contains 441 amino acids which are divided into four parts: N-terminal region, PRD, MTBD, and C-terminal region. Two N-terminal insert parts, N1 and N2 encoded by E2 and E3, are composed of 29 amino

acids in each of them. In MTBD, each microtubule-binding motif, R1 to R4, is composed by about 18 amino acids and 13/14 amino acids in inter-repeat regions IR. The sequences of the repeats are partially conserved. The scheme does not reproduce the relative size of the Tau domains.

Physiologically, Tau is an intrinsically disorder protein (IDP) and generally can be divided into four parts: an N-terminal region, Proline-riche domain (PRD), a MTBD and a C-terminal region (Figure 20, B). These four regions provide to Tau various chemical and physiological properties. MTBD repeats R1 to R4 (31 or 32 residues) have similar sequences and consist of an 18-residue imperfect repeat and of a 13- or 14-residue inter-repeat region (IR) (Lee et al. 1988). It was noted that the presence or absence of the two N-terminals inserts encoded by E2 and E3 may affect the diameter of the assembled MTs in some specific axons (Chen et al. 1992). This suggests that the spacing of MTs depends on the length of Tau N-terminal domain which may in turn increase the axonal diameter (Chen et al. 1992). The N-terminal region (M¹–Y¹⁹⁷) (residue numbering as in the longest human isoform of Tau), including the N-terminal part of the PRD (165-197), is referred to as the projection domain because it projects from the microtubule surface where it may connect to plasmin membrane and other cytoskeletal elements (Buée et al. 2000; Hirokawa et al. 1988). The C-terminal part of Tau (197-441) is called the microtubule binding domain as it is related to the microtubule-associated protein (MAP) function of Tau (Mandelkow et al. 1995; Buée et al. 2000).

2.2 Multiple binding functions

As an IDP, its flexibility and accessibility allow Tau to have numerous binding partners, including signaling molecules, cytoskeletal elements, membrane lipid and nuclear DNA, which suggest multiple functions of Tau proteins in the cells (Morris et al. 2011).

As first described to initialize the tubulin assembly *in vitro*, the four or three repeated microtubule-binding motifs of Tau protein are well characterized to increase the rate of microtubule polymerization and prevent it depolymerization (Panda et al. 1995). The efficiency in promoting tubulin polymerization is different according to 4R or 3R Tau isoforms. It has been demonstrated that the peptide, ²⁷⁴KVQIINKK²⁸¹ located between R1

and R2, is a binding site with two-fold greater affinity for other repeats for the MTs (Goode & Feinstein 1994; Panda et al. 1995). This R1-R2 inter-region (IR1/2) is specifically expressed in adult Tau with 4R and acts as an adult-specific and high affinity anchor to tether Tau to tubulin (Goode & Feinstein 1994). In addition, the amount of Tau protein binding to MTs could regulate the dynamic of motor proteins like kinesin in the axonal transport, as it has been reported that the distribution level of Tau along the MTs has a proximal-to-distal gradient (Kempf et al. 1996). Lower concentration of Tau can promote the initialization of anterograde transport of cargo whereas higher concentration of Tau at the opposite ends of MTs, close to the synapses, might inhibit kinesin activity and facilitate the discharge of the cargo from the motor protein, increasing the efficiency of axonal transport (Dixit et al. 2008).

The stabilization of MTs and regulation of axonal transport are thought to be important roles of Tau in physiological situations. However, the knock-down of Tau by siRNA in primary neuron culture does not decrease the number of MTs or their polymerization state (Qiang et al. 2006), neither the axonal transport (Vossel et al. 2010), suggesting other MAPs might take over Tau function in stabilization of MTs. In addition, Tau is able to bind to and bundle actin filaments, which is mediated by its PRD and MTBD (Figure 21) (Fulga et al. 2007; He et al. 2009). The interaction between Tau and actin filaments may result in microtubule interconnecting with the other cytoskeletal component so as to restrict the flexibility of microtubule in axons (Matus 1994).

In addition, Tau can mediate signaling pathway by working as a scaffold protein (Figure 21), for example, to tether the Fyn kinase. In the absence of Tau protein, Fyn can no longer traffic into postsynaptic sites in dendrites (Ittner et al. 2010). In details, Tau is able to interact with the SH3 domain of Fyn kinase, which preferentially recognizes and binds to a Proline-rich motif 'PXXP' (P refers to Proline residue and X is any other amino acid), and the peptide ²³¹TPPKSPS²³⁷ in Tau match with this consensus sequence (Lee et al. 1998).

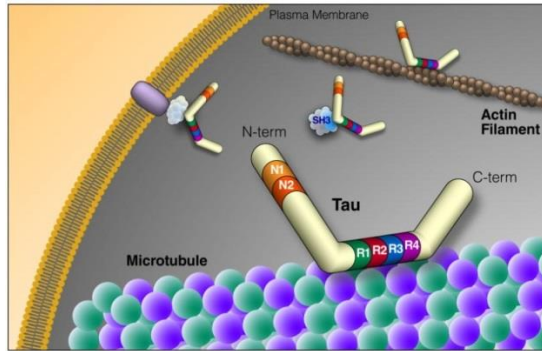


Figure 21: The multiple functions of Tau. In neurons, Tau has numerous binding partners, including MTs, actin filaments and Fyn kinase whose SH3 domain is illustrated to associate with Tau. Hence, in addition to bundle and maintain cytoskeletal proteins, Tau acts also as scaffold protein to carry out the signaling transduction (Morris et al. 2011).

Phospholipase C- γ (PLC- γ), the most abundant PLC isoform in brain cytosol, is also described as Tau binding partner. As Fyn kinase, PLC- γ possesses also a SH3 domain to interact specifically with the Proline-rich domain of Tau. Then, the Tau-mediated activation of PLC- γ hydrolyzes membrane phosphatidylinositol 4,5-bisphosphate (PIP₂) to generate intracellular messengers (Hwang et al. 1996). Another function as an enzyme inhibitor has been also been described. Tau is able to bind to and inhibit the tubulin-deacetylase, histone deacetylase 6 (HDAC6), consequently increasing tubulin acetylation which may regulate indirectly microtubule stabilization (Perez et al. 2009).

In addition to multiple cytosolic functions, Tau protein has been implicated in chromosome stability through interaction with DNA in nucleus (Rossi et al. 2008). It is thus suggested that Tau might act as DNA protector in neurons. Tau can bind to DNA in nucleus in response to heat shock (HS) or oxidative stress to facilitate DNA repair (Sultan et al. 2011). The HS-induced DNA damage can be decreased after the overexpression of human Tau in cells, reversely, more damages of DNA are observed in Tau-knockout neurons culture (Sultan et al. 2011). Recently, the Tau-DNA interaction has been elucidated by nuclear magnetic resonance spectroscopy (NMR) (Qi et al. 2015). Multiple sites along Tau protein, mainly in Proline-rich domain and R2 repeat motif, effectively bind to oligonucleotides *in vitro*. The phosphorylation of Tau at multiple AD-related sites abolishes the *in vitro* interaction with oligonucleotides, suggesting that pathological phosphorylation in AD could disrupt the physiological function of Tau in DNA binding (Qi et al. 2015).

Part 2. The aggregation of neuronal Tau protein

Tau protein in Alzheimer's brain is observed with a typical form described as PHFs with the appearance of α helical superstructure (Figure 22, A). PHFs will further assemble into NFTs which are toxic and fatal to neurons and considered as a hallmarks of Tauopathies. In 1985, Dr. Brion and his colleagues demonstrated by immunolabelling that the NFTs were constituted of Tau protein (Figure 22) (Brion et al. 1985). All the Tau isoforms containing three or four repeated MTBD can be found in PHFs, in which they are highly phosphorylated (Grundke-Iqbal et al. 1986; Lee et al. 1991).

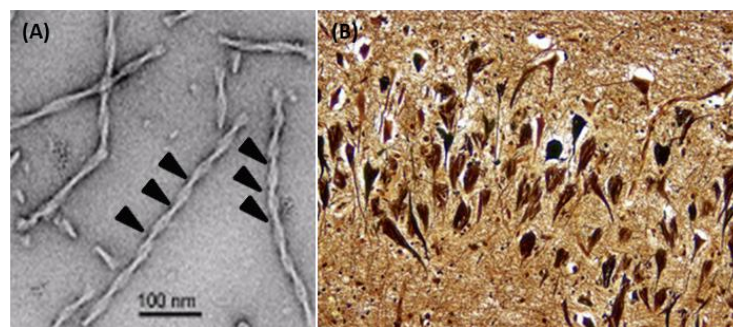


Figure 22: (A) PHFs of Tau protein observed by electron microscope. The filaments are characterized by twisted forms, shown by black arrows. (B) NFTs are deposits of Tau filaments, which are revealed by anti-Tau antibody in human Alzheimer's brain tissue.

As the initialization and development of Tau aggregation is complicated and sophisticated, it is still unclear about the essential sequential event(s) that drive random structure protein into highly morphologic ordered filaments in neurons. In molecular studies, several elements might give us clue(s) to better understand the mechanism(s) of aggregation process. Firstly, Tau possesses several intrinsic events, for example covalent bond of sulfhydryl groups (-SH) and/or hydrophobic peptides, to induce its dimerization and/or polymerization (Schweers et al. 1995; von Bergen et al. 2000). Second, truncation, genetic mutation and post-translational modification such as phosphorylation can be also important event(s) in Tau aggregation process (Goedert et al. 2010). In addition, extra event(s) like polyanionic agent(s) or scaffold protein might be essential to initialize the aggregation. These events include local charge modulation and/or conformational-changes, consistently with

the features observed for other prion-like protein aggregation mechanisms (Goedert et al. 2010).

1. Aggregation nuclei

There are two C residues (C^{291} and C^{322} , located respectively in R2 and R3) in Tau sequence can form intramolecular or intermolecular disulfide bridges by an oxidation process of their sulfhydryl ($-SH$) groups (Figure 23, A). The intermolecular bridge formation mediates Tau dimerization, which might act as a seed of aggregation (Schweers et al. 1995) (Figure 23, B).

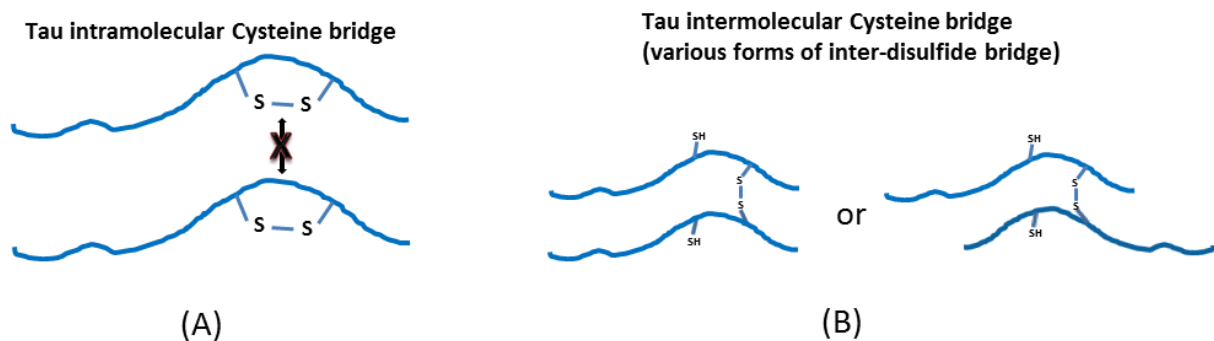


Figure 23: The intramolecular or intermolecular disulfide bond of Tau. (A) Two C residues, present in full-length Tau molecule, can form an intramolecular disulfide bridge via C^{291} and C^{322} , which prevents Tau molecule from forming dimers. (B) The intermolecular Cysteine bridge via C^{291} and/or C^{322} leads to various Tau dimer forms which are proposed to act as seed of the aggregation process.

It is reported that the covalent binding via C^{291} and/or C^{322} is essential and act as a seed for initialization of Tau polymerization (Bhattacharya et al. 2001). There might be however other pathways of aggregation. For example, a mutated Tau fragment, Tau[208-324] with both C residues mutated into A residues, is still able to assemble into fibers *in vitro* (Huvent et al. 2014). Therefore, covalent binding of C residues is not strictly required, at least for Tau[208-324], to initialize aggregation.

In fact, Tau primary sequence contains only about 15% of hydrophobic residues, but an excess of positively charged amino acids resulting in a pI value of 8 to 10 depending of the isoforms, explaining its disorder and highly soluble characters (Uversky et al. 2000). However, two short hydrophobic sequences in the MTBD have been highlighted that are sufficient to

drive soluble Tau into aggregation process in some circumstances. They are two hexapeptides, $^{275}\text{VQIINK}^{280}$ and $^{306}\text{VQIVYK}^{311}$ called as PHF6* peptide and PHF6 peptide, respectively (von Bergen et al. 2000). Both of them are located 11 amino acids away at the N-terminal side of C residues in R2 and R3 of full-length Tau, called htau40 (Figure 24). In particular, PHF6 peptide $^{306}\text{VQIVYK}^{311}$ has been demonstrated as core nucleus of aggregation because Proline-scanning mutagenesis in this hexapeptide significantly interrupts the process of Tau aggregation. Moreover all constructs containing this PHF6 are enable to rapidly aggregate (von Bergen et al. 2000).

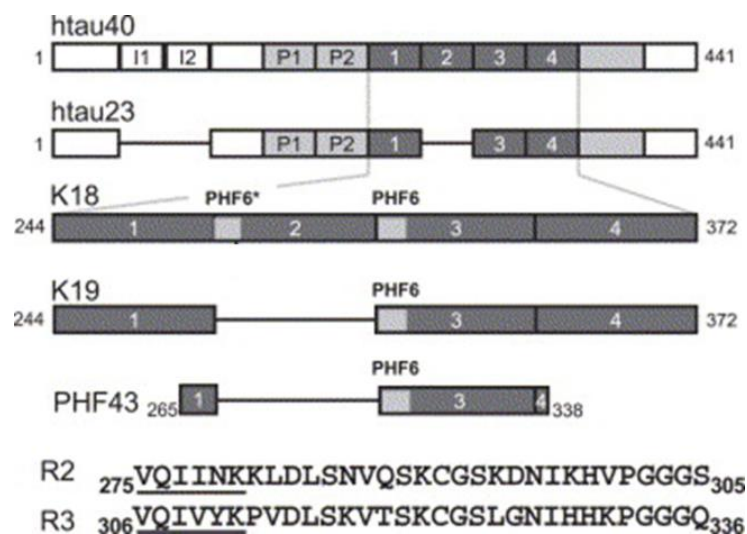


Figure 24: Two isoforms and derived constructs of Tau used over the years in various projects. The longest sequence of Tau in human central nervous system, called htau40 or 2NR4, contains 441 residues. The shortest isoform, htau23 or 0N3R, which lacks the N-terminal insert sequences, as well as the second repeat region, due to alternative splicing of Tau gene. Two constructs, K18 and K19, are derived from htau40 and htau23, containing only the MTBDs, including both of PHF6* ($\text{V}^{275}\text{-K}^{280}$) and PHF6 ($\text{V}^{305}\text{-K}^{311}$) or only PHF6, respectively. PHF sequences are underlined in the amino acid sequence at the beginning of R2 and R3. The peptide PHF43 can be obtained by the proteolysis of K19 by endoprotease. The residue numbering of isoforms and constructs refers to the longest isoform of 441 residues (Von Bergen et al. 2005).

In addition, fragment PHF43, prepared by proteolytic degradation of htau23 (Figure 24), containing only PHF6 and adjacent R3, shows a high potential to aggregate into fibrous structures with β -sheet conformation (Von Bergen et al. 2005). PHF6 peptide within PHF43 (Figure 24) construct has been demonstrated as a core motif to interact with others Tau fragments or isoforms leading into aggregation by forming β -sheet-like interaction (von

Bergen et al. 2000). Moreover, sonicated PHF43 aggregates can work as seeds resulting in htau43 to elongate into *bona fide* PHFs (von Bergen et al. 2000).

Like the PHF6 peptide, the PHF6* peptide has been demonstrated to serve as seed or core nucleus of the aggregation mechanism (Von Bergen et al. 2005), and other minimal fibrillation domains have been also identified in *in vitro* assays, such as peptides 317-335, 391-407 (Pérez et al. 2001) and 314-320 (Abraha et al. 2000), all located in the MTBD, being able to trigger full-length Tau polymerization. In contrast, the acidic N-terminus of full-length Tau cannot be assembled *in vitro* alone, and even decreases the assemble ability in Tau aggregation process (Pérez et al. 2001). Similarly, the C-terminus domain has been suggested to inhibit the assemble process which could be however reversely altered by phosphorylation at S^{396/404} or truncation at various sites from S³²⁰ to the end of the molecule (Abraha et al. 2000).

In PHFs, most of Tau protein adopts an ordered β -sheet structure that is the structural feature shared with other type of disordered proteins in aggregation-related pathologies, such as α -synuclein in Parkinson's disease (PD), islet amyloid polypeptide in type II diabetes and β -Amyloid peptides in AD (Chiti & Dobson 2006).

Circular Dichroism (CD) spectroscopy, Fourier Transform Infrared (FTIR) spectroscopy and X-ray diffraction have been used to detect such β -sheet structure in various forms of Tau aggregates (Von Bergen et al. 2005). A conformation transition is for example observed for PHF43 (Figure 24) by CD, from a disorder structure to an oriented β -sheet structure in the process of aggregation (von Bergen et al. 2000). These techniques simply give an average view of the conformation. In earlier experiments performed with larger constructs or full-length PHFs, for example, the secondary structural transition along the aggregation process was not be detected by CD (Schweers et al. 1994).

NMR spectroscopy, on the other hand, can be used to characterize local secondary structure. As liquid NMR spectroscopy is sensible with the chemical environment of atoms, we can compare the deviation of experimental C α chemical shift with that of random values to predict the secondary structure, even the propensity of local β -strand conformation in full-length Tau can be defined according to the deviation of C α chemical shifts. As shown below, the NMR analysis indicates several peptidic stretches with a propensity to adopt a β -

strand conformation (Figure 25, A and B illustrated by yellow arrow in Tau sequence) (Marco D. Mukrasch et al. 2009). In particular, $^{274}\text{K-L}^{284}$ and $^{305}\text{S-D}^{315}$, included in the sequences of PHF6 and PHF6*, strongly suggest the propensity of β -strand conformation transition in Tau nuclei of aggregation (Marco D. Mukrasch et al. 2009).

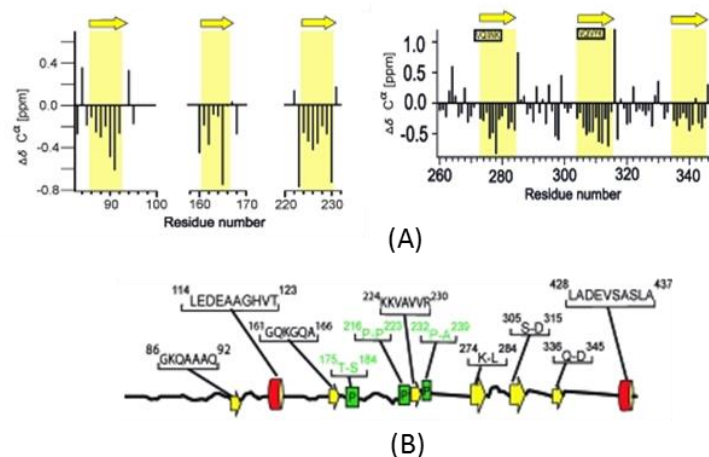


Figure 25: The prediction of secondary structure propensity in full-length Tau by solution NMR spectroscopy. (A) The relative negative C α chemical shifts compared to that of random coil values reveal several continuous stretches with preferential β -strand conformation in solution. The relative C α chemical shift values are given as function of residue number of full-length Tau. (B) The prediction of secondary structure propensity in Tau sequence. Two peptides in red, $^{114}\text{LEDEAAGHVT}^{123}$, and $^{428}\text{LADEVASLASLA}^{437}$, are suggested as α -helical, three short peptides in green squares are represented for polyproline II and six yellow arrows show the regions where over 17% of conformer population has β -structure propensity (Marco D. Mukrasch et al. 2009).

Solid-state NMR (ssNMR) spectroscopy has been used to investigate the core of PHFs assembled *in vitro* from Tau fragment K19 (the sequence of K19 shown in Figure 24). The rigid core of the K19 fibrils is built up by intermolecular stacking of C 322 -C 322 K19 dimers in a parallel, in-register manner (Figure 26, A and B) (Daebel et al. 2012). The β 3-strand (Figure 26, A and B) located in the sequence between V 306 and S 324 sequence, is shown to have two sets of resonances in the spectra, suggesting two possible conformations of cysteine disulfide binding in K19 dimers and two possible arrangements of the β -strand (Figure 26, B) (Daebel et al. 2012).

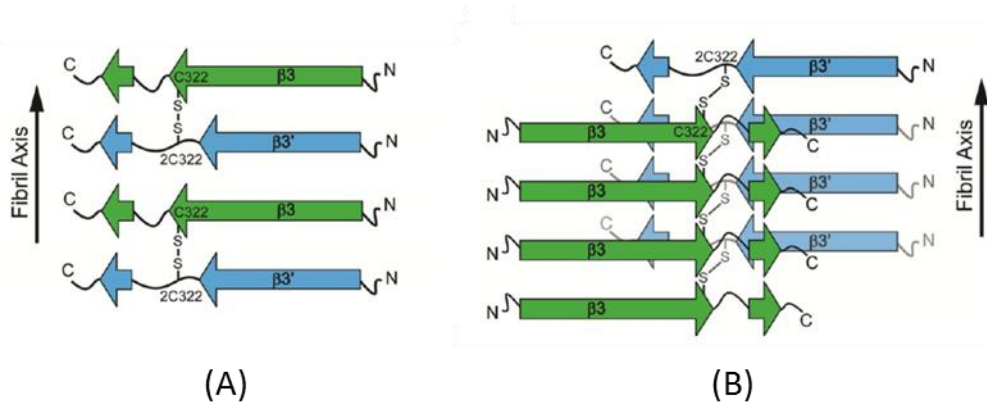


Figure 26: Two models of Tau assembly in fibrils based on ssNMR study of aggregates of the K19 fragment of Tau. (A) Model 1: K19-dimer is formed by parallel β -strands from 2 molecules and perpendicular to the fibril axis, assembled by disulfide bonds parallel to the fibril axis. (B) Model 2: K19-dimer is formed by anti-parallel β -strands from 2 molecules and perpendicular to the fibril axis, assembled by disulfide bonds disposed across the fibril axis (Daebel et al. 2012).

Besides physical measurements, some so-called conformational antibodies, such as Alz50 and MC-1, are used to get insight into structural changes. They recognize Tau in abnormal conformations, in particular the folded conformation of the aggregates, recognizing regions outside the nucleation domains (Jicha et al. 1997). Although these antibodies are widely used to recognize Tau in a potential pathological conformation, it is still unclear the exact nature of their epitopes on Tau.

2. Aggregation cofactors

Because Tau is soluble and flexible in solution, recombinant Tau *in vitro* aggregation has to be stimulated by sulphated glycosaminoglycans as polyanionic cofactors, like heparin or heparin sulfate. In addition, the heparin or heparin sulfate is found able to bind to Tau protein, and induce and accelerate the assembly of Tau isoforms and variable constructs into filaments with similar morphological characteristics as the PHFs extracted from AD brain (Goedert et al. 1996; Pérez et al. 1996). The heparin sulfate has been observed intracellularly accumulated in the neurons during the development of AD (Snow et al. 1990; Goedert et al. 1996). Heparin sulfate proteoglycans (HSPGs) has been recently reported to mediate the

uptake of extracellular Tau fibrils in cells, regulating the trans-cellular aggregate propagation, suggesting a possible role *in vivo* of the HSPGs in the process of Tau pathology propagation in the brain (Holmes et al. 2013). Recent studies show that 3-O-sulphated heparin sulphates can bind to Tau in a chaperone manner, and this binding might induce a conformational changes in Tau, leading to abnormal phosphorylation by different kinases in neurons (Sepulveda-Diaz et al. 2015). Altogether, it is suggested that HSPGs might be involved in Tauopathies, and Tau/HSPGs binding can be also a therapeutic target in neurodegeneration diseases (Holmes et al. 2013).

A liquid-NMR study on Tau/heparin interaction shows that the binding of heparin in the positively charged regions flanking the MTBDs might induce several β -strand structure in Tau sequence, proposing that the heparin molecules not only play a role in charge neutralization but also in conformational perturbation (Sibille et al. 2006). Therefore, intramolecular long range self-contacts and local secondary structure perturbations could both result in a higher propensity for aggregation. On the other hand, there are other polyanionic aggregation cofactors studied in Tau aggregation such as fatty acid like arachidonic acid and docosahexaenoic acid (Wilson & Binder 1997; Gamblin et al. 2000), tRNA (Kampers et al. 1996) and polyglutamic acid.

In addition, some proteins have an ability to trigger the aggregation process of Tau. This is the case of Tau binding to the 14-3-3 protein, a scaffold protein involved in numerous processes in the cells. The 14-3-3 protein is found by immunodetection to be present in NFTs (Umahara et al. 2004). Moreover, 14-3-3 enables Tau association *in vitro* for both phosphorylated Tau and nonphosphorylated Tau. 14-3-3 promotes aggregation in an incubation time-dependent manner, from amorphous aggregates to PHF-like filaments and laterally associated filaments, which are similar with all ultrastructures observed in AD brain (Qureshi et al. 2013). It is thus suggested that 14-3-3 may play an important role in facilitating Tau aggregation in cells.

FKBP52 (FK506-binding protein) is another example of Tau co-factor of aggregation. FKBP52 is well-known as effector of immunosuppressive drugs including FK506 and rapamycin. FKBP52 is highly expressed in brain, and it has been proposed that FKBP52 binds Tau protein with increasing affinity *in vivo* and *in vitro*, depending on Tau phosphorylation

level (Chambraud et al. 2010). This interaction is proposed to be involved in the process of Tauopathy development. Firstly, FKBP52 is antagonistic towards Tau-induced tubulin polymerization. Second, FKBP52 might induce TauP301L oligomers formation *in vitro* (Giustiniani et al. 2014). Additionally, in the transgenic zebrafish model, FKBP52 knockdown significantly reduces the pathological phenotypes associated with the transgenic TauP301L (Giustiniani et al. 2014). FKBP52 has a peptidyl-prolyl *cis/trans* isomerase (PPIases) activity. Other PPIases like FKBP51, FKBP12 and Pin1 have been also shown to interact with Tau and to regulate Tau biological functions as well as its pathogenesis (Blair et al. 2015).

3. Mutation modulated aggregation

Besides structural/molecular factors and other extrinsic co-factors, the genetic mutation in 3R or 4R Tau sequence is also a factor significantly affecting its physiological functions and aggregation processes. Many of Tau mutations bring out different pathological states of Tau. In frontotemporal dementia with Parkinsonism linked to chromosome 17 (FTDP-17), a number of mutations have been identified, such as P301L, a deletion Δ K280 and intronic mutations, which can alter the population ratio of 3R and 4R Tau isoforms (von Bergen et al. 2000; Fischer et al. 2007). Other mutants, R5L and G303V are found in Progressive Supranuclear Palsy (PSP) disease and L266V and G272V in Pick's disease (Table 1 : Impacts of some Tau mutations associated with neurodegenerative diseases (Fontaine et al. 2015)).

Table 1 : Impacts of some Tau mutations associated with neurodegenerative diseases (Fontaine et al. 2015)

Mutation	Impact on phosphorylation and aggregation	Associated Tauopathies	References
R5L	Increases Tau aggregation;	PSP	(Chang et al. 2012)
R406W	Increases Tau aggregation; reduces Tau binding to MTs; Increase pS202 level;	FTDP-17	(Chang et al. 2012; Chris Gamblin et al. 2000; Barghorn et al. 2000)
P301L	Increases Tau aggregation; reduces Tau binding to MTs;	FTDP-17	(Chang et al. 2012; Nacharaju et al. 1999; Chris Gamblin et al. 2000; Barghorn et al. 2000)

	Increase pS202 level;		
P301S	Increases Tau aggregation; reduces Tau binding to MTs;	FTDP-17	(Chris Gamblin et al. 2000; Lossos et al. 2003; Morris et al. 2001; Huey et al. 2006)
G272V	Increases Tau aggregation; reduces Tau binding to MTs; Increase pS202 level;	FTDP-17 Pick's disease	(Chang et al. 2012; Chris Gamblin et al. 2000; Barghorn et al. 2000)
Δ K280	Increases Tau aggregation; reduces Tau binding to MTs;	FTDP-17	(Barghorn et al. 2000; Vogelsberg-Ragaglia et al. 2000; Von Bergen et al. 2001)
G335V	Increases Tau aggregation; reduces Tau binding to MTs;	FTDP-17	(Neumann et al. 2005)
N279K	Increases Tau aggregation; reduces binding of 4R Tau, but not 3R Tau to MTs;	FTDP-17	(Barghorn et al. 2000; Clark et al. 1998; Tsuboi et al. 2002)
Δ N296	Increases Tau aggregation; reduces Tau binding to MTs;	Parkinson's disease, PSP	(Bagnoli et al. 2004)
L266V	Increases Tau aggregation; reduces Tau binding to MTs;	Pick's disease	(Hogg et al. 2003; Kobayashi et al. 2002)

About 20% of cases in inherited FTDP-17 involve mutations in the Tau protein (Rademakers et al. 2004). These mutated Tau proteins are found in the neurofibrillary deposits in young-age onset Tauopathies, strongly suggesting that these Tau variants are related to the pathological aspects, such as weakening the binding to MTs and accelerating the Tau aggregation process (Goedert 2005). For example, the FTDP mutations like G272V, N279K, R406W, P301L and Δ K280 (see the table above) cause a moderate decrease in microtubule interactions and stabilization, together with an enhanced rate in PHFs formation (Barghorn et al. 2000). Moreover, NMR studies of K18 (see Figure 24), K18 Δ K280 and K18 P301L suggest that missense mutations might increase the β -structure content in core nucleation regions containing PHF* and PHF peptides, and reduce their abilities to bind to MTs (Fischer et al. 2007). Other dysfunctions of mutated Tau have also been described, for example, kinesin protein shows, in *in vitro* assays, a slower rate of translocation along the

MTs assembled by Δ N296, P301L, R406W 4R-Tau mutations, and consequently, the deregulation on kinesin-motor-transport might directly or indirectly result in neuron death in Tauopathies (Yu et al. 2014).

In addition, it is reported that Tau isoforms containing mutations such as G272V, V337M, P301L and R406W, have higher phosphorylation levels compared to wild type Tau in *in vitro* phosphorylation assays with rat brain extract (Alonso et al. 2004). G272V, P301L, R406W mutations have been additionally suggested to be more efficiently phosphorylated by CDK5, than wild type Tau (Han et al. 2009). In spite of different effects on specific-phosphorylation sites, most of Tau mutations display a four-fold increase in S²⁰² phosphorylation level, and this increasing pS²⁰² has an influence on inhibiting the microtubule assembly-promoting activity of Tau *in vitro* (Han et al. 2009). Tau mutants are thus suggested to be more favorable substrate for some kinases although the molecular mechanism(s) that could explain this observation remain to be elucidated.

Tau P301L is a mutation quite commonly used in transgenic mouse animal models. Its overexpression in mice results in hyperphosphorylation of Tau at multiple pathological sites and formation of filaments at young age (Sahara et al. 2002). The dysfunctions of TauP301L are directly linked to several pathological phenotypes, like motor and behavioral deficit (Lewis et al. 2000). Moreover, neuronal lesions, such as development of NFTs, occur in an age- and gene-dose-dependent manner in transgenic mice, imitating well the features of human Tauopathies (Sahara et al. 2002). This offers an appropriate animal model to investigate NFTs-related pathogenesis. Another identified Tau mutation P301S has been used in transgenic mice, resulting in abundant filaments composed of hyperphosphorylated Tau proteins detected in neurons of brain and spinal cord. pS²¹⁴ has been mentioned to be excluded from the P301S phosphorylation sites and activated MAP kinases can extensively co-localize with abnormal phosphorylated P301S Tau in neurons of transgenic mice (Allen et al. 2002).

4. 'Hyperphosphorylation' model in the *in vitro* and *in vivo* studies

The pattern of hyperphosphorylation is made up by a combination of specific phosphorylated sites correlated with the severity of neuronal cytopathology in AD. By mass spectrometry analysis, over 20 PHF-related phosphorylation sites have been reported by mass spectrometry studies (Maho Morishima-Kawashima et al. 1995; Hanger et al. 2002). In addition, variable antibodies have been developed, determining specific phosphorylation site(s) involved in abnormal phosphorylation (Grundke-Iqbal et al. 1986; Biernat et al. 1992; Bramblett et al. 1993; M Goedert et al. 1993; Augustinack et al. 2002). For example, TG3 (against pT²³¹), pS²⁶² and pT¹⁵³ are immunopositive in pre-neurofibrillary tangle (pNFT) in neurons but do not appear to be present in filaments, while pT^{175/181}, 12E8 (pS²⁶²/pS³⁵⁶), pS⁴²², pS⁴⁶ and pS²¹⁴ are observed stained in NFTs, and at the late-stage of neurodegeneration, they are dominantly stained with AT8 (pS²⁰² and pT²⁰⁵), AT100 (pT²¹² and pS²¹⁴) and PHF-1 (pS³⁹⁶ and pS⁴⁰⁴) antibodies (Augustinack et al. 2002). Therefore, AT8, AT100 and PHF-1, especially AT8, antibodies are used to detect abnormal phosphorylation (**Figure 27**) (Braak et al. 2006). Others antibodies used to detect pathological Tau, for instance MC1 and Alz50 rather rely on an aberrant conformational change during pathology evolution (Luna-Muñoz et al. 2005; Jicha et al. 1997; Jeganathan et al. 2008).

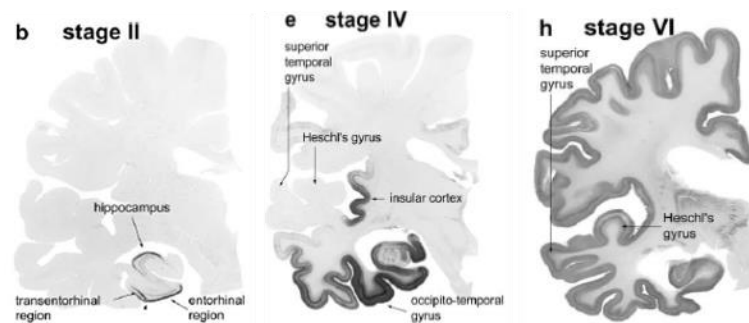


Figure 27: Immuno-labelled-propagation of pathological Tau. The monoclonal antibody AT8 which recognizes the epitope pSer202/pThr205 is used to label the phosphorylated Tau in the development of pathology in AD's brain (Braak et al. 2006).

As Tau phosphorylation level is increased with the evolution of AD, scientists have made a lot of efforts trying to understand the relationship between phosphorylation and Tau aggregation. Tau can be phosphorylated at several sites in physiological circumstances to

regulate polymerization and stabilization of MTs, and other cellular functions (Johnson & Stoothoff 2004; Noble et al. 2013). However, Tau gets increasingly phosphorylated, notably at some pS-P and pT-P sites like pS²⁰²/pT²⁰⁵, pS³⁹⁶/pS⁴⁰⁴, from early onset of pathological cases and remains highly phosphorylated until the fatal fate of the neuron (Augustinack et al. 2002). Several pathological phosphorylated sites have been well-described in AD. These abnormal sites appear in an order manner, from early-stages sites to late-stages phosphorylation. For example, pS²⁶² can be detected in early amorphous, aggregated state of non MTs-associated Tau, and T²³¹ is next getting phosphorylated (Kolarova et al. 2012; Luna-Muñoz et al. 2005). It is then followed by more phosphoepitopes like pS¹⁹⁹, pS²⁰², pT²⁰⁵, pS²⁰⁸ as well as pS³⁹⁶, pS⁴⁰⁴ and pS⁴²² (Porzig et al. 2007; Bramblett et al. 1993; M Goedert et al. 1993).

The highly phosphorylated Tau, modified to a high level at numerous pS/pT-P sites, is often described as abnormally phosphorylation and is code-named hyperphosphorylated Tau. However, the difficulties in the analytical characterization of hyperphosphorylated Tau have rendered the task to give a proper definition of abnormal pathological phosphorylation of Tau difficult. *In vitro* 'hyperphosphorylation' models have been widely used in biochemical studies of Tauopathies, but the corresponding phosphorylation sites are often poorly described. Hyperphosphorylated Tau used in biochemical studies can be purified from brain affected by the disease, from transgenic mice for example, or obtained by phosphorylation of recombinant Tau by rat brain extract or relevant recombinant kinases able to induce abnormal phosphorylation (M Goedert et al. 1993; Bibow et al. 2011).

5. Impact of hyper-phosphorylation on aggregation

Dating back to 1986, Dr. Iqbal and his colleagues demonstrated an abnormal phosphorylation of Tau protein in neurons in AD brain. By immunocytochemistry it was shown that this hyperphosphorylated Tau is an important component in PHFs (Grundke-Iqbal et al. 1986). The density and propagation of NFTs from hippocampus to most of the neocortex are well correlated with the symptoms of the developing dementia (Braak et al. 2006). In addition, it has been proposed that abnormally phosphorylated Tau sequesters normal Tau and other MAPs into oligomers and fibers, preventing its binding to MTs (Iqbal et

al. 2010). The sequestered Tau protein might additionally be assemble into PHFs or SFs in neurons (Iqbal et al. 2009). This property is increasingly considered as a Prion-like phenomenon and might be potentially more toxic than NFTs formation by itself (Iqbal et al. 2013). The hyperphosphorylation is hence considered as an important event in PHFs formation and other Tau pathological studies. It has additionally been found that hyperphosphorylation of Tau can be associated with formation of small oligomeric species, considered as early-stage aggregated species (Iqbal et al. 2013; Tepper et al. 2014). The observation of phospho-Tau containing oligomers in specific brain areas is consistent with the development of functional deficits during Tau pathogenic progression in animal models, suggesting the neurotoxicity of Tau oligomers (Berger et al. 2007).

The link between phosphorylation and aggregation has been explored in a few *in vitro* studies. Tau can be phosphorylated by recombinant expression in insect cells using baculovirus system (Tepper et al. 2014). About 20 phosphorylation sites were identified in this study. This phosphorylated Tau forms fibers *in vitro* but does not aggregate in the insect cells. The fraction of fibers form in the incubated phospho-Tau samples is small and the authors concluded that there is no obvious link between hyperphosphorylation and aggregation (Tepper et al. 2014).

Another study has shown that phosphorylated Tau extracted from AD patient's brain can be aggregated *in vitro*, without the addition of exogenous inducers (Alonso et al. 2001). Moreover, Tau extracted from normal brain or recombinant Tau, phosphorylated *in vitro* by rat brain extracts are able to self-assemble. The authors concluded that a high level of phosphorylation alone is sufficient to cause aggregation (Alonso et al. 2001).

The relationship between phosphorylation and aggregation, although very commonly made, is not so obvious. For example, the aberrant phosphorylation on K-X-G-S motifs (X refers to any amino acid) abolishes the ability of binding to MTs, whereas it also prevents free Tau protein from PHFs formation (Schneider et al. 1999; von Bergen et al. 2000). As S²⁶², S³²⁴ and S³⁵⁶ in KXGS motifs are located in the MTBDs, the phosphorylation *in vitro* at S²⁶², S³²⁴ by the microtubule associated kinase2 (MARK2) and at S²¹⁴ by cAMP-dependent protein kinase (PKA) might disrupt the cysteine-dimerization and inhibit further assembly of Tau into PHFs (Schneider et al. 1999). Besides the KXGS motifs, they are other numerous

phosphorylated sites, notably pS-P and pT-P, showing a weak inhibition of PHFs assembly (Schneider et al. 1999). In contrast, pS¹⁹⁹, pS²⁰⁵, pT²³¹, pS³⁹⁶ and pS⁴⁰⁴, at PRD, generated *in vitro* by GSK3 β make pre-assembled Tau more susceptible to polymerize into large NFTs-like structures, suggesting that hyperphosphorylated Tau is able to promote the oligomers aggregation into irreversible clusters of filaments (Rankin et al. 2005; Rankin et al. 2008).

The hyperphosphorylation is often assumed as an important cause for PHF formation, but the relationship between them is ambiguous and controversial. The question is raised about whether the abnormal phosphorylation is the culprit for Tau aggregation. Could misfolding or conformational changes, or simply change in the electrostatic potential, result in PHFs formation and in further neurodegeneration? Since the mechanisms and functions of Tau hyperphosphorylation in neurons are still unclear, this question remains open since nearly thirty years. Moreover, the number or the level of phosphorylation which could be considered as hyperphosphorylation were never precisely defined neither the minimal pattern of phosphorylation fitting the hyperphosphorylation definition. The responsible kinases that would induce such kind of hyperphosphorylation are also not yet determined.

Part 3. Deregulation of kinases and phosphatases in AD

A large number of post-translational modifications (PTMs) have been described for Tau protein. 63 sites of endogenous Tau were recently identified by mass spectrometry, to be modified by 7 types of PTMs in wild-type mice (Meaghan Morris et al. 2015). PTMs include phosphorylation, acetylation, methylation, ubiquitination, O-linked N-acetylglucosamine (O-GlcNAc) etc. Among these PTMs, phosphorylation is widely studied because its significant impacts on Tau properties, in physiological and pathological conditions. The initial cause(s) of Tau pathology in neurons are still unclear, but aberrant PTMs are certainly responsible for at least part of some changes observed in early stages of the neurodegeneration process.

Both an increased kinase activity and/or a reduced phosphatase activity might result in the hyperphosphorylation of Tau protein in cells. Searching responsible kinases for AD is of interest to find potential therapeutic targets for AD and other neurodegenerative diseases. It has been reported that, by high throughput reverse co-transfection cell-based assay, the protein Tau may be phosphorylated by over 352 human kinases at AD-related specific phosphorylation epitopes (Cavallini et al. 2013). However, the number of relevant kinases in AD is probably smaller (Johnson & Stoothoff 2004).

There are 85 possible targets of phosphorylation sites along full-length Tau sequence, among them, 80 sites of them are S/T residues and 5 sites are Y residues. Recently, 27 phosphorylated sites at S/T/Y residues have been assigned by using mass spectrometry on endogenous Tau from mouse brain. Similarly, phosphorylation has been detected at 26 sites in endogenous Tau of human brain (Meaghan Morris et al. 2015; Funk et al. 2014). Compared to S/T- kinases, Y-kinases are much fewer to regulate Tau phosphorylation, but are also important in its regulation. For example, Fyn kinase, one of Src family kinases, is capable to phosphorylate at Y¹⁸ Tau, inducing the dysfunction of Tau protein as well as synaptic and cognitive impairment in transgenic mouse model of AD (Lee et al. 2004; Chin et al. 2005).

Little is known about specific impact(s) of each phosphorylation site on physiological or pathological functions of Tau protein. The role of Tau kinases still need to be.

1. AD-related kinases

The S/T-kinases are divided into the Proline-directed and the non-Proline-directed kinases. The S or T residues followed by a P residue constitute the S/T-P epitope recognized by Proline-directed kinases, such as Glycogen synthase kinase 3 β (GSK3 β), Cyclin-dependent kinase 5 (CDK5) and extracellular signal-regulated kinase 1/2 (ERK1/2). These kinases are described as AD-related kinases because their target S/T-P motifs are mainly found in the Proline-rich domain and C-terminal region of Tau protein where most of the pathological phosphorylation sites in Tau sequence are described (Mazanetz & Fischer 2007).

GSK3 β kinase was found in the late 1970s as an enzyme involved in the control of glycogen metabolism (Cohen 1979). It is highly expressed in the brain and involved in several central nervous system (CNS) diseases, like ischemic stroke, bipolar disorders, Huntington's disease and AD (Cohen & Goedert 2004; Bhat et al. 2004). In the amyloid pathway in AD, GSK3 kinase is able to phosphorylate T⁶⁶⁸ in the cytoplasmic portion of APP, which accelerates A β ₄₀ and A β ₄₂ generation in mouse brain (Aplin et al. 1996; Jaworski et al. 2011). A specific inhibition of cellular GSK3 β by lithium chloride can successfully reduce of 40-50% the A β levels in the brain of transgenic mice models (Ryder et al. 2003). Lithium chloride can reduce GSK3 β -induced phosphorylation level of protein Tau as well (Hong et al. 1997; Lovestone et al. 1999).

GSK3 β is known as Tau Protein Kinase I (TPKI), capable to generate *in vitro* PHF epitopes which are undetectable in normal brain. CDK5, known as Tau Protein Kinase II (TPKII), is able to accelerate Tau phosphorylation by GSK3 β , suggesting that the priming phosphorylation by CDK5 might indirectly regulate the formation of PHF epitopes (Ishiguro et al. 1993). Therefore, GSK3 β and CDK5 are considered as critical candidates for Tau hyperphosphorylation, converting the normal Tau into PHF-like state.

Priming phosphorylation are able to enhance the activity of GSK3 β toward Tau protein, for example, pS²¹⁴ by PKA or pT²¹² by dual-specificity tyrosine phosphorylated and regulated kinase 1A (DYRK1A) are shown to enhance sequentially the activity of GSK3 β on Tau at specific phosphorylation sites (Woods et al. 2001; Leroy et al. 2010). However, a NMR study

shows that GSK3 β alone can also lead to *in vitro* Tau phosphorylation at S³⁹⁶, S⁴⁰⁰ and S⁴⁰⁴ without priming, while the priming phosphorylation, pS²¹⁴ by PKA, enhances catalytic efficacy of GSK3 β , achieving additional phosphorylation sites on Tau (Leroy et al. 2010).

However, it is still a matter of debate whether the inhibition of GSK3 is able to reduce the Tau-induced neurodegeneration in animal models. There is no more convincing evidence neither to indicate that GSK3 kinase activity is increased in Tauopathies nor that the overexpression of GSK3 directly leads to the formation of Tau filaments in transgenic mouse models (Cohen & Goedert 2004).

Like GSK3 kinase, CDK5 is required for the cell survival and neuronal development (Gilmore et al. 1998; Grant et al. 2001). However, the overexpression of CDK5 and its activator p25 in double transgenic mice models might lead to Tau hyperphosphorylation in the brain, inducing Tau aggregation in pre-tangles neurons (Noble et al. 2003). Moreover, immunolabeling assays reveal that CDK5 and/or GSK3 kinases colocalize with Tau protein in abnormal conformation immunopositive for MC1 antibodies. Other immunohistochemical studies also suggest the association of NFTs with CDK5 and/or GSK3 kinases in neurons (Yamaguchi et al. 1996; Shiurba et al. 1996; Noble et al. 2003). These findings indicate that Tau might be continuously phosphorylated by kinases even after aggregation, but mechanism(s) about the phosphorylation of aggregated Tau by associated kinases are far from clear.

The fact that CDK5 is highly activated in AD is thought to result from its association with the p25 subunit, a degradation product of the p35 subunit. The p35 subunit is converted to p25 by the calcium-dependent calpain protease, and elevated cellular calcium level in AD case would trigger the proteolytic cleavage procedure from p35 to p25 so that the activity of CDK5 will be upregulated by the accumulation of p25 subunit (Kusakawa et al. 2000; Lee et al. 2000). A recent study reveals that p25 preferably binds to GSK3 β over CDK5 and also enhances GSK3 β activity towards Tau hyperphosphorylation in p25-transfected neuronal cells (Chow et al. 2014).

PKA kinase is not a Proline-directed kinase, but reported to be related to AD (Carlyle et al. 2014). The activity of PKA on Tau protein is pertinent to hyperphosphorylation as it gives a prior phosphorylation which will enhance furthermore the hyperphosphorylation either by

ERK family kinases or by GSK3 at several pathological sites (Blanchard et al. 1994; Shi et al. 2004; Leroy et al. 2010). There are 6 predominant phosphorylated sites identified by NMR spectroscopy, after *in vitro* incubation with recombinant PKA kinase: pS²¹⁴, pS²⁰⁸, pS³²⁴, pS⁴¹⁶, pS⁴⁰⁹ and pS³⁵⁶ (Isabelle Landrieu et al. 2006). Among them, pS²¹⁴ is the preferential site (Isabelle Landrieu et al. 2006). pS²¹⁴, as also reported for pS²⁶², decreases the interaction strength of Tau with MTs over 10-folds (Sillen et al. 2007). However, pS²¹⁴ prevents Tau against aggregation into PHF states (Schneider et al. 1999; Sironi et al. 1998).

Another non-Proline-directed kinase, the MARK2 can phosphorylate microtubule-associated protein Tau, as well as MAP2 and MAP4 on their microtubule-binding domains (Illenberger et al. 1996). The overexpression of MARK2 in cells results in Tau hyperphosphorylation at S residues in 'KXGS' motifs which are mostly located in MTBDs of Tau (Drewes et al. 1997). Multiple phospho-sites by MARK2 have been recently identified in *in vitro*, by using NMR analysis: pS²⁶², pS³⁵⁶ and pS³²⁴, which might interfere with Tau/microtubule association (Drewes et al. 1997; Schwalbe et al. 2013).

The type II Ca²⁺/calmodulin-dependent protein kinase (CaMKII) can be regulated by its autophosphorylation and it is shown that a low phosphatase activity is already sufficient to deregulate CaMKII (Bennecib et al. 2001). In presence of inhibitors of protein phosphatases (PPs) such as PP2A and PP-1 *in vitro*, phosphorylation of Tau is observed at S²⁶² and S³⁵⁶ (Bennecib et al. 2001).

Another kinase DYRK1A is also considered to play a role in Tau-induced neurodegenerative diseases. DYRK1A is encoded by a gene located within the Down Syndrome Critical Region (DSCR) on chromosome 21 and is reported as involved in the development of the pathology but also in early-onset AD associated with Down Syndrome (Arron et al. 2006; Frost et al. 2011).

Kinases may have synergistic effects to create Tau phosphorylation pattern observed in AD brain. The combination of activated PKA, CDK5, CaMKII and GSK3 in brain slices of adult rats produces AD-like phosphorylation of Tau protein with phosphorylation detected at S^{198/199/202}, S²¹⁴, T²³¹/S²³⁵, S²⁶², S^{396/404} and S⁴²² by anti-phospho-sites antibodies (Sengupta et al. 2006). This pattern of Tau phosphorylation, observed in brain slices, reduces significantly its biological activity of MTs binding and increases the sequestration of normal Tau. It is

therefore proposed that Tau needs to be phosphorylated sequentially by a combination of kinases to behave similarly to AD-phosphorylated Tau (Sengupta et al. 2006).

2. AD-related phosphatases

In addition to the up-regulation of kinases, the loss of biological functions of protein phosphatases activity, like PP1, PP2A, PP2B and PP5 phosphatases, is also thought to cause aberrant phosphorylation of Tau protein in AD cases. These four phosphatases are able to dephosphorylate Tau *in vitro* with different efficiency at multiple pathological sites: pS¹⁹⁹, pS²⁰², pT²⁰⁵, pT²¹², pS²¹⁴, pS²³⁵, pS²⁶², pS³⁹⁶, pS⁴⁰⁴ and pS⁴⁰⁹. Among these four phosphatases, PP2A is the most efficient phosphatase toward phosphorylated Tau, representing about 71% of total Tau phosphatase activity in human brain (Liu et al. 2005). Each phosphatase seems to have their favorite sites of dephosphorylation, for example, pS¹⁹⁹ and pS²⁰² are most efficiently dephosphorylated by PP2A and PP5, whereas pS³⁹⁶ and pS⁴⁰⁴ can be efficiently dephosphorylated by PP2B (Liu et al. 2005). The activity of PP2A in AD brain is diminished, suggesting an impact of PP2A downregulation on Tau phosphorylation in AD brain. For example, anesthesia-induced hypothermia inhibits PP2A activity, resulting in the increase of Tau phosphorylation in mouse models (Whittington et al. 2014).

PP2A is a heterodimeric or heterotrimeric complex composed by two or three subunits: the catalytic C subunit, scaffolding A subunit and regulatory B subunit which is not present in the heterodimer. The presence of the regulatory B subunit improves the efficiency of PP2A towards certain substrates, such as Tau protein for example (Figure 28, A) (Sontag et al. 2012; Xu et al. 2008). The PP2A/B α subunit facilitates the dephosphorylation process of GSK3-mediated phosphorylated Tau. The heterodimeric PP2A without regulatory B subunit exhibits a reduced ability in Tau dephosphorylation assay (Xu et al. 2008).

PP2A holoenzyme (heterotrimeric complex) can directly interact with Tau and MAP2 on the binding sequence, 'RTPPKSP', but not with the equivalent phosphorylated sequence, 'RpTPPKSP' (Figure 28, B and C) (Sontag & Sontag 2014). This sequence is also the binding target of Fyn kinase. It is thus possible that Fyn kinase competes with PP2A holoenzyme to interact with Tau or MAP2. As the deregulation of Fyn-Tau interaction has been described in

some neurodegeneration processes (Lee et al. 2004; Bhaskar et al. 2005; Ittner et al. 2010), an overexpression of Fyn kinase might result in the downregulation of PP2A holoenzyme-mediated Tau dephosphorylation, stimulating the aberrant phosphorylation process of Tau (Figure 28, C).

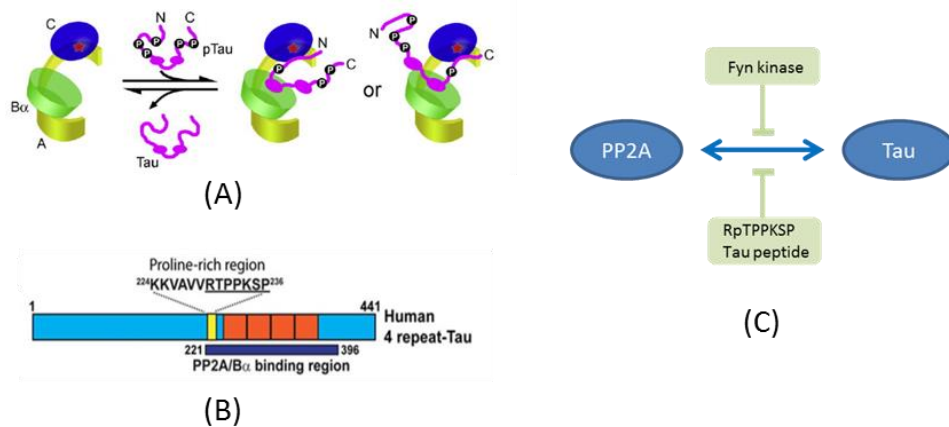


Figure 28: Dephosphorylation of Tau protein by PP2A phosphatase. (A) The A subunit of PP2A works as a scaffold to adapt two other subunits; the B α subunit regulates the interaction of phosphatase with phospho-Tau; the C subunit exerts its catalytic activity to dephosphorylate Tau (B) Along full-length human Tau sequence, fragment [221-396] is the binding region of PP2A holoenzyme containing B α subunit. A ‘RTPPKSP’ peptide is reported as PP2A binding site and is found in the Proline-rich region of Tau protein, corresponding to residues [230-237]. (C) The interaction of PP2A and Tau can be regulated by various events, for example competition with Fyn kinase or ‘RpTPPKSP’ Tau peptide (Sontag et al. 2012; Xu et al. 2008).

It was shown using NMR spectroscopy that the phosphorylation of Tau can regulate the activity of PP2A (Figure 29) (Landrieu et al. 2011). The phosphorylation at T²³¹ can decrease the rate of dephosphorylation at pS²⁰² and pT²⁰⁵. A mutated phospho-Tau, with T²³¹ replaced by A residue, is more efficiently dephosphorylated at the AT8 epitope compare to wild type phospho-Tau (Figure 29, compare A and C). This mechanism of regulation could be due to the docking of PP2A in the ‘RT²³¹PKKSP’ Tau sequence while the equivalent phosphorylated RpT₂₃₁PKKSP’ is hardly binding to PP2A holoenzyme (Figure 28, B) (Sontag et al. 2012; Xu et al. 2008). Therefore a phosphorylation at T²³¹, described as an early event in the AD development, could decrease the efficiency of PP2A activity at the AT8 epitope, leading to its accumulation at later stages of the disease (Landrieu et al. 2011).

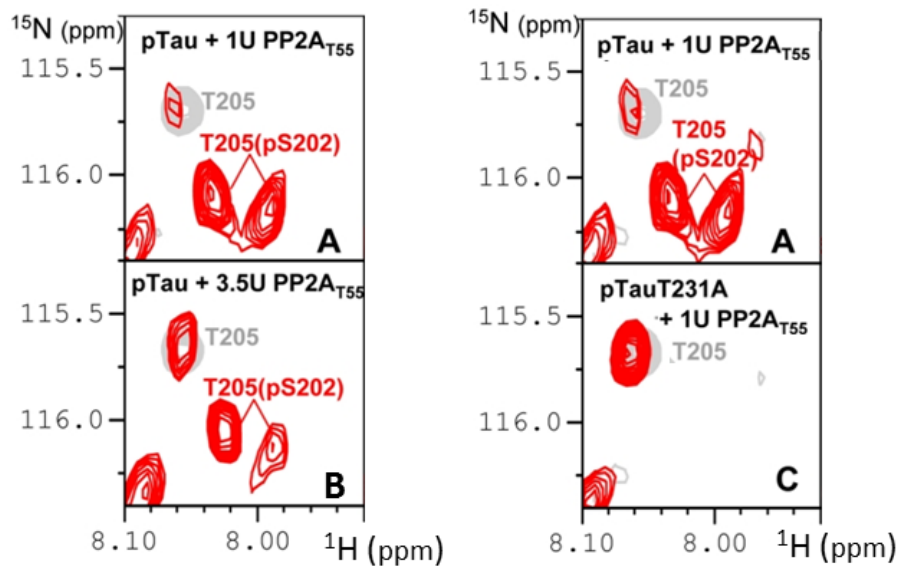


Figure 29: [H, ^{15}N] 2D HSQC spectra of Tau dephosphorylation at AT8 epitope, $\text{pS}^{202}/\text{pT}^{205}$. The spectrum of Tau (in grey) is overlapped with that of CDK2-mediated pTau dephosphorylated by PP2A heterotrimeric complex (in red) (PP2A_{T55} in Figure 28, A). (A) When pT^{205} is dephosphorylated, two resonances corresponding to T^{205} will appear: one the same chemical shift as that in Tau HSQC spectrum ($\text{T}^{205}\text{S}^{202}$), and another one corresponding also to T^{205} but located near a pS^{202} . In presence of 1U PP2A_{T55}, most of T^{205} is dephosphorylated whereas the S^{202} residue remains still mostly phosphorylated. (B) When PP2A_{T55} is increased to 3.5U, the intensity of resonance corresponding to T^{205} (pS^{202}) is reduced, and resonance intensity of T^{205} increased, which means pS^{202} residue is getting more dephosphorylated. (C) Only one T^{205} peak is observed in red spectrum of pTau T231A with only 1U of PP2A (conditions of experiment A) (Landrieu et al. 2011).

Besides the direct regulation of PP2A towards Tau protein, the downregulation of PP2A might be involved in multiple pathological mechanisms in AD. For example, mice lacking phosphatase PP2A B subunit PR61/B'delta develop progressively hyperphosphorylation of Tau in brain and spinal cord by deregulation of CDK5 and GSK3beta (Louis et al. 2011). Conversely, the aberrant stimulation of kinases, for instance GSK3 β , might also induce inactivation of PP2A via several mechanisms (Sontag & Sontag 2014).

3. A brief history of ERK kinase and MAPK cascades

ERK kinase was first studied in the context of insulin signaling. At that time, ERK was named MAP kinase because insulin-stimulated ERK kinase can phosphorylate MAP2 on Serine and Threonine residues *in vitro* (Ray & Sturgill 1988). Meanwhile, this MAP kinase was also found as an upstream kinase to phosphorylate the ribosomal protein S6 kinase (S6K II) in response of to a variety mitogens (Sturgill et al. 1988). MAP kinase was isolated from the extract of stimulated cells as a 40 kDa phospho-protein (Ray & Sturgill 1988). As this kinase can be stimulated by various environmental factors, its name was finally settled on ERK.

In the next decades, ERK has been studied as a prototypical member of a series of S/T kinases which are sequentially phosphorylated and activated in signal transduction pathways called the Mitogen-Activated Protein kinase (MAPK) cascades (Figure 30). In response to extracellular stimuli and environmental changes, including mitogens, hormones, stresses as well as physical changes like temperature, osmotic pressure etc., MAPK cascades are activated. MAPKs regulate various cellular processes such as proliferation, differentiation, stress response, and apoptosis (Yoon & Seger 2006). The MAPK cascades can be initially activated by a small GTP-binding protein (e.g., Ras). Then, this initial signal is rapidly and directly transmitted to protein kinases, most commonly MAPK kinase kinases (MAP3Ks). Once MAP3Ks are activated, the sequential phosphorylation and activation will take place in downstream kinases of the cascades. MAP3Ks phosphorylate MAPK kinase (MAPKK), such as MEK1/2, which will then phosphorylate its specific downstream component MAPK, such as ERK1/2, p38 etc., and sometimes there will be the next tier MAPK-activated protein kinases (MAPKAPK) phosphorylated (Figure 30) (Yoon & Seger 2006).

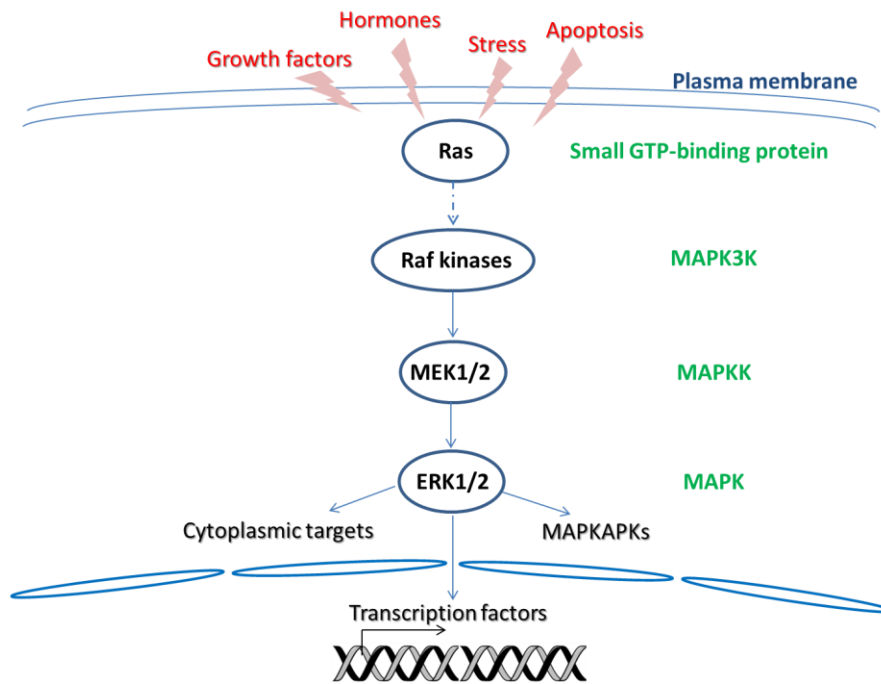


Figure 30: The MAP kinase signaling cascades. MAPK, ERK1/2, can be simulated in response to various extracellular signals, such as growth factors, hormones, stress or apoptosis. Such kind of signal activates small GTP-binding protein Ras, then the signal is transduced through several MAP4Ks which are not shown in figure, but a dotted line represents an indirect mechanism involved in MAP3K, Raf kinase, activation. The following steps are MAPKK, MEK1/2, activation by Raf that in turn is able to phosphorylate and activate MAPK, ERK1/2. MAPK may regulate ultimately MAPKAPs or other cytoplasmic targets such as Tau protein. In some cases, the phosphorylated protein is a transcription factor that will translocate into the cellular nucleus to mediate gene expression.

Each part of the MAPK signal cascades is composed of several components which are encoded from distinct genes and usually translated to a series of altered splicing isoforms. Over 70 genes so far have been identified to encode nearly 200 distinct components in the whole system of MAPK cascades (Keshet & Seger 2010). The ERK1/2 cascade has been mainly studied in case of cancers because of its important roles in cellular proliferation and differentiation. In the cascade, ERK1/2 as MAPKs is activated by its specific MAPK kinase, MEK1/2. The activation of ERK1/2 enzymatic activity is reported to require the dual-phosphorylation on both Tyrosine and Threonine residues in the 'TEY' motif located in the activation loop (Figure 31), while ERK1/2 monophospho-isoforms with 'pTEY' or 'TEpY' motif are also detected in cells (N. Anderson et al. 1990).

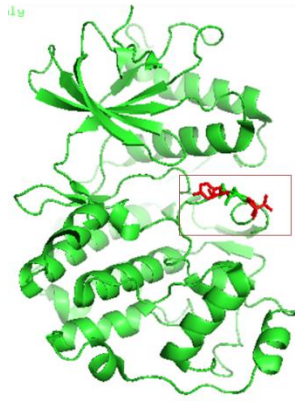


Figure 31: ERK2 3D structure in inactivated state. The ‘TEY’ motif is located in the activation loop which is shown boxed in red line. The T and Y residues are illustrated by red sticks. ERK2 PDB code: 4P3Q.

The monophosphorylated ERK1/2 isoforms can be generated *in vitro* by dephosphorylation of the dual-phosphorylated ERK1/2 by specific phosphatases like PP2A for the pT residue and protein tyrosine phosphatases (PTPs) for the pY residue (Sudhakaran Prabakaran et al. 2011). Monophospho-isoforms of ERK have been detected by nanoUPLC-MS in cellular extracts (Hahn et al. 2013). Different phospho-isoforms of ERK1/2 kinases may have distinct biological effects, intracellular localization and tissue-specific repartition (Hunter 2007). For example, the TEpY ERK phospho-isoform is reported in ERK-related regulation of Golgi structure in cell cycle (Cha & Shapiro 2001) and the pTEY ERK has been detected in intact cardiac myocytes (Sugden et al. 2010). The crystallographic structure of TEpY ERK1 shows that the conformation of the activation loop can be distinguished from loop conformations of unphospho-isoform and dual-phosphorylated isoform (Kinoshita et al. 2008). The distribution and specific functions in cells of the mono-phosphorylated ERK at ‘TEY’ motif are not yet fully elucidated.

4. MAP kinase Erk1/2 in Alzheimer's disease

The stress-related kinases like stress-activated C-Jun N-terminal kinase (SAPK/JNK), the MAPK p38 and the ERK1/2 kinases are relevant in the hyperphosphorylation of Tau protein in AD. The JNK signal pathway, a MAP kinases pathway, is associated with amyloid deposition and Tau phosphorylation on several pathological phospho-epitopes such as pT²⁰⁵ and pS⁴²² sites (Morishima et al. 2001; Reynolds et al. 1997). p38 is able to phosphorylate Tau protein on disease-related phosphoepitopes (Cavallini et al. 2013), and additionally plays other roles in neuroinflammation, excitotoxicity and synaptic plasticity (Munoz & Ammit 2010).

ERK1/2 kinase is a proline-directed kinase candidate in Tau-induced neurodegeneration. ERK1/2 is highly expressed in neurons and able to phosphorylate *in vitro* the neuronal Tau protein into the Alzheimer-like/PHF-like state with most of the pathological phospho-epitopes immunopositive (pS⁴⁶, pS¹⁹⁹, pS²⁰², pS²³⁵, pS³⁹⁶, pS⁴⁰⁴ and pS⁴²²) (Drewes et al. 1992). Disease-specific phosphoepitopes such as pS⁴²² can be fully reconstituted by ERK2, but not by either GSK3 or CDK5 kinase (Grueninger et al. 2011). In addition, ERK-mediated phosphorylation would decrease over 10-fold the affinity of Tau protein for the MTs, substantially reducing the microtubule stabilization (Drechsel et al. 1992).

There are several additional evidence showing dysfunctions of ERK1/2 in neuronal pathology. First, an activated ERK1/2 can lead to the death of some specific neuron sets, which could induce neurodegenerative disorders (Subramaniam & Unsicker 2010). Second, the overexpression of a ERK1/2 upstream regulator, ITPKB (inositol triphosphate 3-kinase B), might be related to increased ERK1/2 activation in cerebral cortex of AD patient brains. The ITPKB/ERK1/2 pathway might be an important regulator in Tau phosphorylation in AD (Stygelbout et al. 2014). In addition, activated ERK1/2 can be observed at early stages of aberrant Tau phosphorylation and co-localizes with phosphorylated Tau deposits in a subset of neurons and glial cells (Ferrer et al. 2001). Moreover, it is observed that both of ERK1/2 and its activator MEK1/2 are present in initial AD stages I-III and accumulate with the progressive development of neurofibrillary degeneration in the following stages of disease development (Pei et al. 2002).

However, it is recently shown that the phosphorylation level of Tau protein is not altered whether the ERK1/2 kinases are inhibited or activated, either in cell culture or in mice model, and Tau phosphorylation level is unchanged in MEK1 knock-out mice model where ERK1/2 is supposed to be inhibited (Noël et al. 2014).

It is thus still controversial whether ERK1/2 is indeed a responsible kinase for Tau hyperphosphorylation, but a lot of evidence supports its involvement in Tau pathology.

Part 4. Docking interactions

1. Strategies of modular interactions in protein kinases and phosphatase networks

The kinases and phosphatases, like other enzymes, possess the active site to accommodate their substrates and perform their activity. However, for each kinase or phosphatase, the active site is able to recognize a range of similar short amino acid sequences, called substrate motifs, which cannot explain by themselves the selectivity towards the right targets when working in the huge network of cellular signaling. A large number of those kinases and phosphatases resort to additional protein-protein interactions to achieve both specificity and catalytic efficiency. The protein interaction system relies on additional separated globular domains or docking grooves that can be located far from the active site (Figure 32, a and b) (Remenyi et al. 2006).

The globular docking domains found in various enzymes are folded and stable modules regulating protein-protein interactions that provide the specificity to distinguish related substrates. SH2 and SH3 domains are such globular domains that are found in Src, Alb, Hck and Csk protein kinases and SHP protein phosphatase. SH2 domain for instance recognizes phospho-tyrosine peptides. In the Fyn kinase, one Src family kinase, the sequence 'PXXP' (X is any amino acid) is identified as the site employed for the interaction with SH3 domain (Hongtao et al. 1994). These domains therefore make important contribution to the kinases or phosphatases interactions with their substrates (Miller 2003). In contrast to globular domains physically distinct from the catalytic domains, docking grooves can be integrated in the protein structure. They are usually composed by a few amino acids located at the protein surface, mainly positively charged and hydrophobic residues forming pockets or grooves (Remenyi et al. 2006). Even within the same family, kinases and phosphatases can differently develop docking grooves to select their appropriate docking motifs from a large array of substrates (Figure 32, c) (Bhattacharyya et al. 2006).

In some cases, modular domains (e.g., SH2 domain) or docking grooves are additionally characterized as phosphorylation-dependent in the manner of recognizing their docking motifs. Their substrates or up-stream kinases have first to be phosphorylated in the docking

motifs so as to be recognized (Figure 32, d). Conversely, the PP2A phosphatase interaction with its docking sequence in Tau is perturbed by phosphorylation of T²³¹ (Landrieu et al. 2011). In summary, docking interactions aid to improve the efficiency and specificity of kinases/phosphatases recognition of substrates.

On the other hand, docking interactions can additionally make allosteric modification in the catalytic domain and active site, directly regulating its catalytic activity (Figure 32, e). For instance, a docking interaction can induce an allosteric structural modification of the active site of phosphorylated p38 α , accelerating therefore the phospho-transfer reaction (Tokunaga et al. 2014).

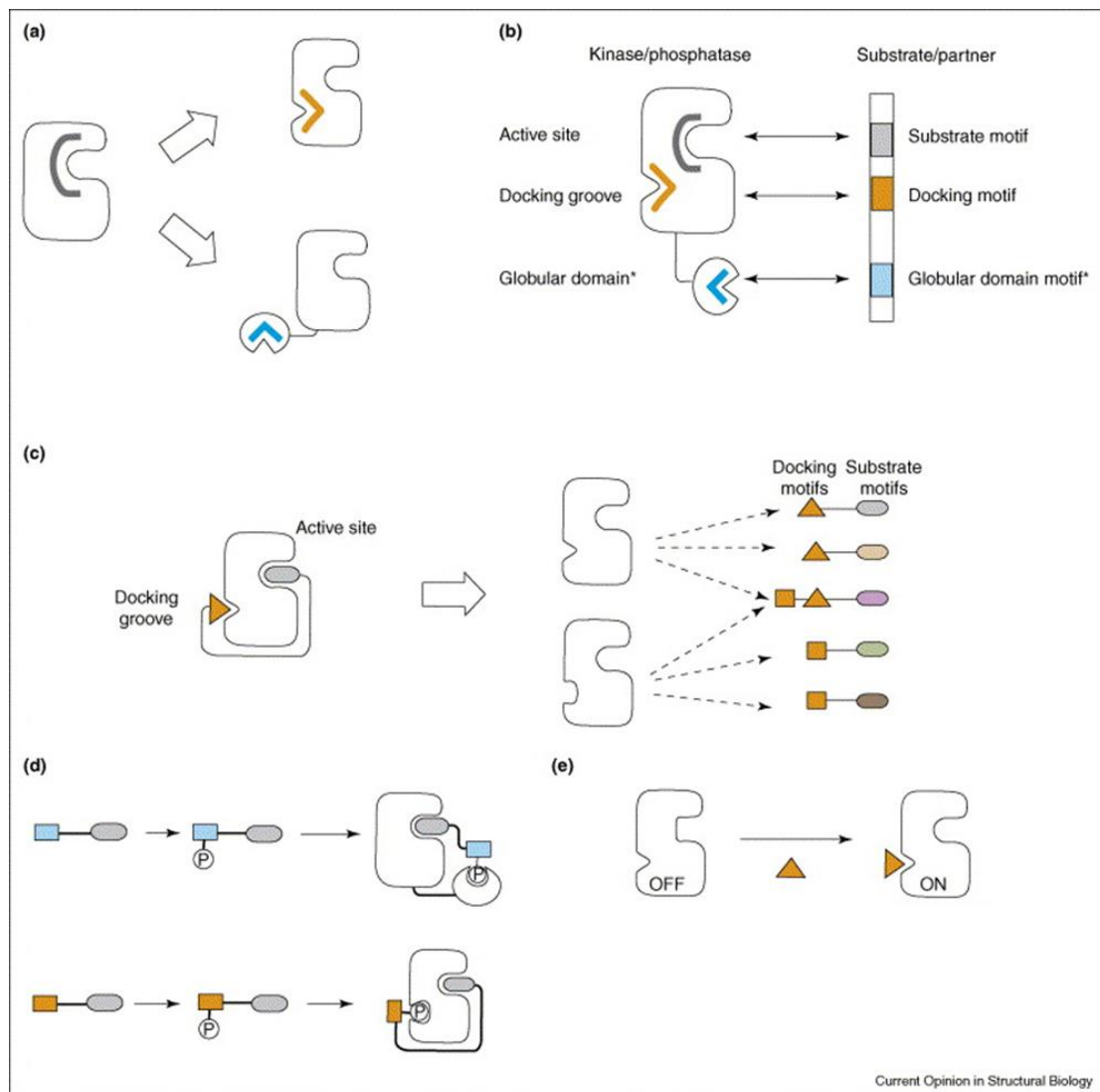


Figure 32: Protein-protein interactions mediated by modular domains and docking grooves. (a) The catalytic function site, outlined in grey, of kinases or phosphatases is physically separated from protein-protein recognition part which could be a docking groove

illustrated in orange or a globular modular domain in blue. (b) The active site, docking groove and globular domain each target a corresponding peptide motif in substrates or partners. (c) As the active sites of kinases or phosphatases generally have limited selectivity for the recognition of substrates, the docking groove contributes to the specificity of protein-protein interaction. (d) In addition to the simple peptide motifs for the docking groove or modular domain, in some cases, the phosphorylation of peptide motif is required for the docking-groove or modular-domain mediated interaction. (e) Docking interaction can sometimes induce an allosteric modification in kinases or phosphatases catalytic site which will regulate the catalytic function for example, switch on its activity (Remenyi et al. 2006).

There are other protein-protein interaction mechanisms observed in cell signal pathways. Unlike the simple enzyme-substrate complex in which the target recognition and catalytic function occur on the basis of one protein structure, the connectivity and catalytic elements could be ultimately separated with different proteins, each of which might be genetically independent. In these cases, the interaction seems to be more complicated and often needs one or more protein partners, defined as adapters and scaffolds, to assemble the complex. The PP2A phosphatase is an example of such an organization. The adapter or scaffold proteins (in the case of PP2A, subunit A) act as an organizing platform to recruit other specifically recognized molecule components in the same complex. With the help of these molecules, catalytic elements would be bound to their upstream partners and substrates or downstream protein partners, in particular in signal transduction. The recruitment of these molecular partners is usually adopted in the manner of globular domain or docking groove recognition (Figure 33).

Compared to scaffold-mediated complexes involving more than two protein partners, adapter proteins generally link only two protein partners (Bhattacharyya et al. 2006). Here below is the example of the CDKs kinases, which are major components of cell cycle division machinery, required to associate with their regulatory adaptor, a cyclin protein, to perform their enzymatic activity. CDK2 kinase, for example, associates first with cyclin E to initiate the DNA synthesis driving cells from G1 to S phase, and is then activated by binding to Cyclin A in order to regulate transcriptional expression and others cellular functions in S phase progression. The interaction of CDK2 and Cyclin A has a high affinity and about 35% of CDK2 surface is involved in the interaction according to the crystal structure of human CDK2/Cyclin A complex (Jeffrey et al. 1995; Morgan 1997). A dual mode of recognition is employ to gain

substrate specificity: the sequence S/T-P-X-R/K (X refers to any amino acid) of the phospho-acceptor in substrate is recognized by CDK2 while Cyclin A binds R/K-X-L recruitment motif of the same substrate (Lowe et al. 2002). The adaptor protein cyclin A is able to tightly bind to CDK2 and also recruit of substrate motifs to carry out the kinase efficiency.

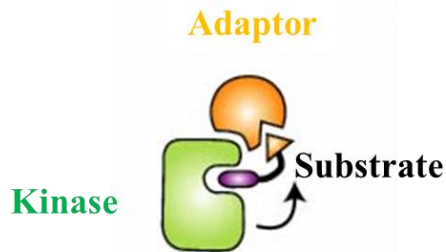


Figure 33: A model of adaptors as mediators for the connectivity of protein partners. The adaptor molecule shown in orange on the left links two components together, kinase molecule in green and substrate whose two distinct motifs are respectively recognized by adaptor and kinase (Bhattacharyya et al. 2006).

2. Conserved docking sites in substrates of MAP kinases

As widely implicated in diverse cellular mechanisms, MAP Kinases are able to form complexes with a large variety of substrates while they are recognized by various up-stream activators and phosphatases. Given this promiscuity, it is an interesting question how each MAP kinase selectively recognizes its own substrates but not those of closely-related kinases. From the genetic studies, it appears that no extra globular domain in MAP kinases contributes to the connectivity with the substrates. Data suggests that a modular docking domain is conserved within MAP kinases that increases the affinity with up-stream activators or down-stream substrates and supports the efficiency of the catalytic activity (Bardwell & Thorner 1996; Holland & Cooper 1999; Sharrocks et al. 2000)

The MAP kinases preferentially phosphorylate an identical P-X-S/T-P motif including a minimal consensus sequence S/T-P (Davis 1993; Songyang et al. 1996). It is thus of interest to understand the additional specificity elements that target its specific substrates. From the studies about the interaction of JNK, one of the MAP kinases, and its substrate c-Jun, it has been revealed that a δ domain positioned at the N-terminal of the S/T-P motifs is necessary

to increase its phosphorylation efficiency. The δ domain is composed of a consensus of 14 amino acids, including the sequence $K-X_2-R/K-X_4-L-X-L$ (X is any amino acid), located about 20 amino acids away from two nearby phospho-acceptor sites (Hibi et al. 1993; Kallunki et al. 1994). Another example is ERK kinase for which a similar docking site has been identified in the transcription factor Elk-1 (Yang et al. 1998a; Yang et al. 1998b). Both JNK and ERK1/2 docking sites recognize the $K-X-R-K-X_3-L-X-L$ consensus sequence, suggesting that these kinases share common substrates, e.g. Elk-1.

In the last twenty years, a number of studies have identified such kind of docking sites from substrates, up-stream activators or scaffold proteins of various classes of MAP kinases and have demonstrated that a MAPK-docking site is constituted by a conserved consensus amino acid sequence $(R/K)_2-X_{2-6}-\Phi_A-X-\Phi_B$ (Φ is hydrophobic residue, X is any amino acid), defined as a D-docking site, D-motif or KIM-motif (kinase interaction motif) (Bardwell & Thorner 1996; Holland & Cooper 1999; Sharrocks et al. 2000).

3. ERK1/2 and other MAP kinases recruitment grooves

In MAPK signaling pathway, MAP kinases are able to accurately choose their own protein partners. By examining the primary amino-acid sequence, a putative or identified D-docking site is found in almost all substrates of known members of MEK kinase family (Bardwell & Thorner 1996). In the consensus sequence of MAPK-docking sites, two or more basic residues are considered to anchor or direct the docking motif to bind its docking groove in MAP kinases. A cluster of acidic residues are conserved as part of the kinase docking groove to serve an electrostatic interaction with positive charged residues in D-docking motif of substrates (Tanoue et al. 2000). Besides charged residues, adjacent hydrophobic amino acids on the surface of MAP kinases are also important in substrate selectivity by hydrophobic interaction with residues of Φ_A and Φ_B in docking sites (Xu et al. 2001). Altogether, the acidic residues and hydrophobic residues, named as Φ_A and Φ_B , are found located in C-terminal region, far from the catalytic region of MAPK, playing a role in the specificity of docking sites recognition, and here called as D-Recruitment Site (DRS) or Common Docking (CD) domain (Brunet & Pouyssegur 1996; Xu et al. 2001; Tanoue et al. 2000).

In case of the ERK2 kinase, it has been reported that the mutation of two negatively charged D³¹⁶ and D³¹⁹ residues (in the sequence of *Rattus* ERK2) into N residues disrupts the interaction between ERK2 and MKP3 (MAPK phosphatases 3) (Camps et al. 1998). In addition, these two D residues are located in the C-terminal lobe of ERK2 where both of their side chains (shown in red in Figure 34) are exposed on the surface. Moreover, Tanoue T *et al* have shown that either of D³²¹ or D³²⁴ mutation to N residue in *Xenopus* ERK2 sequence will significantly decrease its binding affinity with MEK1 compared to that of wild-type ERK2. These data show the importance of these two D residues in the MAPK-docking-mediated interaction (Tanoue et al. 2000).

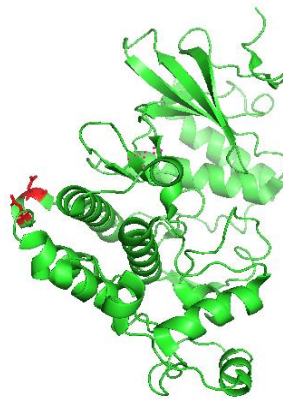


Figure 34: The structure of *homo sapiens* ERK2 composed by 362 amino acids. The side chains of D319 and D321 residues are illustrated in red. PDB code: 4H3Q.

CD domains are conserved in other MAP kinases in their C-terminal part, as shown in the sequence alignment of Figure 35. Besides the two D residues (shown in red in Figure 35, a) conserved in all MAPK sequences, the surrounding sequence also shows a conserved pattern. For instance, E and H residues are highly conserved at the N and C-terminals in a 'DXXD' motif (Figure 35, a).

Three major and typical MAP kinases, ERK1/2, JNKs and p38s, are recognized and activated by their own upstream regulator MEK kinases in a D-docking-mediated interaction. As ERK1/2, JNK1 and p38 α share a 40%-50% identical amino-acid sequence (Caffrey et al. 1999) and a similar docking domain sequence. A significant decrease of binding ability has revealed that the mutation of relevant D residue in docking domain sequence will perturb or disrupt the interaction of JNK or p38 with their MEK kinases (Tanoue et al. 2000). JNK and

p38 thus share a common docking domain with ERK2 which regulate the binding with various MEK kinases, phosphatases and substrates (Figure 35, b). The interface mapping of MAPKs and their substrates has been undertaken by multiple methods, such as mutagenesis analysis, hydrogen exchange mass spectrometry (HXMS) and x-ray crystallography (Tanoue et al. 2000; Lee et al. 2004; Zhou et al. 2006; Liu et al. 2006).

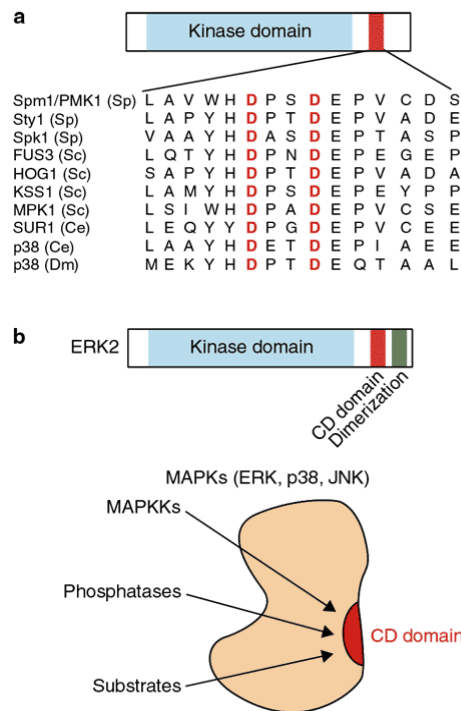


Figure 35: The CD groove is conserved in MAP kinases. (A) Two acidic residues Asp (D written in red in amino acid sequence) are found at the C-terminal lobe in almost all the MAP kinase families. (B) In terms of ERK1/2, p38 and JNK, major MAP kinase families, the CD domain shown in red is conserved separately from the catalytic domain and serves to bind various protein partners such as MAPKKs, Phosphatases and Substrates (Tanoue et al. 2000).

Some D-docking motifs in substrates show selectivity to either of ERK1/2, JNK or p38 while other D-docking motifs are able to recognize multiple MAP kinases (Bardwell et al. 2009; Sharrocks et al. 2000). To understand the selectivity, some D-docking peptides derived from protein partners were separately prepared and designed to bind to ERK1/2, p38 α or JNK1 respectively. From the study of crystal structures of the MAP kinases with these various

peptides, it turns out that ERK2 and p38 α can be distinguished from JNK based on docking consensus but not ERK2 from p38 α selectivity (Garai et al. 2013).

However, based on structural studies a simple docking consensus can still not explain how the specificity of MAPK-docking peptide is achieved. It suggests that more factors besides the core docking site, such as region lengths and distinct compositions, are also important to define the selectivity of D-docking site towards some specific MAP kinases. Two hydrophobic pockets, in addition to Φ_A and Φ_B , are found on the surface of ERK2 and p38 α , but not of JNK1 (Peti & Page 2013). These hydrophobic pockets are generally located between the positively charged CD groove and the Φ_A -X- Φ_B pockets. They are named as upper pocket (Φ_U) and lower pocket (Φ_L). Therefore, the consensus for D-docking site could be finally defined as (R/K) $_2$ -X-X- Φ_U -X $_{4-6}$ - Φ_L -X $_2$ - Φ_A -X- Φ_B or the reversible consensus Φ_B -X- Φ_A -X $_2$ - Φ_L -X $_{4-6}$ - Φ_U -X-X-(R/K) $_2$ (Figure 36) (Garai et al. 2013). Not all of the hydrophobic pockets would be necessarily used in D-docking interaction: D-docking sites can contain none of Φ_U and Φ_L residues or either of them or both of them (Garai et al. 2013). For example, only three hydrophobic residues, Φ_A , Φ_B and Φ_L are present in JNK-specific peptides which results in D-docking peptides much easily discriminated between JNK and p38/ERK than between p38 and ERK. It has been shown that some JNK-specific peptides do not bind either p38 or ERK and reversibly, p38-specific or ERK-specific peptides do not bind JNK. In contrast, the peptides derived from p38-specific or ERK-specific protein partners can also interact with the other kinase, but in a looser way (Peti & Page 2013). It has been reported that the discrimination factor of p38-specific or ERK-specific peptides is less than 4-fold (Garai et al. 2013; Peti & Page 2013).

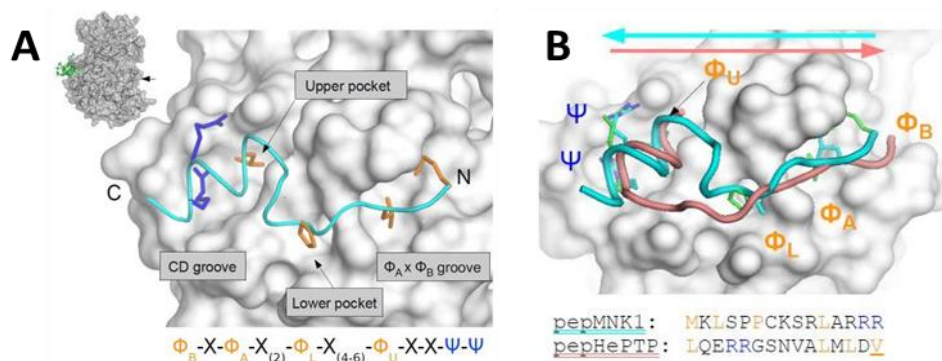


Figure 36: Crystal structure of ERK2-peptide complexes. (A) Zoomed crystal structure of docking interaction of ERK2 with pepMNK1 peptide (PDB code: 2Y9Q). The docking domain

is at the opposite side of the activation loop, shown by arrow in the inset, in ERK2 crystal structure. The peptide is derived from MNK1 and occupies the docking groove in a C- to N-terminus order. The multiple hydrophobic pockets dedicated to docking interaction on ERK2 surface are identified by arrows in the CD groove. The consensus of D-docking site is summarized, Ψ and Φ represent positively charged residues (in blue) and hydrophobic residues (in orange) respectively, and X is any amino acid. (B) Overlapped crystal structures of ERK2-pepMNK1 and ERK2-pepHePTP interactions. The binding of pepHePTP (PDB code: 2GPH), linear motif in cyan, is in the N- to C-terminus orientation, in reverse to the pepMNK binding way, shown in red. The Ψ residues are highlighted in blue in the sequence and the Φ residues in orange (Garai et al. 2013).

MAP kinases show specificity in the recognition of their upstream activators, MAPK kinases, in the signal cascade: ERK1/2 is recognized by MEK1/2; p38 is phosphorylated by MEK3/6, but also by MEK4, and JNK1/2/3 might be activated by MEK4 and MEK7 as well (Lawrence et al. 2008; Cuenda & Rousseau 2007; Johnson & Nakamura 2007; Wang et al. 2007). These activation pathways are thought to be regulated by D-docking interactions. It has been investigated that the specificity of recognition between peptides from MEKs and MAP kinases, are structurally and functionally close to each other (Bardwell et al. 2009). The results of this study show that MEKs-derived peptides bind generally much better to their cognate MAP kinases than to their non-cognate MAP kinases, however, MEK6-derived D-site peptides are able to inhibit the activity of non-cognate ERK2 as well as to inhibit their cognate p38 (Bardwell et al. 2009). ERK2 is a weak discriminator of its cognate and non-cognate MEK-derived peptides, thus suggesting that multiple regions, at least two domains in addition to D-docking domain, are implicated in the ERK-MEK interaction (Robinson et al. 2002). D-docking domains are important to discriminate their protein partners, but require additional contacts to enhance their specificity (Robinson et al. 2002; Bardwell et al. 2009).

4. F-docking sites and F-docking domain

In the complex of ERK2 and Elk-1, another docking site besides D-docking site was identified and characterized. Its amino acid sequence 'FXFP' (X represents any amino acid), called an F-docking site first described by Jacobs. D, *et al* in 1998, mediates the interactions with ERK2 but not JNK. The 'FXFP' motif is also identified in other Elk subfamily of ETS

proteins, such as LIN-1 and Aop/Yan which appear as well as Elk-1 to be directly regulated by ERK2. When the 'FXFP' motif is altered, in particular F residues, the phosphorylation by ERK2 of these transcription factors is substantially reduced. For example, after the mutation of 'FQF' motif in Elk-1 fragment [307, 428] by 'AAA', the Michaelis constant (K_m) is increased threefold and the catalytic efficiency (V_{max}/K_m) is thus decreased by threefold (Jacobs et al. 1999). Therefore, it is suggested that this 'FXF' docking site provides an additional affinity and increases sequence specificity in the interactions between ERK and its substrates. 'FXF' is the shortest and the cardinal motif in F-docking site. However, a peptide library screening has shown that F residues could be replaced by other aromatic residues as Y or W while maintaining the structural function in F-docking interface (Sheridan et al. 2008).

Compared to D-docking domain, the recruitment of F-docking site is much less characterized. There is no clear crystallographic information given to define F-docking Recruitment Site (FRS) in MAP kinases. However, some hydrophobic residues, such as L²³⁵, have been identified as crucial part of FRS in ERK2 structure by using hydrogen exchange mass spectrometry coupled with mutation analysis (Lee et al. 2004). Therefore, it has been proposed that the FRS is formed as an hydrophobic pocket sterically close to the activation loop on the surface of ERK2 (Lee et al. 2004). Sheridan D.L. *et al* proposed a model for interaction of a typical F-docking motif (acetyl-SFQFP-amide) onto a known ERK2 structure. From this *in-silico* model, we can see that the aromatic group of two F residues at position +1 and position +3 are oriented into the hydrophobic pocket and well captured by hydrophobic interactions on the surface of ERK2 (Figure 37) (Sheridan et al. 2008).

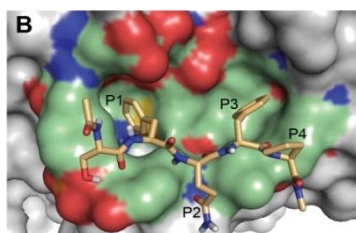


Figure 37: Proposed model for FRS-peptide interactions. A pentapeptide ligand is used to model the interaction between activated ERK2 and 'FXF' motif. The peptide sequence is acetyl-SFQFP-amide (represented by stick in orange). The first F residue at the N-terminus is noted as P1 and others residues are marked as P2, P3 and P4 until the peptide C-terminus. The two F residues, at P1 and P3, show a strong selectivity for the hydrophobic pocket (green) on the surface of ERK2. The crystal structure data of activated ERK2 is from PDB with code 2ERK and the model of binding was obtained by AutoDock (Sheridan et al. 2008).

The p38 α isoform has within its amino acid sequence a conserved F-docking motif and from the results of peptide library screening, it has been found that p38 α , as well as ERK2, are highly selective for peptides containing aromatic residues at +1 and +3 position in a 'FQFP' motif. Therefore, it is suggested p38 α also binds to F-docking peptide. The consensus for p38 α as well as ERK1/2 is proposed as F/W-X-F/Y/W located within a 20 amino acids range from the C-terminus of the phosphor-acceptor site. No F-docking peptide was shown to bind to JNK2. Structurally, it was observed that the L²³⁵ residue, engaged in the F-docking interacting pocket in ERK2, is conserved in almost all the p38 family members, but a W residue is present in the corresponding pocket in JNK isoforms. The substitution by a residue of larger size would explain a conformational alteration on the surface of JNK2 which could perturb the binding of aromatic residues (Sheridan et al. 2008).

Objectives

Tau is an intrinsically disordered protein, abundantly expressed in human central nervous system. Tau is getting attention on the one hand because it is an important component of the neurofibrillary tangles found in neurons in Alzheimer's disease and an actor of the associated neurodegeneration. On the other hand, its multiple biological functions in healthy neurons are yet to be fully unraveled.

A well-known role of Tau protein is the stabilization of MTs polymerized from tubulins and the regulation of axonal transport in neurons. This function is negatively regulated by phosphorylations, ensuring the dynamics of the system. However, under pathological conditions, a hyperphosphorylation of Tau is observed that seems to lead to loss of crucial functions and to gain of toxicity in neurons. Therefore, phosphorylation, a simple chemical modification, is sufficient to change Tau properties to switch from physiological component to cause of pathogenesis. Despite large research effort, the molecular mechanisms of Tau phosphorylation still need to be fully elucidated and their impact on Tau functions remain poorly understood.

The extracellular-regulated kinase 2 (ERK2) is one important kinase, among several relevant candidates, involved in Tau hyperphosphorylation. One reason the link between phosphorylation and function is not clearly resolved, despite its huge interest, is the difficulty in characterization of phosphorylated Tau forms. We here used nuclear magnetic resonance (NMR) spectroscopy as a useful analytical tool for characterization of both Tau phosphorylation at multiple sites and its interaction with other binding partners. In this context, the aim of my thesis is a better understanding of the link between Tau phosphorylations and their impacts on physiological and pathological Tau functions.

In my thesis, I first have identified the *in vitro* ERK2-mediated phosphorylation pattern of Tau protein by NMR spectroscopy. In addition, I have compared the enzymatic activities of phospho-isoforms of ERK2 toward Tau as substrate. Three phospho-isoforms are generated when ERK2 is activated *in vitro* or in cells culture (Sudhakaran Prabakaran et al. 2011; Sugden et al. 2010; Hahn et al. 2013).

Next, we have tried to define the contribution of ERK2 kinase in rat brain extract kinase activity towards Tau protein. Tau phosphorylated by the kinase activity of rat brain extract is used in *in vitro* biochemical experiments as a model of Tau hyperphosphorylation.

Experiments by NMR or by other biochemical techniques were performed to inhibit ERK2 activity in rat brain extract, as well as to compare the phosphorylation pattern by rat brain extract with that by ERK2.

Third, to better understand the molecular mechanism of Tau recognition by ERK2, docking sites of Tau were identified by NMR experiments. Tau peptides involved in ERK binding were designed and prepared to confirm the recognition sequence by ERK2.

The result gave insights into Tau recognition by ERK2 and provided data to better understand the molecular mechanisms of Tau hyperphosphorylation and dysfunctions in Alzheimer's disease.

Two studies were next undertaken to investigate the consequences of ERK-mediated Tau phosphorylation on its physiological and pathological function. In the first case, the impact of ERK2 phosphorylation on DNA-binding was studied. We observe that multiple phosphorylations in the proline-rich domain of Tau have an effect in distance on the interaction with oligonucleotides on the microtubule binding domain. In the second case, we showed that ERK2-phosphorylation stimulates Tau self-assembly, in the same manner as observed for the rat brain hyperphosphorylated Tau.

We conclude that ERK2 is a kinase of Tau that can induce a pathological form of Tau, more sensitive to aggregation and unable to insure its protective role of DNA binding.

Results

Part 1

ERK2-mediated Tau phosphorylation and the recognition of multiple docking sites by ERK2 kinase

In this study, I have focused on the analysis of the kinase activity of ERK2 towards Tau. As an analytical tool, NMR spectroscopy is used to characterize the phosphorylation pattern of Tau by ERK2. We have observed that ERK2 kinase is able to generate *in vitro* almost all of the 'pS/pT-P' motifs (14 out of 17, except pT111-P, pT212-P and pT217-P). Phosphorylation of S/T residues corresponding to 12 to 15 sites has also been reported (Biernat et al. 1992; M Goedert et al. 1993; Alonso et al. 2001) after *in vitro* incubation of brain-extracted or recombinant Tau with rat brain extract in presence of okadaic acid (OA) to inhibit phosphatase, in particular, pS/pT phosphatase PP2A. The site-specific, precise pattern of the hyperphosphorylation of Tau by rat brain extract was however never investigated. All of ERK2-phosphorylated sites identified in ERK2-phosphorylated Tau can also be found in Tau phosphorylated by rat brain extracts, according to our NMR analysis. As it is reported that Tau phosphorylated by rat brain extract is capable to self-aggregate *in vitro*, a similar aggregation experiment was also performed for Tau phosphorylated by ERK2 kinase.

The observation of Tau aggregates was carried out by transmission electron microscopy. The aggregates are observed after a short incubation time at 35°C in both samples of phospho-Tau, with phosphorylation generated by either ERK2 or rat-brain-extract. Several micrometer-size objects are found with twisted filaments resembling the PHFs observed in AD's affected brain. The aggregation induced by the phosphorylation of Tau is not as massive as the heparin-induced Tau aggregation and concerns only a fraction of the protein in the sample. Nevertheless it is specific as it is not observed in the unphosphorylated Tau samples.

Additionally, MAP kinases are known to recognize their protein substrates not only by their specificity for a targeted S or T phosphorylation site but also by binding to peptidic linear motifs located outside of the phosphorylated motif, called docking sites (Tanoue et al. 2000; Bardwell et al. 2009). We have used NMR spectroscopy to identify ERK2-docking sites along the Tau sequence. Two main docking sites were found in the MTBDs of Tau. To our knowledge, this is the first substrate of ERK2 identified with multiple docking sites. Measure of the dissociation constant K_d showed a weak interaction, characteristics of transient protein-protein interactions. These results support the hypothesis that ERK2 activation under stress conditions might have a detrimental effect for Tau function and participate in AD physio-pathology.

These results are described and discussed in the included manuscript that will be submitted for publication.

We have performed additional experiments related to ERK2 characterization that will be here below presented and are not included in the manuscript. We have first tried to determine which kinases in the rat brain extract could be responsible for Tau phosphorylation. We additionally investigated the kinase activity of various activated isoforms of the ERK2 kinase. First, experiments were designed to find out which kinase(s) in the rat brain extract could be linked to specific phosphorylation sites of Tau in rat brain extract. We use commercial inhibitors described to be specific for ERK2, GSK3 β and PKA. However, there is no evidence to show, based on the NMR experiments to detect the phosphorylations, that ERK2 as well as GSK3 β inhibitors could inhibit Tau phosphorylation by rat brain extract. In addition, even though Tau phosphorylation is inhibited by PKA inhibitor, the results were not encouraging because S/T-P motif phosphorylations were also inhibited although PKA is not a Proline-directed kinase. Our interpretation of these experiments is that the PKA inhibitor we used is a peptide that may disrupt the recognition by ERK2 kinase of the Tau protein. The inhibitor is indeed a peptide whose amino acid sequence is compatible with the consensus sequence of ERK docking site described before (Tanoue et al. 2000).

We next search other ways to investigate the active kinases in the rat brain extract and in particular whether the ERK1/2 kinase activity could be found. PEA-15 (15kDa phosphoprotein enriched in astrocytes) is a protein described to specifically inhibit ERK activity due to the specific binding of PEA-15 to both ERK1/2 activation loop and docking groove (Mace et al. 2013). We thus prepared the recombinant PEA-15 protein and added it to the phosphorylation mix. PEA-15 was able to effectively inhibit the phosphorylation by rat brain extract. Nevertheless, this inhibition was not completely specific as we observe the reduction of phosphorylation level of some pS residues that should not be targeted by ERK2 as they are not included in S/T-P motifs. The rat brain extract is thus a complex mixture of kinases and it seems based on these experiments that it is not so easy to specifically target one of these kinases with inhibition. It might be due to the interconnection of these kinases that can activate one another or phosphorylate Tau depending of specific pattern of phosphorylation, as it is the case for example for GSK3.

Finally, we attempted to use a monoclonal antibody targeted at dually phosphorylated ERK1/2 (anti-pTEpY ERK1/2) in rat brain extract, which recognizes and directly blocks the activation loop of ERK kinase. We observe an inhibition effect on Tau phosphorylation analyzed by SDS-PAGE, but no further NMR experiment has been performed due to the difficulty to use a large amount of antibody in the inhibition assays. We were thus not able to show the specific inhibition of ERK-phosphorylated sites by NMR spectroscopy.

These inhibition assays suggest active ERK1/2 kinase might be present in rat brain extract and also involved in Tau phosphorylation by rat brain extract. This part of the experiments are however not included in the manuscript as they remain some ambiguities in the conclusions of these kinase-specific inhibition assays.

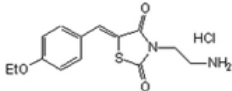
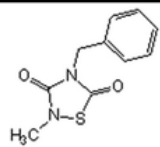
Analysis of kinase activity in rat brain extract

1. Inhibition of kinases of rat-brain-extract in Tau phosphorylation assays

By comparing NMR spectra of Tau phosphorylated by ERK2 and by rat brain extract, I obtain a very similar phosphorylation pattern. Our hypothesis is that the activity from the rat brain extract mainly comes from ERK2 kinase or related MAP kinases. Three additional phosphorylated sites in the rat brain extract phosphorylated Tau, not included in Pro-directed motifs, are modified by other unidentified kinases. Several kinase-specific inhibition assays have been performed to further investigate the activity of kinases, in particular ERK2 kinase, in rat brain extract. Inhibitors of ERK2 kinase as well as PKA kinase and GSK3 β are used to inhibit specific kinase activity in Tau phosphorylation assays by rat brain extract. The commercial inhibitors used in the experiments are listed in the Table 2.

In the mixture of phosphorylation reaction (2.5 ml), 4 μ M ¹⁵N-labelled Tau is incubated with 500 μ l rat brain extract with around 7mg/ml total protein concentration. Kinase-specific inhibitors are added in each reaction mixture with 20 μ M final concentration. After 24H incubation at 37°C, samples are first analyzed by SDS-PAGE. Compared to the control of phospho-Tau without kinase-specific inhibitor, the inhibition effects are not observed with the ERK2 (Figure 38, A, lane 3) or GSK3 β inhibitors (data not shown), whereas the sample containing the PKA inhibitor shows a decreased phosphorylation, appearing as a faster migration of part of the phosphorylated Tau in the gel (Figure 38, A, lane 4).

Table 2: Kinase-specific inhibitors

Inhibitors	Molecular representation	Solubility	References
Non-ATP-competitive ERK inhibitor		DMSO	#1049738-54-6, Millipore <i>Hancock, CN. et al. 2005</i>
Non-ATP-competitive PKA inhibitor	Amino acid sequence: T-Y-A-D-F-I-A-S-G-R-T-G-R-R-I	H ₂ O	#539684, Millipore
Non-ATP-competitive GSK3beta inhibitor I		DMSO	#327036-89-5 Millipore

NMR Spectroscopy is next used to better understand the inhibition effect on Tau phosphorylation by PKA inhibition. In 2D HSQC spectrum shown in Figure 38, B, the residues potentially phosphorylated by the PKA kinase, corresponding to phosphorylated S residues not included in S/T-P motifs pS²⁰⁸, pS³⁵⁶ and pS²⁶², are indeed not detected in the Tau protein phosphorylated in presence of the PKA inhibitor. However, other S/T residues that we do not expect to be phosphorylated by PKA because they are included in S/T-P motifs are also inhibited by the PKA inhibitor. In presence of PKA inhibitor, the phosphorylation at S²⁰⁸ and S³⁵⁶ is dramatically inhibited, but also the phosphorylation of T¹⁵³-P, S²⁰²-P and T²⁰⁵-P. In addition, T¹⁷⁵-P, S¹⁹⁹-P, S²³⁵-P and S³⁹⁶-P have a significant decrease in phosphorylation level (Figure 38, C). Because of that observation, we could not conclude on a specific effect of the inhibitor.

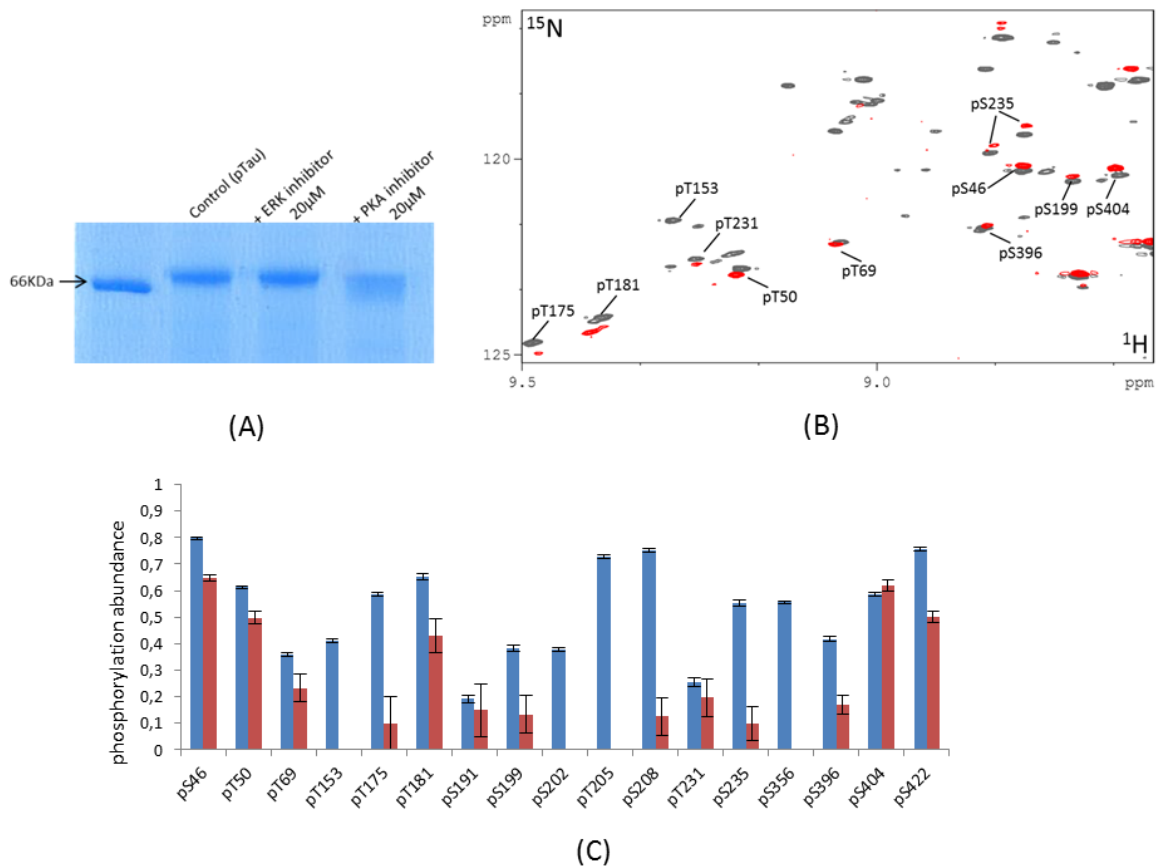


Figure 38: Inhibition of Tau phosphorylation by addition of kinase-specific inhibitors in rat brain extract. (A) SDS-PAGE analysis of inhibition effect on rat-brain-extract-mediated Tau phosphorylation. The control sample of Tau phosphorylation is a band migrating at a position corresponding to about 66kDa (the BSA marker in a molecular weight marker mix). The ERK2-phosphorylated Tau has a slower migration (lane 2). The presence of 20µM ERK2 inhibitor in the phosphorylation assay does not affect the migration, showing no evidence

of inhibition. Migration of the Tau sample phosphorylated in presence of 20 μ M PKA inhibitor is faster compared to the phosphorylated protein in lane 3, and more heterogenous. (B) Overlapped [^1H , ^{15}N] 2D HSQC zoom-in spectra of phospho-Tau incubated with rat brain extract (in grey) and phospho-Tau incubated with rat brain extract in presence of PKA inhibitor, in the same conditions (in red). The phospho-sites are annotated in the spectra. (C) Relative phosphorylation abundance of phospho-sites in Tau sequence. The relative phosphorylation abundance is correlated with the relative integrals of resonances of phospho-residues in the HSQC spectra.

In terms of non-ATP competitive ERK inhibitor 76, it is described to specifically bind to ERK2 in the adjacent space of the docking groove and inhibit cell proliferation in cells assay (Hancock et al. 2005). We do not observe inhibition in the rat brain extract phosphorylation assays but at that point we cannot be sure that our hypothesis of ERK2 activity in the extract is valid. We thus repeated the inhibition assays but this time with recombinant ERK and again failed to observe indication of inhibition by SDS-PAGE. These experiments of inhibition thus remain non conclusive. Despite direct binding of inhibitor76 to ERK2 docking groove (Hancock et al. 2005), we still observe a kinase activity in our assays in its presence. Our hypothesis is that in presence of abundant substrate, the activity is not sufficiently inhibited to be observed after a long incubation period. We also observed later in the course of this work, as described in the included manuscript, that the docking sites of Tau do not seem to be necessary for Tau to be phosphorylated by ERK2, at least in our *in vitro* condition with concentrated substrate. This might explain why an inhibitor targeting the docking groove of ERK2 is not efficient.

2. Inhibition ERK2 activity by PEA-15 *in vitro*

Scaffold proteins might have regulatory influence on MAP kinases. PEA-15, consisting of a death effector domain (DED) and a short carboxyl-terminal tail, has been shown by crystallographic studies to occupy ERK2 docking groove and bind to the activation loop in different phospho-isoforms (Mace et al. 2013). In addition, fluorescence assays show that PEA-15 is able to bind to ERK1/2 in different activation states, but poorly bind to another MAP kinase, p38 (Callaway et al. 2007). PEA-15 is considered as a regulator for ERK2 activity in cells (Formstecher et al. 2001; Whitehurst et al. 2004). It is suggested that PEA-15 might

be able to compete with other ERK substrates by blocking docking interaction, and a significant decrease and slow-down activity of ERK1/2 has been observed in Elk-1 phosphorylation *in vitro* after binding to PEA-15 (Callaway et al. 2007; Callaway et al. 2005).

Therefore, PEA-15 might be an effective inhibitor of enzymatic activity of ERK kinase in *in vitro* conditions. We first confirmed the inhibition effect of PEA-15 in Tau phosphorylation assay by recombinant active ERK2 *in vitro*. The mixture of 16 μ M PEA-15 with 0.5 μ M pTEpY ERK2 is incubated with 50 μ M Tau protein for 3H under conventional phosphorylation conditions. Control reactions are done with neither of ERK2 kinase and PEA-15, and with ERK2 kinase but no PEA-15. Reactions were stopped by heating at 75°C for 15min. The migration of each Tau sample in SDS-PAGE shows that the phosphorylation degree of Tau is apparently decreased in presence of PEA-15 compared to ERK-mediated Tau phosphorylation without PEA-15: Tau phosphorylated in presence of PEA15 appears to migrate faster in the gel, although not as fast as the unphosphorylated Tau control sample (Figure 39).

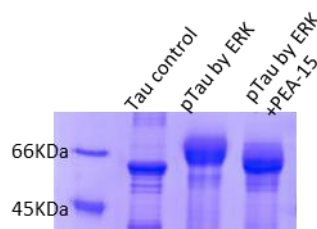
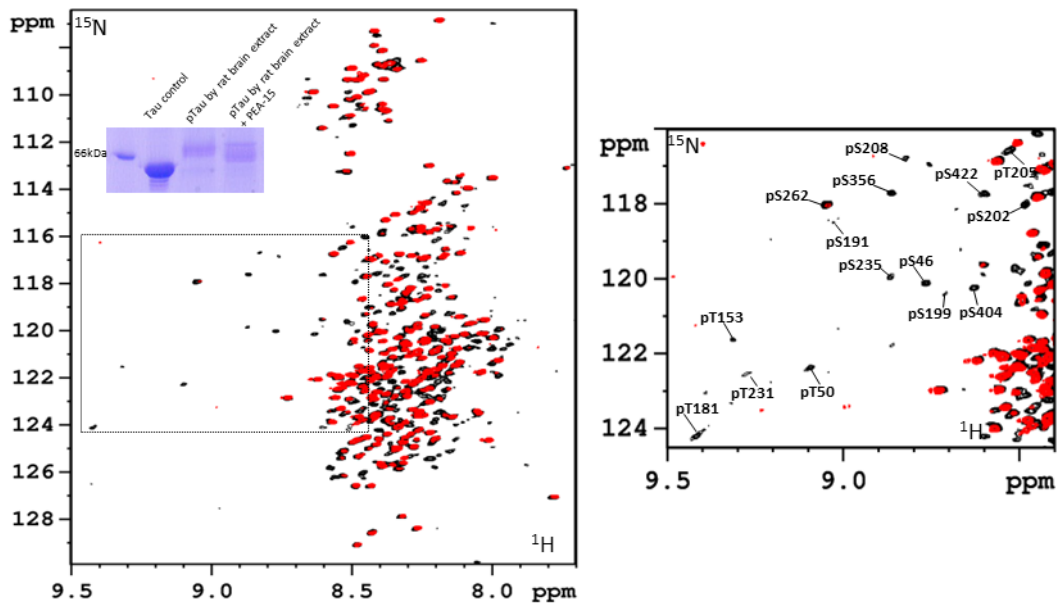


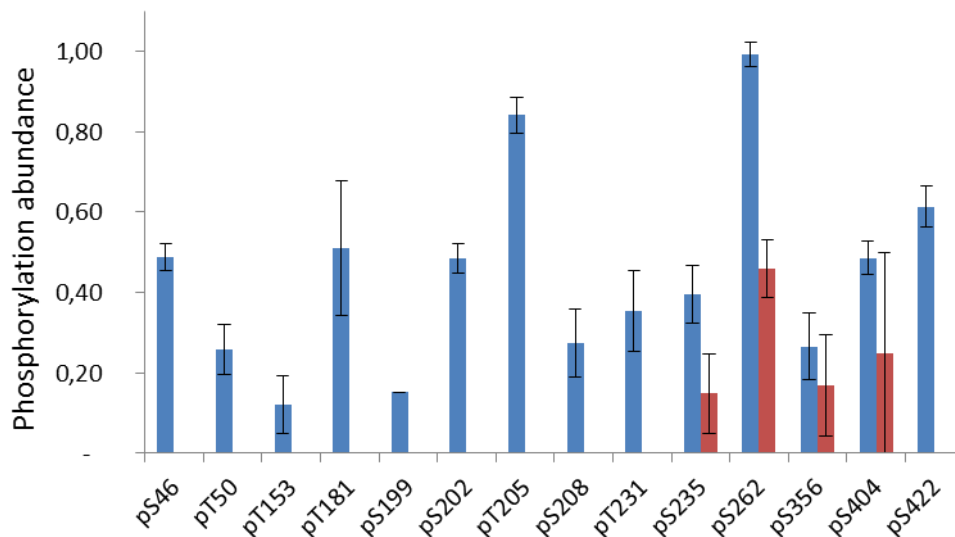
Figure 39: SDS-PAGE analysis of Inhibition effect of PEA-15 in ERK2-mediated Tau phosphorylation. Three samples are prepared: Tau control, ERK2-mediated Tau phosphorylation control and ERK2-mediated phosphorylation in presence of PEA-15. Around 5 μ g of each Tau sample is loaded in 12% acrylamide gel analyzed by SDS-PAGE. The migration of the sample prepared in presence of PEA-15 appears faster, around 60kDa, compared to ERK2-mediated phosphorylation without PEA-15.

As PEA-15 is capable of significantly decrease ERK2-mediated phosphorylation, it was next used in inhibition assays of Tau phosphorylation by rat brain extract. The preparation of rat brain extract and the compositions in the reaction of Tau phosphorylation by rat brain extract is described in 'attached Manuscript: "The study of posttranslational modifications of Tau protein by Nuclear Magnetic Resonance spectroscopy: phosphorylation of Tau protein

by ERK2 recombinant kinase and rat brain extract and acetylation by recombinant Creb-binding protein.” The inhibition assay is performed under the same reaction conditions, but in presence of 15 μ M inhibitor PEA-15. The mixture is next inactivated by heating at 75°C for 15min and the SDS-PAGE analysis is carried out before the preparation of sample for NMR analysis. In SDS-PAGE analysis, a faster migration is observed for phospho-Tau obtained in presence of PEA-15, indicating that PEA-15 partially inhibits the kinase activity of the rat brain extract, probably by inhibiting ERK1/2 activity in the extract (Figure 40). NMR study showed details about the inhibition of PEA-15 on specific phospho-sites. Overlaying the spectra of ¹⁵N-labelled Tau phosphorylated by rat brain extract with that of ¹⁵N-labelled Tau phosphorylated by rat brain extract in presence of PEA-15 showed that most of the resonances assigned as phospho-residues loss their intensities, in particular pS/pT in proline-directed motifs which can be found in ERK-phosphorylated Tau (Figure 40). Therefore, it suggests that active ERK1/2 kinase is present in the rat brain extract and takes an important part in the total kinase activity in rat brain extract. Residual phosphorylation is observed for pS²³⁵ and pS⁴⁰⁴ indicating that their phosphorylation might be partly mediated by other kinases. However, some decrease intensity is also observed for pS²⁶² and pS³⁵⁶ compared to the phospho-Tau obtained without PEA-15. These sites are not included in Pro-directed motifs and thus not expected to be phosphorylated by ERK1/2. It may be that inhibition of certain phosphorylation sites by ERK1/2 may interfere with phosphorylation by other kinases, or that the inhibition of ERK1/2 kinase may directly or indirectly influence the regulation of other kinases. Therefore, this experiment although strongly suggesting an ERK1/2 activity in the rat brain extract is not completely conclusive.



(A)



(B)

Figure 40: Inhibition of rat-brain-extract-mediated Tau phosphorylation by PEA-15. (A) SDS-PAGE analysis, shown included in the HSQC spectrum on the left, suggests that the presence of PEA-15 partly inhibits Tau phosphorylation by rat brain extract as the band migration is faster compared to the phosphorylated sample without PEA-15. In the NMR study, the 2D HSQC spectrum of ^{15}N -labelled phosphorylated Tau by rat brain extract (in black) is overlaid with the spectrum of ^{15}N -labelled phosphorylated Tau inhibited by PEA-15 (in red). Comparison of the red spectrum with the black one clearly indicates that most of the resonances corresponding to phospho-residues are not detected in the red spectrum. The phospho-residues are assigned in the region of the spectrum corresponding to the phospho-residues (on the right). Resonances are still detected for pS²³⁵, pS²⁶², pS³⁵⁶ and pS⁴⁰⁴. (B) The phosphorylation abundance of phospho-sites by rat brain extract

without or in presence of PEA-15. The phosphorylation levels are represented by relative integrals of corresponding resonances in HSQC spectra, and the error bars are calculated by S/N ratios of resonances for phospho-sites.

3. Inhibition ERK1/2 activity by anti-pTEpY ERK1/2 antibodies in rat brain extract

Besides PEA-15, the monoclonal anti-double-phosphorylated ERK1&2 antibodies (anti-pTEpY ERK1&2 antibodies) is also used as specific inhibitor of ERK activity. First, to confirm the presence of active ERK in the brain extracts, brain extracts from three individual mice are prepared and probed by anti-pTEpY ERK antibodies by western blot analysis. A positive signal is detected at a size expected for the ERK1/2 kinase (Figure 41, A). As positive control, 40ng, 80ng and 120ng of recombinant pTEpY ERK2 are deposited in the last three lanes of gel and are indeed recognized by anti-pTEpY ERK1/2 antibodies. 7 μ l of mice brain extracts at around 7 μ g/ μ l of total protein concentration are deposited in the first three lanes. Compare to the intensities of the control samples, an estimation of 50ng of active ERK kinase is present in 49 μ g of total protein in each gel sample from mice brain extracts. Based on this assay, the concentration of active pTEpY ERK is estimated at about 0.1 μ M in mice brain extracts.

As we show that anti-pTEpY ERK1/2 antibodies recognize both recombinant pTEpY ERK and active ERK in mice brain extracts, we next use it to block the activity of ERK1/2 in rat brain extract. To ensure the blockage of ERK activity, we mix a large excess of anti-pTEpY ERK1/2 antibodies with rat brain extract, so 22.5 to 30 μ g anti-pTEpY ERK antibodies are mixed with around 20 μ g rat brain extract, then incubated with 8 μ M Tau protein in 25 μ l phosphorylation buffer at 37°C for 24H reaction. The samples are analyzed by SDS-PAGE to compare the migration of the resulting phosphorylated Tau in comparison with unphosphorylated Tau and phospho-Tau obtained under the same condition without addition of anti-pTEpY ERK1/2 antibodies (Figure 41). The migration in acrylamide gel herein showed that anti-pTEpY ERK1/2 antibodies decrease the phosphorylation degree of Tau by rat brain extract, but do not inhibit entirely Tau phosphorylation compared to the migration position for Tau control (Figure 41). However, further NMR study about blockage of ERK activity in rat brain extract was not possible due to the limitation of the quantities of anti-pTEpY ERK1/2 antibodies available. SDS-PAGE analysis for the inhibition of ERK1/2 activity

assay at least confirms the presence of active ERK in the extract and its contribution in Tau phosphorylation by rat brain extract *in vitro*.

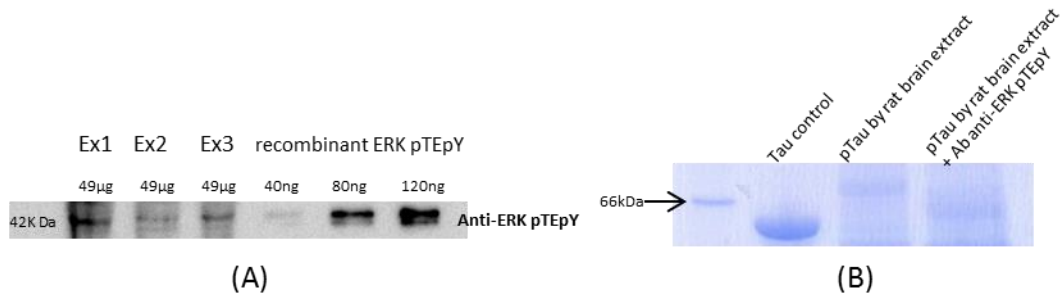


Figure 41: (A) Estimation of the amount of pTEpY ERK1/2 in mice brain extracts using monoclonal anti-pTEpY ERK1/2 antibodies (anti-diERK1/2, 1.5-2.0mg/ml, SIGMA 9692) and western blotting. Three independent mice brain extract were prepared and the total protein concentration in brain extract estimated by Bradford colorimetric assay. 7µl of three mice brain extracts at 7µg/µl total protein concentration, and 40ng, 80ng and 120ng of recombinant pTEpY ERK2 are loaded on the acrylamide gel. (B) The anti-pTEpY ERK1/2 antibodies is used to inhibit ERK1/2 activity on Tau phosphorylation by rat brain extract. Around 8µg of each Tau samples are loaded in 12% acrylamide gel. Compared to the band for Tau control that appears at a position corresponding to 60kDa and for Tau phosphorylated by rat brain extract that appears at position corresponding to 70kDa, the band for phospho-Tau obtained in presence of anti-pTEpY ERK1/2 antibodies has an intermediate migration, around 65kDa. The sample is also more heterogenous in its degree of phosphorylation and the band appeared consequently as a smear.

4. Conclusion:

The active ERK kinase is detectable either in rat or mouse brain extracts. The kinase activity of brain extracts can be inhibited by addition of PEA-15 and by monoclonal anti-active ERK1/2 antibodies that both specifically target ERK. In addition to the similar pattern of phosphorylation observed by ERK2 and rat brain extract, as defined by NMR spectroscopy and described in the included manuscript, these results strongly suggest that the ERK2 kinase corresponds to a major part of the kinase activity in the extracts. However, it was difficult to be completely specific in our inhibition of the kinase activity, and we had to add large amount of the inhibiting proteins. For these reasons, the results are not conclusive.

manuscript in preparation:

Characterization of the neuronal Tau protein as a target of the ERK kinase

Haoling Qi^{1,2}, Sudhakaran Prabakaran³, François-Xavier Cantrelle^{1,2}, Béatrice Chambraud⁴, Jeremy Gunawardena³, Guy Lippens^{1,2}, Isabelle Landrieu^{1,2}

1 UMR8576 CNRS-Lille University, F-59000 Lille, France.

2 FraBio3688 F-59000 Lille, France.

3 Department of Systems Biology, Harvard Medical School, Boston, MA 02115, USA.

4 INSERM, Unité mixte de recherche 788, Université Paris XI, Kremlin Bicêtre, France

Characterization of the neuronal Tau protein as a target of the ERK kinase

Haoling Qi^{1,2}, Sudhakaran Prabakaran³, François-Xavier Cantrelle^{1,2}, Béatrice Chambraud⁴, Jeremy Gunawardena³, Guy Lippens^{1,2}, Isabelle Landrieu^{1,2}

From: ¹ UMR8576 CNRS-Lille University, F-59000 Lille, France. ² FraBio3688 F-59000 Lille, France. ³ Department of Systems Biology, Harvard Medical School, Boston, MA 02115, USA. ⁴ INSERM, Unité mixte de recherche 1195, Université Paris SUD, Le Kremlin Bicêtre, France

Running title: *Phosphorylation of Tau by ERK2*

To whom correspondence should be addressed: Dr Isabelle Landrieu, RMN, IRI Building (CNRS) Parc scientifique de la Haute Borne 50, avenue de Halley, 59650 Villeneuve d'Ascq FRANCE Telephone:+33362531702 E-mail: isabelle.landrieu@univ-lille1.fr

Keywords: Tau protein (Tau), Extracellular-signal-regulated kinase (ERK), protein-protein interaction, nuclear magnetic resonance (NMR), aggregation

ABSTRACT

Tau neuronal protein has a central role in neurodegeneration and is implicated in Alzheimer's disease development. Dysregulation of Tau in pathological conditions is correlated with abnormal phosphorylation that impairs its interaction with other proteins. Tau is found aggregated in neurons affected by the disease, typically in paired helical filaments constituted of hyperphosphorylated Tau. Molecular mechanisms leading to pathological Tau are unknown. Here, we characterized Tau phosphorylation by ERK2 kinase, a MAP kinase that responds to extracellular signals. Analysis of *in vitro* phosphorylated Tau by activated recombinant ERK2 with NMR spectroscopy revealed phosphorylations of 15 Ser/Thr sites. *In vitro* phosphorylation of Tau using rat brain extract and subsequent NMR analysis identified the same sites. Phosphorylation with rat brain extract is known to result in transformation of Tau into an AD-like state. Our results indicated that phosphorylation of Tau by ERK2 kinase alone was sufficient to produce the same characteristics. We then investigated the mechanism of ERK2 phosphorylation of Tau. Kinases are known to recognize their protein substrates not only by their specificity for a targeted Ser or Thr phosphorylation site but

also by binding to peptidic linear motifs located outside of the phosphorylated motif, called docking sites. We identified two main docking sites along the Tau sequence using NMR spectroscopy. Our results suggest that ERK2 dysregulation in Alzheimer's disease could lead to abnormal phosphorylation of Tau resulting in the pathology of the disease.

INTRODUCTION

Tau is an intrinsically disordered protein whose primary sequence is divided into several functional domains: an N-terminal region, a Proline-Rich Domain (PRD), a MicroTubule Binding Domain (MTBD) constituted of partially repeated sequences R1 to R4, and a C-terminal region (**Fig. 1A**). Both PRD and MTBD are involved in microtubule stabilizing activity of Tau (1, 2).

Phosphorylation of Tau is an essential process to regulate its physiological function(s); however, abnormal phosphorylation of Tau has been linked to neuronal dysfunction (365). In Alzheimer's disease (AD) Tau is hyperphosphorylated and aggregated (6). The longest Tau protein isoform (441-residue) has 80 Threonine (T) and Serine (S) residues, exposed as Tau is an intrinsically disordered protein, subject to modification by numerous kinases (7). Mass

spectrometry (MS) analyses have identified around 45 sites to be phosphorylated on Tau aggregates, extracted from AD patients, with a typical paired helical filament (PHF) morphology (8, 9) against 15 to 30 in soluble Tau extracted from mice (10) or normal human brain (11). Monoclonal antibodies such as the AT8 (recognizing pS202/pT205, (12)) or the PHF1 (pS396/pS404, (13)) antibodies are often used as empirical disease markers (5). Proline-directed kinases, with a S/T-P phosphorylation consensus motif, such as Cyclin-dependant kinase 5 (CDK5, (14, 15)) with its activator protein p25, glycogen synthase kinase (GSK3, (16)), stress-activated protein kinases (JNK, (17) and p38, (18)) and extracellular-signal-regulated kinase (ERK1/2, (19)), are considered as potential therapeutic targets against Tau hyperphosphorylation (20). A clear understanding of the mechanism of abnormal phosphorylation of Tau and Tau species responsible for neuronal dysregulation are still lacking. Characterization of the disease-related kinases and the related specific patterns of phosphorylation are therefore of interest to develop new strategies to counteract the pathological processes.

ERK2 kinase belongs to the mitogen-activated protein kinase (MAPKs) family and is activated by dual phosphorylation on a Thr-X-Tyr sequence in its activation loop by MAP kinase kinases (MKK) (21,23). Human ERK2 is phosphorylated on Thr183 and Tyr185 by MEK kinase. MAP kinases have classical kinase structure with a N-terminal lobe folded as a beta sheet associated to a larger C-terminal domain constituted of alpha-helices (24). The activation loop is located at the hinge between these domains and shows a large conformational change upon phosphorylation (25). The mechanisms regulating specificity and efficiency of kinases are not fully understood but involve the binding of kinase docking grooves to binding motifs on their protein substrates,

constituted of linear peptides (26, 27). Interaction regions distinct from the catalytic pocket were found to be involved in the recognition of both ERK1/2 upstream regulators and downstream substrates (28, 29). The ERK docking site is targeted by proteins that contain a linear motif called D-recruitment site (DRS or D-site), defined by a loose consensus of about 10 amino acid residues $\Psi_{1-3} X_{3-7} \Phi X \Phi$ (Ψ , Φ , and X refer to positively charged, hydrophobic, or any intervening residues, respectively, and subscripts refer to the number of residues, (30)). Additionally, the same docking groove on ERK2 can accommodate a reverse consensus revD-site $\Phi X \Phi X_{3-7} \Psi_{1-3}$, bound in a C- to N- orientation (30, 31). Interactions of the conserved D and revD motifs with the MAP kinase docking site have been characterized at the atomic level in complexes of ERK2 with peptide fragments from several protein partners (30, 32,34). Another docking motif was found, called F-recruitment site (FRS or F-site) that recognizes a Phe-X-Phe motif (35).

ERK1/2 kinase activation in AD brain is well documented (36,38). Previous studies propose that ERK1/2 is able to transform Tau into an AD-like state, although mainly documented by the detection of the AT8 epitope (19). To better define the phosphorylation sites that participate in the reconstitution of this AD-like state of Tau (19), we used NMR spectroscopy. We observed that 14 out of the 17 S/T-P sites are phosphorylated by activated recombinant ERK *in vitro*. Another well-known *in vitro* model of Tau hyperphosphorylation is obtained by incubation with rat brain extracts blocked for dephosphorylation by okadaic acid (39). We compared phosphorylation patterns of Tau obtained using rat brain extract with phosphorylation pattern obtained using *in vitro* activated recombinant ERK2. A similar pattern of Tau phosphorylation was indeed observed, reinforcing the point that ERK kinase by itself can transform Tau into an hyperphosphorylation state. We then studied Tau-ERK2 interaction. We mapped the

interaction sites of ERK2 along the Tau sequence and demonstrate an interaction mediated by two docking sites in the MTBD that is distal to the PRD containing most of the ERK phosphorylated sites of Tau. We conclude that Tau and ERK2 form a dynamic complex, Tau being the first example of an ERK2 substrate with multiple docking sites. These conclusions expand our view on the potential role of ERK2 in Tau neurodegeneration pathway in AD and shed light on the molecular mechanisms leading to pathological Tau formation.

EXPERIMENTAL PROCEDURES

Molecular cloning cDNA encoding peptides Tau[220-240] and Tau[271-294] were amplified from Tau full length cDNA by PCR. The cDNA were cloned by a ligation independent protocol into vector pETNKI-HisSUMO3-LIC (40).

Preparation of recombinant proteins The longest isoform of Tau (441 amino acid residues) and the Tau fragments Tau[165-245], and Tau[244-372] (K18) were expressed and purified as recombinant proteins from *Escherichia coli* B121(DE3) (New England Biolabs) using pET15b plasmid (Invitrogen) under the control of T7lac promoter. Tau fragment Tau[220-240], Tau[271-294] were expressed as N-terminal fusion with the SUMO protein presenting a N-terminal HisTag from a modified pET vector (40).

Bacteria were grown in LB medium at 37°C and recombinant protein production induced with 0.4mM Isopropyl-1-thio- β -D-galactopyranoside. Isotope labeling was performed using a modified M9 medium containing in addition to the M9 salts, MEM vitamin mix 1X (Sigma), 1g of ^{15}N NH_4Cl and 4g of glucose or 2g of ^{13}C glucose and 200mg of complete medium powder (Celtone Complete Medium, Cambridge Isotope Laboratories) per liter of bacterial culture. Briefly, Tau protein, Tau[165-245] and Tau[244-372] fragments were purified by first heating the bacterial extract 15 minutes at 75°C. Purification next consisted

in cation exchange chromatography with a sodium phosphate buffer at pH 6.5 (Hitrap SP sepharose FF, 5 ml, GE healthcare) for Tau and Tau[165-245] and Ni-chelating chromatography for Tau[244-372] (Hitrap Ni-sepharose FF, 5 ml, GE healthcare). Full length Tau protein and Tau fragments were then buffer exchanged against ammonium bicarbonate (Hiload 16/60 desalting column, GE Healthcare) for lyophilisation. His-SUMO Tau[220-240], His-SUMO Tau[271-294] were purified by affinity chromatography on Ni-NTA resin following standard conditions. The fusion proteins were buffer-exchanged using a PD-10 column (G25 resin, cut-off of 7kDa, GE Healthcare) against 10mM HEPES pH7.6, 100mM NaCl, 1mM DTT to be frozen for conservation.

Recombinant His₆-tagged p42 MAP kinase (ERK2) from *Xenopus laevis* was prepared by growing bacteria transformed with a ERK recombinant T7 expression plasmid in LB medium until induction by 1mM IPTG of the protein production for a period of 4 hours, at 37°C. His-ERK2 was purified by affinity chromatography on Ni-NTA resin following standard conditions. After analysis on SDS-PAGE, the pooled fractions were buffer-exchanged using a PD-10 column (GE Healthcare) against conservation buffer 50mM Tris-HCl, 150mM NaCl, 0.1mM EGTA, 50% glycerol, pH 7.5 and kept frozen at -80°C. Activated-ERK2 was prepared as previously described (41).

To label Tau with CF₃ attached on its native Cys residues (C291 and C322), 100 μM ^{15}N Tau or ^{15}N Tau[244-372] in 50mM ammonium bicarbonate were first thoroughly reduced by incubation for 2H at 22°C with 1mM Tris (hydroxymethyl) phosphine reducing agent. The protein samples were next incubated with 2mM 2-iodo-N-trifluoroethyl acetamide (EnamineStore) in dimethyl sulfoxide at 22°C for 3H. The excess of 2-iodo-N-trifluoroethyl acetamide was removed by desalting. The ^{15}N CF₃-Tau samples were lyophilized.

In vitro phosphorylation of Tau protein ^{15}N -labelled recombinant Tau was used as substrate to assay the activity of activated ERK2 kinase. $100\mu\text{M}$ of ^{15}N Tau or ^{15}N Tau[165-245] is incubated with $1\mu\text{M}$ of ERK2 kinase enzyme at 37°C during 3h in $200\mu\text{L}$ of phosphorylation buffer 50mM Hepes pH 8.0, 50mM NaCl, 12.5mM MgCl_2 , 2.5mM ATP, 2mM DTT, 1mM EDTA, 2mM EGTA and protease inhibitor cocktail (ROCHE, Complete Inhibitors without EDTA). To identify the phosphorylation sites by NMR spectroscopy ^{15}N , ^{13}C -doubly labeled Tau was incubated in the same conditions overnight with the activated recombinant ERK2 kinase. Enzymatic incubation was terminated by 15 min heating at 75°C followed by centrifugation. The phosphorylation mixture was buffer-exchanged using desalting centrifugal devices (0.5ml bed of G25 resin, cut-off of 7KDa , Thermo Scientific Zeba Desalting Columns) against NMR buffer (50mM deuterated-Tris, pH 6.65, 25mM NaCl, 2.5mM EDTA, 1mM DTT and 10% D_2O). Phosphorylation of the Tau[165-245] by ERK2 followed the same protocol. The rat brain extract was prepared by homogenizing a brain (about 2g) in 5ml of homogenizing buffer (10mM Tris.Cl pH 7.4, 5mM EGTA, 2mM DTT, $1\mu\text{M}$ okadaic acid (Sigma) supplemented with $20\mu\text{g/ml}$ Leupeptin and 40mM Pefabloc (39). Ultracentrifugation was next performed at 100000g for 1 hour at 4°C . The supernatant was directly used for its kinase activity. Total protein concentration was estimated to be 7mg/ml by Bradford colorimetric assay. The ^{15}N -Tau protein ($1-1.5\text{mg}$) was dissolved at 10M in 2.5mL of phosphorylation buffer (2mM ATP, 40mM Hepes.KOH pH 7.3, 2mM MgCl_2 , 5mM EGTA, 2mM DTT complemented with a protease inhibitor cocktail (Complete $\hat{\text{I}}$, Roche) and $1\mu\text{M}$ okadaic acid (Sigma)). The phosphorylation reaction was performed at 37C for 24H with $500\mu\text{l}$ of brain extract. The mixture was next heat-inactivated at 75°C for 15min . Reaction mixtures were buffer-exchanged against 50mM

Ammonium bicarbonate before lyophilization. Phosphorylation of the Tau[165-245] by rat brain extract kinase activity followed the same protocol. The samples were prepared by solubilizing the lyophilized powder into NMR buffer. Each set of experiment was independently repeated two or three times.

NMR Spectroscopy Analysis of the phospho-Tau samples by NMR spectroscopy was performed at 293K or 298K on Bruker 600MHz and 900MHz spectrometers equipped with a triple resonance cryogenic probehead (Bruker, Karlsruhe, Germany). TMSP (Trimethylsilyl propionate) was used as the reference (0 ppm , part per million). $100\mu\text{M}$ ^{15}N Tau in volume of $200\mu\text{l}$ in 3mm tubes was sufficient to obtain the $2\text{D } ^1\text{H}, ^{15}\text{N}$ HSQC (Heteronuclear Single Quantum Correlation) spectra with 32 scans. HSQC 2D experiments to map the interaction between the Tau protein and recombinant ERK2 kinase were recorded at 293K on a 900MHz Spectrometer with 64 scans per increment, as a complex matrix of 2048×416 complex points for $14 \times 25\text{ ppm}$ spectral widths in the proton and nitrogen dimensions, respectively. HNCACB 3D spectra were recorded for ^{15}N , ^{13}C phospho-Tau obtained both with rat brain extract and recombinant ERK2 kinase with a standard Bruker pulse sequence. A 3D HNCaNNH spectrum (42) was additionally used in the assignment. 3D HNCACB experiments were acquired to confirm the assignment of the Tau residues in ^{15}N , ^{13}C His-SUMO Tau[220-240] and ^{15}N , ^{13}C His-SUMO Tau[271-294]. For Fluor NMR experiments, the lyophilized ^{15}N CF_3 -Tau and ^{15}N CF_3 -Tau[244-372] were suspended in Phosphate NMR Buffer consisting in Phosphate Buffer Saline, pH7.4, 2.5mM EDTA and 2mM DTT. $50\mu\text{M}$ of CF_3 -Tau or CF_3 -Tau[244-372] in $200\mu\text{l}$ Phosphate NMR buffer were titrated with increasing concentration of His-ERK2 ($25\mu\text{M}$, $50\mu\text{M}$, $100\mu\text{M}$, $125\mu\text{M}$, $162\mu\text{M}$ and $220\mu\text{M}$). The $1\text{D } ^{19}\text{F}$ spectra were recorded at 293K , with 1024 scans, on a Bruker 600MHz Avance NMR

spectrometer equipped with a 5mm CPQCI $^1\text{H}/^{19}\text{F}-^{13}\text{C}/^{15}\text{N}$ cryogenic probehead (Bruker, Karlsruhe, Germany). The chemical shifts in 1D ^{19}F spectra were referenced by using the fluor resonance of external Trifluoroacetic acid at -76 ppm.

NMR data processing Spectra were processed with Bruker TopSpin 3.1 software. Data analysis, peak picking and calculation of peak volumes were done with Sparky 3.114 software (T. D. Goddard and D. G. Kneller, SPARKY 3, University of California, San Francisco). Assignment of resonances of pT and pS phosphorylated residues is based on the typical ^1H and ^{13}C chemical shifts of these residues (43). pS and pT resonances were assigned to a specific residues in phospho-Tau primary sequence using as additional information the ^{15}N , ^{13}C and ^1H chemical shifts of their N-terminal residue (44646) (Table 1). Resonance integration was performed by summing all the intensities over a box enclosing the peak of interest. To account for variations between spectra, integration volumes were normalized to the integration value of the C-terminal residue, which is isolated in the spectrum and not influence by the phosphorylation(s). To estimate level of phosphorylation at each site, we first estimated the level of phosphorylation on T153 residue using the resonances of A152. A152 has two distinct resonances in the 2D ^1H , ^{15}N spectrum depending on the phosphorylation status of T153 residue. The ratio of the integration volumes of these A152 resonances gives an estimation of the phosphorylation degree of T153. We next use this value to correlate integration volumes of resonances with phosphorylation level of the corresponding phospho-residue.

Interaction of ERK2 with Tau, Tau fragments and Tau peptides ERK2 buffer-exchange after storage was done using desalting centrifugal devices (1.5ml bed of G25 resin, cut-off of 7kDa, Thermo Scientific Zeba Desalting Columns). ERK2 protein in Tris NMR buffer was then

concentrated to a volume of 200 μl using a centrifugal concentrator (0.5ml, 30K membrane, Amicon Ultra) up to 250 μM . The concentrated enzyme solution was directly used to suspend lyophilized ^{15}N Tau, ^{15}N Tau[244-372] (K18) and ^{15}N Tau[165-245] to a final concentration of 50-80 μM labeled samples. For the interaction with Tau peptides, ^{15}N His-Sumo Tau[220-240] peptide or ^{15}N His-SUMO Tau[271-294] peptide were directly mixed with ERK2 in the NMR buffer to a final concentration of 50 μM labeled peptides. The ERK2 samples were prepared freshly prior to the NMR experiments due to the tendency of the ERK2 protein to precipitate in the NMR buffer conditions.

RESULTS

Identification of Tau amino acids phosphorylated in vitro by ERK2 - We here use NMR spectroscopy to identify the phosphorylation sites of Tau *in vitro* modified by ERK2 kinase. On incubation with MEK-activated recombinant ERK2 (doubly phosphorylated on T183EY185), several additional resonances can be observed in the ^1H , ^{15}N 2D spectrum for the resulting phospho-Tau, compared to the spectrum of the unphosphorylated Tau (compare **Fig. 1 B** and **C**). These resonances are typical for the HN amide resonances of pS and pT residues (43, 45), indicating that Tau is indeed phosphorylated at many sites by ERK2. Phosphorylation sites were identified using 3D triple resonance NMR spectroscopy on a ^{15}N , ^{13}C -labelled Tau phosphorylated *in vitro* by activated ERK2. Of the 17 pS/pT-P sites 14 sites along the Tau sequence were found phosphorylated by ERK2 (**Fig. 2A, B, Table 1**). ERK2 phosphorylates T50, T153, T175, T181, T205, T231, S235, S404 and S422 with a stoichiometry over 50%, estimation based on peak integration (46)(**Fig. 2B, Table 1**). In addition, a minor phosphorylation is observed for S191 which is not a Pro-directed site (**Fig. 2, Table 1**). Phosphorylation by ERK2 of a Tau[165-245] fragment encompassing the PRD of

Tau allowed to confirm the identification of the phosphorylation sites located in this domain (**Fig. 2C**). Comparison with previous assignments of the NMR amide cross peaks corresponding to Tau Proline-directed phosphorylation sites, generated by CDK2/CycA3 or GSK3 kinases (47, 48), further confirmed identifications of the ERK2 phosphorylation sites located in the PRD and C-terminal region.

Comparison of ERK2-phosphorylated Tau with an hyperphosphorylation model of Tau

Phosphorylation of S/T residues corresponding to 12 to 15 sites has similarly been reported after incubation of Tau with rat brain extract (12, 39, 49). The site-specific, precise pattern of the hyperphosphorylation of Tau by rat brain extract was however never investigated. We therefore use NMR spectroscopy to establish the map of Tau amino acid residues phosphorylated by kinases in rat brain extract and compare with those phosphorylated by ERK2 kinase. Rat brain extracts were used to *in vitro* phosphorylate recombinant ^{15}N -labelled Tau. The corresponding ^1H , ^{15}N 2D spectrum of the phosphorylated Tau showed additional resonances in the region for pT and pS residues, compared to the spectrum of the unphosphorylated Tau (**Fig. 1**, compare **D** and **B**). Comparison of 2D spectra of Tau phosphorylated by either activated ERK2 or rat brain extracts shows that many resonances assigned to the ERK2 phosphorylated sites have a match in the brain extract phosphorylated Tau (**Fig. 2A** and **B**). To confirm that the similarity in the phospho-Tau spectra reflects a shared phosphorylation pattern, phosphorylation sites were identified using 3D triple resonance NMR spectroscopy on a ^{15}N , ^{13}C -labelled Tau phosphorylated *in vitro* by rat brain extract. The major modified sites of Tau correspond to pS46, pT50, pT153, pT175, pT181, pS202, pT205, pS208 pT231, pS262, pS356, pS396, pS404 and pS422 (**Fig. 2**). This analysis confirmed that the

overlapping resonances in the 2D spectra indeed correspond to the same phosphorylated residues. The level of phosphorylation for these residues is also similar between Tau phosphorylated by the rat brain extract or the activated ERK2 (**Fig. 2B**). A few additional Tau phosphorylation sites are also identified exclusively from the incubation with the rat brain extract including pS208, pS262 and pS356 that are not proline-directed sites (**Fig. 2B**). Phosphorylation with the brain extract of Tau[165-245] fragment, corresponding to the PRD, resulted in detection in the corresponding 2D ^1H , ^{15}N HSQC of resonances corresponding to phosphorylated residues. These phosphorylated sites matched those found in the PRD embedded in the full-length phosphorylated Tau protein (**Fig. 2D**), confirming the assignment. The data showed that the pattern of phosphorylation obtained solely by ERK2 kinase activity is similar to the one of the hyperphosphorylated Tau obtained by incubation with rat brain extract.

Identification of ERK2 docking site(s) on the Tau protein

MAP kinases recognize their substrates not only by the phosphorylation S/T-P motifs but also by docking motifs. We thus next investigated the mechanism of Tau recognition by ERK2. In order to map potential docking sites, 2D spectra of ^{15}N -Tau mixed with recombinant ERK2 were compared to a reference spectrum from the ^{15}N -Tau protein free in solution (**Fig. 3A, D**). The resonances in these spectra are sensitive to their chemical environment and the local protein dynamics, an interaction affecting their chemical shifts and/or intensities. At a 1:5 ^{15}N Tau/ERK2 molar ratio, an interaction indeed translates into an important broadening for numerous resonances compared to the reference spectrum (**Fig. 3A, D**). Assignment of the Tau protein resonances has been previously completed by us and others (50, 51) and was used to map the interaction region(s) based on the 2D spectra perturbations. Peak intensities were compared for 187

resonances corresponding to residues dispersed along the 441 amino-acid residue Tau sequence (**Fig. 3F**). The data showed interaction of ERK2 localized mainly in the MTBD of Tau (Tau[244-372]) (also called K18 (1)). To increase the resolution, the interaction experiment was repeated to increase the resolution with Tau fragments, Tau[165-245] corresponding to the PRD and Tau[244-372] corresponding to the MTBD (**Fig.3, Fig.4**). Addition of ERK2 to the ^{15}N -Tau[165-245] resulted in minor perturbations of the resonances in the corresponding 2D spectrum (**Fig.3B**) while an interaction of ERK2 with Tau[244-372] is clearly observed as the intensity of several resonances in its spectrum is affected (**Fig.3C,E, Fig.4A**). The intensity of the resonances corresponding to amino-acids included in Tau[274-288] and Tau[306-318] segments strongly decreased in presence of ERK2 (**Fig. 4A**, I/I0 below 40%). The sequences of these peptides can accommodate a D-site K₂₇₄VQIINKKLDL_{L284} and revD-site V₃₀₆QIVYKPV_{DL}SK₃₁₇ docking peptides, respectively (**Fig. 4B**). These ERK2 docking sequences also correspond to respectively the PHF6* (V₂₇₅QIINK₂₈₀) and PHF6 (V₃₀₆QIVYK₃₁₁) peptides described as nuclei of Tau aggregation (52). Resonance intensities of residues in Tau[346-358] segment also showed a decrease upon ERK2 interaction but to a lesser extent (**Fig. 4A**, I/I0 below 60%). This region could correspond to a secondary binding site of interaction, although it is not clear if it fits a classical ERK2 docking site.

Apparent K_d were calculated using fluor NMR spectroscopy (53) to confirm that the main binding is located in the MTBD (**Fig.5**). The Tau protein and Tau[244-372] (MTBD) were labelled with fluor attached on the native Cys residues C291 and C322 along the sequence (**Fig. 4**). Chemical shift value perturbation of the fluor signal along titration of the ERK2 protein on the labelled Tau or Tau fragment showed a saturation behaviour typical of an interaction (**Fig. 5**). The similar apparent K_d values of 73 μM for

Tau and 179 μM for Tau[244-372] fragment indicated that the main binding indeed occurs within the Tau[244-372] segment. K_d in the 100 μM -range is compatible with docking function of the interaction. The data demonstrate that the main binding sites of Tau for ERK2 are localized in the MTBD of Tau, in the Tau[244-372] segment, outside of the regions containing ERK2 phosphorylation sites.

Tau peptides interaction with ERK2

kinase Two peptides were next chosen to confirm whether they interact individually, or not, with the ERK2 kinase docking site. The first peptide derived from the Tau sequence, Tau[220-240] in the PRD, contains several ERK2 phosphorylation sites but no interaction site for ERK2. On the other hand, F[271-294]Tau contains the Tau[274-284] sequence here above defined as an ERK2 docking site. As the Tau[271-294] peptide showed a limited solubility (PHF6*), fusions with the SUMO protein were used, both for the recombinant expression and 2D spectra acquisition. SUMO being a small folded protein, the overlap with the Tau peptide signals was reasonable and therefore allowed a correct analysis of the Tau resonances (**Fig. 6**). Overlay of the 2D ^1H , ^{15}N HSQC of the fusion peptides alone or mixed with ERK2 confirms that the resonance perturbations affected only those resonances corresponding to the Tau peptides and not to the SUMO fusion protein (**Fig. 6**). The resonances corresponding to the Tau residues in SUMO-Tau[220-240] are only slightly affected by addition of ERK2 kinase (**Fig. 6A, C**). To the contrary, addition of the kinase to the SUMO-Tau[271-294] affected peak intensities of most of the resonances and principally residues 274 to 284 (**Fig. 6B, D**). The peptides Tau[220-240] and Tau[271-294] behaved in their interaction with ERK2 in the same manner embedded in the protein or isolated from their context. The data confirmed the sequence K₂₇₄ to L₂₈₄ as a docking site of ERK2. Despite the presence in the Tau[220-240] of predicted D

and revD docking sites consensus sequences (**Fig. 4**), no binding to ERK2 is observed.

DISCUSSION

We have here identified using NMR spectroscopy Tau phosphorylation sites modified *in vitro* by the recombinant ERK2 MAP kinase and rat brain extracts. We demonstrate that the Tau phosphorylation patterns observed with *in vitro* phosphorylation by ERK2 kinase and rat brain extracts were similar, with most of the 17 S/T-P motifs modified. Accordingly, incorporation of 14 to 16 phosphates on S/T-P sites per Tau molecule was reported by the MAPK activity purified from the brain extract (19). Our previous analysis of Tau phosphorylation patterns obtained *in vitro* by several Tau kinases showed that none of them has the capacity to modify such a large number of phosphorylation sites (44, 47, 48, 54). Phosphorylation by brain extracts is a method to obtain *in vitro* phosphorylated Tau (12, 39) with AD-like characteristics (49), such as a reduced electrophoretic mobility on SDS-PAGE and positive immunodetection of the AT8 epitope (12, 39) and the pS396/pS404 epitope (55). Our work shows that the ERK2 kinase by itself has also the potential to modify the Tau protein into a phosphorylation state resembling the one of the AD-Tau.

Our analytical characterization of Tau phosphorylation showed that ERK2 kinase is promiscuous as most of Tau S/T-P motifs were phosphorylated. The question of how MAP kinases recognize specific substrates is only partially answered. We characterized interaction of ERK2, mediated by two main docking sites, in the MTBD of Tau. To our knowledge, Tau is the first example of ERK2 protein substrate to contain a combination of docking sites. A similar combination of 3 D-docking sites was described in the regulatory disordered N-terminal region of MKK7 used for the specific recognition by the JNK MAP kinase (56, 57). Another type of a modular system of recognition was previously proposed

consisting of a combination of the D-docking site and F-docking site, although in this case it corresponds to two distinct binding grooves of ERK2 (35). Two binding sites on the substrates for one recognition groove of ERK2 allows the formation of a dynamic complex (58), defined as involving more than 2 transient interfaces between the binding partners. The high concentration of interaction sites on a flexible ligand such as Tau, termed allovalency, increases the probability of the rebinding of the protein partner (59).

Comparison of the Tau interacting peptides with the degenerate ERK2 recognition sequence $\Psi_{1-3}X_{3-7}\phi X\phi$ (with Ψ for Arg/Lys residues, x for any residue and ϕ for hydrophobic residues, the indices corresponding to the number of residues (29, 30) shows that the first peptide Tau[274-284] corresponds to predicted classical D-docking along the Tau sequence (**Fig. 4**). However, the second peptide Tau[306-317] that was experimentally defined as interacting with ERK2 is best fitted with a reverse recognition sequence (30), starting from hydrophobic residues, as $\phi X\phi X_{3-7}\Psi_{1-3}$. It is proposed that the classical D-motif docking peptides efficiently distinguished only JNK from ERK2 and p38, and only motifs containing a reversed N- to C-terminal consensus sequence compared to classical D motifs could discriminate between the latter two MAPKs (30). The use of a combination of these linear motifs could thus be a solution to compensate the lack of specificity of promiscuous active sites (60). We showed that Tau[165-245] fragment does not contain a docking site for ERK2. Nevertheless, phosphorylation of Tau[165-245] by activated ERK2 kinase showed a similar pattern and level of phosphorylation as with the full length Tau substrate (**Fig. 2**). This suggests that the enzymatic activity is not affected by the docking and that the phosphorylation of the PRD might not require the ERK2 docking in the MTBD, at least in the equilibrium conditions of our experiments. The essentiality of docking

sites for ERK2 to exert its efficient kinase activity is not established (29, 61, 62). Kinetic studies demonstrate that docking sites that interact with either the DRS or the FRS have little effect on the intrinsic catalytic activity of ERK2 (61). In a proteomic study, a D-docking peptide was found only on 17% of the substrates within 20 amino acid of the phospho-site (62). However, a peptide-based study shows to the contrary that a docking site is necessary to mimick a ERK2 substrate (29). It might be in the case of Tau that the docking sites are crucial only in a cellular context to manage specificity and competition rather than to stimulate activity (63).

Activation of ERK1/2 is increased in AD neurons (64), is found in association with abnormally phosphorylated early Tau deposits (65) and is linked to the progression

of the neurofibrillary degeneration through the Braak stages of AD (36, 66). Activation of ERK1/2 also responds to fibrillar amyloid beta deposits in mature hippocampal neuronal culture (67), to an increase activity of IPTKB (38) and oxidative stress (68), all affecting Tau phosphorylation. ERK1/2 phosphorylation of Tau could thus take place in cells upon stress-signaling or once the phosphorylation fails to be counteracted by an efficient dephosphorylation. The ERK kinase is thus accordingly considered as a Tau kinase that could be involved in AD patho-physiology. We here reinforce this view by showing that the ERK2 kinase has the capacity by itself to phosphorylate Tau on many sites. These results support the hypothesis that ERK activation under stress conditions might have a detrimental effect for Tau function and participate in AD physio-pathology.

Acknowledgements: We thank O. Dounane for its technical assistance.

FOOTNOTES

The NMR facilities were funded by the Région Nord, CNRS, Pasteur Institute of Lille, European Community (FEDER), French Research Ministry and the University of Sciences and Technologies of Lille I. We acknowledge support from the TGE RMN THC (FR-3050, France). This study was supported by a grant from the LabEx (Laboratory of Excellence), DISTALZ (Development of Innovative Strategies for a Transdisciplinary approach to Alzheimer's disease), and in part by the French government funding agency Agence Nationale de la Recherche TAF. PS and JG were supported by the US National Institutes of Health under R01 GM081578.

The abbreviations used are: AD, Alzheimer's disease; ERK2, Extracellular-regulated kinase2; MTBD, microtubule binding domain; PHF, paired helical filament; PRD, proline rich domain.

Conflict of interest: The authors declare that they have no conflicts of interest with the contents of this article.

Author contributions: H.Q., S.P., and I.L. conducted most experiments, F-X.C. conducted most NMR data acquisition, H.Q. and I.L. performed NMR data analysis, B.C. conducted experiments to prepare rat brain extract and advised on the manuscript, I.L., S.P., G.L., J.G. and H.Q. wrote the manuscript I.L., S.P., G.L. and J.G. conceived the idea for the project

REFERENCES

1. Gustke, N., Trinczek, B., Biernat, J., Mandelkow, E. M., and Mandelkow, E. (1994) Domains of tau protein and interactions with microtubules. *Biochemistry (Mosc.)*. **33**, 9511622
2. Goode, B. L., Denis, P. E., Panda, D., Radeke, M. J., Miller, H. P., Wilson, L., and Feinstein, S. C. (1997) Functional interactions between the proline-rich and repeat regions of tau enhance microtubule binding and assembly. *Mol Biol Cell*. **8**, 353665
3. Alonso, A. C., Zaidi, T., Grundke-Iqbal, I., and Iqbal, K. (1994) Role of abnormally phosphorylated tau in the breakdown of microtubules in Alzheimer disease. *Proc Natl Acad Sci U A*. **91**, 556266
4. Stoothoff, W. H., and Johnson, G. V. (2005) Tau phosphorylation: physiological and pathological consequences. *Biochim Biophys Acta*. **1739**, 280697
5. Gotz, J., Gladbach, A., Pennanen, L., van Eersel, J., Schild, A., David, D., and Ittner, L. M. (2010) Animal models reveal role for tau phosphorylation in human disease. *Biochim Biophys Acta*. **1802**, 860671
6. Grundke-Iqbal, I., Iqbal, K., Tung, Y. C., Quinlan, M., Wisniewski, H. M., and Binder, L. I. (1986) Abnormal phosphorylation of the microtubule-associated protein tau (tau) in Alzheimer cytoskeletal pathology. *Proc Natl Acad Sci U A*. **83**, 491367
7. Martin, L., Latypova, X., Wilson, C. M., Magnaudeix, A., Perrin, M. L., Yardin, C., and Terro, F. (2013) Tau protein kinases: involvement in Alzheimer's disease. *Ageing Res Rev*. **12**, 2896309
8. Hasegawa, M., Morishima-Kawashima, M., Takio, K., Suzuki, M., Titani, K., and Ihara, Y. (1992) Protein sequence and mass spectrometric analyses of tau in the Alzheimer's disease brain. *J Biol Chem*. **267**, 17047654
9. Morishima-Kawashima, M., Hasegawa, M., Takio, K., Suzuki, M., Yoshida, H., Watanabe, A., Titani, K., and Ihara, Y. (1995) Hyperphosphorylation of tau in PHF. *Neurobiol Aging*. **16**, 365671; discussion 371680
10. Morris, M., Knudsen, G. M., Maeda, S., Trinidad, J. C., Ioanoviciu, A., Burlingame, A. L., and Mucke, L. (2015) Tau post-translational modifications in wild-type and human amyloid precursor protein transgenic mice. *Nat Neurosci*. **18**, 118369
11. Funk, K. E., Thomas, S. N., Schafer, K. N., Cooper, G. L., Liao, Z., Clark, D. J., Yang, A. J., and Kuret, J. (2014) Lysine methylation is an endogenous post-translational modification of tau protein in human brain and a modulator of aggregation propensity. *Biochem J*. **462**, 77688
12. Biernat, J., Mandelkow, E. M., Schroter, C., Lichtenberg-Kraag, B., Steiner, B., Berling, B., Meyer, H., Mercken, M., Vandermeeren, A., Goedert, M., and et al. (1992) The switch of tau protein to an Alzheimer-like state includes the phosphorylation of two serine-proline motifs upstream of the microtubule binding region. *EMBO J*. **11**, 159367
13. Jeganathan, S., Hascher, A., Chinnathambi, S., Biernat, J., Mandelkow, E. M., and Mandelkow, E. (2008) Proline-directed pseudo-phosphorylation at AT8 and PHF1 epitopes induces a compaction of the paperclip folding of Tau and generates a pathological (MC-1) conformation. *J Biol Chem*. **283**, 32066676
14. Baumann, K., Mandelkow, E. M., Biernat, J., Piwnica-Worms, H., and Mandelkow, E. (1993) Abnormal Alzheimer-like phosphorylation of tau-protein by cyclin-dependent kinases cdk2 and cdk5. *FEBS Lett*. **336**, 417624
15. Kobayashi, S., Ishiguro, K., Omori, A., Takamatsu, M., Arioka, M., Imahori, K., and Uchida, T. (1993) A cdc2-related kinase PSSALRE/cdk5 is homologous with the 30

- kDa subunit of tau protein kinase II, a proline-directed protein kinase associated with microtubule. *FEBS Lett.* **335**, 17165
16. Ishiguro, K., Shiratsuchi, A., Sato, S., Omori, A., Arioka, M., Kobayashi, S., Uchida, T., and Imahori, K. (1993) Glycogen synthase kinase 3 beta is identical to tau protein kinase I generating several epitopes of paired helical filaments. *FEBS Lett.* **325**, 1676-72
 17. Reynolds, C. H., Utton, M. A., Gibb, G. M., Yates, A., and Anderton, B. H. (1997) Stress-activated protein kinase/c-jun N-terminal kinase phosphorylates tau protein. *J Neurochem.* **68**, 1736644
 18. Reynolds, C. H., Nebreda, A. R., Gibb, G. M., Utton, M. A., and Anderton, B. H. (1997) Reactivating kinase/p38 phosphorylates tau protein in vitro. *J Neurochem.* **69**, 19168
 19. Drewes, G., Lichtenberg-Kraag, B., Doring, F., Mandelkow, E. M., Biernat, J., Goris, J., Doree, M., and Mandelkow, E. (1992) Mitogen activated protein (MAP) kinase transforms tau protein into an Alzheimer-like state. *Embo J.* **11**, 213168
 20. Mazanetz, M. P., and Fischer, P. M. (2007) Untangling tau hyperphosphorylation in drug design for neurodegenerative diseases. *Nat Rev Drug Discov.* **6**, 464679
 21. Anderson, N. G., Maller, J. L., Tonks, N. K., and Sturgill, T. W. (1990) Requirement for integration of signals from two distinct phosphorylation pathways for activation of MAP kinase. *Nature.* **343**, 65163
 22. Boulton, T. G., Yancopoulos, G. D., Gregory, J. S., Slaughter, C., Moomaw, C., Hsu, J., and Cobb, M. H. (1990) An insulin-stimulated protein kinase similar to yeast kinases involved in cell cycle control. *Science.* **249**, 6467
 23. Seger, R., Ahn, N. G., Boulton, T. G., Yancopoulos, G. D., Panayotatos, N., Radziejewska, E., Ericsson, L., Bratlien, R. L., Cobb, M. H., and Krebs, E. G. (1991) Microtubule-associated protein 2 kinases, ERK1 and ERK2, undergo autophosphorylation on both tyrosine and threonine residues: implications for their mechanism of activation. *Proc Natl Acad Sci U A.* **88**, 614266
 24. Zhang, F., Strand, A., Robbins, D., Cobb, M. H., and Goldsmith, E. J. (1994) Atomic structure of the MAP kinase ERK2 at 2.3 Å resolution. *Nature.* **367**, 704611
 25. Canagarajah, B. J., Khokhlatchev, A., Cobb, M. H., and Goldsmith, E. J. (1997) Activation mechanism of the MAP kinase ERK2 by dual phosphorylation. *Cell.* **90**, 859669
 26. Adams, P. D., Sellers, W. R., Sharma, S. K., Wu, A. D., Nalin, C. M., and Kaelin, W. G., Jr. (1996) Identification of a cyclin-cdk2 recognition motif present in substrates and p21-like cyclin-dependent kinase inhibitors. *Mol Cell Biol.* **16**, 6623633
 27. Brown, N. R., Noble, M. E., Endicott, J. A., and Johnson, L. N. (1999) The structural basis for specificity of substrate and recruitment peptides for cyclin-dependent kinases. *Nat Cell Biol.* **1**, 438643
 28. Tanoue, T., Adachi, M., Moriguchi, T., and Nishida, E. (2000) A conserved docking motif in MAP kinases common to substrates, activators and regulators. *Nat Cell Biol.* **2**, 11066
 29. Fernandes, N., Bailey, D. E., Vanvraken, D. L., and Allbritton, N. L. (2007) Use of docking peptides to design modular substrates with high efficiency for mitogen-activated protein kinase extracellular signal-regulated kinase. *ACS Chem Biol.* **2**, 6656-73
 30. Garai, A., Zeke, A., Gogl, G., Toro, I., Fordos, F., Blankenburg, H., Barkai, T., Varga, J., Alexa, A., Emig, D., Albrecht, M., and Remenyi, A. (2012) Specificity of linear motifs that bind to a common mitogen-activated protein kinase docking groove. *Sci Signal.* **5**, ra74

31. Mace, P. D., Wallez, Y., Egger, M. F., Dobaczewska, M. K., Robinson, H., Pasquale, E. B., and Riedl, S. J. (2013) Structure of ERK2 bound to PEA-15 reveals a mechanism for rapid release of activated MAPK. *Nat Commun.* **4**, 1681
32. Liu, S., Sun, J. P., Zhou, B., and Zhang, Z. Y. (2006) Structural basis of docking interactions between ERK2 and MAP kinase phosphatase 3. *Proc Natl Acad Sci U A.* **103**, 5326631
33. Zhou, T., Sun, L., Humphreys, J., and Goldsmith, E. J. (2006) Docking interactions induce exposure of activation loop in the MAP kinase ERK2. *Structure.* **14**, 101169
34. Ma, W., Shang, Y., Wei, Z., Wen, W., Wang, W., and Zhang, M. (2010) Phosphorylation of DCC by ERK2 is facilitated by direct docking of the receptor P1 domain to the kinase. *Structure.* **18**, 1502611
35. Jacobs, D., Glossip, D., Xing, H., Muslin, A. J., and Kornfeld, K. (1999) Multiple docking sites on substrate proteins form a modular system that mediates recognition by ERK MAP kinase. *Genes Dev.* **13**, 163675
36. Pei, J. J., Braak, H., An, W. L., Winblad, B., Cowburn, R. F., Iqbal, K., and Grundke-Iqbal, I. (2002) Up-regulation of mitogen-activated protein kinases ERK1/2 and MEK1/2 is associated with the progression of neurofibrillary degeneration in Alzheimer's disease. *Brain Res Mol Brain Res.* **109**, 45655
37. Swatton, J. E., Sellers, L. A., Faull, R. L., Holland, A., Iritani, S., and Bahn, S. (2004) Increased MAP kinase activity in Alzheimer's and Down syndrome but not in schizophrenia human brain. *Eur J Neurosci.* **19**, 271169
38. Stygelbout, V., Leroy, K., Pouillon, V., Ando, K., D'Amico, E., Jia, Y., Luo, H. R., Duyckaerts, C., Erneux, C., Schurmans, S., and Brion, J. P. (2014) Inositol trisphosphate 3-kinase B is increased in human Alzheimer brain and exacerbates mouse Alzheimer pathology. *Brain.* **137**, 537652
39. Goedert, M., Jakes, R., Crowther, R. A., Six, J., Lubke, U., Vandermeeren, M., Cras, P., Trojanowski, J. Q., and Lee, V. M. (1993) The abnormal phosphorylation of tau protein at Ser-202 in Alzheimer disease recapitulates phosphorylation during development. *Proc Natl Acad Sci U A.* **90**, 5066670
40. Luna-Vargas, M. P., Christodoulou, E., Alfieri, A., van Dijk, W. J., Stadnik, M., Hibbert, R. G., Sahtoe, D. D., Clerici, M., Marco, V. D., Littler, D., Celie, P. H., Sixma, T. K., and Perrakis, A. (2011) Enabling high-throughput ligation-independent cloning and protein expression for the family of ubiquitin specific proteases. *J Struct Biol.* **175**, 11369
41. Prabakaran, S., Everley, R. A., Landrieu, I., Wieruszeski, J. M., Lippens, G., Steen, H., and Gunawardena, J. (2011) Comparative analysis of Erk phosphorylation suggests a mixed strategy for measuring phospho-form distributions. *Mol Syst Biol.* **7**, 482
42. Weisemann, R., Ruterjans, H., and Bermel, W. (1993) 3D triple-resonance NMR techniques for the sequential assignment of NH and ¹⁵N resonances in ¹⁵N- and ¹³C-labelled proteins. *J Biomol NMR.* **3**, 113620
43. Bienkiewicz, E. A., and Lumb, K. J. (1999) Random-coil chemical shifts of phosphorylated amino acids. *J Biomol NMR.* **15**, 20366
44. Landrieu, I., Lacosse, L., Leroy, A., Wieruszeski, J. M., Trivelli, X., Sillen, A., Sibille, N., Schwalbe, H., Saxena, K., Langer, T., and Lippens, G. (2006) NMR analysis of a Tau phosphorylation pattern. *J Am Chem Soc.* **128**, 3575683
45. Theillet, F.-X., Smet-Nocca, C., Liokatis, S., Thongwichian, R., Kosten, J., Yoon, M.-K., Kriwacki, R. W., Landrieu, I., Lippens, G., and Selenko, P. (2012) Cell signaling, post-translational protein modifications and NMR spectroscopy. *J. Biomol. NMR.* **54**, 2176236

46. Theillet, F. X., Rose, H. M., Liokatis, S., Binolfi, A., Thongwichian, R., Stuiver, M., and Selenko, P. (2013) Site-specific NMR mapping and time-resolved monitoring of serine and threonine phosphorylation in reconstituted kinase reactions and mammalian cell extracts. *Nat Protoc.* **8**, 1416632
47. Amniai, L., Barbier, P., Sillen, A., Wieruszeski, J. M., Peyrot, V., Lippens, G., and Landrieu, I. (2009) Alzheimer disease specific phosphoepitopes of Tau interfere with assembly of tubulin but not binding to microtubules. *FASEB J.* **23**, 1146652
48. Leroy, A., Landrieu, I., Huvent, I., Legrand, D., Codeville, B., Wieruszeski, J. M., and Lippens, G. (2010) Spectroscopic studies of GSK3{beta} phosphorylation of the neuronal tau protein and its interaction with the N-terminal domain of apolipoprotein E. *J Biol Chem.* **285**, 33435644
49. Alonso, A., Zaidi, T., Novak, M., Grundke-Iqbal, I., and Iqbal, K. (2001) Hyperphosphorylation induces self-assembly of tau into tangles of paired helical filaments/straight filaments. *Proc Natl Acad Sci U A.* **98**, 692368
50. Smet, C., Leroy, A., Sillen, A., Wieruszeski, J. M., Landrieu, I., and Lippens, G. (2004) Accepting its random coil nature allows a partial NMR assignment of the neuronal Tau protein. *Chembiochem.* **5**, 1639646
51. Mukrasch, M. D., Bibow, S., Korukottu, J., Jeganathan, S., Biernat, J., Griesinger, C., Mandelkow, E., and Zweckstetter, M. (2009) Structural polymorphism of 441-residue tau at single residue resolution. *PLoS Biol.* **7**, e34
52. von Bergen, M., Friedhoff, P., Biernat, J., Heberle, J., Mandelkow, E. M., and Mandelkow, E. (2000) Assembly of tau protein into Alzheimer paired helical filaments depends on a local sequence motif ((306)VQIVYK(311)) forming beta structure. *Proc Natl Acad Sci U A.* **97**, 5129634
53. Marsh, E. N. G., and Suzuki, Y. (2014) Using (19)F NMR to probe biological interactions of proteins and peptides. *ACS Chem. Biol.* **9**, 124261250
54. Lippens, G., Amniai, L., Wieruszeski, J. M., Sillen, A., Leroy, A., and Landrieu, I. (2012) Towards understanding the phosphorylation code of tau. *Biochem Soc Trans.* **40**, 6986703
55. Lichtenberg-Kraag, B., Mandelkow, E. M., Biernat, J., Steiner, B., Schroter, C., Gustke, N., Meyer, H. E., and Mandelkow, E. (1992) Phosphorylation-dependent epitopes of neurofilament antibodies on tau protein and relationship with Alzheimer tau. *Proc Natl Acad Sci U A.* **89**, 538468
56. Ho, D. T., Bardwell, A. J., Grewal, S., Iverson, C., and Bardwell, L. (2006) Interacting JNK-docking sites in MKK7 promote binding and activation of JNK mitogen-activated protein kinases. *J Biol Chem.* **281**, 13169679
57. Kragelj, J., Palencia, A., Nanao, M. H., Maurin, D., Bouvignies, G., Blackledge, M., and Jensen, M. R. (2015) Structure and dynamics of the MKK7-JNK signaling complex. *Proc Natl Acad Sci U A.* **112**, 3409614
58. Mittag, T., Marsh, J., Grishaev, A., Orlicky, S., Lin, H., Sicheri, F., Tyers, M., and Forman-Kay, J. D. (2010) Structure/function implications in a dynamic complex of the intrinsically disordered Sic1 with the Cdc4 subunit of an SCF ubiquitin ligase. *Structure.* **18**, 4946506
59. Klein, P., Pawson, T., and Tyers, M. (2003) Mathematical modeling suggests cooperative interactions between a disordered polyvalent ligand and a single receptor site. *Curr Biol.* **13**, 1669678
60. Ubersax, J. A., and Ferrell, J. E., Jr. (2007) Mechanisms of specificity in protein phosphorylation. *Nat Rev Mol Cell Biol.* **8**, 530641

61. Lee, S., Warthaka, M., Yan, C., Kaoud, T. S., Ren, P., and Dalby, K. N. (2011) Examining docking interactions on ERK2 with modular peptide substrates. *Biochemistry (Mosc.)*. **50**, 9500610
62. Courcelles, M., Fremin, C., Voisin, L., Lemieux, S., Meloche, S., and Thibault, P. (2013) Phosphoproteome dynamics reveal novel ERK1/2 MAP kinase substrates with broad spectrum of functions. *Mol Syst Biol.* **9**, 669
63. Futran, A. S., Link, A. J., Seger, R., and Shvartsman, S. Y. (2013) ERK as a model for systems biology of enzyme kinetics in cells. *Curr Biol.* **23**, R97269
64. Arendt, T., Holzer, M., Grossmann, A., Zedlick, D., and Bruckner, M. K. (1995) Increased expression and subcellular translocation of the mitogen activated protein kinase kinase and mitogen-activated protein kinase in Alzheimer's disease. *Neuroscience*. **68**, 5618
65. Ferrer, I., Blanco, R., Carmona, M., Ribera, R., Goutan, E., Puig, B., Rey, M. J., Cardozo, A., Vinals, F., and Ribalta, T. (2001) Phosphorylated map kinase (ERK1, ERK2) expression is associated with early tau deposition in neurones and glial cells, but not with increased nuclear DNA vulnerability and cell death, in Alzheimer disease, Pick's disease, progressive supranuclear palsy and corticobasal degeneration. *Brain Pathol.* **11**, 144658
66. Braak, H., and Braak, E. (1991) Neuropathological staging of Alzheimer-related changes. *Acta Neuropathol.* **82**, 239659
67. Ferreira, A., Lu, Q., Orecchio, L., and Kosik, K. S. (1997) Selective phosphorylation of adult tau isoforms in mature hippocampal neurons exposed to fibrillar A beta. *Mol Cell Neurosci.* **9**, 220634
68. Perry, G., Roder, H., Nunomura, A., Takeda, A., Friedlich, A. L., Zhu, X., Raina, A. K., Holbrook, N., Siedlak, S. L., Harris, P. L., and Smith, M. A. (1999) Activation of neuronal extracellular receptor kinase (ERK) in Alzheimer disease links oxidative stress to abnormal phosphorylation. *Neuroreport.* **10**, 241165

FIGURE LEGENDS

Figure 1. Phosphorylation of Tau. **A.** Scheme of the domain organization of Tau protein, limits of the domains are indicated by the amino acid number in the sequence, MTBD is the Microtubule Binding Domain **B** to **D** ^1H , ^{15}N HSQC 2D spectra of **B** Tau **C** Tau phosphorylated by MEKK-activated recombinant ERK2 **D** Tau phosphorylated by rat brain extract kinase activity. The region of the spectrum containing resonances corresponding to phosphorylated S/T residues is boxed in **C** and **D** spectra. Detailed annotation of the resonances corresponding to phosphorylated residues is provided in Fig. **2B**.

Figure 2. Comparison of Tau phosphorylation by activated recombinant ERK2 and rat brain extracts. **A** Overlaid details of ^1H , ^{15}N HSQC 2D spectra of the phosphorylated Tau by activated ERK2 (in red) or by rat brain extract (in black). The enlarged region corresponds to the boxed region in **Fig. 1C and D**. Resonances corresponding to assigned phosphorylated Tau residues are annotated. **B** Level of phosphorylation for each pS/pT Tau residue presented as black bars for Tau phosphorylated by the rat brain extract, and red bars by activated ERK2. Each experiment was repeated twice, the standard deviation around the average value is shown by error bars. The level of phosphorylation is estimated based on the integrals of resonance peaks, as described in methods. **C** and **D** ^1H , ^{15}N HSQC 2D spectrum of Tau[165-245] modified by incubation at 37°C **C** for 3 hours with activated recombinant ERK2 kinase or **D** overnight with rat brain extract. The annotated resonances were assigned to phosphorylation sites by comparison with the ^1H , ^{15}N HSQC 2D of Tau protein phosphorylated by activated recombinant ERK2 kinase or rat brain extract, in the same conditions.

Figure 3. ERK interacts with the MTBD of Tau. **A-C** Overlaid 2D spectra corresponding to **A** free Tau (black) and Tau with 5 molar excess of ERK (superimposed in red), **C** free Tau[165-245] or PRD (black) and Tau[165-245] with 1 molar equivalent of ERK2 (superimposed in green) **C** free Tau[244-372] or MTBD (black) and Tau[244-372] with 1 molar excess of ERK2 (superimposed in blue). Boxed regions in **A** and **C** are enlarged and annotated in **D** and **E**. **F** Relative intensities I/I0 of corresponding resonances in the 2D spectra of Tau with 5 molar excess of ERK (I, red in **A**) or free in solution (I0, black in **A**), for residues along the Tau sequence.

Figure 4. ERK2 main interaction sites can be matched to docking sequences **A** relative intensities I/I0 of corresponding resonances in the 2D spectra of Tau[244-372] with 1 molar excess of ERK (I, blue in **Fig. 4C**) or free in solution (I0, black in **Fig. 4C**). Double arrows indicate the interaction regions along the sequence: Tau[274-288], Tau[306-318] and Tau[346-358]. **B** Sequence of Tau. Perturbations of resonance intensities are coloured coded as red for residues with a I/I0 below 0.5 and as orange below 0.6. Residues with no information for the corresponding resonance are in gray. Sequences defined in the interaction experiment match the consensus D-site $\Psi\text{X}_7\Phi\text{X}\Phi$ and revD-site $\Phi\text{X}\Phi\text{X}_7\Psi$ (Ψ : positively charged residues, ϕ : hydrophobic residues, X any residue) of ERK docking sites, as indicated below the sequences of Tau[274-284] and Tau[309-317]. Tau[244-372] or MTBD is indicated by green arrows along the sequence, Tau[220-240] and Tau[271-294] peptides (**Fig. 7**) by red and black arrows, respectively. The PHF6* and PHF6 peptides in the R2 and R3 repeats, respectively, are boxed.

Figure 5. Determination of K_d of Tau/ERK interaction. **A** Superimposed 1D Fluor NMR spectra of CF₃-Tau[244-372] *upper panel* and CF₃-Tau *lower panel* **B** Saturation curves based on the chemical shift perturbation of the Fluor signal of CF₃-Tau and CF₃-Tau[244-372]. The signal of only one CF₃-Cys was monitored along the titration, the second one being broadened.

Figure 6. Interaction of Tau peptides with ERK2 **A-B** Detail of overlaid ¹H, ¹⁵N HSQC 2D spectra of **A** ¹⁵N His-SUMO Tau[220-240] and **B** ¹⁵N His-SUMO Tau[271-294] free in solution (in black) or with 1 molar excess of ERK kinase (superimposed in red). Relative intensities ratio I/I₀ for corresponding resonances in these spectra are shown in **C** and **D**, respectively.

Supplementary Table

Table S1 Sequence specific assignment of resonances corresponding to phosphorylated residues in ERK phospho-Tau. ¹H, ¹⁵N, CA, CB columns correspond to the chemical shifts (in ppm) of atoms from the assigned phospho-residues indicated in column 1. The amino-acid type at the direct N-terminus of each phospho-residue is displayed in column i-1 residue type and the chemical shifts of the corresponding CA and CB atoms in CA-1 and CB-1 columns.

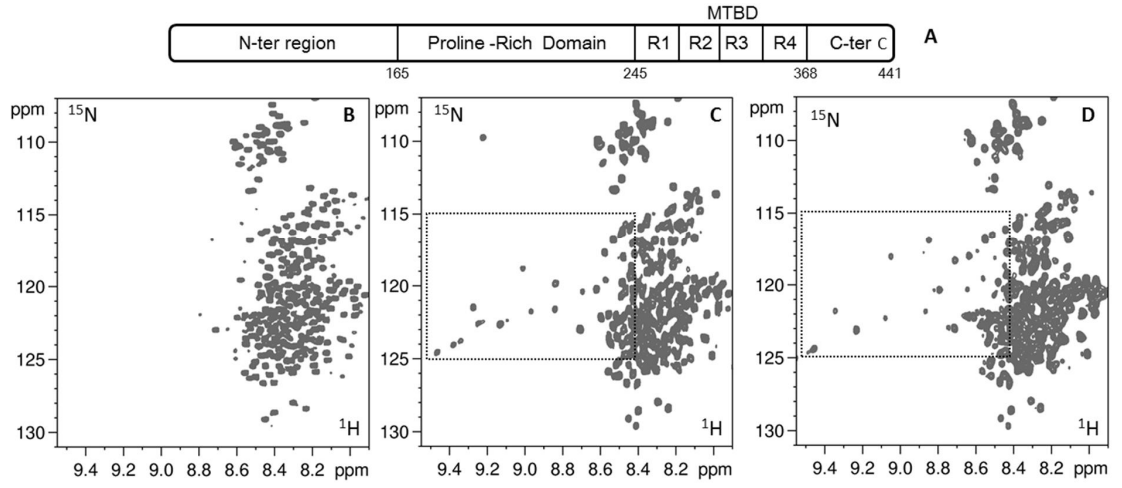


Figure 1

Phosphorylation of Tau by ERK2

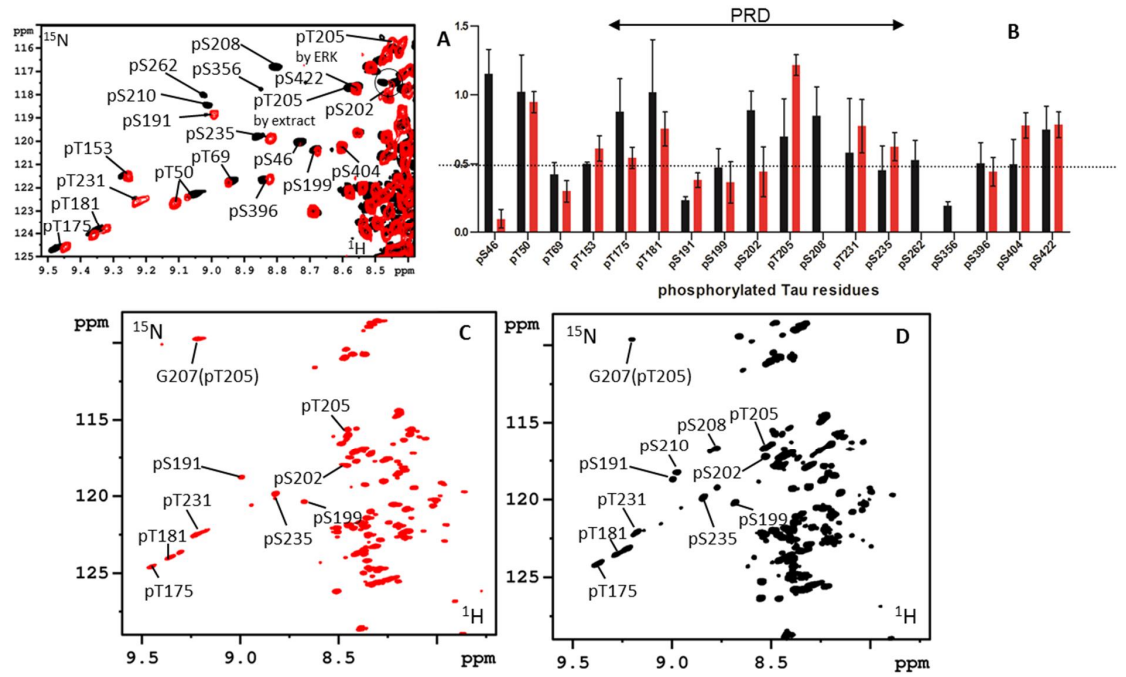


Figure 2

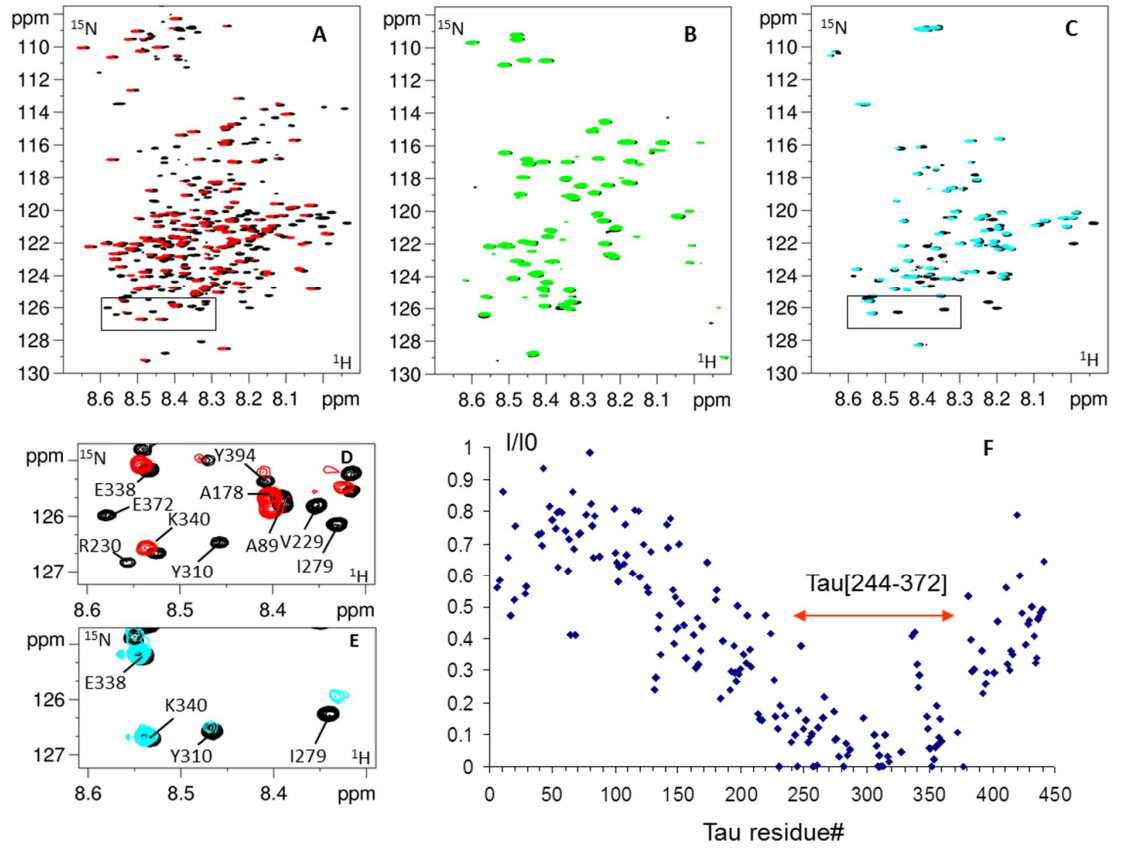


Figure 3

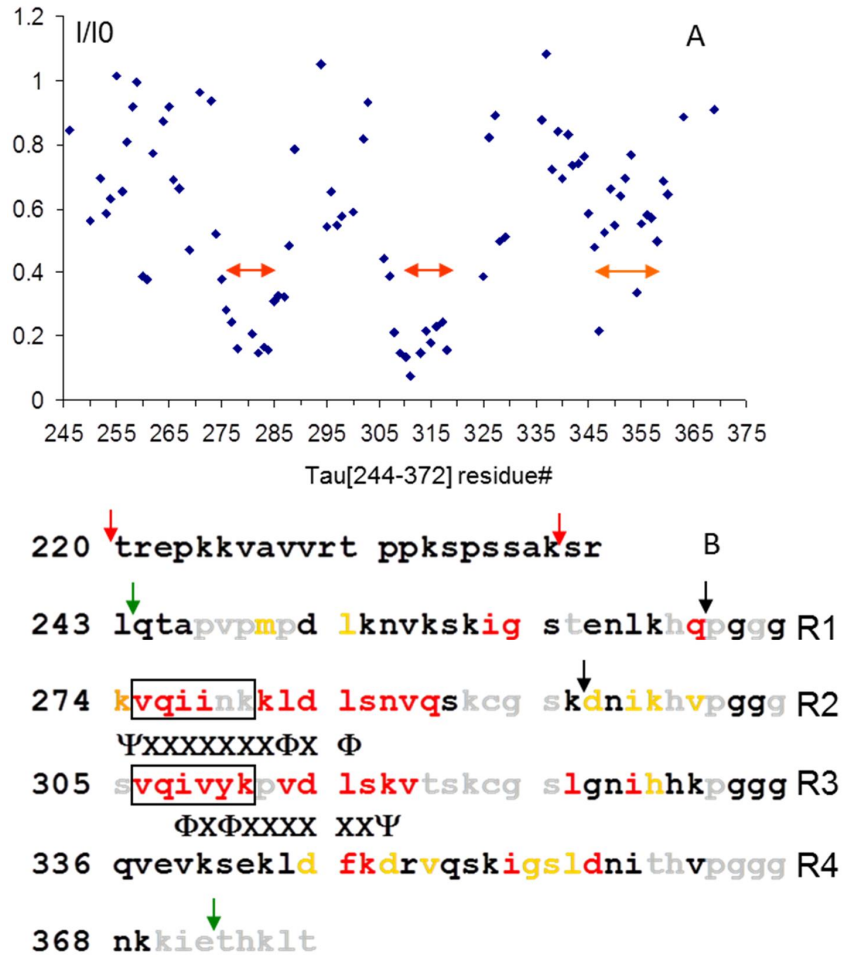


Figure 4

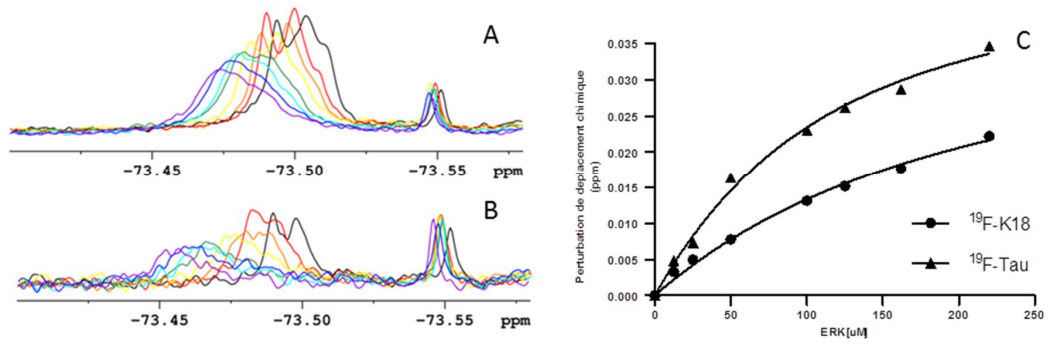


Figure 5

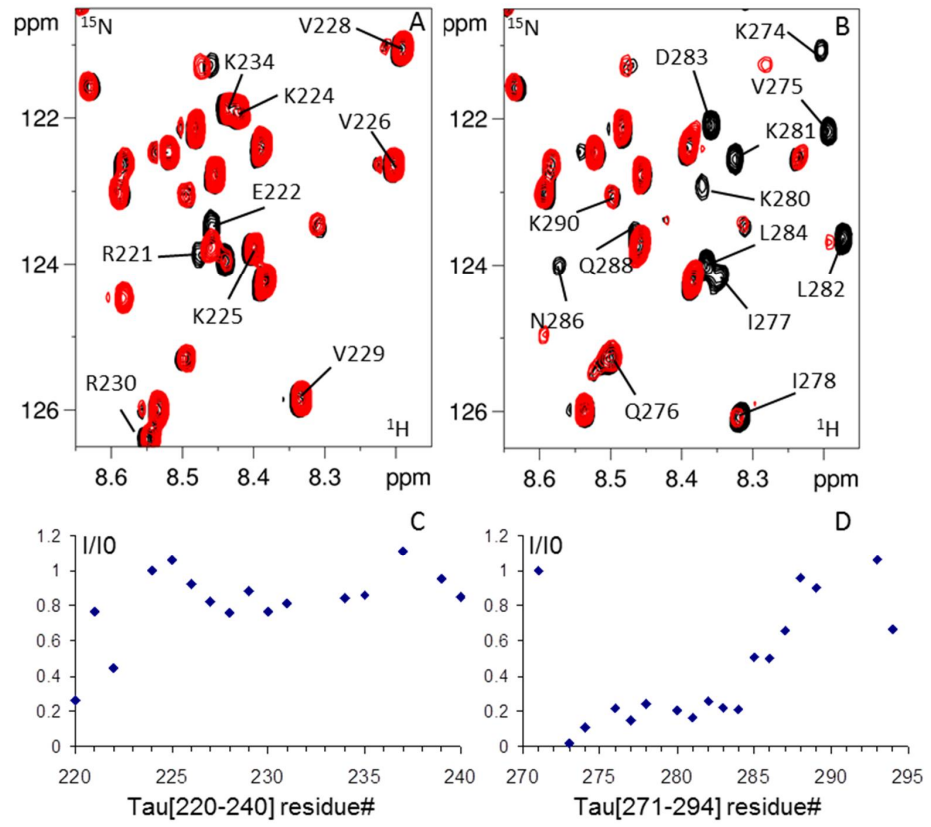


Figure 6

Phosphorylation of Tau by ERK2

	¹⁵ N	¹ H	CA	CB	CA-1	CB-1	i-1 residue type
pS46	120.4	8.80	56.1	64.9	57.4	30.9	Glu
pT50	123.5	9.30	61.1	72.2	55.6	30.2	Gln
pT69	122.5	9.13	60.7	72.2	58.4	64.1	Ser
pT153	121.8	9.35	61.1	72.2	52.4	19.4	Ala
pT175	125.1	9.59	61.5	72.4	55.7	33.3	Lys
pT181	124.5	9.49	61.3	72.4	55.9	33.3	Lys
pS191	119.0	9.04	58.3	65.6	56.0	33.3	Lys
pS199	120.6	8.71	56.0	65.0	57.7	64.3	Ser
pS202	117.9	8.54	55.7	65.3	45.0	-	Gly
pT205	117.1	8.62	60.4	71.8	45.0	-	Gly
pT231	123.0	9.33	60.9	72.2	55.8	31.0	Arg
pS235	120.0	8.85	55.8	65.2	56.5	33.3	Lys
pS396	121.8	8.86	56.5	64.5	56.5	34.1	Lys
pS404	120.4	8.66	55.9	70.0	61.7	70.0	Thr
pS422	118.2	8.65	56.2	65.0	54.3	41.6	Asp

Table 1

Part 2

Analysis of the kinase activity of the activated
isoforms of ERK2 kinase

The ERK kinase is a MAPK, activated by dual phosphorylation on a 'TXY' sequence in its activation loop by its upstream activator MKK, whereby the latter themselves are activated after binding of an extracellular ligand to a Tyrosine receptor kinase (Davis 1993; Pearson G et al. 2001). For human Erk1, the 'TEY' sequence contains T²⁰² and Y²⁰⁴ whereas it corresponds to T¹⁸³ and Y¹⁸⁵ for human ERK2. The crystallographic data of ERK TEpY suggests a distinct and stable conformation to favor the phosphorylation at T residue in 'TEY' motif (Takayoshi Kinoshita et al. 2008). Phosphorylated ERK1/2 is regulated by either phosphotyrosine phosphatases or dual specificity S/T and Y phosphatases known as MAP kinase phosphatases (MKPs) (Pearson G et al. 2001). ERK kinase family consists of two major classes, ERK 1 and ERK 2 (ERK1/2) who share nearly 90% identical amino acid sequences from human proteins. ERK1/2 can be commonly activated by MEK1/2 kinases via the phosphorylation at 'TEY' motifs. The active form of ERK1/2 kinases is commonly considered as pTEpY ERK, dual-phosphorylated ERK at both T and Y residues in 'TEY' motif in activation loop. However, evidence show that mono-phosphorylated ERK isoforms, solely phosphorylated at T or Y residue, might exist in cells and have distinct physiological functions related to intracellular localization and tissue-specific distribution, for example, TEpY ERK2 might be involved in ERK-related regulation of Golgi structure (Cha & Shapiro 2001). Endogenous pTEY ERK1/2 has been detected and separated from other ERK phospho-isoforms in myocytes by MonoQ FPLC (Fast Protein Liquid Chromatography) and a basal enzymatic activity of pTEY ERK1/2 has been demonstrated by *in vitro* assays, suggesting that pTEY ERK1/2 might be an active isoforms in cells in contrast to the general thought of that pTEpY ERK1/2 is the only active form (Sugden et al. 2010). However, it still remains unclear the specificity and efficiency of TEpY ERK and pTEpY ERK. We were thus interested to characterize the enzymatic activity of both ERK phospho-isoforms in our *in vitro* conditions. As T and/or Y residues in 'TEY' motif of ERK1/2 kinase can be phosphorylated, they are four phospho-patterns for 'TEY' motif: TEY ERK, pTEY ERK, TEpY ERK and pTEpY ERK. We characterize, in this study, the enzymatic activity of these ERK phospho-isoforms in Tau *in vitro* phosphorylation by using NMR spectroscopy as an analytical tool.

1. Comparison of ERK2 phospho-isoform enzymatic activity with Tau

Characterization of Tau phosphorylation has been already performed with the MEK-activated pTEpY ERK2, with a double phosphorylation in its activation loop (Figure 42).

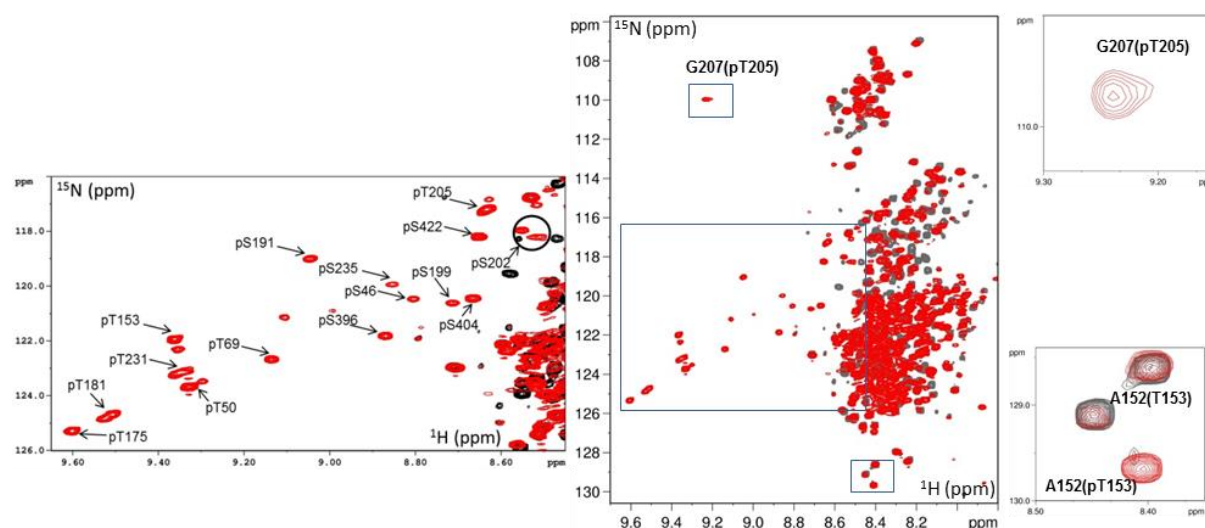


Figure 42: $[^1\text{H}, ^{15}\text{N}]$ HSQC spectrum of ^{15}N -labelled recombinant Tau phosphorylated by active ERK2 (pTEpY ERK2 isoform) overlaid on spectrum of ^{15}N -labelled recombinant Tau in grey. All the resonances corresponding to phosphorylated residues are found in a characteristic region of the spectrum indicated by the blue-line box. The assignment of the resonances of phosphorylation sites is given in the left zoom-out HSQC spectrum in which 15 phospho-sites are marked. As the chemical environment is modified, some neighbor residues also undergo change in their chemical shift. For example, the G²⁰⁷ resonance has a large chemical shift change (see box in spectrum) when its neighbor residue S²⁰²/T²⁰⁵ is phosphorylated (Gandhi et al. 2015). Upon T¹⁵³ phosphorylation, A¹⁵² has a split resonance, one additional corresponding to pT¹⁵³ and one for the remaining T¹⁵³.

We next examined the activity and specificity of the ERK2 protein with single phosphorylation in the activation loop towards the Tau protein sites. pTEY and TEpY phospho-isoforms are obtained by differential dephosphorylation by the PP2A and PTP phosphatases, respectively (Sudhakaran et al., 2011). Distribution of the phospho-isoforms is evaluated by mass spectrometry to ensure that the pTEpY phospho-isoform is residual in these kinase preparations (Figure 43). It is indeed difficult to convert 100% of pTEpY ERK (probably already a heterogenous form of ERK) obtained by incubation with MEK kinase into pure pTEY ERK or TEpY ERK by incubation with the phosphatases. pTEY ERK fraction is minor

in the pTEpY ERK and TEpY ERK samples. The pTEY ERK2 sample is not contaminated by pTEpY isoform while the TEpY sample shows a residual fraction of pTEpY isoform.

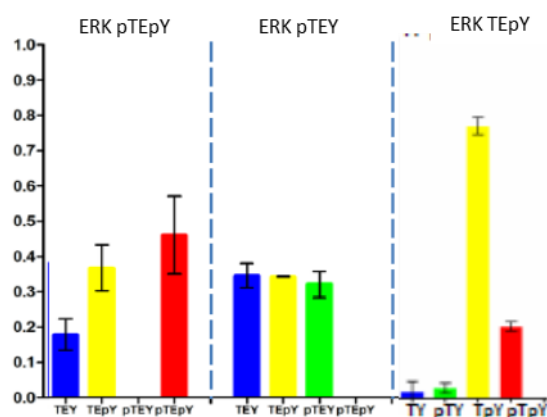


Figure 43: Distribution of different phospho-isoforms in pTEpY ERK2, pTEY ERK2 and TEpY ERK2 samples by MALDI-TOF analysis. The mass spectroscopy experiment is performed by Dr. Sudhakaran in group of Prof. J.Gunawardena in Harvard medical school, USA.

Comparison of the NMR 2D ^1H , ^{15}N HSQC of Tau shows that incubation with unphosphorylated ERK2 does not lead to any phosphorylation of the substrate (Figure 44). Similarly in the spectrum of the TEpY ERK2 phospho-isoform (Figure 44, C) only residual phosphorylation of T⁵⁰, T²⁰⁵ and S²³⁵ is observed that could correspond to activity from the 20% pTEpY ERK2 phospho-isoform remaining in the enzyme preparation (Figure 43), as defined by quantitative MALDI-TOF method (Sudhakaran et al., 2011). By contrast, both the pTEY and pTEpY phospho-isoform show an efficient phosphorylation of the Tau protein, on multiple sites (Figure 44, A and B). Quantitative MS analysis attests that the pTEY ERK2 and pTEpY ERK2 enzyme preparations were not cross contaminated (Figure 43).

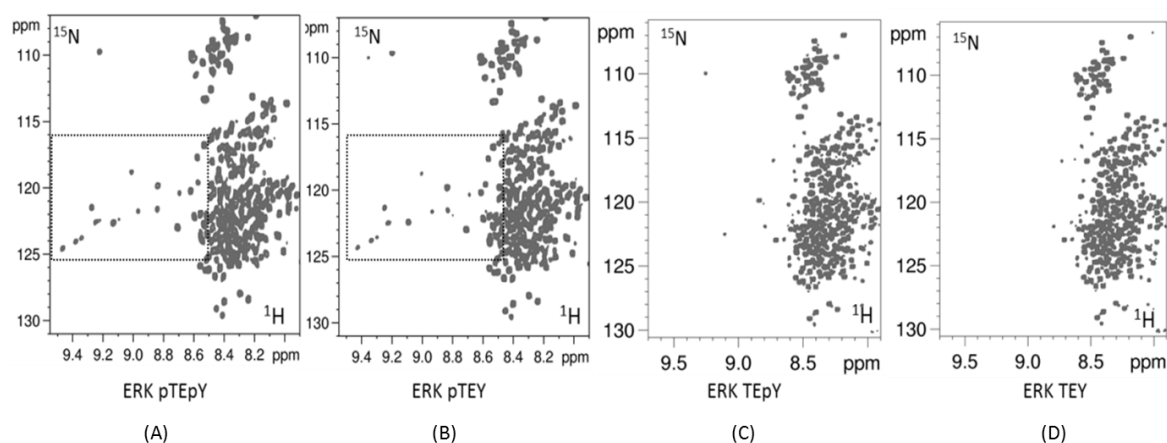


Figure 44: ERK activation-dependent phosphorylation of Tau Comparison of ^1H , ^{15}N HSQC 2D spectrum of ^{15}N Tau incubated for 3 hours at 37°C with ERK2 phospho-isoforms (A) TEY ERK2, (B) pYET ERK2, (C) pTEY ERK2 and (D) pTEpY ERK2. Additional resonances are observed in the region above 8.6ppm on the proton scale for the Tau protein modified by both the pTEY (A) and pTEpY ERK2 (B) phospho-isoforms compared to C and D. Comparison of the pattern of Tau phosphorylation by these latter phospho-isoforms is given in the diagram in Figure 9. Mass spectrum analysis of the phospho-isoform distribution for the various enzyme mixes are given in Figure 43.

To confirm the observed activity of mono-phosphorylated ERK2 isoforms, we mutated T and Y residues respectively by V and F residues. We then phosphorylated Tau with the mutated *in vitro* activated ERK2, following the same procedure as with pTEpY ERK2. The activity of mutated ERK2 phospho-isoforms is tested by NMR analysis of Tau phosphorylation under the same condition. As shown in Figure 45, VEpY ERK2 is nearly inactive in Tau phosphorylation, which is consistent with our observation that TEpY ERK2 has hardly any enzymatic activity. However, pTEF ERK2 also showed only a weak activity in Tau phosphorylation (Figure 45). In this case, our hypothesis is that pTEF ERK2 is not properly activated because the priming phosphorylation at Y residue is important for the phosphorylation of T residue (Takayoshi Kinoshita et al. 2008).

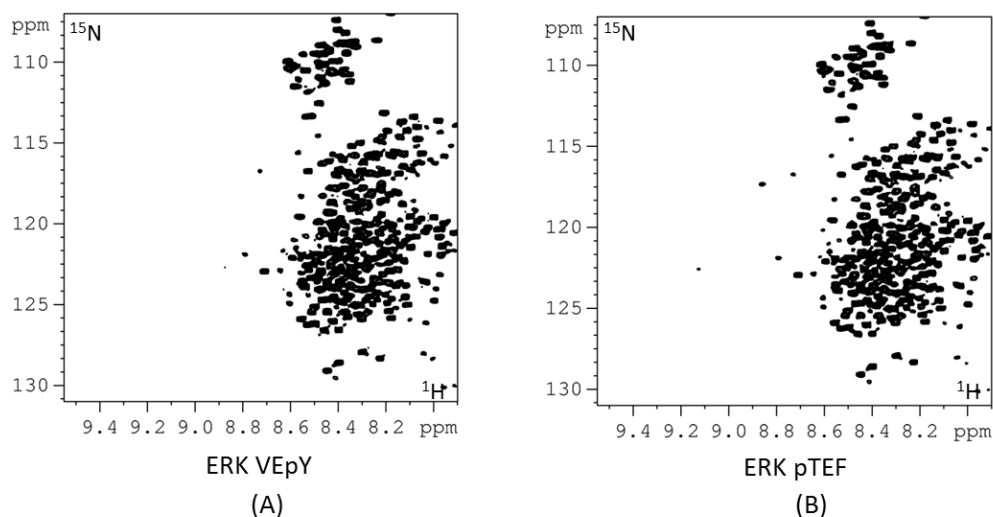


Figure 45: The enzymatic activity of activated mutated ERK2 kinase on protein Tau. (A) 2D HSQC spectrum of ^{15}N Tau prepared with phosphorylated ERK2 mutated at T by V residue in activation motif 'TEY'. (B) 2D HSQC spectrum of ^{15}N Tau prepared with phosphorylated ERK2 mutated at Y by F residue in activation motif 'TEY'.

In conclusion, in analysis of ^{15}N -labelled Tau samples by NMR spectroscopy, multiple sites are found phosphorylated by active ERK2 kinase. A mono-phosphorylated isoform of ERK2 at T residue in 'TEY' motif has nearly the same capacity of phosphorylation on Tau *in vitro* as pTEpY ERK2 which is usually considered as fully activated ERK2 form. ERK2 mutations at T and Y residue in 'TEY' motif confirm that the sole phosphorylation at Y residue in VEpY ERK2 is not sufficient to activate ERK and that the phosphorylation of the Y residue might be necessary to phosphorylate the T residue by MEK1.

In our analytical studies, the phosphorylation level is analyzed by integrating the volume of resonances of phosphorylated residues in HSQC spectra for Tau phosphorylated by pTEY ERK2 and pTEpY ERK2 samples (Figure 44, A and B). Comparison of the resonances corresponding to the phosphorylated residues confirms a similar specificity pattern, the same sites being modified in similar proportions (Figure 46, A). The pTEY ERK2 however contains a slightly higher level of unphosphorylated ERK2 that could account for a general lower level of phosphorylation for Tau phosphorylated with the pTEY enzyme preparation (Figure 43). The population of active fraction in pTEpY ERK2 sample is 15% more than that in pTEY ERK2 sample. The lower level of phosphorylation could nevertheless be the result of a less active enzyme. To compare the activity of the activated-ERK2 isoforms, NMR-based kinetic assays were performed by following Tau phosphorylation by pTEY ERK2 and pTEpY

ERK2 for 1H, 2H and 3H incubation periods. As shown in Figure 46, A, pTEpY ERK2 seems to have a faster kinetics of phosphorylation. We need additional experiments to confirm these preliminary data and our methodology is not well adapted for these experiments as a large quantity of enzyme is required. ERK2 kinase is unstable under certain *in vitro* conditions like high concentration, low salt concentration, temperature, etc., resulting in precipitation of the kinase. It is thus also difficult to quantitatively and qualitatively reproduce the experiments.

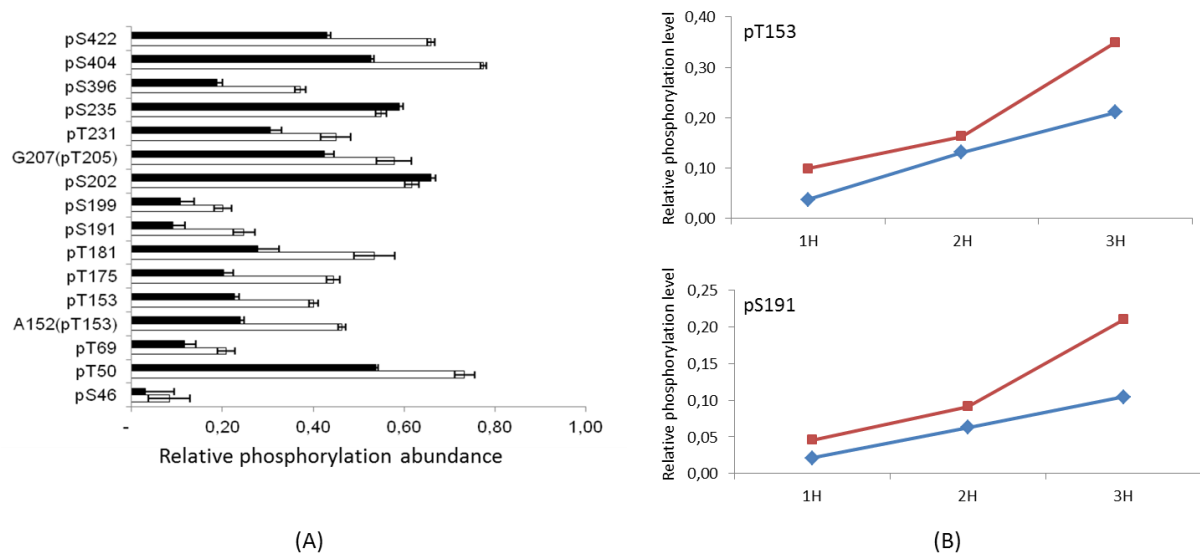
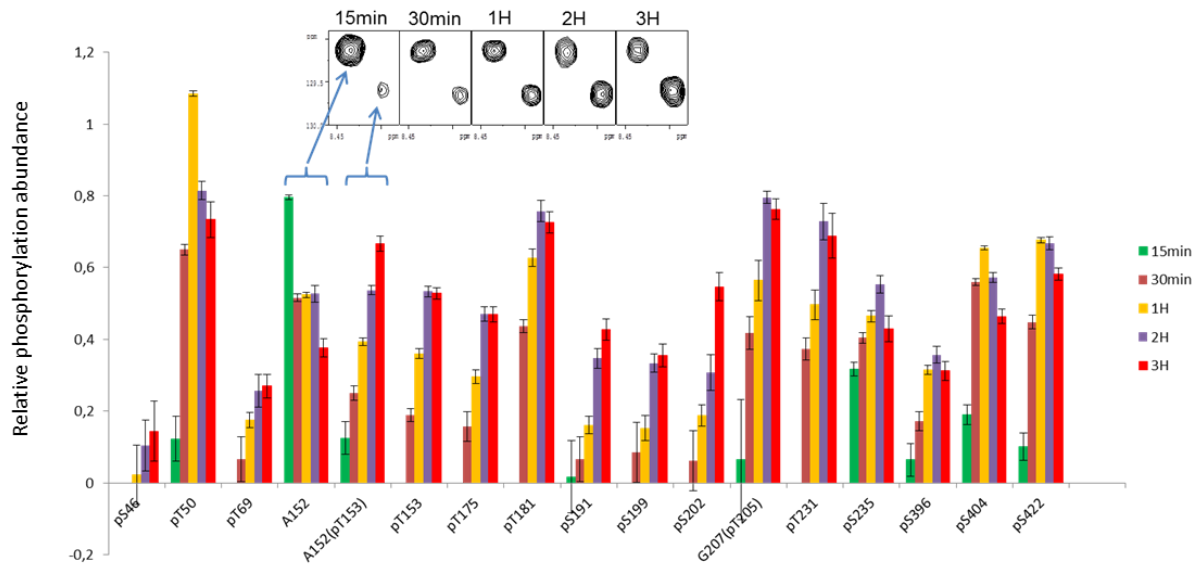


Figure 46: (A) The diagram displays the relative integrals of the resonances corresponding to Tau phospho-residues. The value of 1 is the average integrals of 3 isolated peaks corresponding to Tau residues dispersed in the primary sequence. Bars in black correspond to the phosphorylation of Tau by the pTEY ERK2 phospho-isoform and in white by the pTEpY ERK2 phospho-isoform. Error bars take into account the data variability due to the S/N ratio. **(B)** Kinetic assays of Tau phosphorylation by pTEY ERK2 (blue diamonds) and pTEpY ERK2 (red squares). Phosphorylation level of T¹⁵³ and S¹⁹¹ residues at 1H, 2H and 3H incubation, estimated by the normalized integrals of corresponding resonances in HSQC spectra (one spectrum per time point).

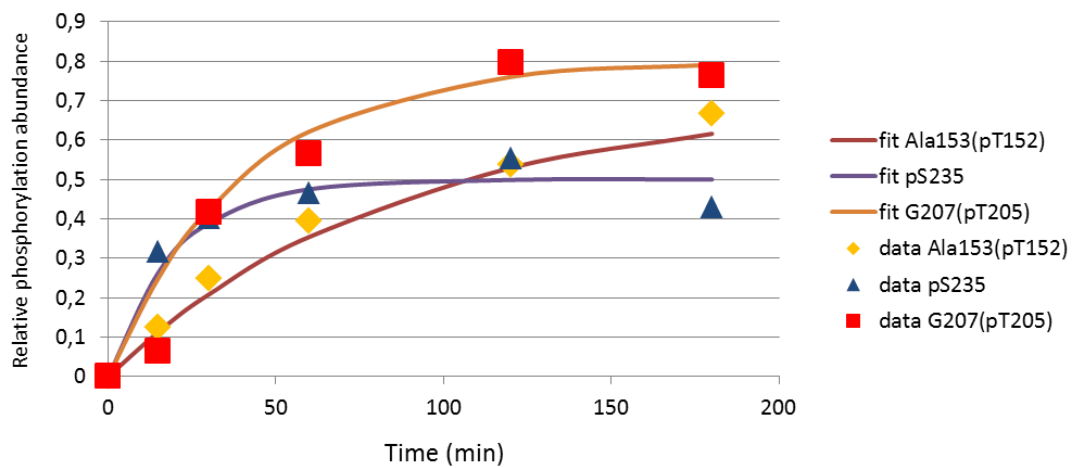
Therefore, we concluded that both pTEY ERK2 and pTEpY ERK2 have a similar site-specificity *in vitro* Tau phosphorylation and pTEpY ERK2 seems to have a better catalytic efficiency.

2. Site-specific rate of phosphorylation

In order to further define the ERK2 preferential sites along the Tau sequence, a time course of phosphorylation was also performed with pTEpY ERK2, with one 2D spectrum acquired for each time point of reaction. The relative integrals of resonances corresponding to identified phosphorylated residues were used to evaluate the level of modification at a specific phosphorylation site for each time point. A site-dependent kinetics of phosphorylation is shown in graph in Figure 47, A. The neighbour residue and its resonance integral can also be used to monitor a specific phosphorylation, for example A¹⁵² resonance is affected by the phosphorylation at T¹⁵³ (Figure 47, A). A fast phosphorylation rate is observed for pS²³⁵, pS⁴⁰⁴ and pS⁴²² with a peak already detected in the HSQC after 15 minutes of incubation with ERK2. Most sites are modified by over 40% phosphorylation after 3H reaction time, such as pT⁵⁰, pT¹⁵³, pT¹⁷⁵, pT¹⁸¹, pT¹⁹¹, pS²⁰², pT²⁰⁵, pT²³¹, pS²³⁵, pS⁴⁰⁴ and pS⁴²², while S⁴⁶ and T⁶⁹ at the N-terminus of Tau have are around 20% phosphorylation (Figure 47, A). After 2H reaction, almost all of sites are saturated in the conditions of the *in vitro* assay (Figure 47, A). All data from the HSQC spectra on phosphorylation time courses can be fitted by exponential equations. The constant time of phosphorylation reaction for each site would be given as shown in Figure 47, B and C. Three data sets of A¹⁵²/pT¹⁵³, pS²³⁵ and G²⁰⁷/pT²⁰⁵ are shown as examples (Figure 47, B). The phosphorylation of S²³⁵ is the most rapid, with a time constant of 20 min, followed by time constant for G²⁰⁷/pT²⁰⁵ at 40 min and A¹⁵²/pT¹⁵³ at 85 min (Figure 47, C). The other major sites pT⁵⁰, pT¹⁸¹, pT²⁰⁵, and more significantly pS²⁰², have a slower rate of phosphorylation (Figure 47, C).



(A)



(B)

Phospho-sites	Constant T (min)	Phospho-sites	Constant T (min)
pS46	75	pS199	30
pT50	35	pS202	85
pT69	40	G207(pT205)	40
A152(pT153)	85	pT231	45
pT153	90	pS235	20
pT175	40	pS396	38
pT181	45	pS404	25
pS191	45	pS422	25

(C)

Figure 47: Kinetics of Tau phosphorylation by active ERK2 *in vitro*. (A) The fraction of phosphorylation at each site of Tau is correlated with the relative integrated volume of phospho-site resonance in the HSQC spectrum. HSQC are acquired for each time point of incubation, for samples with 15 min (green), 30 min (brown), 1 H (yellow), 2 H (violet) and 3 H (red) reaction time. In the graph, each resonance volume is normalized by that of the C-terminal L⁴⁴¹ residue to account to variations between spectra. The error bars reflect the

Signal/Noise ratio. (B) Site-specific kinetic of Tau phosphorylation by pTEpY ERK2. Graphical representation of the build-up of relative resonance integrals corresponding to Tau T/S residues with increasing phosphorylation due to incremental incubation periods, for a representative enzymatic reaction. Each data point in the plot corresponds to an integral in a 2D spectrum of the Tau protein incubated with activated-ERK2 for a time. Triangles and diamonds correspond to the resonance of pS²³⁵ and the A¹⁵² located next to pT¹⁵³, respectively, and squares are for the resonance of G²⁰⁷ located next to pT²⁰⁵. Integral values of the resonances during a representative phosphorylation experiment (as shown in A) are fitted with mono-exponential functions of the type $1-(e^{-t/T})$ with time t and constant T in minutes. T constants are given in (C). (C) Time constants (T, in minutes) of the phosphorylation of Tau on specific sites by pTEpY ERK2.

Part 3

**NMR characterization of Tau interaction with DNA
and its regulation by Tau phosphorylation**

One physiological function of Tau in cells is to protect DNA in stress conditions (Violet et al. 2014; Sultan et al. 2011). This Tau function has been less studied than other roles of Tau in neurons, such as for example its role in MTs stabilization. As other functions of Tau are known to be regulated by phosphorylation, such is the case for its interaction with MTs, interaction of Tau with DNA could also be modulated by PTMs. Although phosphorylation of Tau in the nucleus has been reported, this aspect was never investigated (Lu et al. 2013; Alvarez et al. 2012; Lu et al. 2013). In this study, NMR spectroscopy is used to characterize the interaction of Tau with double-stranded oligonucleotides (referred to as DNA in this study). We have defined two main interaction sites, located in the C-terminal part of PRD and in R2 repeat in MTBDs. We additionally have investigated the impact of Tau phosphorylation on this interaction. Several Tau constructs were necessary to elucidate the molecular detail of Tau interaction with DNA.

I contributed in this work first by preparing Sumo-Tau peptides and interpret NMR data to elucidate their interactions with DNA. To confirm the interaction sites of Tau with DNA, we have used peptides whose sequences correspond to interaction site identified by NMR spectroscopy in the full length protein. I selected two Tau peptides as F[220-240]Tau and F[271-294]Tau, corresponding to amino acid sequences located in C-terminal part of PRD and R2 repeat of MTBDs, respectively. The peptide in the R2 repeat corresponds to one of Tau nuclei of aggregation, called PHF6* and is not very soluble (von Bergen et al. 2000).

To prepare the peptides, we used recombinant DNA construct to obtain a fusion with a N-terminal Sumo3 protein, a small folded protein consisting of 103 amino acids. The cDNA cloning of Tau peptides, the preparation of ¹⁵N-labelled His-Sumo Tau peptides for NMR spectroscopy analysis are described in 'Materials and Methods'. We have used the fusion proteins for the NMR analysis. As the resonances for Sumo residues are well dispersed in HSQC spectra, in contrast to that of Tau peptides which are more restricted in the central spectra, the overlap between the signal of Tau and those of the SUMO were limited enough to allow the assignment of the peptide signals and the interaction experiments. In addition, there is no chemical shift perturbation of the signals corresponding to the Sumo protein in presence of DNA seen in the [H, ¹⁵N] 2D HSQC spectra of ¹⁵N-labelled His-Sumo Tau peptides. I also contributed to the study of the regulation of the interaction of DNA and Tau by Tau phosphorylation. Using Tau samples phosphorylated by mouse brain extract, we have shown

that the phospho-Tau does not interact with the DNA. This suggests that pathological Tau phosphorylation could affect the physiological function of Tau mediated by DNA binding.

paper (published on January 27, 2015)

**Nuclear Magnetic Resonance Spectroscopy characterization of Tau
interaction with DNA and its regulation by phosphorylation**

Nuclear Magnetic Resonance Spectroscopy Characterization of Interaction of Tau with DNA and Its Regulation by Phosphorylation

Haoling Qi,^{†,‡} François-Xavier Cantrelle,[†] Houda Benhelli-Mokrani,^{§,@} Caroline Smet-Nocca,[†] Luc Buée,^{||,⊥} Guy Lippens,[†] Eliette Bonnefoy,[§] Marie-Christine Galas,^{||,⊥} and Isabelle Landrieu^{*,†,‡}

[†]UMR8576 CNRS-Lille University, 59655 Villeneuve d'Ascq, France

[‡]Interdisciplinary Research Institut (IRI), 59655 Villeneuve d'Ascq, France

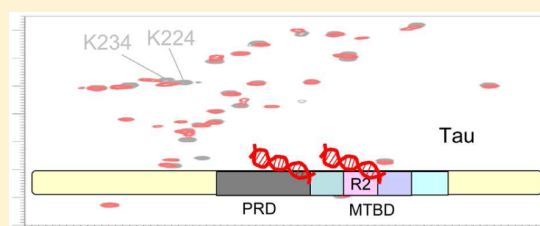
[§]UMR-S1007 Inserm-Paris Descartes University, Sorbonne Paris Cité, 75270 Paris, France

^{||}UMR-S1172, (JP)Arc Alzheimer & Tauopathies Inserm-Lille University, Medicine Faculty, 59045 Lille, France

[⊥]CHRU, Memory Clinic, 59045 Lille, France

S Supporting Information

ABSTRACT: The capacity of endogenous Tau to bind DNA has been recently identified in neurons under physiological or oxidative stress conditions. Characterization of the protein domains involved in Tau–DNA complex formation is an essential first step in clarifying the contribution of Tau–DNA interactions to neurological biological processes. To identify the amino acid residues involved in the interaction of Tau with oligonucleotides, we have characterized a Tau–DNA complex using nuclear magnetic resonance spectroscopy. Interaction of an AT-rich or GC-rich 22 bp oligonucleotide with Tau showed multiple points of anchoring along the intrinsically disordered Tau protein. The main sites of contact characterized here correspond to the second half of the proline-rich domain (PRD) of Tau and the R2 repeat in the microtubule binding domain. This latter interaction site includes the PHF6* sequence known to govern Tau aggregation. The characterization was pursued by studying the binding of phosphorylated forms of Tau, displaying multiple phosphorylation sites mainly in the PRD, to the same oligonucleotide. No interaction of phospho-Tau with the oligonucleotide was detected, suggesting that pathological Tau phosphorylation could affect the physiological function of Tau mediated by DNA binding.



Several neurological disorders have been linked to alterations of protein–DNA interactions potentially leading to perturbation of gene expression, although the proteins involved are not considered transcription factors *per se*.¹ The proteins α -synuclein (α Syn), Prp prion protein, SOD1 (superoxide dismutase 1), Tau, and amyloid $A\beta$ peptides are examples of such proteins. Called amyloid proteins, they have in common, on one hand, their sensitivity to aggregation and, on the other, their capacity to translocate into the nucleus and interact with DNA.¹ The amyloid proteins also share the characteristic of being associated with neurological disorders: Parkinson's disease, spongiform encephalopathy, amyotrophic lateral sclerosis, and Alzheimer's disease (AD). Their interaction with DNA can result in an increase in their aggregation propensity,² as was shown, at least *in vitro*, for α Syn or Prp,^{3,4} and/or lead to gene expression modification as proposed upon the nuclear translocation of amyloid $A\beta$ 1–42.^{5–7} This suggests that the interaction of these amyloid proteins with DNA might make an important contribution to the disease. To understand the part of amyloid protein–DNA interactions related to the establishment of such diseases, it is necessary to determine the protein regions involved in DNA complex formation.

The involvement of Tau in the development of AD pathology has been predominantly linked to the loss of its function as a microtubule-associated protein. The molecular mechanisms of Tau-linked pathways associated with neurodegeneration are, however, far from being totally elucidated. Recently, the importance of the multifunctional aspect of Tau has strongly emerged.⁸ Tau-dependent global heterochromatin relaxation leading to aberrant gene expression in *Drosophila*⁹ and cell cycle reactivation is one example of a mechanism by which Tau has been implicated in the establishment of pathogenesis beyond its role as a microtubule stabilizer.

Even though Tau is mainly described as an axonal protein, it can also be localized in the nucleus of neurons and other cell types^{10–14} where it was shown to directly or indirectly bind the DNA.^{12,14–16} The DNA binding capacity of Tau appears to be related to its DNA protective function, because Tau has been shown to prevent neuronal genomic DNA from damage under physiological or heat-shock conditions^{14,17} and to promote chromosome stability.^{16,18} This is in agreement with the *in vitro* observation that Tau binds the minor groove of the DNA

Received: November 26, 2014

Revised: January 21, 2015

Published: January 26, 2015

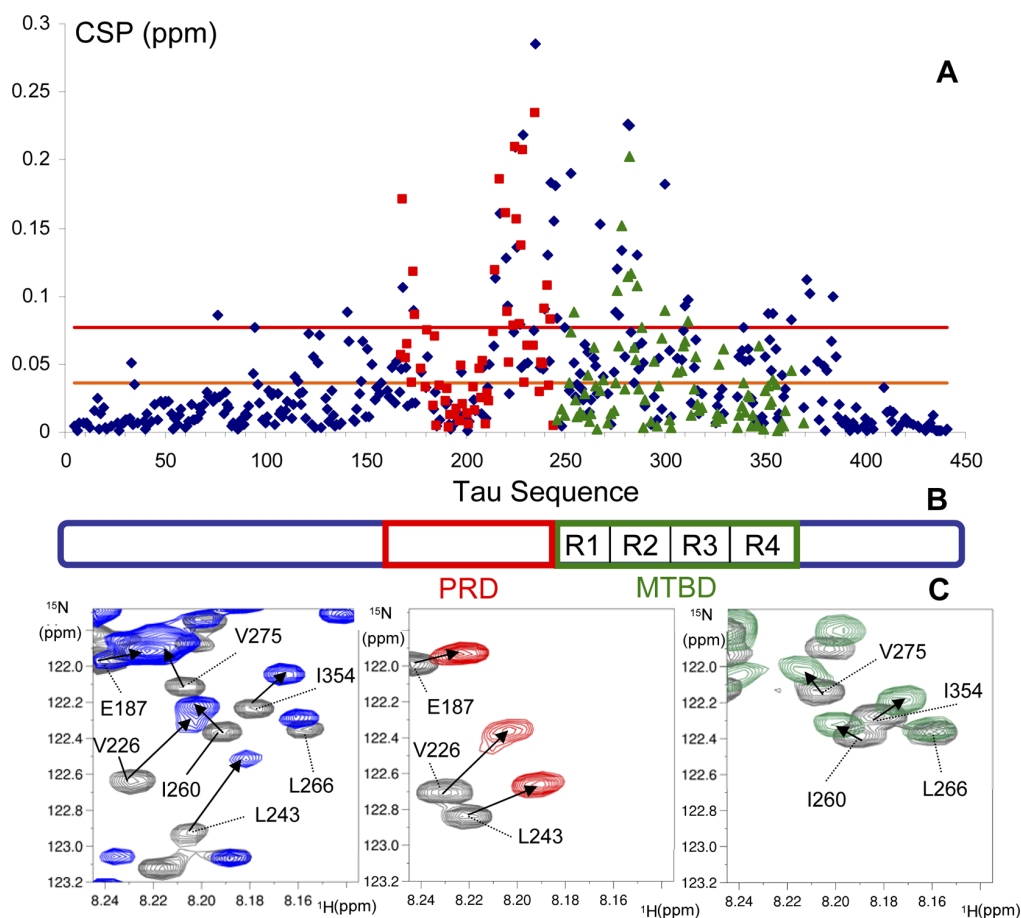


Figure 1. Mapping of Tau interaction sites with the GSAT oligonucleotide. (A) Combined ^1H , ^{15}N CSP, calculated as defined in Materials and Methods, of resonances in two-dimensional (2D) ^1H - ^{15}N HSQC spectra of full-length [^{15}N]Tau (blue diamonds), F[165–245]Tau or PRD (red squares), and F[244–372]Tau or MTBD (green triangles). CSP are differences calculated between the spectra of the protein with a molar ratio of the GSAT oligonucleotide of 2 and of the protein free in solution, for every assigned resonance along the sequence. The orange threshold corresponds to the average CSP and the red one to the average CSP plus one standard deviation for the Tau data. (B) Schematic Tau protein that highlights the PRD (red box) and repeat regions R1–R4 in the MTBD (green box) along the Tau sequence. CSP along the Tau amino acid sequence are shown in Figure S4 of the Supporting Information. (C) Details of overlaid 2D ^1H - ^{15}N HSQC spectra of [^{15}N]Tau, [^{15}N]F[165–245]Tau, and [^{15}N]F[244–372]Tau (from left to right, respectively) free in solution (gray spectra) and with a molar ratio of GSAT oligonucleotide of 2 (spectra superimposed in blue, red, and green, respectively).

double helix, protecting DNA from oxidative damage or thermal denaturation.^{14,19,20}

Tau activity is physiologically regulated by multiple post-translational modifications, and aberrant phosphorylations have been systematically linked to its dysfunction. Hyperphosphorylated Tau is the main component of the paired helical filaments, the aggregated form of Tau found in neurons of patients suffering from AD. Multiphosphorylation was proposed to induce the detachment of Tau from the microtubules and to impair axonal transport, leading eventually to neuronal death. The work on the pathological aspect of Tau phosphorylation has mainly focused on its relationship with Tau aggregation or microtubule stabilization. Very few studies have examined the effect of phosphorylation on the stress-related DNA protective role of Tau. Phosphorylation of Tau has been observed in the case of the nuclear fraction of Tau in neuroblastoma N2a cells and in mouse brains exposed to formaldehyde²¹ as well as in neuroblastoma cells infected with herpes simplex virus type 1,²² showing the relevance of establishing the consequences of Tau phosphorylation on its DNA binding capacity. Additionally,

formaldehyde treatment of N2a cells induces the co-occurrence of Tau hyperphosphorylation and DNA damage,²¹ and *in vitro*, Tau phosphorylation by GSK3 kinase reduces its capacity to protect DNA against thermal denaturation or reactive oxygen species,²³ suggesting that phosphorylation could be related to the dysfunction of the nuclear fraction of Tau.

In this context, we have focused our interest on the determination of the regions of Tau protein involved in its interaction with DNA. Several regions of Tau have been defined along its primary sequence: an N-terminal region, a proline-rich domain (PRD), a microtubule binding domain (MTBD) consisting of four partially repeated sequences (R1–R4), and a C-terminal region (Figure 1). The sequences described as being responsible of nucleating Tau aggregation,²⁴ called PHF6* and PHF6, are located at the beginning of the R2 and R3 repeats, respectively, in the MTBD. Both the PRD and the MTBD are involved in the microtubule stabilizing activity of Tau.^{25,26}

The amino acid composition of the intrinsically disordered Tau protein is enriched with a few residue types that represent

most of its primary sequence. This is the case of the 44 lysine residues corresponding to 10% of the amino acid composition of the longest 441-amino acid Tau isoform and the 80 Ser/Thr residues, potential sites of phosphorylation. When combined in a Tau protein phosphorylated at multiple sites, the modification of charge distribution could lead to a very complex regulation of Tau interactions. We have previously shown that the analytical capacity of nuclear magnetic resonance (NMR) spectroscopy allows us to define interaction sites between Tau and a protein or a ligand such as heparin at the level of an amino acid residue.²⁷ Similarly, the phosphorylation pattern of the Tau samples used in the interaction assays can be defined in a global manner, visualizing all the single-site modifications in one experiment.^{28,29} With these analytical capacities, we have used NMR spectroscopy to investigate the interaction of Tau with a 22 bp oligonucleotide, whose sequence was derived from murine γ -satellite DNA, to define the regions of Tau involved in its interaction with DNA. Additionally, we have used phosphorylated forms of Tau protein, characterized by NMR, to investigate the impact of a multiple-phosphorylation pattern on the Tau–DNA interaction.

MATERIALS AND METHODS

Annealing of Oligonucleotides for the NMR Experiments. The forward AT-rich 5'-ATTTAGAAATGTCCACTGTAGG-3' oligonucleotide (Eurofins MWG Operon, Ebersberg, Germany) and its reverse complement (80 nmol each) were mixed in 1 mL of annealing buffer [65 mM Tris-HCl (pH 7.7), 15 mM MgCl₂, and 1.5 mM EDTA]. The oligonucleotide mix was subjected to a 3 min denaturation at 95 °C followed by a slow cooling via a 1 °C step every minute to 10 °C. The annealed oligonucleotides [called double-stranded (ds) AT-rich or GSAT oligonucleotide] were purified on a MonoQ HR 5/5 anion exchange resin equilibrated in TE buffer [10 mM Tris-HCl (pH 7.7) and 1 mM EDTA]. A NaCl salt gradient was used to separate the major annealed fraction from the residual oligonucleotides. The collected fractions were pooled and buffer exchanged against 50 mM ammonium bicarbonate before lyophilization. The lyophilized ds AT-rich oligonucleotide was suspended in NMR buffer [50 mM deuterated Tris-*d*₁₁ (pH 6.6), 25 mM NaCl, and 2.5 mM EDTA]. The same procedure was used to prepare ds GC-rich oligonucleotide from the GC-rich sequence 5'-ATCCAGAGGTGTCCACTGTAGG-3'.

Isotopic Labeling of Recombinant Tau Protein. The Tau protein used in this study is the longest isoform, 441 amino acid residues, expressed as a recombinant protein without any tag from the recombinant pET15b *Escherichia coli* expression vector in BL21(DE3) strains. Tau fragments were expressed as fusion protein with an N-terminal histidine tag for F[244–372]Tau or without any tag for F[165–245]Tau, from the same expression vector. Tau peptides F[220–240]Tau and F[271–294]Tau were expressed as a fusion with the SUMO protein presenting an N-terminal His tag from a modified pET vector.³⁰

For uniform ¹⁵N labeling, the protein production was conducted in M9 medium with 1 g of ¹⁵NH₄Cl, a supplement of 300 mg of [¹⁵N]ISOGRO complete medium (Isotech), and a MEM vitamin cocktail (Sigma) per liter of growth medium. Two grams of [¹³C₆]glucose was used for the doubly labeled proteins instead of 4 g of glucose for sole ¹⁵N labeling. Production of recombinant protein was started with 0.4 mM isopropyl 1-thio- β -D-galactopyranoside, and bacterial growth

was then pursued for a 4 h period, at 37 °C. A first purification step was obtained by heating the bacterial protein extract for 15 min at 75 °C. The Tau protein and Tau fragments were recovered in the soluble fraction after centrifugation at 15000g for 30 min. Purification of the [¹⁵N]Tau protein and [¹⁵N]F[165–245]Tau was performed by cation exchange chromatography in 50 mM phosphate buffer (pH 6.3) and 1 mM EDTA (5 mL Hitrap SP Sepharose FF column, GE Healthcare). [¹⁵N]F[244–372]Tau, [¹⁵N]Sumo-F[220–240]Tau, and [¹⁵N]Sumo-F[271–294]Tau were purified on nickel resin (5 mL HisTrap, GE Healthcare) according to the manufacturer's standard protocol. The pooled fractions from the chromatography purification step were transferred to ammonium bicarbonate by desalting on a 15/60 Hiprep Desalting Column (G25 resin, GE Healthcare) and lyophilized. [¹⁵N]Tau, [¹⁵N]Tau fragments, and [¹⁵N]Sumo-fused Tau peptides were suspended in NMR buffer [50 mM deuterated Tris-*d*₁₁, 30 mM NaCl (pH 6.7), 2.5 mM EDTA, and 2 mM DTT]. The same purification procedures were followed for the doubly ¹⁵N- and ¹³C-labeled proteins. The acquisition of two-dimensional (2D) NMR spectra for the Tau, Tau fragments, and peptides in the presence of the GSAT oligonucleotide, suspended in the same buffer as the proteins, was performed at a protein final concentration in the range of 45–100 μ M.

Phosphorylation of Recombinant Tau. The mouse brain extract was prepared by homogenizing a half brain (~0.2 g) in 500 μ L of homogenizing buffer [10 mM Tris-HCl (pH 7.4), 5 mM EGTA, 2 mM DTT, and 1 μ M okadaic acid (Sigma)] supplemented with 20 μ g/mL leupeptin and 40 mM Pefabloc. The suspension was first crudely homogenized manually with a potter in 1.5 mL tubes followed by several passages through a 20 gauge needle. Ultracentrifugation was next performed at 100000g for 1 h in 1.5 mL tubes. The [¹⁵N]Tau protein was dissolved at 10 μ M in 10 mL of phosphorylation buffer [2 mM ATP, 40 mM Hepes-KOH (pH 7.3), 2 mM MgCl₂, 5 mM EGTA, and 2 mM DTT supplemented with a protease inhibitor cocktail (Complete, Roche) and 1 μ M okadaic acid (Sigma)]. The phosphorylation reaction was performed at 37 °C for 24 h with 500 μ L of mouse brain extract. The mixture was next heat inactivated at 75 °C for 15 min. After centrifugation, the supernatant was transferred to ammonium bicarbonate by desalting on a 15/60 Hiprep Desalting Column (G25 resin, GE Healthcare) and lyophilized. Phosphorylation by the recombinant CDK2/CycA3 kinase was previously described in detail.²⁹

Acquisition of Data. TMSP-*d*₄ (trimethyl silyl propionate, 1 mM) used as a proton chemical shift internal reference (0 ppm) and 5% D₂O were added to the protein sample. ¹H–¹⁵N HSQC 2D spectra were recorded at 293 K on a 900 MHz Avance III NMR spectrometer equipped with a triple-resonance cryogenic probehead (Bruker, Karlsruhe, Germany). Three-dimensional (3D) HNCACB spectra were acquired at 600 MHz for assignment of Tau peptide resonances on 300 μ M ¹⁵N- and ¹³C-labeled Sumo-F[220–240]Tau and Sumo-F[271–294]Tau. Assignment of the DNA-bound Tau resonances was based on the gradual chemical shift observed in the titration experiments and a 3D HNCACB spectrum acquired on a 300 μ M ¹⁵N- and ¹³C-labeled F[165–245]Tau with a 0.5 molar ratio of the GSAT oligonucleotide.

Data Analysis. Spectra were processed using Bruker TOPSPIN 2.1 (Bruker). Peak picking were performed using Sparky (T. D. Goddard and D. G. Kneller, SPARKY 3, University of California, San Francisco). The chemical shift perturbations (CSP) of individual amide resonances were

calculated with the following equation, taking into account the relative dispersion of the proton and nitrogen δ chemical shifts: $CSP = [(\delta^1H_{bound} - \delta^1H_{free})^2 + 0.2(\delta^{15}N_{bound} - \delta^{15}N_{free})^2]^{1/2}$. Bound and free subscripts in the formula stand for the δ in the oligonucleotide-bound protein state and free protein state, respectively.

RESULTS

Interaction of Full-Length Tau Protein with a Double-Stranded AT-Rich Oligonucleotide. A detailed molecular study of the interaction of Tau with DNA was conducted using a double-stranded AT-rich oligonucleotide whose sequence is found present within pericentromeric γ -satellite AT-rich DNA (GSAT). A 936 bp fragment from this chromosomal region was previously shown to interact with Tau by an electrophoretic mobility shift assay (EMSA).¹³ An oligonucleotide was chosen instead of this DNA fragment to facilitate experiments by nuclear magnetic resonance spectroscopy (NMR). The capacity of recombinant Tau to form protein–DNA complexes with the AT-rich 22 bp GSAT oligonucleotide *in vitro* was confirmed by an EMSA (Figure S1 of the Supporting Information). The double-stranded GSAT oligonucleotide used in the experiments was purified by anion exchange chromatography to ensure the homogeneity of the preparation. The principle of the mapping experiment by NMR is the comparison of 2D spectra of ¹⁵N-labeled Tau acquired in the presence of the GSAT oligonucleotide with respect to the spectra of ¹⁵N-labeled Tau alone (Figure S2 of the Supporting Information). The resonances in these spectra correspond to ¹H–¹⁵N amide correlations and are assigned to an amino acid residue in the protein sequence. The assignment of Tau resonances has previously been completed by us and others.^{31–33} These resonances are perturbed in intensity and/or chemical shifts in case their chemical environment or their conformation is modified and can thus be used to monitor the interaction between molecular partners. Addition of the GSAT oligonucleotide to Tau indeed induced many CSP in the [¹⁵N]Tau 2D HSQC spectrum (Figure 1). To investigate whether this interaction is dependent on the oligonucleotide sequence, the experiments were similarly performed with a second oligonucleotide with a higher GC content, which was annealed and purified as the GSAT oligonucleotide. [¹⁵N]Tau 2D HSQC spectra in the presence of one oligonucleotide or the other can be superimposed (compare red and green signals in Figure S3A,C of the Supporting Information), showing that the interaction with Tau is mediated through the backbone of the nucleic acid, in a manner independent of the nature of the bases. Because of the disordered nature of Tau and its large size, the signal overlap precludes a complete coverage of the CSP. Despite the missing data for some residues (Figure S4 of the Supporting Information), the numerous CSP observed along the Tau sequence revealed a complex interaction consisting of multiple binding sites (Figure 1 and Figure S4 of the Supporting Information).

Interaction of a Double-Stranded GSAT Oligonucleotide with the PRD and MTBD of Tau. To confirm and further define the amino acids of Tau participating in the interaction with the GSAT oligonucleotide, two fragments of Tau sequence that encompass the regions found to be involved in the interaction of Tau with the GSAT oligonucleotide were used. Tau fragments corresponding to the PRD F[165–245]Tau and to the MTBD F[244–372]Tau (also called K18) were complexed with the GSAT oligonucleotide (Figure 1 and

Figure S2 of the Supporting Information). Comparison of the extent and direction of the respective CSP (Figures 1 and 2)

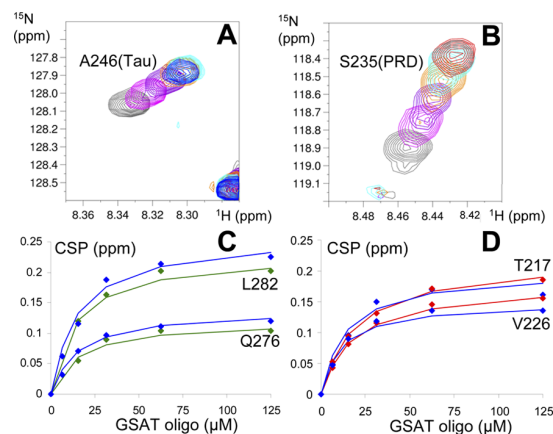


Figure 2

Figure 2. Affinity of Tau for the GSAT oligonucleotide. (A and B) Details of overlaid 2D ¹H–¹⁵N HSQC spectra of [¹⁵N]Tau and F[165–245]Tau, respectively, free in solution (gray spectra) and with 0.1, 0.25, 0.5, and 1 molar ratios of GSAT oligonucleotide (spectra superimposed in pink, purple, orange, and cyan, respectively). The final titration point of a 2 molar ratio of GSAT oligonucleotide is (A) the blue resonance for Tau and (B) the red resonance for F[165–245]Tau. (C and D) Saturation curves were obtained by plotting the gradual CSP observed for resonances corresponding to amino acid residues in the Tau binding sites vs the increasing amount of GSAT oligonucleotide. Diamonds correspond to the experimental data, and the solid curve corresponds to the fit by the equation $(CSP)_{max} \times [oligo]/(K_D + [oligo])$, with $(CSP)_{max}$ being the CSP attained at saturation and $[oligo]$ being the concentration of added GSAT oligonucleotide. (C) CSP of the resonances of L282 and Q276 in Tau (blue) and F[244–372]Tau (green). (D) CSP of the resonances of T217 and V226 in Tau (blue) and F[165–245]Tau (red).

indicated that the PRD and MTBD interacted with the GSAT oligonucleotide in a similar manner isolated or embedded in full-length Tau (Figures 1 and 2). Overall, the data obtained during NMR analysis of Tau–DNA interaction identified the second half of the PRD, from amino acid R209 to A246, as the region of Tau protein predominantly involved in anchoring the 22 bp GSAT oligonucleotide. In addition, the N-terminal part of the R2 repeat containing the PHF6* sequence involved in Tau aggregation,²⁴ from amino acid K267 to S289, was identified as a second site of interaction with the GSAT oligonucleotide. Titrations of the GSAT oligonucleotide into Tau, the MTBD samples, and the PRD samples were used to calculate dissociation constants (K_D) that characterize these interactions. Gradual CSP along the titration (Figure 2A,B) can be fit to a saturation curve (Figure 2C,D) to derive the K_D values for every residue that shows a CSP above the average for Tau resonances at saturation (above the red threshold in Figure 1A). In the PRD, the average K_D value calculated on the basis of the resonances of eight residues present between L215 and S241 residues of Tau was $10.5 \pm 2.4 \mu M$ and in the case of the F[165–245]Tau fragment was $19.2 \pm 0.8 \mu M$. In the MTBD fragment, the average K_D value calculated on the basis of the resonances of seven residues present between V275 and N286 residues of Tau was $11.3 \pm 1.7 \mu M$ and in the case of the F[244–372]Tau fragment was $15.7 \pm 3.3 \mu M$. The K_D calculated for some residues of Tau located outside of these

main interaction regions showed lower affinity, with a value of $30.6 \pm 8.4 \mu\text{M}$ for six residues located between Q351 and A384 residues and a value of $19.1 \pm 3 \mu\text{M}$ for T169 and K174 residues. These data showed that the GSAT oligonucleotide binds to the PRD and R2 repeat with similar affinity, confirming both regions as the main binding sites. The data obtained with the isolated domains indicate that both the PRD and the MTBD can bind the GSAT oligonucleotide in an independent manner. The similar affinities observed for the isolated domains compared to that of the full-length Tau confirmed the independence of these sites within the Tau protein for oligonucleotide binding. A combination of those binding sites would indeed have led to a significantly higher affinity of Tau compared to those of the isolated domains. However, the presence of both binding sites within the Tau protein could account for the lower K_D observed for Tau compared to those of both fragments, as the concentration of binding sites is double compared to that of the isolated fragments.

Interaction of the GSAT Oligonucleotide with Tau Peptides. To gain further insight into the minimal regions of Tau protein necessary to establish an interaction with the GSAT oligonucleotide, shorter peptides of Tau were used. These Tau peptides were the F[220–240]Tau peptide consisting of an amino acid sequence present in the PRD and the F[271–294]Tau peptide consisting of an amino acid sequence present in R2 of the MTBD, including the PHF6* sequence. Both peptides were chosen as they showed interaction with the GSAT oligonucleotide when embedded in the Tau sequence (Figure 1 and Figure S4 of the Supporting Information). Because the F[271–294]Tau peptide displayed poor solubility, fusions with the SUMO protein were used, both for recombinant expression and for acquisition of 2D NMR spectra. Because SUMO is a small folded protein, the overlap with the Tau peptide signals was reasonable and therefore allowed a correct analysis of the Tau resonances. Comparison of the 2D HSQC spectra of ^{15}N -labeled Tau SUMO peptides obtained after addition of an equimolar concentration of the GSAT oligonucleotide with the spectra of the peptide alone showed limited CSP (Figure 3). In the case of the SUMO-

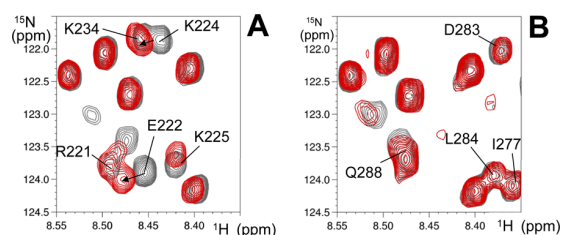


Figure 3. Mapping of Tau interaction sites with the GSAT oligonucleotide. Details of overlaid 2D ^1H - ^{15}N HSQC spectra of (A) [^{15}N]Sumo-F[220–240]Tau from the Tau PRD and (B) [^{15}N]Sumo-F[271–294]Tau from the Tau MTBD free in solution (gray) and with a 1 molar ratio of GSAT oligonucleotide (superimposed in red). Resonances from the Tau peptides are labeled.

F[220–240]Tau peptide, CSP were observed between amino acids 222 and 229 (Figure 3A and Figure S5A of the Supporting Information), while for the SUMO-F[271–294]Tau peptide, the spectrum was not modified after addition of the GSAT nucleotide (Figure 3B and Figure S5B of the Supporting Information). The CSP in the spectrum of SUMO-

F[220–240]Tau are, however, small compared to those observed for the resonances corresponding to the same sequence embedded in larger fragments (compare Figure 1A with Figure S5A,B of the Supporting Information). The 20-amino acid Tau peptides were thus not able to interact efficiently with the GSAT oligonucleotide on their own, showing that a minimal length is required to anchor the 22-base oligonucleotide.

Modulation of Interaction of Tau with the GSAT Oligonucleotide by Tau Phosphorylation.

Interactions of Tau with several molecular partners are known to be modulated by phosphorylation. We thus next addressed the question of the influence of Tau phosphorylation on the capacity of Tau to interact with DNA. To investigate this aspect, we first used an *in vitro* phosphorylated Tau protein obtained by incubating [^{15}N]Tau with a mouse brain extract that contains a complex mixture of kinases known to phosphorylate Tau.³⁴ During these experiments, phosphatase activities were blocked by okadaic acid. Under these conditions, Tau protein was phosphorylated at multiple sites (Figure 4A).

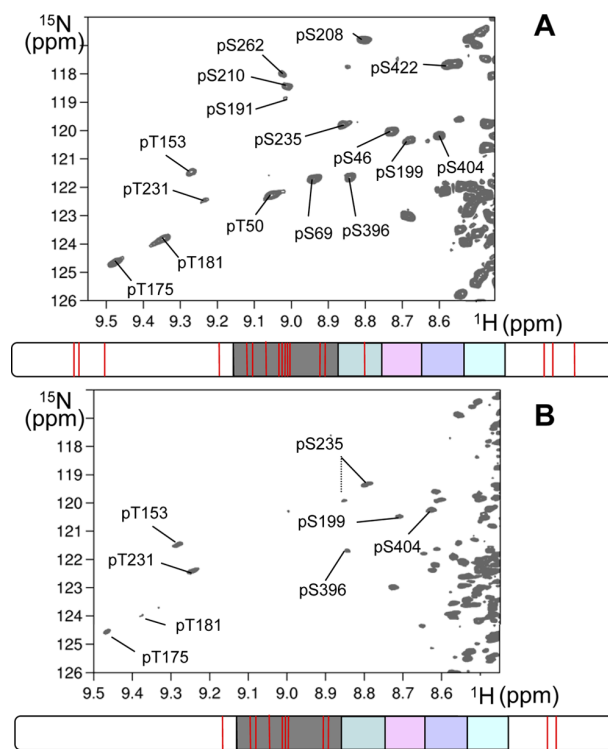


Figure 4. Phosphorylation patterns of Tau. Details of 2D ^1H - ^{15}N HSQC spectra of [^{15}N]Tau phosphorylated with (A) mouse brain extracts and (B) CDK2/CycA3 recombinant kinase. Resonances corresponding to phosphorylated Ser and Thr residues are labeled. The schematic Tau protein highlights the repeat regions, color-coded light blue, pink, purple, and green. The detected phosphorylation sites are represented by red bars.

Analysis of the phosphorylated forms of Tau using NMR spectroscopy showed new resonances in the region corresponding to pSer and pThr residues that were absent in the spectrum of the unphosphorylated form of Tau. A total of 18 resonances of phosphorylated residues could be detected. The phosphorylation sites obtained here with a mixture of kinases were identified by comparing the chemical shifts of their resonances

with those of resonances of phosphorylation sites obtained by incubating Tau with individual recombinant kinases that we have previously described.^{28,29,35} These phosphorylations affected all the regions of Tau: the N-terminal region (pS46, pT50, pS69, and pT153), the PRD (pT175, pT181, pS191, pS199, pS202, pT205, pS208, pS210, pT231, and pS235), the MTBD (pS262), and the C-terminal region (pS396, pS404, and pS422) (scheme in Figure 4A). Incubation of this phosphorylated form of Tau with the GSAT oligonucleotide resulted in no detectable interaction as translated by the absence of perturbation in the resulting 2D spectrum obtained in the presence of the GSAT oligonucleotide as compared to the spectrum of free phospho-Tau (Figure S3B,D of the Supporting Information). The experiment was repeated with the second oligonucleotide having a higher GC content that also showed no interaction with the phosphorylated Tau sample (Figure S3B,D of the Supporting Information). Phosphorylations of Tau at multiple sites, mainly located in the PRD, thus abolish its interaction with the oligonucleotides. The interaction assay of a phosphorylated Tau isoform with the GSAT oligonucleotide was repeated with a Tau protein displaying a reduced phosphorylation profile, obtained by using the recombinant CDK23/CycA3 kinase (Figure 4B) whose pattern of Tau phosphorylation we have previously thoroughly characterized.²⁹ The major CDK phosphorylation sites located in the oligonucleotide Tau binding region were limited to pT231 and pS235 residues of the PRD. Despite this lower level of phosphorylation, as compared to that observed after incubation of Tau with the kinase activity of brain extracts, the CDK phospho-Tau was unable to bind to the GSAT oligonucleotide (Figure 5). No binding was observed not only in the PRD in the case of CDK phospho-Tau (Figure 5B) or CDK phospho-F[165–245]Tau (Figure S6 of the Supporting Information) but also in the MTBD in phospho-Tau (Figure 5D). Despite the distance between the GSAT oligonucleotide binding site present in the R2 repeat and the phosphorylation sites in the

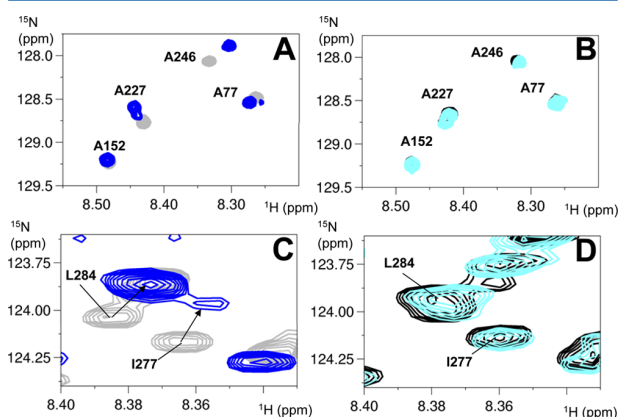


Figure 5. Phosphorylation of Tau with CDK2/CycA3 decreases its capacity to interact with oligonucleotides. Details of overlaid 2D ^1H – ^{15}N HSQC spectra of (A and B) [^{15}N]Tau free in solution (gray) and with a 1 molar ratio of GSAT oligonucleotide (superimposed in blue) and (B and D) [^{15}N]CDK2 phospho-Tau free in solution (black) and with a 1 molar ratio of GSAT oligonucleotide (superimposed in cyan). Panels A and B show regions of alanine residues; A227 and A246 are located in the PRD. I277 and L284 in panels C and D are located in the R2 repeat.

PRD, the phosphorylation events do globally affect the interaction.

DISCUSSION

The interaction of Tau with a 22 bp oligonucleotide was investigated using NMR spectroscopy to obtain a detailed description of the region(s) of Tau protein involved in the establishment of Tau–DNA interactions. Our first interrogation was about the specificity of the interaction because the C-terminal part of Tau is very rich in lysine residues that could potentially drive unspecific electrostatic interactions. It seems not to be the case, as we observe a localized interaction of the oligonucleotide predominantly with the second part of the PRD of Tau and the R2 repeat in the MTBD. Tau interacted with the AT-rich as well as with the GC-rich oligonucleotides, suggesting that Tau–DNA interaction is mediated by the DNA backbone.

Protein–nucleic acid interaction involves Lys/Arg basic residues, both being well represented in the Tau–GSAT oligonucleotide interacting domains. Additionally, polar residues such as Ser/Thr or Gln/Asn residues, well represented in the PRD, are favored in establishing contacts with the DNA backbone. The amino acid composition of the PHF6* peptide present in the MTBD is, however, less typical of a DNA-interacting sequence as it contains several hydrophobic residues that are usually under-represented at protein–DNA interfaces.³⁶ The larger side chains of the hydrophobic residues indeed prevent access of the protein backbone atoms to the DNA.

This result is nevertheless in agreement with recent work on the thermodynamics of the Tau–DNA interaction, based on surface plasmon resonance (SPR), which has identified hydrophobicity as an important contributor to the stabilization of the interaction.³⁷ Interaction of the GSAT oligonucleotide with the R2 sequence of Tau was clearly detected by CSP, in the case of both the full-length Tau protein and the F[244–372]Tau (K18) fragment, showing that the oligonucleotide is able to interact with the isolated MTBD in a manner independent of the flanking sequences. The involvement of the PRD and MTBD of Tau in oligonucleotide binding, as determined using an EMSA, has been previously reported,²⁰ as well as the capacity of these two domains to independently interact with oligonucleotide sequences. Isolated peptide sequences located in the interaction regions, F[220–240]Tau from the PRD or F[271–294]Tau from the R2 repeat, only weakly interacted with the GSAT oligonucleotide. This suggests that a minimal protein length is required for the oligonucleotide to anchor, which is not found in the 20-amino acid peptide sequences.

Phosphorylation of the nuclear fraction of Tau has not yet been thoroughly characterized, but a recent study supports the idea that Tau can be phosphorylated on several sites in the nuclear compartment.²¹ We here showed that phosphorylation strongly reduces the level of interaction of Tau with the GSAT oligonucleotide, with only very small CSP detected in phospho-Tau spectra upon addition of the oligonucleotide. A bulk electrostatic effect can be invoked to explain the loss of Tau–DNA interaction, because phosphorylations reduce the net positive charge.³⁸ However, this electrostatic model implies that the phospho sites have to be located in the proximity of the polybasic region.³⁸ The phospho-Tau proteins used in our study were phosphorylated at numerous Ser/Thr residues mainly located in the PRD, the only phosphorylation site

detected in the MTBD being pS262 in the case of Tau phosphorylated by the brain extracts. Despite this observation, the interaction is abolished by phosphorylation not only in the PRD but also in the repeats. The large number of acidic residues introduced by phosphorylation of Ser/Thr residues could explain the loss of interaction in the PRD, but the link is not straightforward between multiple phosphorylations in the PRD and loss of interaction in the MTBD. We indeed showed that the isolated MTBD can bind in a manner independent of the PRD to the oligonucleotide. The phosphorylation sites closest to the Tau R2 repeat DNA binding site (F[271–294]Tau) are pT231/pS235 present in the PRD, located some 40 amino acid residues away in the primary sequence, in a disordered protein context. However, several structural studies point to the fact that Tau is not an entirely disordered polymer but shows a complex network of transient long-range interactions between distant domains of the protein mediated by electrostatic effects.^{33,39–41} Intramolecular FRET (Forster resonance energy transfer) measurements have suggested that Tau retains some global folding even in its “natively unfolded” state.⁴⁰ The conclusion that Tau is not a fully extended polymer was also drawn from PRE (paramagnetic relaxation enhancement) NMR experiments combined with SAXs data³³ and from conformational ensemble approaches.⁴¹ More specifically, the N-terminal and C-terminal domains of Tau are found to dynamically fold back on the central part of the Tau protein,^{33,41} in a model called a “paperclip”.⁴⁰ The PRD was additionally shown to contact repeat R3.³³ These weak contacts between distant domains of the Tau protein, in particular between the PRD and the MTBD, could potentially explain the long-range effect of the phosphorylations in the PRD affecting the DNA binding of the MTBR.

In vitro phosphorylation of Tau by GSK3 was recently shown to decrease the capacity of Tau to interact with DNA in an EMSA.²³ Phosphorylated Tau expressed in Sf9 cells was also shown to lose its capacity to interact with calf thymus DNA by SPR.³⁷ pT181 and pS396 were immuno-detected in the GSK3 phospho-Tau protein,²³ and pS202/pT205 and pT212/pS214 were detected by the AT8 and AT100 antibodies, respectively, in the sf9-expressed Tau.³⁷ These phosphorylation patterns do not support the idea that phosphorylations have to be located on sites close to the interaction regions with the DNA to prevent the interaction. As immunodetections do not allow a global survey of the resulting Tau phosphorylation pattern, contrary to the NMR analysis, additional phosphorylations in the GSK3 phospho-Tau or sf9-expressed phospho-Tau might have occurred without detection.

In vivo, the phospho-Tau protein detected in replicating HEK cells by the PHF1 antibody does not colocalize with the condensed chromosomes, suggesting that phosphorylations can prevent the Tau–DNA interaction.³⁷ Nuclear shuttling of Tau into the nucleus upon heat shock results in a decrease in the level of Tau phosphorylation.¹⁴ Additionally, the capacity of Tau to protect neurons against hyperthermia-induced DNA damage was correlated to an increased level of binding of dephosphorylated Tau to DNA.¹⁴ It is thus possible that the fraction of Tau translocating and transiently remaining in the nucleus under stress conditions is mainly dephosphorylated. In the reverse, recovery of cells after heat shock is associated with an increased level of Tau phosphorylation and a concomitant decrease in the level of nuclear Tau. Nevertheless, nuclear phosphorylated Tau was detected under other stress conditions; the treatment of neuroblastoma cells with form-

aldehyde and GSK3 kinase was proposed in this case to phosphorylate Tau in the nucleus. Interestingly, accumulation of phosphorylated Tau in the nuclei under formaldehyde treatment co-occurred with DNA alteration.²³ We here describe that the phosphorylation of Tau, mainly in its PRD, results in a loss of its capacity to interact with nucleotide sequences. Such a pattern of phosphorylation would thus result in the inability of Tau to bind DNA and could consequently induce a loss of its DNA protective function. Therefore, hyperphosphorylation could be linked to pathological aspects of Tau function in the nucleus.

■ ASSOCIATED CONTENT

🔗 Supporting Information

Recombinant Tau forms a protein–DNA complex with the GSAT oligonucleotide in EMSA experiments (Figure S1). Recombinant Tau forms a protein–DNA complex with the GSAT oligonucleotide in NMR experiments (Figure S2). Comparison of interaction of Tau with ds AT-rich and GC-rich oligonucleotides. Phosphorylation of Tau by rat brain extract decreases its capacity to interact with both oligonucleotides (Figure S3). CSP due to the interaction with the GSAT oligonucleotide mapped onto the amino acid residue sequence of the PRD and repeat regions of Tau (Figure S4). CSP along the sequences of [¹⁵N]Sumo-F[220–240]Tau and [¹⁵N]Sumo-F[271–294] peptides upon addition of the GSAT oligonucleotide (Figure S5). Comparison of the interaction of ¹⁵N F[165–245]Tau and ¹⁵N CDK-phospho F[165–245]Tau with the GSAT oligonucleotide (Figure S6). This material is available free of charge via the Internet at <http://pubs.acs.org>.

■ AUTHOR INFORMATION

Corresponding Author

*UMR8576 CNRS-Lille University, 59658 Villeneuve d’Ascq, France. Telephone: +33 3 62531714. Fax: +33 3 62531. E-mail: isabelle.landrieu@univ-lille1.fr.

Present Address

@H.B.-M.: UFIP CNRS6286, Nantes University, 44322 Nantes, France.

Author Contributions

H.Q. and F.-X.C. contributed equally to this work.

Funding

The NMR facilities were funded by the Région Nord, CNRS, Pasteur Institute of Lille, European Community (FEDER), French Research Ministry, and the University of Sciences and Technologies of Lille I. We acknowledge support from the TGE RMN THC (FR-3050, France). This study was supported by a grant from the LabEx (Laboratory of Excellence) DISTALZ (Development of Innovative Strategies for a Transdisciplinary approach to Alzheimer’s disease), and in part by the French government funding agency Agence Nationale de la Recherche MALZ EPITAUDNA.

Notes

The authors declare no competing financial interest.

■ ACKNOWLEDGMENTS

We thank L. Delattre for technical assistance, Dr J. Lopez for the Tau assignment and Dr B. Chambraud for help with the brain extract protocols.

■ ABBREVIATIONS

AD, Alzheimer's disease; CSP, chemical shift perturbations; EMSA, electrophoretic mobility shift assay; GSAT, γ -satellite AT-rich DNA; HSQC, heteronuclear single-quantum spectrum; MTBD, microtubule binding domain of the Tau protein; NMR, nuclear magnetic resonance spectroscopy; SPR, surface plasmon resonance; PRD, proline-rich domain of the Tau protein.

■ REFERENCES

- (1) Camero, S., Benitez, M. J., and Jimenez, J. S. (2013) Anomalous protein-DNA interactions behind neurological disorders. *Adv. Protein Chem. Struct. Biol.* 91, 37–63.
- (2) Liu, C., and Zhang, Y. (2011) Nucleic acid-mediated protein aggregation and assembly. *Adv. Protein Chem. Struct. Biol.* 84, 1–40.
- (3) Nandi, P. K., Leclerc, E., Nicole, J. C., and Takahashi, M. (2002) DNA-induced partial unfolding of prion protein leads to its polymerisation to amyloid. *J. Mol. Biol.* 322, 153–161.
- (4) Cherny, D., Hoyer, W., Subramaniam, V., and Jovin, T. M. (2004) Double-stranded DNA stimulates the fibrillation of α -synuclein in vitro and is associated with the mature fibrils: An electron microscopy study. *J. Mol. Biol.* 344, 929–938.
- (5) Ohyagi, Y., Asahara, H., Chui, D. H., Tsuruta, Y., Sakae, N., Miyoshi, K., Yamada, T., Kikuchi, H., Taniwaki, T., Murai, H., Ikezoe, K., Furuya, H., Kawarabayashi, T., Shoji, M., Checler, F., Iwaki, T., Makifuchi, T., Takeda, K., Kira, J., and Tabira, T. (2005) Intracellular A β 42 activates p53 promoter: A pathway to neurodegeneration in Alzheimer's disease. *FASEB J.* 19, 255–257.
- (6) Barucker, C., Sommer, A., Beckmann, G., Eravci, M., Harmeier, A., Schipke, C. G., Brockschneider, D., Dyrks, T., Althoff, V., Fraser, P. E., Hazrati, L. N., George-Hyslop, P. S., Breitner, J. C., Peters, O., and Multhaup, G. (2015) Alzheimer Amyloid Peptide A β 42 Regulates Gene Expression of Transcription and Growth Factors. *J. Alzheimer's Dis.* 44, 613–624.
- (7) Barucker, C., Harmeier, A., Weiske, J., Fauler, B., Albring, K. F., Prokop, S., Hildebrand, P., Lurz, R., Heppner, F. L., Huber, O., and Multhaup, G. (2014) Nuclear translocation uncovers the amyloid peptide A β 42 as a regulator of gene transcription. *J. Biol. Chem.* 289, 20182–20191.
- (8) Morris, M., Maeda, S., Vossel, K., and Mucke, L. (2011) The many faces of tau. *Neuron* 70, 410–426.
- (9) Frost, B., Hemberg, M., Lewis, J., and Feany, M. B. (2014) Tau promotes neurodegeneration through global chromatin relaxation. *Nat. Neurosci.* 17, 357–366.
- (10) Loomis, P. A., Howard, T. H., Castleberry, R. P., and Binder, L. I. (1990) Identification of nuclear tau isoforms in human neuroblastoma cells. *Proc. Natl. Acad. Sci. U.S.A.* 87, 8422–8426.
- (11) Brady, R. M., Zinkowski, R. P., and Binder, L. I. (1995) Presence of tau in isolated nuclei from human brain. *Neurobiol. Aging* 16, 479–486.
- (12) Greenwood, J. A., and Johnson, G. V. (1995) Localization and in situ phosphorylation state of nuclear tau. *Exp. Cell Res.* 220, 332–337.
- (13) Sjoberg, M. K., Shestakova, E., Mansuroglu, Z., Maccioni, R. B., and Bonnefoy, E. (2006) Tau protein binds to pericentromeric DNA: A putative role for nuclear tau in nucleolar organization. *J. Cell Sci.* 119, 2025–2034.
- (14) Sultan, A., Nessler, F., Violet, M., Begard, S., Loyens, A., Talahari, S., Mansuroglu, Z., Marzin, D., Sergeant, N., Humez, S., Colin, M., Bonnefoy, E., Buee, L., and Galas, M. C. (2011) Nuclear tau, a key player in neuronal DNA protection. *J. Biol. Chem.* 286, 4566–4575.
- (15) Villasante, A., Corces, V. G., Manso-Martinez, R., and Avila, J. (1981) Binding of microtubule protein to DNA and chromatin: Possibility of simultaneous linkage of microtubule to nucleic acid and assembly of the microtubule structure. *Nucleic Acids Res.* 9, 895–908.
- (16) Rossi, G., Dalpra, L., Crosti, F., Lissoni, S., Sciacca, F. L., Catania, M., Di Fede, G., Mangieri, M., Giaccone, G., Croci, D., and Tagliavini, F. (2008) A new function of microtubule-associated protein tau: Involvement in chromosome stability. *Cell Cycle* 7, 1788–1794.
- (17) Violet, M., Delattre, L., Tardivel, M., Sultan, A., Chauderlier, A., Caillierez, R., Talahari, S., Nessler, F., Lefebvre, B., Bonnefoy, E., Buee, L., and Galas, M. C. (2014) A major role for Tau in neuronal DNA and RNA protection in vivo under physiological and hyperthermic conditions. *Front. Cell. Neurosci.* 8, 84.
- (18) Rossi, G., Conconi, D., Panzeri, E., Redaelli, S., Piccoli, E., Paoletta, L., Dalpra, L., and Tagliavini, F. (2013) Mutations in MAPT gene cause chromosome instability and introduce copy number variations widely in the genome. *J. Alzheimer's Dis.* 33, 969–982.
- (19) Hua, Q., and He, R. Q. (2003) Tau could protect DNA double helix structure. *Biochim. Biophys. Acta* 1645, 205–211.
- (20) Wei, Y., Qu, M. H., Wang, X. S., Chen, L., Wang, D. L., Liu, Y., Hua, Q., and He, R. Q. (2008) Binding to the minor groove of the double-strand, tau protein prevents DNA from damage by peroxidation. *PLoS One* 3, e2600.
- (21) Lu, J., Miao, J., Su, T., Liu, Y., and He, R. (2013) Formaldehyde induces hyperphosphorylation and polymerization of Tau protein both in vitro and in vivo. *Biochim. Biophys. Acta* 1830, 4102–4116.
- (22) Alvarez, G., Aldudo, J., Alonso, M., Santana, S., and Valdivieso, F. (2012) Herpes simplex virus type 1 induces nuclear accumulation of hyperphosphorylated tau in neuronal cells. *J. Neurosci. Res.* 90, 1020–1029.
- (23) Lu, Y., He, H. J., Zhou, J., Miao, J. Y., Lu, J., He, Y. G., Pan, R., Wei, Y., Liu, Y., and He, R. Q. (2013) Hyperphosphorylation results in tau dysfunction in DNA folding and protection. *J. Alzheimer's Dis.* 37, 551–563.
- (24) von Bergen, M., Friedhoff, P., Biernat, J., Heberle, J., Mandelkow, E. M., and Mandelkow, E. (2000) Assembly of tau protein into Alzheimer paired helical filaments depends on a local sequence motif ((306)VQIVYK(311)) forming β structure. *Proc. Natl. Acad. Sci. U.S.A.* 97, 5129–5134.
- (25) Gustke, N., Trinczek, B., Biernat, J., Mandelkow, E. M., and Mandelkow, E. (1994) Domains of tau protein and interactions with microtubules. *Biochemistry* 33, 9511–9522.
- (26) Goode, B. L., Denis, P. E., Panda, D., Radeke, M. J., Miller, H. P., Wilson, L., and Feinstein, S. C. (1997) Functional interactions between the proline-rich and repeat regions of tau enhance microtubule binding and assembly. *Mol. Biol. Cell* 8, 353–365.
- (27) Sibille, N., Sillen, A., Leroy, A., Wieruszkeski, J. M., Mulloy, B., Landrieu, I., and Lippens, G. (2006) Structural impact of heparin binding to full-length Tau as studied by NMR spectroscopy. *Biochemistry* 45, 12560–12572.
- (28) Landrieu, I., Lacosse, L., Leroy, A., Wieruszkeski, J. M., Trivelli, X., Sillen, A., Sibille, N., Schwalbe, H., Saxena, K., Langer, T., and Lippens, G. (2006) NMR analysis of a Tau phosphorylation pattern. *J. Am. Chem. Soc.* 128, 3575–3583.
- (29) Amniai, L., Barbier, P., Sillen, A., Wieruszkeski, J. M., Peyrot, V., Lippens, G., and Landrieu, I. (2009) Alzheimer disease specific phosphoepitopes of Tau interfere with assembly of tubulin but not binding to microtubules. *FASEB J.* 23, 1146–1152.
- (30) Luna-Vargas, M. P., Christodoulou, E., Alfieri, A., van Dijk, W. J., Stadnik, M., Hibbert, R. G., Sahtoe, D. D., Clerici, M., Marco, V. D., Littler, D., Celie, P. H., Sixma, T. K., and Perrakis, A. (2011) Enabling high-throughput ligation-independent cloning and protein expression for the family of ubiquitin specific proteases. *J. Struct. Biol.* 175, 113–119.
- (31) Lippens, G., Wieruszkeski, J. M., Leroy, A., Smet, C., Sillen, A., Buee, L., and Landrieu, I. (2004) Proline-directed random-coil chemical shift values as a tool for the NMR assignment of the tau phosphorylation sites. *ChemBioChem* 5, 73–78.
- (32) Smet, C., Leroy, A., Sillen, A., Wieruszkeski, J. M., Landrieu, I., and Lippens, G. (2004) Accepting its random coil nature allows a partial NMR assignment of the neuronal Tau protein. *ChemBioChem* 5, 1639–1646.
- (33) Mukrasch, M. D., Bibow, S., Korukottu, J., Jeganathan, S., Biernat, J., Griesinger, C., Mandelkow, E., and Zweckstetter, M. (2009)

Structural polymorphism of 441-residue tau at single residue resolution. *PLoS Biol.* 7, e34.

(34) Goedert, M., Jakes, R., Crowther, R. A., Six, J., Lubke, U., Vandermeeren, M., Cras, P., Trojanowski, J. Q., and Lee, V. M. (1993) The abnormal phosphorylation of tau protein at Ser-202 in Alzheimer disease recapitulates phosphorylation during development. *Proc. Natl. Acad. Sci. U.S.A.* 90, 5066–5070.

(35) Leroy, A., Landrieu, I., Huvent, I., Legrand, D., Codeville, B., Wieruszeski, J. M., and Lippens, G. (2010) Spectroscopic studies of GSK3 β phosphorylation of the neuronal tau protein and its interaction with the N-terminal domain of apolipoprotein E. *J. Biol. Chem.* 285, 33435–33444.

(36) Luscombe, N. M., Laskowski, R. A., and Thornton, J. M. (2001) Amino acid-base interactions: A three-dimensional analysis of protein-DNA interactions at an atomic level. *Nucleic Acids Res.* 29, 2860–2874.

(37) Camero, S., Benitez, M. J., Cuadros, R., Hernandez, F., Avila, J., and Jimenez, J. S. (2014) Thermodynamics of the interaction between Alzheimer's disease related tau protein and DNA. *PLoS One* 9, e104690.

(38) Serber, Z., and Ferrell, J. E., Jr. (2007) Tuning bulk electrostatics to regulate protein function. *Cell* 128, 441–444.

(39) von Bergen, M., Barghorn, S., Jeganathan, S., Mandelkow, E. M., and Mandelkow, E. (2006) Spectroscopic approaches to the conformation of tau protein in solution and in paired helical filaments. *Neurodegener. Dis.* 3, 197–206.

(40) Jeganathan, S., von Bergen, M., Brtlich, H., Steinhoff, H. J., and Mandelkow, E. (2006) Global hairpin folding of tau in solution. *Biochemistry* 45, 2283–2293.

(41) Schwalbe, M., Ozenne, V., Bibow, S., Jaremko, M., Jaremko, L., Gajda, M., Jensen, M. R., Biernat, J., Becker, S., Mandelkow, E., Zweckstetter, M., and Blackledge, M. (2014) Predictive atomic resolution descriptions of intrinsically disordered hTau40 and α -synuclein in solution from NMR and small angle scattering. *Structure* 22, 238–249.

0 50 100 200 Tau (ng)

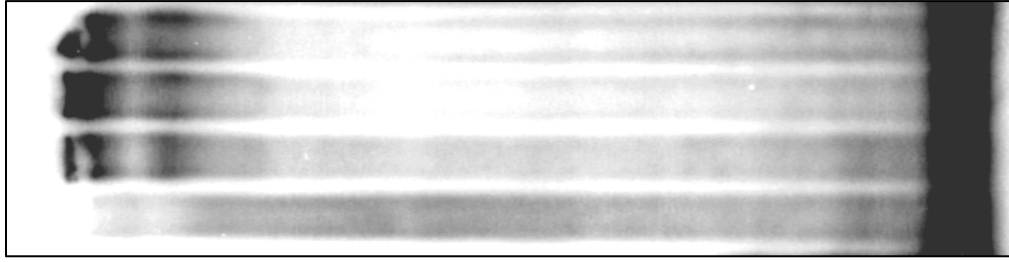


Figure S1. Recombinant Tau forms a protein-DNA complex with GSAT oligonucleotide. Various concentrations of recombinant Tau protein (50, 100 and 200 ng) were incubated with a constant amount of the ^{32}P -labeled 24 base pair double-stranded GSAT oligonucleotide in the presence of unlabeled double-stranded sonicated salmon sperm DNA as random non-sequence specific DNA competitor. The complexes were resolved on a TBE-polyacrylamide gel. After drying, radioactivity was visualized using PhosphorImager. The arrow indicates the migration direction, the star, Tau/DNA complexes and the arrowhead, the free probe. Tau/GSAT complex formation was observed starting with the lowest concentration of Tau as translated by the probe retardation with the intensity of complex formation increasing as the amount of Tau protein used in the experiment was increased.

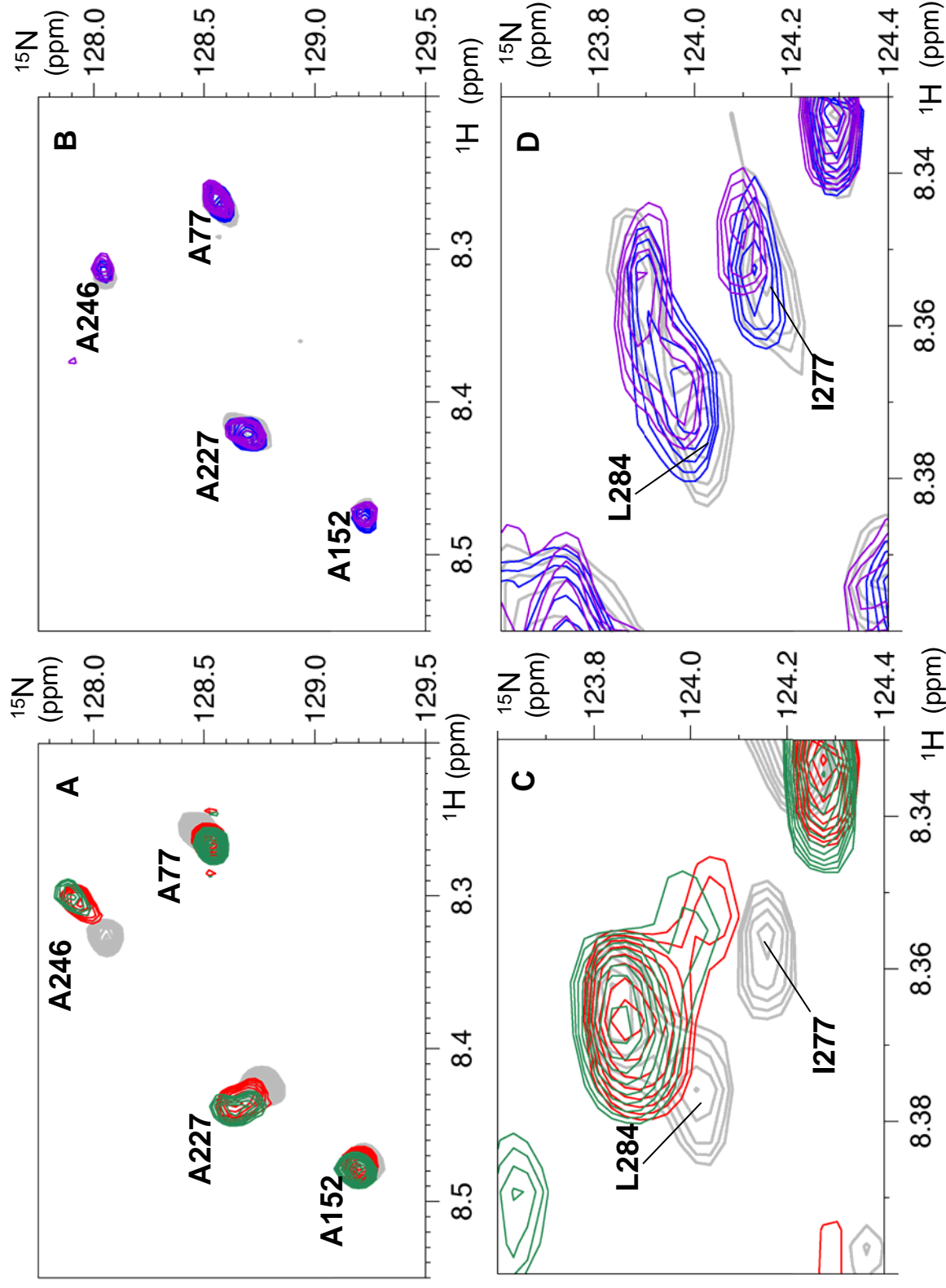


Figure S2. Comparison of Tau interaction with ds AT-rich and GC-rich oligonucleotides. Details of overlaid 2D [^1H , ^{15}N] HSQC spectra of **A** and **C** ^{15}N Tau free in solution (gray) and with 2 molar ratios of AT-rich ds oligonucleotide (superimposed in red) or GC-rich ds oligonucleotide (superimposed in green). **B** and **D** ^{15}N phospho-Tau free in solution (gray) and with 1 molar amount of AT-rich ds oligonucleotides (superimposed in blue) or GC-rich ds oligonucleotides (superimposed in purple). **A** and **B** show regions of Alanine residues, A227 and A246 are located in the PRR and in **C** and **D**, I277, L284 are located in the R2 repeat. phospho-Tau phosphorylation pattern is shown in **Figure 4A**.

162	qkgqana	tri	pa	pp	ap	kt	pp	ss	ge	pp	ks	PRR
192	gdrsgys	g	g	g	g	g	g	g	g	g	g	
222	epkqvav	vr	pp	ks	ps	aks	sr					
243	lqta	vp	md	l	kn	vs	ks	igs	ten	lk	hq	R1
274	kvqi	ink	ld	l	sn	vs	ks	cgs	kn	ik	vp	R2
305	svqi	vyk	pvd	l	sk	vt	sk	cgs	lgn	ih	hk	R3
336	qvevk	sek	ld	fk	dr	vq	ks	igs	ld	ni	th	R4
368	nk	ie	th	kl	tf	re	na	ka	ka			

Figure S3. Amino acid residue sequence of the PRR region and repeat regions of Tau. The repeat regions, R1 to R4, are highlighted along the sequence in light green, pink, purple and light blue, respectively. The PHF6* in R2 and PHF6 in R3 peptides are boxed. CSP along the Tau amino acid sequence is shown in **Figure 1**. The residues coloured orange have a CSP above the average CSP, the red one above the average CSP plus one standard deviation. The CSP of residues coloured in gray are not available. F[265-245]Tau and F[271-294]Tau Tau fragment sequences are delineated by red and green arrows, respectively.

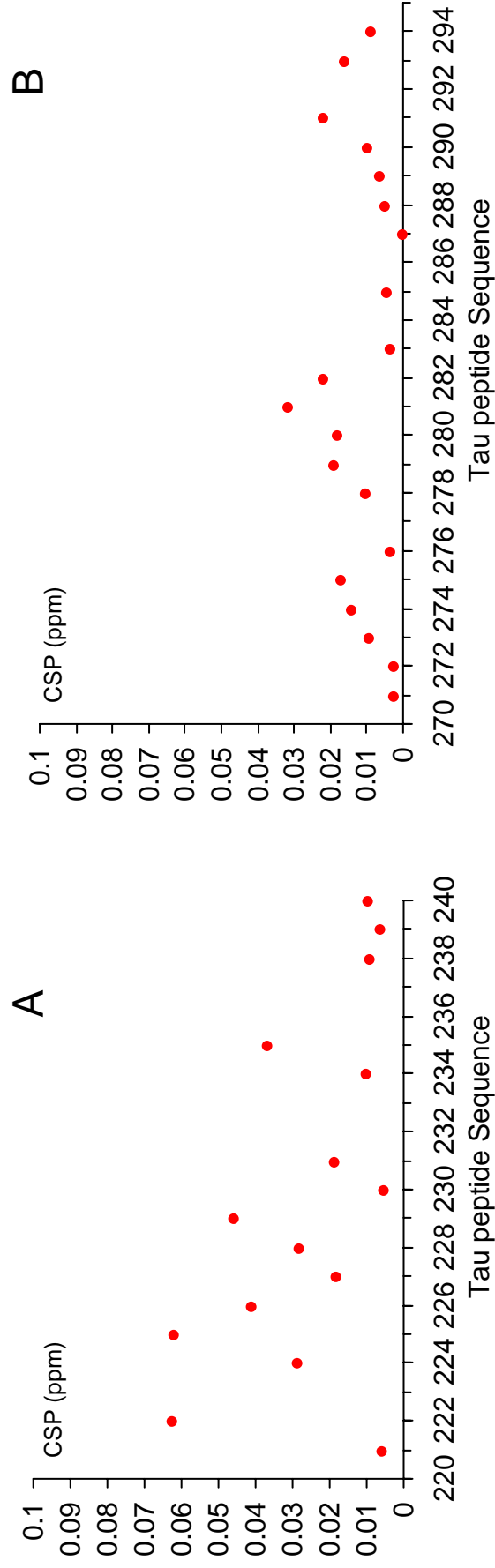


Figure S4. Mapping of Tau interaction sites with GSAT oligonucleotide. CSP in ppm, calculated as defined in methods, of resonances in 2D [^1H , ^{15}N] HSQC spectra of **A** ^{15}N -Sumo-F[220-240]Tau and **B** ^{15}N -Sumo-F[271-294]Tau with 1 molar ratio of GSAT oligonucleotides *versus* free in solution, for every assigned resonances along the sequence. Details of the corresponding spectra are shown in **Figure 3**.

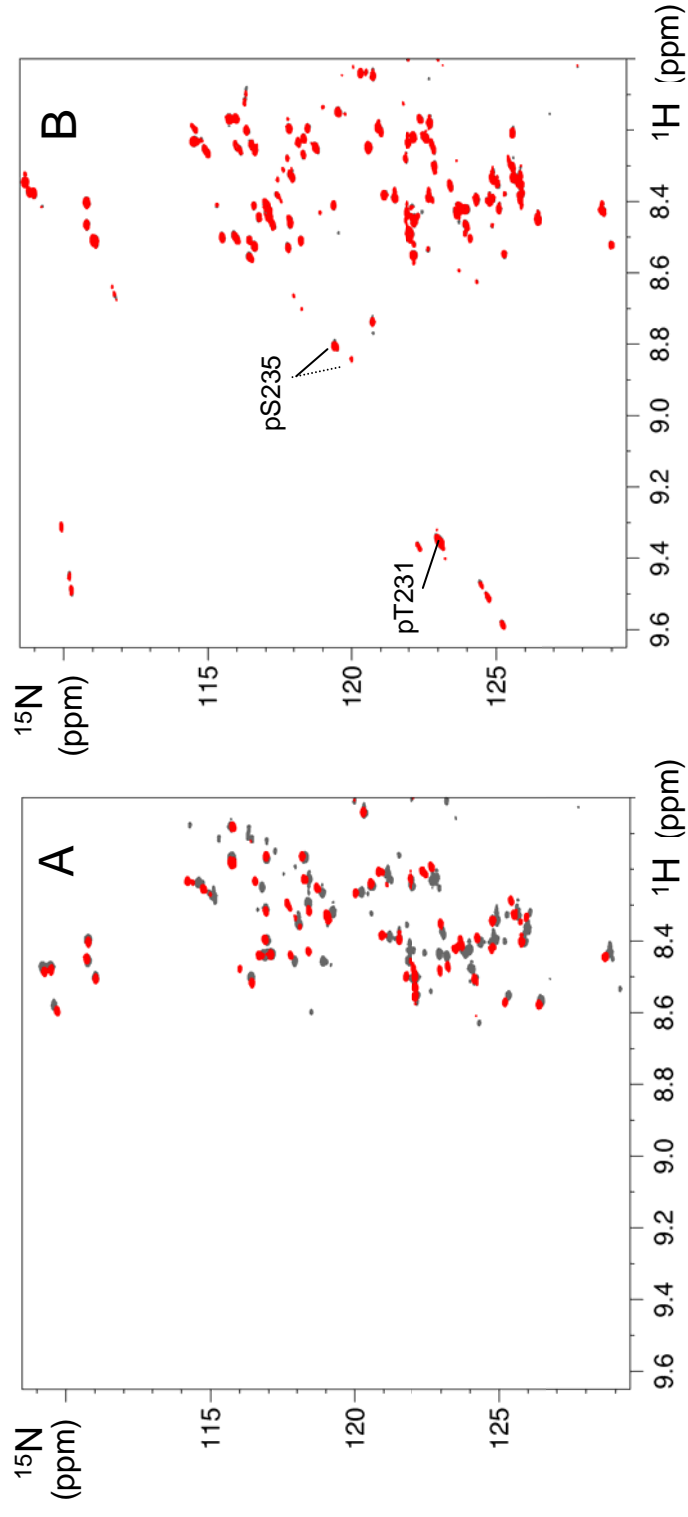


Figure S5. Phosphorylation of Tau with CDK2/CycA3 decreases its capacity to interact with GSAT oligonucleotide. Overlaid 2D [^1H , ^{15}N] HSQC spectra of **A** ^{15}N F[165-245]Tau free in solution (gray) and with 1 molar amount of GSAT oligonucleotide (superimposed in red). **B** ^{15}N CDK2 phospho-F[165-245]Tau free in solution (gray) and with 1 molar amount of GSAT oligonucleotide (superimposed in red).

Discussion

I have used NMR spectroscopy in the research projects to characterize enzymatic activity with Tau as substrate, and to investigate the interaction between Tau and ERK2 kinase or other binding partners.

1. Analytical characterization of Tau phosphorylation by ERK2 and by brain extracts

Tau is an excellent substrate for ERK2 as most of the 17 pS/pT-P motifs were here found modified *in vitro* by this kinase. Accordingly, incorporation of 14 to 16 phosphates on S/T-P sites per Tau molecules was reported by the MAPK activity purified from the brain extract (Drewes et al. 1992). MAPK ERK2 kinase purified from brain is immuno-positive at some AD-related phospho-epitopes like AT8 epitope pS²⁰²/pT²⁰⁵ and PHF-1 epitope pS³⁹⁶/pS⁴⁰⁴ (Drewes et al. 1992). Based on these early observations, ERK2 kinase has been proposed of being able to convert Tau into a PHF-state or AD-state.

The Tau phosphorylation sites here identified as modified by recombinant ERK2 only partially overlapped with those reported earlier by NanoES-MS. The NanoES-MS is a very sensitive method compared to NMR spectroscopy but with a yield difficult to quantify. The sensitivity of MS could lead to detection of minor phosphorylation sites not observed by NMR. 11 pS/pT-P motifs have been identified in recombinant Tau *in vitro* phosphorylated by active recombinant ERK2, with 2-4 phosphate incorporation per Tau molecule (Reynolds et al. 2000). pT²¹² and pT²¹⁷ were not found modified in our NMR study but well by nanoES-MS. This could thus be due to a low level of modification at these positions. However several proline-directed sites like T⁵⁰, S⁶⁹, T¹⁵³ and S¹⁹⁹ are not detected as phosphorylation sites in the MS study of ERK-mediated Tau phosphorylation in contrast with our NMR studies (Table 3) (Reynolds et al. 2000). We also reported based on the NMR data a single phosphorylation of an S residue not included in a Pro-directed motif, and not found in the MS study. There is no obvious explanation for these differences, except the experimental *in vitro* conditions.

In our NMR studies, the phosphorylation pattern of recombinant Tau obtained by incubation with rat brain extract matches the ERK2-mediated Tau pattern of phosphorylation. The main difference corresponds to phospho-sites, such as pS²⁰⁸, pS²⁶² and pS³⁵⁶ that are not included in Pro-directed motifs.

A previous study by LC-MS/MS also investigated the phosphorylation of Tau extracted from human brains of cognitively normal persons. More sites are identified in this study than

in our NMR-based characterization of Tau phosphorylated *in vitro* by rat brain extract. Again, the overlap between the results is very poor: more non-proline directed sites are identified by the MS study such as pT⁷¹, pS¹⁸⁵, pS¹⁹⁸, pS²⁰⁸, pS²¹⁴, pS²⁶², pS⁴⁰⁰ and pT⁴⁰³. Although there are only 17 Pro-directed phosphorylation sites, those also do not match between both studies with pS⁴⁶, pT⁵⁰, pT¹⁵³ found only in the NMR study and pT²¹⁷ only in the MS study. In our NMR spectra, they are some minor peaks in the region expected for phosphorylated residues that are not assigned because they are too weak to obtain signal in a third dimension. They could correspond to the missing phosphorylations in the NMR study.

An additional recent study also investigated the phosphorylation of Tau extracted from mouse brains. This study also reports on the difficulty of identifying phosphorylation in the densely phosphorylated region of the PRD and C-terminal region. For example, identifying that there is one or two phosphorylations in the S¹⁹⁸-S²¹⁰ peptide but without being able to assign these phosphorylations to a specific residue in the sequence (potentially S¹⁹⁸ and/or S¹⁹⁹ and/or S²⁰² and/or T²⁰⁵ and/or S²⁰⁸ and/or S²¹⁰) (Meaghan Morris et al. 2015).

This technical challenge of MS could account for part of the differences that are found between the MS and NMR studies, besides the experimental set-up. A strong consensus seems to emerge only for a few sites such as the AT8 epitope pS²⁰²/pT²⁰⁵ and the AT180 epitope pT²³¹ with pS²³⁵ in addition and in the C-terminus pS³⁹⁶/pS⁴⁰⁴. Note that these sites are usually described as pathological sites of phosphorylation and that the analytical studies here discussed do not target pathological Tau *per se*. However, the use of phosphatases inhibitors in these analytical studies may reproduce this pathological situation by pushing the equilibrium towards phosphorylation.

Table 3: Comparison of endogenous Tau phosphorylation in normal human or mice brain tissue with recombinant Tau phosphorylated by ERK2 or by rat brain extract in NMR studies and MS studies (Reynolds et al. 2000; Funk et al. 2014; Meaghan Morris et al. 2015).

Site	LC-MS/MS	MS	nanoES-MS	NMR	
	Endogenous human Tau	<i>Endogenous mice Tau</i>	Tau phosphorylated by ERK2	Tau phosphorylated by ERK2	Tau phosphorylated by R.B.E
S46			+	+	+
T50			-	+	+
S61 T63 S64 ^a		+			
S69		+	-	+	+
T71 ^a	+				
T111		+			
T153			-	+	+
T169 ^a		+			
T175	+	+	+	+	+
T181	+	+	+	+	+
S185 ^a	+				
S198 ^a	+	+			
S191 ^a		+		+	+
S199	+	+	-	+	+
S202	+	+	+	+	+
T205	+	+	+	+	+
S208 ^a	+		-	-	+
T212		+	+		
S214 ^a	+	+			
T217	+	+	+		
T231	+	+	+	+	+
S235	+	+	+	+	+
S262 ^a	+	+		-	+
S237 ^a		+			
S356 ^a		+	-	-	+
T373 T377 ^a		+			
T386 ^a		+			
S396	+	+	+	+	+
S400 ^a	+	+	-	-	
T403 ^a	+				
S404	+	+	+	+	+
S409 S412 S413 T414 S416 ^a		++			
S422				+	+

The identified phospho-sites in mice endogenous Tau is annotated in the number conserved in human 441-residue Tau.

R.B.E.: rat brain extract

a: non-proline sites

+: identified phospho-sites

-: identified non phospho-sites

Blank: unidentified sites

2. Kinase activity in rat brain

In rat brain extract, several kinases contribute by their enzymatic activities to Tau phosphorylation. There are non-proline-directed kinases in rat brain extract that may phosphorylate S²⁰⁸, S²⁶² and S³⁵⁶. A likely candidate is MARK2 kinase that has been reported to phosphorylate S²⁶² and S³⁵⁶ (Schwalbe et al. 2013). Among the Pro-directed kinase, ERK1/2 is the most likely choice. We have shown that ERK by itself can phosphorylate the S/T-P motifs of Tau also targeted by the rat brain extract activity. We showed that there is active ERK2 in the rat brain extract and that we can inhibit the kinase activity of rat brain by using specific inhibitors of ERK2, antibodies directed against the activation loop and the PEA15 protein.

Because our approach to identify the kinases in the rat brain extract by using specific inhibitors of kinases left some ambiguity, another possibility will be to combine two or more kinases to phosphorylate Tau *in vitro* and analyze the phosphorylation pattern by NMR spectroscopy. It is better to mix the kinases because a phosphorylation at one site may influence phosphorylation of the closest phosphorylation sites (Augustinack et al. 2002). This is well described for GSK3 that needs a priming phosphorylation (Woods et al. 2001; Leroy et al. 2010; Shi et al. 2004). The reverse may also be true and a phosphorylation at a position could prevent phosphorylation of the closest sites.

3. Pathological aspects of Tau phosphorylation

Several evidence support that ERK1/2 is highly activated in AD brains, either in response to IPTKB (Inositol triphosphate 3-kinase B) (Stygelbout et al. 2014) or to oxidative stress (Perry et al. 1999). It is still however not known whether or how much ERK1/2 contribute by its activity to the abnormal phosphorylation of Tau in disease-related cases. We have found that ERK2 the ability to generate properties associated with abnormally phosphorylated Tau, as was reported for the phosphorylation of Tau obtained by rat brain extract in presence of phosphatase inhibitor OA. The similarity is not only because of the multiple phospho-sites and similar phosphorylation pattern by ERK2 kinase and by rat brain extract, but also due to a similar capacity of aggregation by both of phosphorylated Tau.

In our studies, Tau aggregation experiments are performed *in vitro*, following the conditions described by Alonso et al. (Alonso et al. 2001). After 4H aggregation process, similar aggregates can be observed by electron microscopy for Tau phosphorylated both by ERK2 and by rat brain extract, but not for the unphosphorylated Tau (Figure 48). The aggregation might be triggered by Tau phosphorylation by both recombinant ERK2 and rat brain extract (Figure 48). The aggregation that we observed is however not the massive one that we usually observed in heparin-induced Tau or Tau fragments aggregation (Huvent et al. 2014), but concerns only a small fraction of the incubated sample. We could not observe kinetics of aggregation. It could be due to the small amount of aggregates in the sample, Thioflavin T (ThT), a fluorescent dye much used to quantify heparin-induced Tau fibers and amyloid aggregates being not a sensitive one.

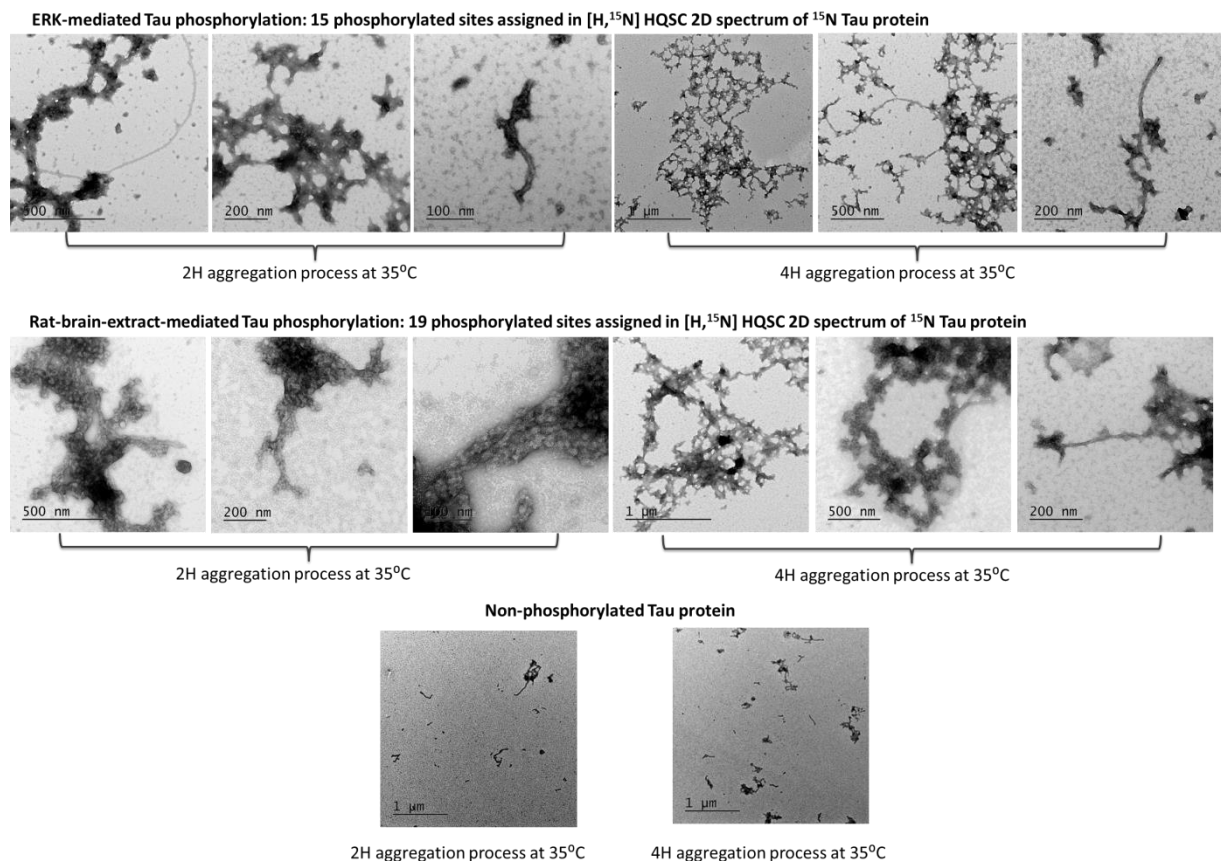


Figure 48: Tau aggregation observed by transmission electron microscopy. The aggregation assays are of Tau phosphorylated by recombinant ERK2 and by rat brain extract. Non-phosphorylated Tau sample is used as control.

Hyperphosphorylation of Tau has some reported pathological impacts such as decrease in MTs-binding affinity and increase ability in aggregation process. However, concerning this last point, very few studies have experimentally linked phosphorylation and aggregation. It is still controversial whether hyperphosphorylation is the key cause of aggregation of Tau protein (Alonso et al. 2001), or both hyperphosphorylation and aggregation occur independently. First, the hyperphosphorylation is never precisely defined at the molecular level. The definition of hyperphosphorylation is by itself not clear: high stoichiometry of phosphates per Tau molecule or some specific phospho-sites such as epitopes of AT8? The modifications related to pathological cases that result in the change of Tau properties and induce the toxicity of Tau protein are not precisely defined (Iqbal et al. 2010).

In endogenous Tau of normal brain tissue, there are only 2-3 moles of phosphates per mole of protein molecule whereas much higher phosphates incorporation is found for endogenous Tau extracted from AD-related brain tissue, with up to 10 moles or more of phosphate (Kopke et al. 1993). In addition, it has been demonstrated by mass spectroscopy that Tau isolated from cognitively normal human brain or wild type mice brain is phosphorylated *in vivo* at numerous sites, even at several described disease-related sites (Table 3), but there is no filamentous aggregation process occurring (Funk et al. 2014). The highly phosphorylated human recombinant Tau expressed in insect cells by using baculovirus expression system is modified at 12 phosphorylation sites, as defined by MS, and does not form aggregates in the insect cells, despite its high concentration during expression (Tepper et al. 2014). In these studies, the stoichiometry is not defined and it could be that each phosphorylation site is only modified at a low level or that only some of the phosphorylation sites are modified to a higher level. This level of modification could be too low to induce aggregation. Soluble hyperphosphorylated Tau extracted from AD human brain tissue, with 5-9 moles phosphate/mole protein, has been reported to be able to be self-assembled into fibers (Alonso et al. 2001), and also to sequester normal non-hyperphosphorylated Tau (Kopke et al. 1993; Alonso et al. 1994; Maeda et al. 2007). Again, the brain-extracted Tau proteins in these studies are not well characterized from an analytical point of view. We cannot exclude that some additional events such as various isoforms or truncated fragments, other posttranslational modifications or chaperone molecule also being brought with Tau molecules extracted from brain do mutually result in aggregation process.

There is no consensus however about the level of phosphorylation that would be needed or which sites would be involved in increasing Tau capacity of nucleation. In our hand, Tau protein solely phosphorylated by ERK2 is more sensitive to aggregation than the nonphosphorylated Tau but the aggregation observed in the sample only affect a small fraction of the sample compared to heparin induced aggregation. It is difficult to say whether it could make a difference in a cellular environment. The aggregation process in AD is very slow and takes years to invade the brain.

4. Interaction of Tau with ERK2 kinase and other binding partners

Conserved docking sequences are observed in most activators and substrates of MAP kinases. Their docking sequences have subtle variations for the recognition by specific MAP kinase, such as ERK or JNK. Along the Tau sequence, two main docking sites, F[274-284] and F[306-317], located in R1 and R2 of MTBDs, have been identified for ERK2 kinase. These interaction sites are compatible with a classic and reverse ERK-docking consensus sequences, respectively. These D-site peptides target the ERK docking groove, consisting of two negative charged Aspartic acid (Asp316 and Asp319 in human ERK2) and several hydrophobic residues, which are located far from its activation loop (Figure 49, A). Besides two main D-sites peptide in Tau sequence, there are other three possible docking sequences that we observe affected in presence of ERK2 by NMR analysis. The signal corresponding to these three sequences are less affected than for the two main docking sites and they may thus represent additional docking sites with less affinity to bind to ERK2. The docking sites are located outside the region where most of the ERK2-mediated phospho-sites are found, in the PRD. (Figure 49, B). However, we have observed that ERK2 can also efficiently phosphorylate *in vitro* the fragment of Tau corresponding to its isolated PRD without any docking sites. In our experimental conditions, with a concentrated substrate available, the docking interaction is not necessary for the enzymatic activity of ERK2 towards Tau.

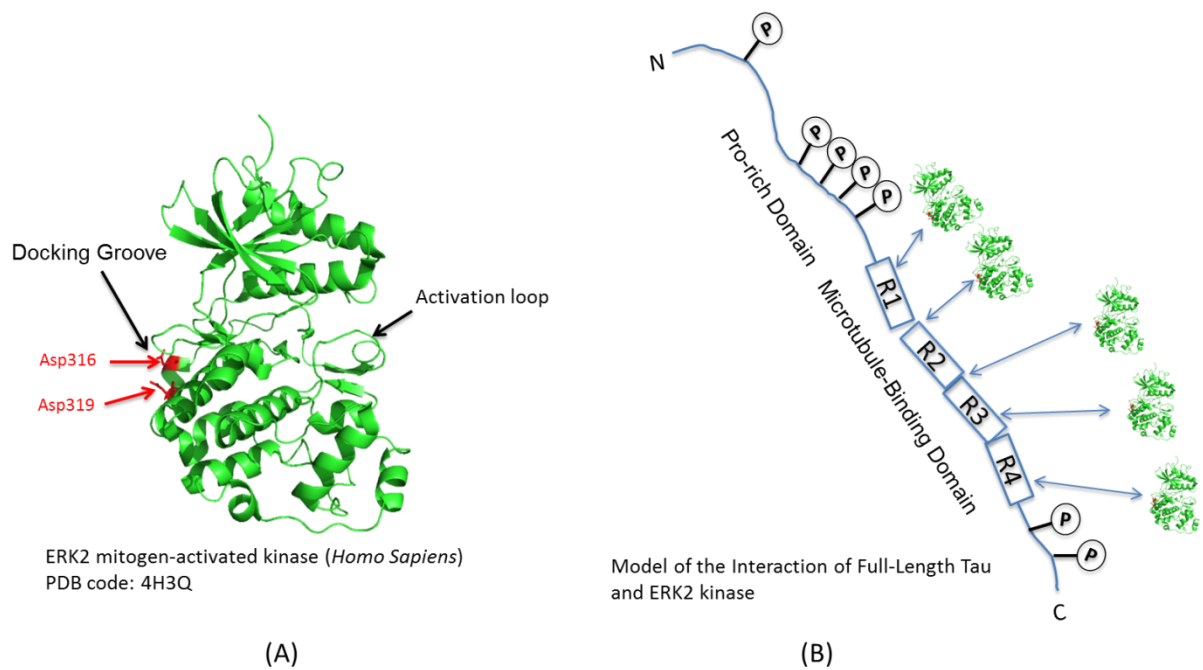


Figure 49: (A) Crystallographic structure of human ERK2 (PDB: 4H3Q). (B) A model of the interaction of full-length Tau with ERK2 kinase.

The role of MAPK docking sites in kinase activity efficiency is still controversial. P38 α , another MAP kinase similar to ERK2 has almost the same docking sequence consensus in its binding partners (Tanoue et al. 2000). NMR studies have shown that a substrate containing this docking sequence does not increase significantly the efficiency of p38 α final phospho-transfer, with only 1.5 fold of phosphorylation increase compared to an equivalent peptide without a docking sequence (Figure 50, A and B) (Tokunaga et al. 2014). For p38, the docking sequence has a mild impact on allosteric effect to increase enzymatic activity when the p38 α docking groove is occupied (Tokunaga et al. 2014). As for ERK2, a slight impact on the catalytic efficiency has also been observed after the occupation either of the DRS or FRS by a mimetic substrate containing a docking peptide (Sunbae et al. 2012). However, even if the effect is modest, it is always difficult to evaluate the impact it can have in a cellular context as docking interactions play an important role to recognize ERK1/2 upstream or downstream partners, and distinguish from other close family members in cellular signaling network (Remenyi et al. 2006). In the case of Tau, the intracellular impact of multiple docking sites may be crucial to regulate ERK1/2 specific binding and substrate competition (Futran et al. 2013), and may upregulate Tau phosphorylation under pathological circumstances as the

activation of ERK1/2 is found increased in AD neurons (Arendt et al. 1995; Perry et al. 1999; Ferrer et al. 2001).

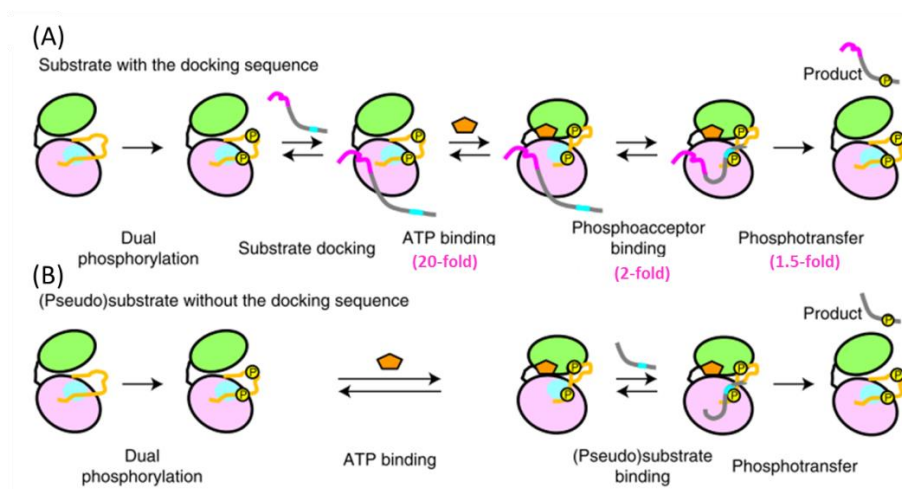


Figure 50: Schematic representation of p38 α in enzymatic phosphorylation process with or without substrate docking. (A) A substrate with docking sequence binds to activated p38 α before the ATP and phosphoacceptor site binding. (B) A pseudo-substrate without the docking sequence as solely phosphoacceptor for p38 α enzymatic activity (Tokunaga et al. 2014).

The inhibition of ERK2 interaction was assayed by using mutations of residues in the docking groove. The two charged Asp residues in the docking groove of ERK2 are important for the recognition of D-sites (Figure 49, A and B). A mutated ERK2 D321/324N loses most interaction with MAPK partners such as MEK1, MAPK phosphatase MKP3 and MAPK-activated protein kinase MNK1 in GST pull-down assays (Tanoue et al. 2000). However, our NMR studies showed that Asp to Asn mutated ERK (a construct of mutant *Xenopus* ERK2 D321/324N given by Dr. Prabakaran, Harvard Medical School, Asp321 and Asp324 corresponding to Asp316 and Asp319 of human ERK2) cannot significantly abolish the interaction with Tau in the conditions of our experiment. We compare the relative intensities of full-length Tau in presence of D321/324N ERK2 with that of K18 F[244-372] binding to wild-type ERK2. Tau K18 fragment contains two main ERK2 docking sites, whose corresponding relative intensities while binding to wild type ERK2 can be used to compare the inhibition effect of D321/324N ERK2 on full-length Tau interaction with the same molar ratio. As shown in Figure 51, there is still a significant decrease of relative resonance intensities of Tau residues around the two main docking sites F[274-284] and F[309-317]

observed upon interaction of Tau with ERK2 D321/324N (Figure 51, blue diamonds in the graph), suggesting that these mutations are not sufficient to abolish Tau interaction with ERK2 mutated at D321/324N residues in docking groove (Figure 51).

Our NMR studies are conducted at high concentration of proteins and only qualitatively characterize the interaction. However, the same profile of relative intensity suggests that the affinity of ERK2 for Tau is not significantly affected by the mutation of the D residues in the docking sites. As the docking groove of ERK2 consists of negatively charged Aspartic acids and several hydrophobic residues, the absence of inhibition of interaction by the D residue mutations suggests the hydrophobic pocket in the ERK2 docking groove might be sufficient for the interaction with Tau docking sites. Accordingly, a structural study by crystallography of the docking interaction of JNK-pepMKK7 shows that MKK7 peptide interaction is well defined in the JNK hydrophobic pockets, whereas the contacts with the positively charged residues in the peptide reveals a looser and less well-defined interaction on the docking groove of JNK1 (Kragelj et al. 2015).

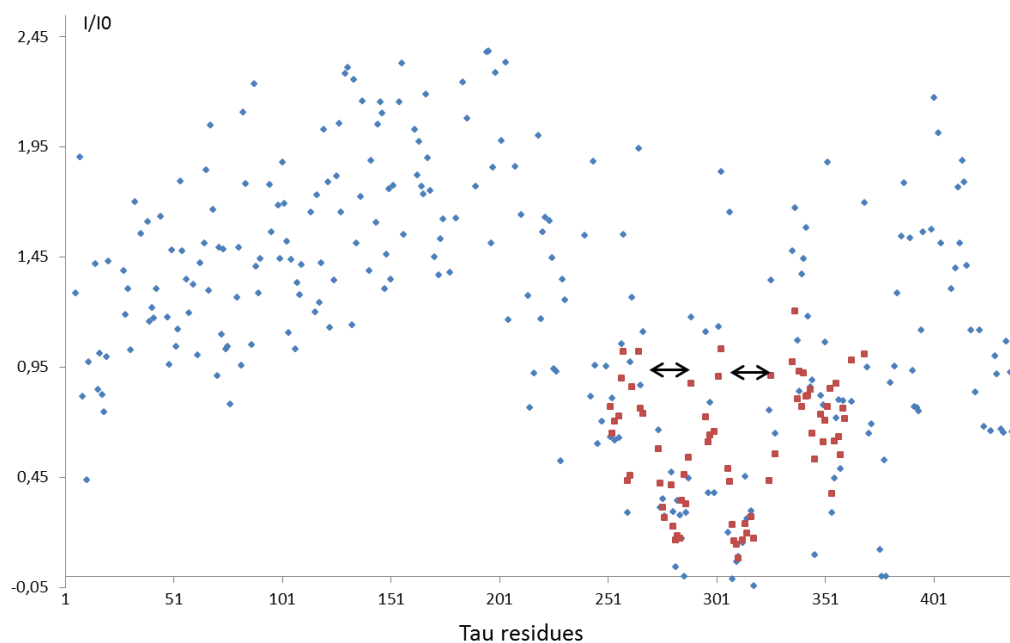


Figure 51: Relative intensities I/I_0 of corresponding resonances in 2D HSQC spectra of full-length Tau with mutant ERK2 D321/324N in 1:2 molar ratio (diamantes in blue), and K18 Tau, F[244-372] with wild type ERK2 in the same molar ratio (squares in red). Two main docking sites F[274-284] and F[309-317] are represented by black arrow.

5. The regulation of Tau/DNA interaction by phosphorylation

Multiple binding sites are observed in Tau protein interacting with a 22-base pair oligonucleotide. Two main interaction sites were identified in NMR studies with oligonucleotidic sequences, the second half of PRD, F[209-246] and N-terminal parts of R2 of MTBDs, F[267-289]. We have investigated the effect of phosphorylation on the Tau/DNA interaction. We have observed that the phosphorylation of Tau, both by rat brain extract and the CDK2/CycA3 kinase, abolish the interaction.

The phosphorylation at pT²³¹/pS²³⁵, observed in both the phosphorylated samples, is directly located in the interaction site Tau F[209-246]. They are also numerous phosphorylation sites in the vicinity of this fragment in the PRD (pS¹⁹⁹, pS²⁰², pT²⁰⁵ for example). These phosphorylations may thus neutralize positive charges of Tau and induce electrostatic effect to inhibit Tau/DNA interaction. However, besides Tau F[209-246], the interaction site Tau F[267-289] located in the MTBR also has a reduced affinity for DNA upon Tau phosphorylation. In the rat brain extract-phosphorylated Tau, the only phosphorylation close to this sequence is pS²⁶². In the CDK-phosphorylated Tau, there are no phosphorylation in the MTBD. Despite these observations, the interaction of DNA with Tau F[267-289] is reduced upon Tau phosphorylation, with both patterns of Tau phosphorylation. This suggests that the phosphorylation may have global impact on the Tau protein interaction rather than only a local one.

Tau has been described to have a dynamic transient conformation with long range interactions which might be mediated by electrostatic effects, conformation described as 'paperclip' (Jeganathan et al. 2006). Therefore, the phosphorylation, not only in proximate interaction sites but also in distant domain might be able to alter the dynamic complex of Tau protein and reduce its interactions with nucleotide sequences (Camero et al. 2014).

Little is known at this stage about the effect of phosphorylation on Tau nuclear function of DNA protection from damages (Sultan et al. 2011). We show that phosphorylation affects the binding of Tau to DNA, in agreement with recent results that suggest that abnormally phosphorylated Tau loses its ability to bind to DNA *in vivo* (Camero et al. 2014). Phosphorylation thus may lead to dysfunction of Tau in the nuclear compartment.

Perspectives

NMR spectroscopy is useful to characterize *in vitro* the enzymatic activity of kinases on Tau protein as substrate. Previous studies have been already undertaken in our laboratory, for example, characterization of Tau phosphorylation by PKA, GSK3, and CDK2/CycA3 (Isabelle Landrieu et al. 2006; Laziza Amniai et al. 2009; Leroy et al. 2010). In addition, numerous phosphorylation sites by ERK2 kinase are also identified in my thesis, which constitute a similar phosphorylation pattern with that generated by rat brain extract *in vitro*. There are phospho-sites corresponding to non-proline directed residues assigned in spectra of phospho-Tau obtained by incubation with rat brain extract. Study on characterization of other kinase activities *in vitro*, such as MARK2 kinase, on Tau protein by NMR spectroscopy, will allow to investigate potential kinase activities besides ERK2 kinase in rat brain extract. Besides NMR, MS and immunoblotting with phospho-specific antibodies could provide more sensitive approaches to detect phosphorylated residues of Tau modified to a low level in our *in vitro* conditions. The phosphorylation of Tau is considered as a therapeutic target in neuronal degeneration disease. The analytical studies on Tau phosphorylation by rat brain extract and various recombinant kinases give us basic insight on specificity and efficiency towards phosphorylated sites *in vitro*, supporting other relevant *in vitro* or *in vivo* investigations.

On the other hand, the docking groove of ERK2 kinase is structurally independent on its activation loop, but it may serve as essential event to distinguish the specificity of ERK in selecting phosphorylation targets from other MAP kinases, such as JNK and p38. These related MAP kinases are also proline-directed kinases and show a subtle difference from ERK1/2 in targeting S/T sites on Tau phosphorylation *in vitro* (Reynolds et al. 2000). Experiments of phosphorylation of peptides derived from ERK docking sites in Tau linked with 'S/T-P' motif might be designed to investigate specificity and/or efficiency of different MAP kinases in Tau phosphorylation. Further experiments should additionally define whether interaction between Tau docking sites and ERK kinase might increase the catalytic activity of ERK2 kinase. Peptides derived from Tau main docking sites might be used to carry out competition assays in Tau interaction with ERK2 in order to reduce local concentration of ERK2 kinase along MTBDs in Tau. In addition, like ERK kinase, p38 also possesses a similar docking interaction domain which has been shown to have an allosteric effect on its substrate phosphorylation. It is not yet fully elucidated if there is allosteric effect of docking

interaction between ERK2 and Tau. Hence, it would be interesting to compare kinetic of reaction of active ERK2, pTEpY ERK2 or pTEY ERK2, on Tau phosphorylation without or in presence of excess of corresponding docking peptides in Tau sequence. As multiple sites are phosphorylated by active ERK2 kinase, it might be more practical to perform kinetic assays by using modular peptides containing ERK2 catalytic targets with or without main docking sites derived from Tau sequence, under our *in vitro* conditions.

In addition, it is interesting to characterize the interaction of Tau with other binding partners which might be related to the Tauopathies development. Investigation of Tau interaction with regulatory subunits of PP2A phosphatase by NMR spectroscopy is one example. Preliminary results are presented below.

Protein phosphatase PP2A is the main phosphatase to dephosphorylate phosphorylated Tau in the brain. PP2A deregulation in AD is thought to be involved in the hyperphosphorylation of Tau. The subunit B of PP2A holoenzyme is known to be a regulatory unit associated with the catalytic unit C. Subunit B was shown to directly bind Tau, participating in the regulation of phosphorylated-Tau dephosphorylation by PP2A (Xu et al. 2008; Sontag et al. 2012). Crystallographic data of the B55 subunit suggest that a central groove, negatively charge, on the top surface of subunit B might be the anchor point for Tau binding. Native PAGE analysis have further delineated two Tau fragments, F[197-259] and F[265-328], capable of binding to PP2A holoenzyme, most likely on subunit B (Xu et al. 2008).

Here, we have tried in preliminary experiments to define the mapping of the interaction site of the regulatory subunit B on Tau by NMR spectroscopy. The recombinant His-B55 α is expressed by Bac-to-Bac[®] baculovirus expression system (Invitrogen) in insect cells. For the purification of His-B55 α , a first step consists in Ni-NTA chelating chromatography in HEPES buffer (25mM HEPES, pH 7.5, 300mM NaCl, 2mM TCEP), followed by an elution step with 250mM Imidazole in HEPES buffer. The elution fractions are next pooled and dialyzed against the ion-exchange buffer (20mM HEPES, pH 7.5, 50mM NaCl, 1mM TCEP, 10% Glycerol) to perform an anion-exchange chromatography step (HiTrap Q FF column, 5ml, GE Healthcare). His-B55 α pool is lastly submitted to a gel filtration chromatography step (Superdex 75 10/300, GE Healthcare) in NMR buffer (20mM HEPES, pH 6.7, 150mM NaCl, 1mM TCEP) and prepared for NMR study. The NMR interaction experiments are undertaken

with ^{15}N Tau with or without B55 α protein, and 2D HSQC spectra are recorded at 293K on a Bruker900MHz Avance III NMR spectrometer equipped with a triple resonance cryogenic probehead (Bruker, Karlsruhe, Germany). The experiments were performed with 40 μM ^{15}N Tau in presence, or not, of 45 μM subunit B55 α . The duration of acquisition with 64 scans is 11 hours.

The relative intensities (I/I0) of resonances of corresponding residues in spectra of ^{15}N Tau in presence of B55 α protein in 1:1 molar ratio (I) compared with ^{15}N Tau in control (I0) (Figure 52) are reported along the sequence of Tau. The plot shows a clear interaction of the B55 α with Tau F[274-287], as the relative intensities of the resonances assigned to residues in this fragment have large decrease of intensity in presence of B55 α . A second fragment F[308-318] is found which also shows perturbation of the resonance intensities of the residues included in this fragment. The decrease of intensities is smaller than for F[274-287] sequence, suggesting a lesser affinity for the latter. We here have further shown two precise interaction sites. A third weak interaction site could be located around Q³⁵⁰ to S³⁵⁶ residues as some of the corresponding resonances show a slight perturbation of their intensities (Figure 52, A). PP2A-binding domain has been suggested to encompass the MTBDs and sequence at its N-terminus, in the PRD, approximately from 221 to 396 in Tau sequence (Sontag et al. 1999). We did not see an interaction with the $^{224}\text{KKVAVVRTPPKSP}^{236}$ peptide in Tau to the B55 α subunit. This result is not inconsistent with previous report that the synthetic $^{224}\text{KKVAVVRTPPKSP}^{236}$ Tau peptide can bind to B55 α regulatory subunit and be competitive with Tau binding to B55 α -contained PP2A phosphatase (Sontag et al. 1999; Sontag et al. 2012). Yet, we did not characterized the difference in B55 α interaction of $^{224}\text{KKVAVVRTPPKSP}^{236}$ peptide sole and embedded in Tau sequence, the electrostatic effect or transient conformation change may be one factor to influence the interaction of B55 α with $^{224}\text{KKVAVVRTPPKSP}^{236}$ peptide in Tau.

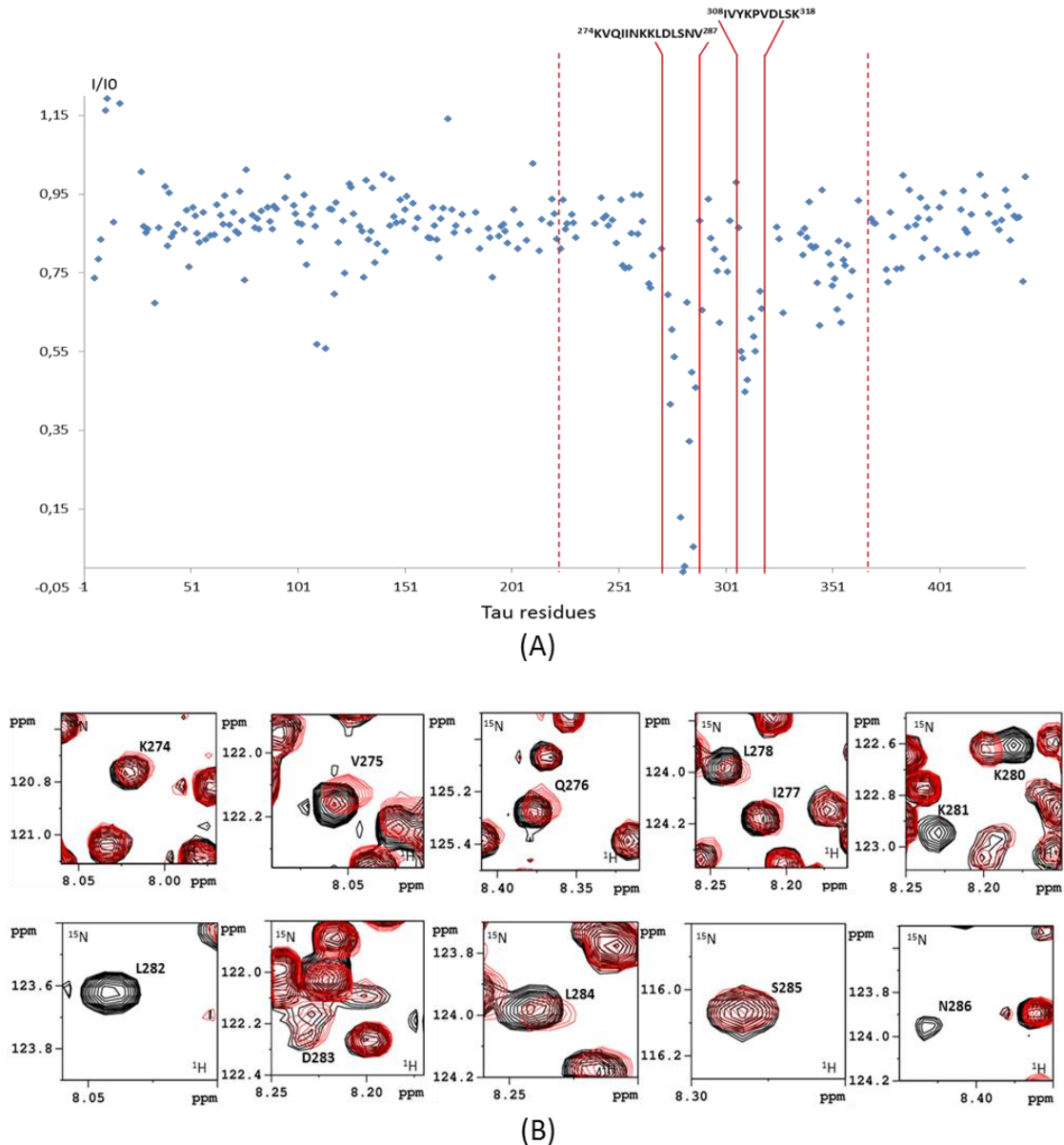


Figure 52: (A) The relative intensity I/I_0 of corresponding resonances in spectra of ^{15}N Tau in presence of PP2A subunit B55 α with 1:1 molar ratio (I, red spectra in B), or free in solution (I0, black spectra in B). 280 out of 441 residues of full-length Tau are shown here. The interaction sites can be mapped in Tau sequence. The most important site is defined as F[274-287] (peptide sequence delineated by continuous red lines and shown above the plot), and a second potential interaction site F[308-318] (same as previous). These interaction sites are included within the previously described B55 α interaction region, approximately from 221 to 396 shown by dotted red lines (Sontag et al. 1999). (B) Overlaid detail of the HSQC spectra of Tau (in black) and Tau with B55 subunit 1:1 molar ratio (superimposed in red). The Tau spectra show the core of the interaction site as located from L278 to L284, the corresponding resonances losing most of their resonance intensity compared to those of neighboring residues after binding to subunit B55 α of PP2A.

To determine the core of B55 α -binding sites, the resonances of the residues in F[274-287] embedded in Tau sequence were individually monitored (Figure 52, B). According to the overlapped spectra, K²⁸⁰, K²⁸¹ and L²⁸² and N²⁸⁶ residues almost totally lose their intensity in presence of B55 α (spectrum in red) compared to Tau free in solution (spectrum in black). This finding is surprisingly similar with what is observed in overlapped spectra of ¹⁵N His-SUMO Tau [274-294] with or without wild-type ERK2 kinase, in which K²⁷⁴ to N²⁸⁶ are the core site of the docking interaction with ERK2.

We have observed multiple interaction sites in Tau sequence both for the regulatory subunit B55 α and to ERK2 kinase. The peptide F[274-287] was found to bind to both B55 α and ERK2, meaning that there is at least one competitive binding site to B55 α and ERK2 under in vitro interaction conditions. The insight of Tau/B55 α interaction gives us interesting perspectives in regulation mechanism of ERK2 kinase and PP2A phosphatase on Tau protein, and two main approaches are thus considered for further studies.

Based on preliminary results of Tau/B55 α interaction sites, it is first considered to confirm and to characterize the B55 α docking sites in Tau sequence, using Tau fragments and peptides as previously done for mapping ERK2 docking sites. In addition, biochemical approaches like fluorescence anisotropy or/and ¹⁹F NMR can be used to characterize the dissociation constant of B55 α interaction with various Tau constructs. Since we find the same core interaction sites F[274-286] for Tau binding to ERK2 kinase and B55 α of PP2A phosphatase, it is interesting to next investigate the binding competition of Tau protein to ERK2 and B55 α , by using such core interaction sites.

The second part will be to investigate the impact of phosphorylation in interaction regulation. Previous studies show that the phosphorylation of T²³¹ residue in ²³⁰RTPPKSP²³⁶, peptide in Tau sequence, is sufficient to abolish its interaction with B55 α (Sontag et al. 2012). In addition, pT²³¹ can negatively influence PP2A regulation in pS²⁰²/pT²⁰⁵ dephosphorylation, a mutated T²³¹ by A residue can efficiently increase dephosphorylation of Tau by PP2A phosphatase, at least at the AT8 epitope (Landrieu et al. 2011). Phosphorylation at T²³¹ could have an effect on docking sites interaction, even if they are located at a long distance in the sequence, as we observed in the case of the modulation of the interaction of DNA oligonucleotides with Tau. Electrostatic effects might mediate a complex network of intrinsic

transient interactions between distant domains of protein, which might regulate Tau binding to its partners (Marco D. Mukrasch et al. 2009; Von Bergen et al. 2006; Jeganathan et al. 2006; Bibow et al. 2014). We would next test the interaction of ERK2 and B55 with wild type Tau or T231A mutated Tau phosphorylated by CDK2/CycA3 or by ERK2 kinase to validate the hypothesis that the phosphorylation could have a long range effect on the interaction. More local phosphorylation in the MTBD by MARK2 for example (Schwalbe et al. 2013) could also be assayed to evaluate its influence on B55 α docking sites interaction.

As we did not observe the interaction between ²³⁰RTPPKSP²³⁶ embedded in Tau and B55 α in our preliminary results, independent peptide including 'RTPPKSP' sequence might be interesting to incubate with B55 α under the same conditions and to compare its binding effect with the sequence embedded in Tau. In case we observe an interaction, the inhibition effect of phosphorylation of T residue in 'RTPPKSP' sequence in B55 α binding on the interaction could then be analyzed by NMR.

Altogether, the Tau/B55 α interaction combined with Tau/ERK2 interaction might give a very interesting study to discover the molecular mechanism of the regulation of PP2A phosphatase and ERK2 kinase on Tau protein that plays an important role in Tau hyperphosphorylation and dysfunctions.

Materials and Methods

manuscript in preparation:

The study of posttranslational modifications of Tau protein by Nuclear Magnetic Resonance spectroscopy: phosphorylation of Tau protein by ERK2 recombinant kinase and rat brain extract and acetylation by recombinant Creb-binding protein.

Haoling Qi,^{1,2} Clément Despres,^{1,2} Sudhakaran Prabakaran,³ François-Xavier Cantrelle,^{1,2} Béatrice Chambraud,⁴ Jeremy Gunawardena,³ Guy Lippens,^{1,2} Caroline Smet-Nocca,^{1,2} Isabelle Landrieu^{1,2}

1 Lille University, CNRS, UMR 8576, F-59 000 Lille, France

2 Research Federation FraBio 3688, F-59655 Villeneuve d'Ascq, France

3 Department of Systems Biology, Harvard Medical School, Boston, MA 02115, USA.

4 INSERM, Paris-Saclay University, UMR1195, Le Kremlin Bicêtre, France

Summary

Nuclear magnetic resonance (NMR) spectroscopy can be used as an analytical tool to investigate posttranslational modifications of protein. NMR is a valuable tool to map the interaction regions of protein partners. Here we present protocols that have been developed in the course of our studies of the neuronal Tau protein. Tau is found aggregated in the neurons of Alzheimer's disease patients. Development of the disease is accompanied by increased, abnormal phosphorylation and acetylation of Tau. We have used NMR to investigate how these posttranslational modifications of Tau affect the interactions with its partners. We present here detailed protocols of *in vitro* phosphorylation of Tau by recombinant kinase, ERK2 or kinase activity of rat brain extracts, and acetylation by recombinant Creb-binding protein (CBP) acetyltransferase. The analytical characterization of the modified Tau by NMR spectroscopy is additionally described.

Keywords

phosphorylations, acetylations, ERK kinase, Creb-binding protein, acetyltransferase, NMR spectroscopy, recombinant proteins

1. Introduction

Tau protein is hyperphosphorylated in the paired helical filaments (PHF) found in neurons in brain affected by Alzheimer's disease . The longest Tau protein isoform (441-residue) has 80 Threonine (T) and Serine (S) residues exposed since Tau is an intrinsically disordered protein to modification by numerous kinases (Martin et al. 2013). In the PHF Tau isoform, up to about 45 phosphorylation sites can be modified (Hasegawa et al. 1992; M. Morishima-Kawashima et al. 1995) while 15 to 30 Tau phosphorylation sites were identified by mass spectrometry in Tau extracted from mice (M. Morris et al. 2015) or cognitively normal human brain. Most of them correspond to proline-directed sites located in the proline rich region of Tau. Given the number and the proximity of these phosphorylation sites, to identify the phosphorylation sites in a phosphorylated Tau sample and to evaluate the level of modification for each of these sites are

difficult (M. Morris et al. 2015). Recently, acetylation of Tau protein was shown to be associated with Tauopathies (Cohen et al. 2011; Min et al. 2010). In this case, the lysine residues are modified by an acetyl group on the NH₃ moiety of the side chain, neutralizing the positive charge of the lysine and modifying the steric characteristics of the side chain. Mass spectrometry analysis revealed 14 lysine residues were acetylated in Tau samples purified from mice, and these were mainly located in the microtubule binding region of Tau (M. Morris et al. 2015).

In addition, these posttranslational modifications affect the binding of Tau to several molecular partners, an aspect of interest to study by NMR spectroscopy (Qi et al. 2015). The need for *in vitro* modified Tau for these NMR experiments has led us to develop protocols to generate the required amount of modified protein. In addition, we have used NMR spectroscopy to characterize enzymatically modified Tau samples with success (I. Landrieu et al. 2006; L. Amniai et al. 2009; Smet-Nocca et al. 2010; Theillet et al. 2012; Kamah et al. 2014). Given the improvement of the probe sensitivity, we can now work with samples in the 10 μM range, in volumes that can be limited to 200 μl. A typical good sample of Tau would be 1 mg in 200 μl or 100 μM of Tau protein. This still is a lot of material compared to most of the applications of biochemistry, such as the immunodetection for the phosphorylation characterization or the GST pull-down for the interaction investigations. Yet compared to these methods we can obtain information at the molecular and define the interaction sites up to the residue. Hence the drawback of the material quantity is compensated by the resolution of the results.

We will here first describe the preparation of isotopically labeled Tau for NMR investigation. The *in vitro* phosphorylated samples of Tau by rat brain extract have been used for years as a model of hyperphosphorylated Tau (Biernat et al. 1992; M. Goedert et al. 1993; Alonso et al. 1994). Phosphorylation by rat brain extract has been described in Goedert, et al. 1993 (M. Goedert et al. 1993). The protocol here presented is an adaptation to the need of biophysical analysis requiring the preparation of sufficient quantity of protein. In the course of our investigation, we also observed that a Tau protein phosphorylated by ERK2 is modified on numerous sites described as

pathological sites of phosphorylation, and thus represents an interesting model of hyperphosphorylated Tau. ERK2 is activated by phosphorylation by MEK, (Boulton et al. 1990; N. G. Anderson et al. 1990; Seger et al. 1991). The acetylation of Tau is obtained *in vitro* by a fragment of the CBP protein, a histone acetyltransferase (Kamah et al. 2014). In addition to the modified, isotopically-labeled Tau protein preparation, we describe the NMR strategy used for the identification of the PTMs.

2. Materials

2.1. Recombinant ^{15}N -Tau, ^{15}N , ^{13}C -Tau and $^{15}\text{N}_2$ -Lysine/ ^{13}C -Tau preparation components

1. TaupET15B recombinant T7 expression plasmid (Novagen)
2. BL21(DE3) transformation competent *E.coli* bacteria (New England Biolabs)
3. Autoclaved LB Broth, Lennox (DIFCO)
4. Autoclaved M9 buffer: 6 g Na_2HPO_4 , 3 g KH_2PO_4 , 0.5 g NaCl per liter
5. Autoclaved 1 M MgSO_4 ,
6. Autoclaved 100 mM CaCl_2
7. MEM vitamin complements 100X (Sigma), (see note 1)
8. 100 mg/ml stock solution of ampicillin antibiotics,
9. 1 M stock solution of IPTG (Isopropyl β -D-1-thiogalactopyranoside)
10. ^{15}N - NH_4Cl (Isotec) or ^{14}N - NH_4Cl
11. $^{13}\text{C}_6$ -Glucose (Isotec) or Glucose
12. $^{15}\text{N}_2/^{13}\text{C}_6$ -L-Lysine hydrochloride (Isotec)
13. ^{15}N -ISOGRO complete medium powder (Isotec) (see note 1)
14. ^{15}N , ^{13}C -ISOGRO complete medium powder (Isotec) (see note 1)
15. The M9 medium is obtained by addition of 1 ml MgSO_4 1 M, 1 ml CaCl_2 100 mM (see note 2), 10 ml MEM vitamin complement 100X (Sigma), 1 ml Ampicillin 100 mg/ml to 1l of M9 buffer. In addition, depending on the isotope labeling scheme, the following components (i, ii

and iii) dissolved in 10 ml of M9 buffer are directly 0.2 μ M filter-sterilized into the M9 medium (see note 3).

i. For the ^{15}N uniform labeling: the isotopes (300 mg of ^{15}N -ISOGRO complete medium, 1 g of ^{15}N - NH_4Cl) and 4 g of glucose

ii. For the ^{15}N , ^{13}C uniform labeling: the isotopes (300 mg of ^{15}N , ^{13}C -ISOGRO complete medium, 1 g of ^{15}N - NH_4Cl and 2 g of $^{13}\text{C}_6$ -glucose, see note 4)

iii. For the selective ^{15}N -Lysine and uniform ^{13}C -labeling: 1 g of ^{14}N - NH_4Cl and 2 g of $^{13}\text{C}_6$ -glucose and 20 minutes before induction 150 mg of $^{15}\text{N}_2/^{13}\text{C}_6$ -L-Lysine hydrochloride.

16. Cation-exchange chromatography CEX A buffer (see note 5): 50 mM phosphate buffer pH6.5, 1 mM EDTA

17. Extraction buffer: CEX A buffer supplemented with Protease inhibitors 1X (1 pellet for 50 ml, EDTA free, Roche) and 2000U DNaseI for 50 ml (20 000U/ml, EUROMEDEX)

18. Cation-exchange chromatography CEX B buffer: CEX A buffer with 1 M NaCl

19. S sepharose FF 5 ml column (GE Healthcare)

20. Lyophilisation buffer: 50 mM Ammonium Bicarbonate

2.2. Recombinant ERK2 preparation components

1. His-ERK2 recombinant T7 expression plasmid

2. BL21(DE3) transformation competent *E.coli* bacteria (New England Biolabs)

3. Autoclaved LB broth Lennox (Difco)

4. 100 mg/ml stock solution of ampicillin antibiotics,

5. 1 M stock solution of IPTG

6. PBS: phosphate buffer saline

7. Extraction buffer: 50 mM NaPi, pH 7.6, 300 mM NaCl, 10 mM Imidazole, Protease inhibitor 1X (1 pellet for 50 ml, EDTA free, Roche), 2000U DNaseI for 50 ml (20 000U/ml, EUROMEDEX)

8. Ni-NTA chromatography cartridge 1 ml (Thermo Science)

9. Wash buffer: 50 mM NaPi pH7.6, 300 mM NaCl, 10 mM Imidazole
10. Elution buffer: 50 mM NaPi pH7.6, 300 mM NaCl, 250 mM Imidazole (see note 6)
11. Activation buffer: 10 mM Hepes.KOH, pH7.3, 1 mM DTT, 5 mM MgCl₂, 100 mM NaCl
12. Dialysis bags (12-14 kDa cut-off, 0.32 ml/cm, Spectrum)
13. Centrifugal concentration devices (10 kDa cut-off, 2 ml, Sartorius)
14. 12% SDS Polyacrylamide precast gels (Pierce)
15. Activation buffer: 10 mM Hepes.KOH, pH7.3, 1 mM DTT, 5 mM MgCl₂, 100 mM NaCl and 10% Glycerol.
16. Conservation buffer: 50 mM Tris-HCl, pH7.5, 150 mM NaCl, 0.1 mM EGTA, 20% Glycerol

2.3. Recombinant GST-MEK1 R4F preparation components

1. GST-MEK1 R4F recombinant pGEX expression plasmid (Mansour et al. 1994)
2. BL21(DE3) transformation competent *E.coli* bacteria (New England Biolabs)
3. Autoclaved LB broth Lennox (Difco)
4. 100 mg/ml stock solution of ampicillin antibiotics
5. 1 M stock solution of IPTG
6. PBS: phosphate buffer saline
7. Extraction buffer: 50 mM Tris-HCl, pH7.5, 1 mM EDTA, 300 mM NaCl, Protease inhibitor 1X (1 pellet for 50 ml, EDTA free, Roche), 2000U DNaseI for 50 ml (20 000U/ml, EUROMEDEX)
8. Glutathione Agarose 4B chromatography cartridge 5 ml (Protino, Macherey Nagel)
9. Wash buffer: 50 mM Tris-HCl, pH7.5, 1 mM EDTA, 300 mM NaCl
10. Elution buffer: 50 mM Tris-HCl, 10 mM Glutathion, pH7.5 (see note 6)
11. Dialysis bags (12-14 kDa cut-off, 0.32 ml/cm, Spectrum)
12. Centrifugal concentration devices (10 kDa cut-off, 2 ml, Sartorius)
13. Activation buffer: 10 mM Hepes.KOH, pH7.3, 1 mM DTT, 5 mM MgCl₂, 100 mM NaCl and 10% Glycerol

14. Conservation buffer: 50 mM Tris-HCl, pH7.5, 150 mM NaCl, 0.1 mM EGTA, 20% Glycerol

2.4. Recombinant ERK2 activation components

1. GST-MEK1 R4F recombinant protein (Methods 3.5, 3.6) or commercial activated-MEK1 (Millipore 14-429)
2. Recombinant His-ERK2 protein in activation buffer or conservation buffer (Methods 3.3, 3.4).
3. PD-10 G25 resin desalting column (GE-Healthcare)
4. Centrifugal concentration devices (10 kDa cut-off, 2 ml, Sartorius)
5. Glutathione Agarose 4B beads (Protino)

2.5. Phosphorylation of Tau by activated ERK2 components

1. 1 mg of ¹⁵N and 5 mg of ¹⁵N, ¹³C lyophilized recombinant full-length Tau (Methods 3.1, 3.2)
2. Activated His-ERK2 in activation buffer (Methods 3.7)
3. Phosphorylation buffer 5X: 250 mM Hepes.KOH, pH8.0, 62.5 mM MgCl₂, 5 mM EDTA, 250 mM NaCl
4. Protease inhibitor 40X (1 pellet in 1 ml, EDTA free, Rocher)
5. PD MidiTrap G25 resin desalting column (GE-Healthcare)
6. Lyophilisation buffer: 50 mM Ammonium Bicarbonate
7. NMR buffer: 50 mM deuterated *d*11Tris.HCl (Isotec), pH6.5, 30 mM NaCl, 2.5 mM EDTA, 1mM DTT (Dithiothreitol), 5% D₂O and 1mM TMSP (Trimethylsilyl propanoic acid)
8. 12% SDS Polyacrylamide precast gels (Pierce)

2.6. Phosphorylation of Tau by rat brain extract components

1. 1 mg of ¹⁵N-labeled recombinant full-length Tau per phosphorylation assay (Methods 3.1, 3.2)

2. 100 μ M okadaic acid (Sigma)
3. Homogenizing buffer H: 10 mM Tris-HCl pH 7.4, 5 mM EGTA, 2 mM DTT, 1 μ M okadaic acid (Sigma) supplemented with 20 μ g/ml Leupeptin and 40 mM Pefabloc
4. HMED buffer 5X: 200 mM Hepes.KOH, pH7.3, 10 mM MgCl₂, 25 mM EGTA, 10 mM DTT
5. PD-10 G25 resin desalting column (GE-Healthcare)
6. Lyophilisation buffer: 50 mM Ammonium Bicarbonate
7. 12% SDS Polyacrylamide precast gels (Pierce)
8. NMR buffer: 50 mM deuterated *d*11Tris-HCl (Isotec), pH6.5, 30 mM NaCl, 2.5 mM EDTA, 1mM DTT, 5% D₂O and 1mM TMSP

2.7. Recombinant CBP preparation components

1. GST-CBP[1202-1848] recombinant T7 expression plasmid (pGEX-6P-1)
2. BL21(DE3) transformation competent *E.coli* bacteria (New England Biolabs)
3. Autoclaved LB Broth, Lennox (DIFCO)
4. 100 mg/ml stock solution of ampicillin antibiotics
5. 1 M stock solution of IPTG
5. PBS 10X: phosphate buffer saline
6. Extraction buffer: PBS 1X pH 7.6, 10% glycerol, 1% Triton X-100, 10 mM EDTA, 2 mM DTT, Protease inhibitor 1X (1 pellet for 50 ml, Roche), 2000U DNaseI for 50 ml (20 000U/ml, EUROMEDEX)
7. Glutathione sepharose resin beads (GE Healthcare): 20 μ l of resin beads/mL of soluble extract
8. Wash buffer: PBS 1X pH 7.6, 10% glycerol, 1% Triton X100, 10 mM EDTA, 2 mM DTT
9. Conservation buffer: 25 mM Hepes.KOH pH 7.8, 0.1 mM EDTA, 1 mM THP (Tris (3-hydroxypropyl) phosphine), 50% glycerol (i.e. acetylation buffer with 50% glycerol)
10. 10% SDS Polyacrylamide precast gels (Pierce)

11. Acetylation buffer: 25 mM Hepes.KOH pH 7.8, 0.1 mM EDTA, 1 mM THP
12. Stock solution of acetyl-coenzyme A (AcCoA) at 20 mM: 25 mg of AcCoA trisodium salt (Sigma) are dissolved in 1.423 ml acetylation buffer and stored at -20°C
13. Stock solution of CBP peptide substrate (Ac-QPVEPKKPVESKSKSGKSAKSKEKQ-NH₂, 8 TFA) at 10 mM: 18 mg of peptide were dissolved in 0.5 ml of deionized water. The pH was adjusted to 7.0 with a solution of NaOH 10M.
14. C18 Zorbax 300SB analytical column 4.6x150 mm (Agilent)
15. 10% TFA (v/v) (Sigma)
16. Acetonitrile (Sigma)
17. Ultrasonic bath
18. Buffers for reverse-phase chromatography: Buffer A (equilibration): 0.1% TFA, 2% acetonitrile in water; Buffer B (elution): 0.1% TFA: 80% acetonitrile in water; both buffers are degassed in an ultrasonic bath for 15 minutes at room temperature

2.8. Acetylation of Tau by CBP components

1. Acetylation buffer: 25 mM Hepes.KOH pH 7.8, 0.1 mM EDTA, 1 mM THP
2. Stock solution of acetyl-coenzyme A (AcCoA) at 20 mM: 25 mg of AcCoA trisodium salt (Sigma) are dissolved in 1.423 ml acetylation buffer and stored at -20°C
3. Recombinant GST-CBP[1202-1848] fragment (Methods 3.11, 3.12)
4. ¹⁵N-labeled or ¹⁵N-Lysine-labeled recombinant Tau protein (Methods 3.1, 3.2)
5. C8 Zorbax 300SB semi-preparative column 9.4x250 mm (Agilent)
6. 10% TFA (v/v) (Sigma)
7. Acetonitrile (Sigma)
8. Ultrasonic bath
9. Buffers for reverse-phase chromatography: Buffer A (equilibration): 0.1% TFA, 2% acetonitrile in water; Buffer B (elution): 0.1% TFA: 80% acetonitrile in water; both buffers are degassed in an ultrasonic bath for 15 minutes at room temperature
10. HiPrep 26/10 desalting column (GE Healthcare)

11. Desalting buffer: 50 mM ammonium bicarbonate

12. NMR buffer: 50 mM NaPi, pH6.4, 25 mM NaCl, 2.5 mM EDTA, 1 mM DTT, 5% D₂O, 1 mM TMSP

3. Methods

3.1. Production of ¹⁵N-Tau, ¹⁵N-Lysine, ¹³C-Tau or ¹⁵N, ¹³C-Tau

Bacterial fermentations have to be performed following the best practices of sterile manipulations.

1. **Day 1:** Tau pET15b recombinant T7 expression plasmid (Novagen) is transformed into BL21(DE3) competent bacterial cells. 50 µl of competent BL21(DE3) bacteria are mixed with 100 ng of the plasmid DNA in a 1.5 ml plastic tube. The mixture is incubated on ice for 30 minutes, followed by heat shock for 30 seconds at 42°C. The tube is placed back on ice for 5 minutes. 1 ml of LB medium at room temperature is added. The bacterial suspension is incubated at 37°C for 30 minutes. 100 µl of the suspension are spread at the surface of a LB plate containing 100 µg/ml of ampicillin antibiotics to select for the colonies having integrated the plasmid. The plate is incubated overnight at 37°C.

2. **Day 2:** a small scale bacterial culture of 20 ml is started by using a few colonies from the selection plate as inoculum. The Tau pET15b bacteria are grown at 37°C for 6 hours in LB medium supplemented with 100 µg/ml of ampicillin, to reach saturation corresponding to an approximate OD600 of 4.0. Meanwhile, 1l of M9 medium is reconstituted by addition of the supplements and isotopes. A large scale culture of 1l is started by inoculating 20 ml of the LB saturated culture into 1l of M9 medium supplemented with 100 µg/ml of ampicillin. The culture is performed in 2l Erlenmeyer culture plastic baffled-flasks placed in an incubator programmed at 10°C and 50 rpm for 14 hours for the uniform ¹⁵N or ¹⁵N, ¹³C-labeling or for 12 hours for the ¹⁵N-Lysine, ¹³C-labeling considering the slower growth phase due to the

absence of complete medium for the later (see notes 7 and 8). The incubator is programmed to switch to 200 rpm and 37°C after this period.

3. **Day 3** Growth is checked by measuring the OD at 600 nm of an aliquot of 1 ml of the culture. For the uniform ^{15}N or ^{15}N , ^{13}C -labeling, when bacterial culture arrived at an OD600 of 0.8 to 1.0, the protein production is induced by addition of 400 μM IPTG. For the ^{15}N -Lysine, ^{13}C -labeling, when bacterial culture reached an OD600 of 0.7 to 0.8, 150 mg of $^{15}\text{N}_2/^{13}\text{C}_6$ -L-Lysine hydrochloride are added and the culture is continued for 20 minutes. Then, the protein production is induced by addition of 400 μM IPTG. The bacterial culture is continued during 4 hours, at 37°C and 200 rpm. Bacterial pellet is collected by centrifugation for 20 minutes at 5500 g in 1l bottles. The bacterial pellet is suspended in 50 ml of PBS buffer and centrifuge in 50 ml plastic tubes at 4000 g. The supernatant solution is removed and the pellet is frozen at -20°C until further use (Figure 1).

3.2. Purification of of ^{15}N -Tau, ^{15}N -Lysine, ^{13}C -Tau or ^{15}N , ^{13}C -Tau

1. The bacterial pellet is unfrozen at room temperature. It is then thoroughly suspended in 45 ml of extraction buffer. Bacterial lysate is obtained by homogenization of this suspension with an Emulsiflex-C3 (Avestin). The insoluble material is removed by centrifugation at 20000 g for 30 minutes.

2. A first purification step is obtained by heating the bacterial protein extract for 15 minutes at 75°C. The Tau protein is recovered in the soluble fraction after centrifugation at 15000 g for 30 minutes.

3. Purification of the ^{15}N -Tau, ^{15}N , ^{13}C -Tau, ^{15}N -Lysine, ^{13}C -Tau protein is performed by cation exchange chromatography on a 5 ml Hitrap SP sepharose FF column. After loading the

sample on the column, the resin is washed with CEX A buffer. The elution of the protein is obtained by a three-step NaCl gradient of with CEX B buffer. The first step corresponds to 10 volumes of column to reach 250 mM NaCl, followed by a second step with 5 volumes of column to reach 500 mM NaCl, and the third step to 2 volumes of the column to reach 1M NaCl (Figure 2).

4. The pooled fractions from the chromatography purification step (corresponding to the box in Figure 2, between 45 and 65 ml) are transferred to lyophilisation buffer by desalting on a 15/60 Hiprep Desalting Column (G25 resin, GE Healthcare) and lyophilized (see note 9 and 10). Injections of 5 ml are repeated 4 to 5 times, depending on the volume of the cation exchange pool (Figure 3).

5. The lyophilized protein is suspended in a buffer suitable for protein modification.

3.3. Production of recombinant ERK2

Bacterial fermentations have to be performed following the best practices of sterile manipulations

1. **Day 1:** His6-tagged p42 MAP kinase from *Xenopus laevis* (His-ERK2) recombinant T7 expression plasmid is transformed into BL21(DE3) competent bacterial cells based on chemical transformation following the same procedure as described in Methods 3.1, 1. Day 1.

2. **Day 2:** a small scale bacterial culture of 10 ml is started by using a few colonies from the selection plates as inoculum. The His-ERK pET BL21(DE3) bacteria are grown overnight in LB medium supplemented with 100 µg/ml of ampicillin to reach saturation corresponding to an approximate OD600 of 4.0.

3. Day 3 A large scale culture of 1l is started by inoculating 10 ml of the overnight culture into 1l of LB medium supplemented with 100 µg/ml of ampicillin. The culture is performed in 2l Erlenmeyer culture plastic baffled flasks placed in an incubator at 37°C and shake at 200 rpm. Growth is checked by measuring the OD at 600 nm of an aliquot of 1 ml of the culture. When bacterial culture arrived at 0.8 to 1.0 of OD₆₀₀, the protein production is induced by addition of 700 µM IPTG. The bacterial culture is continued during 4 hours, at 30°C and 200 rpm. Bacterial pellet is collected by centrifugation for 20 minutes at 5500 g in 1l bottles. The bacterial pellet is suspended in 50 ml of PBS buffer and centrifuged in 50 ml plastic tubes at 4000 g. The supernatant solution is removed and the pellet is frozen at -20°C until further use.

3.4. Purification of recombinant ERK2

1. The bacterial pellet is unfrozen at room temperature. It is then thoroughly suspended in 45 ml extraction buffer. Bacterial lysate is obtained by homogenization of this suspension with an Emulsiflex-C3 (Avestin). The insoluble material is removed by centrifugation at 20000 g for 30 minutes.

2. The soluble bacterial lysate containing the His-ERK2 recombinant kinase (Figure 4 A) is passed through a NTA resin equilibrated in wash buffer. The resin is first washed by wash buffer followed by 5% elution buffer to remove residual lysate. His-ERK2 is eluted by equilibration of the resin into 100% elution buffer. The eluted fractions are collected by 1 ml aliquots which are analyzed by SDS-PAGE before pooling. His-ERK2 is obtained in about 5 ml of pooled fractions at 1.0-1.2 mg/ml concentration. The yield is approximately 5 mg of His-ERK2 per liter of LB broth.

3. His-ERK2 is dialyzed against the activation buffer or the conservation buffer. His-ERK2 in the activation buffer is concentrated up to 3 mg/ml using centrifugal devices. At this step the His-ERK2 (see note 11) is ready for the activation step (methods 3.7). His-ERK2 in conservation buffer is fast frozen in liquid nitrogen and kept at -80°C until further use.

3.5. Production of recombinant GST-MEK1 R4F

Bacterial fermentations have to be performed following the best practices of sterile manipulations

1. **Day 1:** The pGEX plasmid containing the cDNA sequence of recombinant GST-MEK1 R4F MAPK kinase is transformed into BL21(DE3) competent bacterial cells based on chemical transformation following the same procedure as described in Methods 3.1, 1. Day 1.

2. **Day 2:** a small scale bacterial culture of 20 ml is started by using a few colonies from the selection plate as inoculum, in LB medium supplemented with 100 µg/ml of ampicillin, to reach saturation corresponding to an approximate OD₆₀₀ of 4.0.

3. **Day 3:** 1l of BL21(DE3) bacterial culture in LB medium supplemented by 100 µg/ml ampicillin antibiotics is started by adding the 10 ml overnight saturated bacterial culture to the fresh medium. The culture is performed in 2l Erlenmeyer culture plastic baffled flask placed in an incubator at 37°C and shake at 200 rpm. Growth is checked by measuring the OD at 600 nm of an aliquot of 1 ml of the culture. When bacterial culture arrived at 0.8 to 1.0 of OD₆₀₀, the protein production is induced by addition of 700 µM IPTG. The bacterial culture is continued during 4 hours, at 30°C and 200 rpm. Bacterial pellet is collected by centrifugation for 20 minutes at 5500 g in 1l bottles. The bacterial pellet is suspended in 50 ml of PBS buffer and centrifuge in 50 ml plastic tubes at 4000 g. The supernatant solution is removed and the pellet is frozen at -20°C until further use.

3.6. Purification of recombinant GST-MEK1 R4F

1. The bacterial pellets from 2l bacterial culture are unfrozen at room temperature and then thoroughly suspended in extraction buffer. The suspension is homogenized using an Emulsiflex-C3 (Avestin). The insoluble material is next removed by centrifugation at 20000 g for 30 minutes.

2. The soluble bacterial lysate containing the recombinant GST-MEK1 R4F kinase is passed through a Glutathione Agarose 4B chromatography column, containing resin equilibrated with wash buffer, at a slow flow rate of 0.3-0.5 ml/min. The loaded resin is rinsed with wash buffer until the base line at 280 nm is stabilized. The GST-MEK1 R4F protein is collected into elution buffer by 1 ml aliquots. Aliquots are analyzed by SDS-PAGE to choose the fractions to pool.

3. The pooled fractions (Figure 4 B) correspond to about 6 ml at 1 mg/ml. GST-MEK1 R4F protein is dialyzed against the activation buffer_or the conservation buffer. GST-MEK1 R4F protein in activation buffer is concentrated up to 3 mg/ml using centrifugal devices to be used in His-ERK2 activation step (see methods 3.7). GST-MEK1 R4F dialyzed in conservation buffer is flash-frozen in liquid nitrogen and kept at -80°C until further use.

3.7. Activation of recombinant ERK2

1. 1 ml of His-ERK (3 mg/ml, Methods 3.4) is mixed with 1 ml of GST-MEK1 R4F (3 mg/ml, Methods 3.6) in activation buffer in presence of 5 mM ATP and protease inhibitors cocktail 1X in a 5 ml reaction volume, in 15 ml plastic tubes (S. Prabakaran et al. 2011). The activation is carried out at 30°C during 15 hours.

2. If His-ERK2 or GST-MEK1 R4F is frozen in conservation buffer, an additional dialysis step is necessary to make them suspended in activation buffer. Concentration with a centrifugal device is employed to concentrate the kinases for further reaction if needed.

3. 5 μ l is removed from the reaction mixture at various time points to be analyzed by SDS-PAGE to control the progress of the reaction. A slight delay of His-ERK2 migration is observed from 30 minutes of incubation. The amount of soluble His-ERK2 is decreasing during the incubation due to protein precipitation (Figure 5 A). The insoluble material is removed by centrifugation.

4. GST-MEK1 R4F is removed from the reaction mixture by using 500 μ l Glutathione Agarose 4B beads equilibrated in activation buffer. The beads are incubated with slow shaking (rotation of 20 rpm/min) for 1 hour at 4°C with the activation mix and are finally eliminated by centrifugation at 1000 g for 10 minutes. The final activated His-ERK2 is obtained at 0.1-0.15 mg/ml (2.5-4.0 μ M) in 5 ml of reaction volume.

5. 10% Glycerol is added to the activated His-ERK2 in activation buffer. Aliquots of 100 μ l are flash-frozen in liquid nitrogen to be conserved at -80°C until further use.

3.8. Phosphorylation of Tau protein by ERK2 recombinant kinase

1. 100 μ M recombinant ¹⁵N-Tau protein (1 mg lyophilized protein, Methods 3.1) is mixed with 50 μ l activated ERK2 (4 μ M in activation buffer, Methods 3.7, final concentration 1 μ M, see note 12) in presence of 2.5 mM ATP, 1 mM DTT and 1 mM EGTA complemented with protease inhibitors in a total sample volume of 200 μ l in the phosphorylation buffer 1X. The

sample is incubated at 37°C during 3 hours. For the ^{15}N , ^{13}C -Tau protein, the reaction is scaled up to 5 mg lyophilized protein in 1 ml reaction mix.

2. After incubation, the samples are heated at 75°C for 15 minutes and then centrifuged at 20000 g for 15 minutes to remove the ERK2 kinase.

3. The phosphorylated ^{15}N -Tau or ^{15}N , ^{13}C -Tau (Figure 5 B) is desalted into NMR buffer and conserved at -20°C.

4. For NMR spectroscopy analysis, the samples are complemented with 1 mM TMSP (tri-methylsilyl propionate that serves as internal reference), 2 mM DTT and 10% D_2O .

3.9. Preparation of rat brain extract

1. The rat brain (about 1.8 g) is washed immediately after collection in ice-cold homogeneizing buffer.

2. The brain is crudely cut into pieces with dissection scissors and place in homogeneizing buffer (2.5ml/1gr of brain).

3. The rat brain extract is prepared by homogeneizing the brain using a Potter pestle fitted on a tissue grinder and a 10 ml glass tube

4. Ultracentrifugation is performed at 100000 g for 1 hour in a type 50 Ti rotor (Beckman Coulter). The supernatant corresponds to the extract (see note 13).

3.10. Phosphorylation of Tau protein by rat brain extract

1. 4 μM recombinant ^{15}N -labeled Tau protein (around 1 mg protein in 5 ml of total volume) is mixed with 500 μl fresh rat brain extract in HMED buffer 1X. Phosphatases in rat brain extract are blocked by 1 μM okadaic acid. 2 mM ATP and protease inhibitors 1X are added in a final 5 ml reaction volume.
2. The incubation of the phosphorylation mix lasts 24 hours at 37°C. Enzymes in the sample are next inactivated by heating at 75°C during 15 minutes. The sample is centrifuged at 16000 g during 15 minutes to remove out precipitated proteins.
3. Buffer exchange into the lyophilisation buffer is performed using a PD-10 column (G25 resin). 2.5 ml of the inactivated reaction mix is loaded on the column. Operation is repeated to obtain a final volume of 7 ml.
4. The phosphorylated Tau (Figure 5 B) is lyophilized and conserved at -20°C.
5. To analyze by NMR spectroscopy, the lyophilized sample is suspend in 200 μl NMR buffer.

3.11. Production of recombinant GST-CBP acetyltransferase

Bacterial fermentations have to be performed following the best practices of sterile manipulations

1. **Day 1:** The pGEX plasmid containing the cDNA sequence of recombinant CBP[1202-1848] fragment of mouse CBP acetyltransferase is transformed into BL21(DE3) competent bacterial cells based on chemical transformation following the same procedure as described in Methods 3.1, Day 1 except that plates used for colony selection are additionally supplemented with 1% glucose.

2. **Day 2:** a small scale bacterial culture of 10 ml is started by using a few colonies from the selection plate as inoculum, in LB medium supplemented with 1% glucose and 100 µg/ml of ampicillin, to reach saturation corresponding to an approximate OD₆₀₀ of 4.0.

3. **Day 3:** 1l of BL21(DE3) bacterial culture in LB medium supplemented by 1% glucose and 100 µg/ml ampicillin antibiotics is started by adding the 10 ml overnight saturated bacterial culture to the fresh medium. The culture is performed in 2l Erlenmeyer culture plastic baffled flask placed in an incubator at 37°C and shake at 200 rpm. Growth is checked by measuring the OD at 600 nm of an aliquot of 1 ml of the culture. When bacterial culture arrived at 0.8 to 1.0 of OD₆₀₀, the protein production is induced by addition of 200 µM IPTG. The bacterial culture is continued during 4 hours, at 18°C and 200 rpm. Bacterial pellet is collected by centrifugation for 20 minutes at 5500 g in 1l bottles. The bacterial pellet is suspended in 50 ml of PBS buffer and centrifuge in 50 ml plastic tubes at 4000 g. The supernatant solution is removed and the pellet is frozen at -20°C until further use.

3.12 Purification of recombinant GST-CBP acetyltransferase

1. The bacterial pellets from 2l bacterial culture is unfrozen at room temperature and then thoroughly suspended in extraction buffer. The suspension is homogenized using an Emulsiflex-C3 (Avestin). The insoluble material is next removed by centrifugation at 25000 g for 30 minutes.

2. The soluble bacterial lysate containing the recombinant GST-CBP[1202-1848] acetyltransferase (Figure 6) is incubated for 3 hours at 4°C on a roller mixer with Glutathione Sepharose resin beads pre-equilibrated in the extraction buffer. The loaded resin is rinsed 5 times with 12 ml of wash buffer then 5 times with 12 ml of conservation buffer. The beads

are kept as 50% slurry in conservation buffer at -20°C until further use. An aliquot of 15 µl is analyzed by SDS-PAGE.

3.13 Standard analysis of CBP acetyltransferase activity on a peptide substrate

Principle A peptide from the human Thymine DNA Glycosylase (TDG) is used as an efficient substrate to check the activity of every new batch of CBP enzyme. The peptide sequence is Ac-QPVEPKKPVESKKSGKSAKSKEKQ-NH₂ (Ac and NH₂ mean that the N- and C-terminus are acetylated and amidated, respectively). Three acetylation sites which have been previously identified in this peptide are underlined in the peptide sequence (Tini et al. 2002).

1. For the acetylation reaction, 2.5 µl of the peptide solution at 10 mM (final concentration of 100 µM) were added in 212.5 µl of acetylation buffer with 25 µl of the stock solution of AcCoA at 20 mM (final concentration of 2 mM) or 25 µl of acetylation buffer as a control. 10 µl of the slurry of GST-CBP on glutathione beads were added (for a final volume of 250 µl) and the reactions were incubated overnight either at 20°C or 30°C under rotative agitation.

2. Then, the reaction mixtures were centrifuged at 16,000 g for 10 minutes at 4°C and each supernatant was analyzed by reverse-phase chromatography on a C18 column at room temperature. The column is equilibrated at 1 ml/min in Buffer A until the absorbance and conductivity were stable. The total reaction volume (250 µl) was injected in a 1 ml injection loop for 4 ml. Then, the column is washed at 1 ml/min with 2.5 ml of Buffer A and peptides were eluted with a linear gradient of acetonitrile from 0% to 60% buffer B in 30 min at 1 ml/min (Figure 7).

3. Fractions of 0.5 ml were collected and analyzed by MALDI-TOF mass spectrometry. Mass increments of +42 Da ($[M+H]^+$ 2735.82 Da), +84 Da ($[M+H]^+$ 2777.88 Da) and +126 Da ($[M+H]^+$

2819.81 Da) as compared to the mass of the unmodified peptide ($[M+H]^+$ 2693.53 Da) confirmed the incorporation of one, two or three acetyl moieties, respectively (Figure 7, see note 14).

3.14 Acetylation of Tau protein by CBP

1. Acetylation of ^{15}N - or ^{15}N -Lysine, ^{13}C -labeled Tau protein was performed with minor modifications of the conditions described for the TDG peptide. 17.6 mg AcCoA are dissolved in 5 ml acetylation buffer (final concentration of 4 mM) and the solution is filtered on 0.22 μ -filter; this solution is sufficient for 4 acetylation reactions. 5 mg of Tau protein are dissolved in 1.09 ml of AcCoA-containing acetylation buffer (final concentration of 100 μM). For the negative control, AcCoA is omitted and the Tau protein is directly dissolved in acetylation buffer. 100 μl of GST-CBP glutathione beads slurry are added per ml of reaction volume. Then, the acetylation reactions are incubated at 25°C overnight (16 hours) under rotative agitation.
2. The reaction mixtures are centrifuged at 4,000 g for 5 minutes at 4°C. The supernatant is cautiously withdrawn and resin beads are washed twice with 0.2 ml acetylation buffer. The supernatants are pooled and heated at 75°C for 10 min followed by a centrifugation at 4,000 g for 15 min at 4°C to remove potential contaminant proteins that might have eluted from glutathione beads.
3. The acetylation and control reactions are purified by reverse-phase chromatography on a C8 semi-preparative column at room temperature. The column is equilibrated at 4 ml/min in 20% buffer B until the absorbance and conductivity were stable. The protein solution (1.5 ml) was injected in a 2 ml injection loop for 22 ml and proteins are eluted with a linear gradient of acetonitrile from 20% to 60% buffer B in 24 minutes at 4 ml/min (Figure 8).

4. The collected fractions are lyophilized and dissolved in 200 μ l water for SDS PAGE analysis on 10% acrylamide gels. The fraction containing a high concentration of full-length protein is then desalted (Figure 9) in 50 mM ammonium bicarbonate on a Hiprep 26/10 desalting column as described in the Methods 3.2 section 4.

3.15 Assignment of resonances of the phosphorylated residues: identification of the phosphorylation pattern

Principle: A [$^1\text{H},^{15}\text{N}$] HSQC 2D spectrum is recorded to detect the resonances of the phosphorylated S and T residues (see note 15), because they are easily visualized, located around 8.5 to 9.5 ppm of amide proton and 117 to 125 ppm of ^{15}N -amide, outside the bulk of the ^1H , ^{15}N correlations (Figure 10). As shown in Figure 11, phospho-residue resonance assignment is based on [$^1\text{H},^{15}\text{N},^{13}\text{C}$] HNCACB 3D experiment which is recorded in order to link the resonances of the phosphorylated residues observed in the 2D [$^1\text{H},^{15}\text{N}$] HSQC spectrum to a specific pS or pT residue in Tau sequence. CA and CB chemical shift values of pS and pT are typical (Bienkiewicz & Lumb 1999) and allow the identification of the nature of the phosphorylated *i* residue. pS and pT followed by a proline residue also in addition have a typical +2 ppm shift of the CA chemical shift value. The nature of the residue at the *i*-1 position is defined by the chemical shift values of the CA and CB resonances corresponding to the *i*-1 residue (weaker set of signals compared to those of the *i* residue). A few identical phosphorylated patterns possess the same residue at position '*i*-1' and cannot be uniquely identified from the HNCACB experiment alone, as is the case for K-pT175-P and K-pT181-P. Another 3D experiment lifts the redundancy by providing in addition the chemical shift value of ^{15}N of the *i*-1 residue. For example, the resonances corresponding to pT175 and pT181 can be successfully assigned due to the different values of ^{15}N chemical shift observed for K174 and LK180 (Figure 11 and Figure 12).

1. 0.5 to 1 mg of ^{15}N -Tau in 200 μl NMR buffer (50-100 μM) are used to fill a 3 mm tube. A $[\text{}^1\text{H},^{15}\text{N}]$ HSQC 2D spectrum (hsqcetf3gpsi pulse sequence from Bruker, see note 16) (Schleucher et al. 1994) (Figure 10) is recorded at 293K or 298K on a Bruker900MHz Avance III NMR spectrometer equipped with a triple resonance cryogenic probehead (Bruker, Karlsruhe, Germany) with 3072 and 416 points for 14 and 25 ppm in the ^1H and ^{15}N dimensions, respectively. Duration of the acquisition with 64 scans is 9 hours. The spectra were processed by the Bruker TopSpin 3.1 software.

2. Around 4mg of ^{15}N , ^{13}C -Tau in 400 μl NMR buffer (200 μM) are used to fill a NMR Shigemitsu tube. A $[\text{}^1\text{H},^{15}\text{N},^{13}\text{C}]$ HNCACB 3D spectrum (pulse sequence hncacbgpwg3d from Bruker, see note 17) is recorded at 298K on a Bruker900MHz Avance III NMR spectrometer equipped with a triple resonance cryogenic probehead (Bruker, Karlsruhe, Germany) with 2048, 256, 72 points for 14, 25, 61 ppm centred on 4.7, 119, 41 ppm in the ^1H , ^{15}N and ^{13}C three dimensions, respectively. Duration of the acquisition with 16 scans is 4 days and 6 hours. The chemical shift values of 'CA' and 'CB' ^{13}C nuclei of the 'i' and 'i-1' residues are recorded for each $[\text{}^1\text{H},^{15}\text{N}]$ resonance. The spectra are processed by the Bruker TopSpin 3.1 software.

3. $[\text{}^1\text{H},^{13}\text{C}]$ 2D planes are extracted from the $[\text{}^1\text{H},^{15}\text{N},^{13}\text{C}]$ HNCACB 3D experiment (Figure 12 A). Data analysis, peak picking and calculation of peak volumes are done with Sparky 3.114 software (T. D. Goddard and D. G. Kneller, SPARKY 3, University of California, San Francisco).

4. An additional $[\text{}^1\text{H},^{15}\text{N},^{15}\text{N}]$ HNCANN 3D experiment (hncannhgpgw3d pulse sequence from Bruker, see note 18) (Weisemann et al. 1993) is necessary to distinguish redundant phosphorylation patterns. Data acquisition is performed on the same ^{15}N , ^{13}C -Tau sample. $[\text{}^1\text{H},^{15}\text{N},^{15}\text{N}]$ HNCANN experiment is carried out at 298K on a Bruker900MHz Avance III NMR spectrometer equipped with a triple resonance cryogenic probehead (Bruker, Karlsruhe,

Germany) with 3072, 100, 100 points for 14, 21, 21 ppm centred on 4.7, 118.5, 118.5 ppm in the ^1H , ^{15}N and ^{15}N three dimensions, respectively. Duration of the acquisition with 16 scans is 1 day and 22 hours. $[\text{}^1\text{H},^{15}\text{N}]$ 2D planes are extracted from the $[\text{}^1\text{H},^{15}\text{N},^{15}\text{N}]$ HNCANN 3D experiment (Figure 12 B). ^{15}N -chemical shift values in the third dimension of the recorded spectrum correspond to the N chemical shift of the residue at the i and $i-1$ position.

3.16 Assignment of resonances of acetylated residues: identification of the acetylation pattern

Principle: The identification of acetylation sites involves the use of selective ^{15}N -lysine labeling of Tau samples in order to decrease the spectral complexity. The assignment of lysine residues in the non-acetylated Tau samples has been made using the previously described HNCACB and HNCANN three-dimensional experiments acquired on a uniformly ^{15}N -labeled Tau sample (see Method 3.15). On the $[\text{}^1\text{H},^{15}\text{N}]$ HSQC of the ^{15}N -lysine labeled, acetylated Tau sample, one can detect some additional backbone amide resonances together with non-resolved peaks corresponding to the $\text{NH}\epsilon$ acetamide functions of lysine side chains that were referred to as the indicator signal (Figure 13, see note 19) (Kamah et al. 2014) (Theillet et al. 2012). Hence, identification of resonances corresponding to acetylated lysine residues is first required before their assignment. The resonances of acetylated lysine residues are identified in a selectively ^{15}N -lysine labeled, acetylated Tau sample using the $[\text{}^1\text{H},^{15}\text{N}]$ HSQC-TOCSY experiment that enables the detection of the proton resonances of the lysine side chain from either the backbone amide resonance or those of side chain acetamide ($\text{NH}\epsilon\text{-Ac}$, Figure 14).

1. 1 to 2 mg of either uniformly ^{15}N -labeled or selectively ^{15}N -labeled Tau in 200 μl NMR buffer (100-200 μM) are used to fill a 3 mm tube. A $[\text{}^1\text{H},^{15}\text{N}]$ HSQC 2D spectrum (Schleucher et al. 1994) (Figure 13) is recorded at 293K on a Bruker900MHz Avance III NMR spectrometer

equipped with a triple resonance cryogenic probehead (Bruker, Karlsruhe, Germany). For the uniformly labeled sample, data were acquired with 2048 and 512 points for spectral widths of 14 and 30 ppm in the ^1H and ^{15}N -dimensions, respectively, centred on 4.7 ppm and 118.4 ppm. For the selectively ^{15}N -lysine-labeled sample, data were acquired with 2048 and 128 points for spectral widths of 14 and 9 ppm centred on 4.7 ppm and 123.5 ppm in the ^1H and ^{15}N -dimensions, respectively. Duration of the acquisition with 32 scans is 1.325 hours. The spectra were processed by the Bruker TopSpin 3.1 software.²

2. Around 11mg of a ^{15}N -lysine selectively, ^{13}C uniformly-labeled, acetylated Tau sample in 400 μl NMR buffer (600 μM) are used to fill a NMR Shigemi tube. The three-dimensional spectra are acquired under a non-uniform sampling mode on a Bruker 900MHz Avance III NMR spectrometer equipped with a triple resonance cryogenic probehead (Bruker, Karlsruhe, Germany) at 293K. Data processing, peak picking and calculation of peak intensities were performed with the Bruker TopSpin 3.1 software. A [$^1\text{H},^{15}\text{N}$] HSQC-TOCSY spectrum (dipsihsqcf3gpsi3d pulse sequence from Bruker, see note 20) is recorded with 32 scans per increment, a TOCSY mixing time of 120 ms and spectral widths of 16.0, 9.0, and 11.0 ppm in ^1H (F3), ^{15}N (F2), and ^1H (F1) dimensions which are sampled with 3072, 78, and 416 points, respectively. The proton and nitrogen dimensions are centered on 4.7 and 123.5 ppm, respectively.

3. [^1H , ^1H] 2D planes are extracted from the [$^1\text{H},^{15}\text{N}$] HSQC-TOCSY 3D experiment. The chemical shift values of ^1H nuclei of lysine side chain, especially the $\text{H}\epsilon$ chemical shifts, are measured. This latter value allows for discrimination of acetylated lysines from the non-acetylated ones (Figure 14).

4. [$^1\text{H},^{15}\text{N}$] 2D planes are extracted from the [$^1\text{H},^{15}\text{N}$] HSQC-TOCSY 3D experiment at 2.98 ppm and 3.14 ppm in the F1 dimension which corresponds to the $\text{H}\epsilon$ chemical shifts of a non-acetylated and acetylated lysine residue, respectively. Each of this sub-spectrum can be

superimposed to the [^1H , ^{15}N] HSQC of acetylated Tau to discriminate between resonances of non-acetylated and acetylated lysine residues (see Figure 16 A).

5. A [^1H , ^{15}N , ^{13}C] HN(CO)CACB 3D spectrum (hncocacbgpwg3d pulse sequence from Bruker, see note 21) is recorded at 900MHz and 293K with 3072, 40 and 256 points for spectral widths of 14, 9 and 55 ppm in the ^1H , ^{15}N and ^{13}C -dimensions, respectively, centred on 4.7, 123.5, and 43.5 ppm, respectively. Duration of the acquisition with 48 scans is 1 day and 23 hours.

6. [^1H , ^{13}C] 2D planes are extracted from the [^1H , ^{15}N , ^{13}C] HN(CO)CACB 3D experiment. The chemical shift values of 'CA' and 'CB' ^{13}C nuclei of the 'i-1' residues are measured for each [^1H , ^{15}N] lysine resonance enabling residue identification (Figures 15 and 16). To avoid ambiguity related to redundant Xxx-Lys dipeptides (where Xxx is any amino acid) as illustrated in Figure 15 with the Val-Lys340/257 dipeptides, this experiment is combined with HNCACB and HNCANN experiments acquired on ^{15}N -Tau with uniform ^{15}N -labeling (see Methods 3.15) for full assignment of lysine residues in the control, non-acetylated Tau sample. According to this latter strategy, a full sequential assignment enables the identification of the 'i-1' residue of Xxx in each Xxx-Lys dipeptide which is either Glu in the case of Lys340 or Asn in the case of Lys257.

Spectral complexity due to the presence of close acetylation sites is illustrated in Figure 16 for the Lys298 residue. In this case, four resonances are detected for the single Ile-Lys dipeptide. Two of them come from a non-acetylated form of Lys298 and the two remaining from an acetylated Lys298 based on their respective H_α value (Figure 16 A) indicating the proximity of another acetylation site (identified as the Lys294 residue).

4. Notes

1. Complete medium and MEM vitamins addition are not compulsory but help to stimulate the growth and improve the yield. MEM vitamins 100X (SIGMA) are aliquoted by 10 ml and aliquots are stored at -20°C
2. Upon addition of the 100 mM CaCl₂ stock a white precipitate will form.
3. The isotopes are added freshly at the time the bacterial culture is started. They are solubilized in M9 buffer and filtered sterilized at 0.2 µm.
4. To produce ¹⁵N, ¹³C-Tau, 300mg of ¹⁵N, ¹³C-complete medium, 1 g of ¹⁵N-NH₄Cl and 2 g of ¹³C-glucose are suspended in 10 ml of M9 buffer and are 0.2 µM filter-sterilized directly into the M9 medium. Glucose is the limiting factor for the bacterial growth and an OD600 of 1.4-1.6 is usually observed at the end of the fermentation.
5. Tau protein is a disordered protein sensitive to proteases. We find that sterilization (120°C for 20 minutes) of buffers limits Tau degradation. The buffers are 0.22 µm-filtered or autoclaved and stored at 4°C.
6. pH is adjusted after addition of 250 mM imidazole in phosphate buffer and 10 mM reduced Glutathione in Tris buffer, in the elution buffers.
7. We do not reconstitute a complete medium from the Isogro® powder, given the cost of the product, but use it as a culture supplement. Generally, bacterial cultures using M9 media

supplemented with 0.05% Isogro® (w/v) reach the exponential growth phase (as measured by O.D. at 600 nm) after about 4 hours of incubation at 37°C under the conditions described to inoculate the culture. Without Isogro®, the exponential phase of growth is reached after 6 hours at 37°C.

8. The bacterial growth is slow in M9 medium. We use programmable incubators to start the culture at an early morning time, so that the protein production, collection of the bacterial pellet and analytical control of the protein production can be conveniently scheduled during the work day hours.

9. The lyophilized Tau proteins are kept at -20°C

10. Tau protein concentration is difficult to define because its absorption coefficient at 280 nm is low ($A_{280nm}=0.14$ for a solution at 1 mg/ml). To define Tau concentration, we use the surface of the peak of Tau protein absorption at 280 nm in the chromatogram in the desalting step in Ammonium Bicarbonate. This is the most reliable method we have found. This method was validated by analysis of one Tau sample by total amino acid quantification.

11. The His-ERK2 preparation is contaminated with a protein of 66 kDa (Figure 4 A).

12. The activated ERK2 kinase in activation buffer with 10% Glycerol is directly mixed with Tau protein in phosphorylation buffer, without prior buffer exchange.

13. Rat brain extract can be stored at 4°C for a few days only without loss of kinase activity.

14. A peak with a mass increment of +168 Da ($[M+H]^+$ 2861.79 Da) corresponding to the incorporation of four acetyl moieties in our CBP standard substrate from TDG protein can even be detected.

15. In contrast to S/T phosphorylation, Y phosphorylation does not induce a downfield backbone-amide chemical shift of the modified Y residue resonance (Bienkiewicz & Lumb 1999), probably because the phosphorylatable Y hydroxyl group is at a more distal position compare to the one of S and T residues.

16. [^1H , ^{15}N] HSQC pulse sequence from Bruker is hsqcetf3gpsi avance-version (12/01/11): HSQC 2D H-1/X correlation via double INEPT (Insensitive Nuclei Enhanced by Polarization Transfer) using sensitivity improvement, phase sensitive using Echo/Antiecho-TPPI gradient selection with decoupling during acquisition using f3 – channel and flip-back pulse.

17. [^1H , ^{15}N , ^{13}C] HNCACB pulse sequence from Bruker is hncacbgpwg3d avance-version (12/01/11): HNCACB 3D sequence with inverse correlation for triple resonance using multiple INEPT transfer steps (F1(H) -> F3(N) -> F2(Ca -> Cb,t1) -> F3(N,t2) -> F1(H,t3)), on/off resonance CA and CO pulses using shaped pulse, phase sensitive (t1), phase sensitive (t2), using constant time in t2 and water suppression using watergate sequence.

18. [^1H , ^{15}N , ^{15}N] HNCANN pulse sequence from Bruker is hncannhgpwg3d avance-version (12/01/11): (H)N(CA)NNH 3D sequence with inverse correlation for triple resonance using multiple INEPT transfer steps (F1(H) -> F3(N,t1) -> F2(Ca) -> F3(N,t2) -> F1(H,t3)), on/off resonance CA and CO pulses using shaped pulse, phase sensitive (t1), phase sensitive (t2), using semi-constant time in t1 and t2 and water suppression using watergate sequence.

19. In contrast to the phosphorylation sites which are easily identifiable due to the low field chemical shift of their backbone amide resonances (Figure 10), the identification of acetylated lysine is not trivial just by looking to the 2D [^1H , ^{15}N] HSQC spectrum of acetylated ^{15}N -labeled Tau, or even in the ^{15}N -Lys-labeled Tau samples (Figure 13). Furthermore, the CA and CB chemical shifts of lysine residues as extracted from the HNCACB experiment (Methods 3.14, 2) failed to inform about the lysine acetylation state. Only the extremity of the lysine side chain (from C γ to C ϵ) is sensitive to the presence of an acetyl moiety (Smet-NoCCA et al. 2010).

20. [^1H , ^{15}N] HSQC-TOCSY pulse sequence from Bruker is dipsihsqcf3gpsi3d avance-version (12/01/11): TOCSY-HSQC 3D sequence with homonuclear Hartman-Hahn transfer using DIPSI2 sequence for mixing, H-1/X correlation via double inept transfer using sensitivity improvement, phase sensitive (t1), phase sensitive using Echo/Antiecho-TPPI gradient selection (t2), using trim pulses in INEPT transfer, using f3 – channel.

21. [^1H , ^{15}N , ^{13}C] HN(CO)CACB pulse sequence from Bruker is hncocacbgpwg3d avance-version (12/01/11) : HNCOCACB 3D sequence with inverse correlation for triple resonance using multiple INEPT transfer steps (F1(H) -> F3(N) -> F2(C=O) -> F2(C α -> C β ,t1) -> F2(C=O) -> F3(N,t2) -> F1(H,t3)), on/off resonance CA and CO pulses using shaped pulse, phase sensitive (t1), phase sensitive (t2) using constant time in t2 and water suppression using watergate sequence.

Funding

The NMR facilities were funded by the Région Nord, CNRS, Pasteur Institute of Lille, European Community (FEDER), French Research Ministry and the University of Sciences and Technologies of Lille I. We acknowledge support from the TGE RMN THC (FR-3050, France). This study was supported by a grants from the LabEx (Laboratory of Excellence), DISTALZ (Development of Innovative

Strategies for a Transdisciplinary approach to Alzheimer's disease), and in part by the French government funding agency Agence Nationale de la Recherche TAF. SP and JG were partially supported on NIH R01-GM08157.

Figure captions

Figure 1 : Induction of recombinant Tau expression in BL21(DE3) bacteria. Lane1: BL21(DE3) bacteria before the expression induction by IPTG. Lane2: BL21(DE3) bacteria 4 hours after induction. The band of recombinant Tau protein is shown by black arrow around 66 kDa.

Figure 2: Cation exchange chromatography purification step of the ^{15}N -Tau. The chromatogram shows the absorbance at 280 nm in milli-absorption units (graph in blue) and the percentage of CEX buffer B (graph in marron). The peak corresponding to ^{15}N -Tau is boxed in black.

Figure 3: Desalting of ^{15}N -Tau into ammonium bicarbonate buffer from the previous purification step of cation exchange chromatography (Figure 2). The protein elution is monitored at 280 nm. Four injections of 5 ml ^{15}N -Tau are performed for one CEX chromatography. Red lines correspond to injections (5 ml loop). Collected ^{15}N -Tau fractions are shown in black dotted box.

Figure 4: (A) SDS-Polyacrylamide Gel Electrophoresis (SDS-PAGE) is run to monitor the preparation steps of His-ERK2. 5-10 μl of samples collected from the purification steps are run through 12% SDS-Polyacrylamide Gel. Line1: bacterial lysate; Line2: soluble extract; Line3-4: washing fractions collected with 5% elution buffer. Line5-7: purified sample fractions. Eluted His-ERK2 corresponds to the band appearing at 42 kDa in Line5. A number of contaminating proteins are removed by washing the resin with 5% elution buffer (see lines3-4). (B) Analysis of purified GST-MEK1 R4F by SDS-PAGE. 5 μl collected from the elution step are run through 12% SDS-Polyacrylamide Gel. GST-MEK1 R4F fusion protein (up) and GST (bottom) are labeled. The GST tag is expected at 26 kDa and the GST-MEK1 R4F at 68 kDa. The multiple bands correspond to degradation products of the fusion protein.

Figure 5: (A) Time course of His-ERK2 *in vitro* activation by GST-MEK1R4F. 5 μ l of samples are removed from the reaction mix at initial time, 30 minutes, 180 minutes and at 16 hours (overnight) incubation time. From 30 minutes of incubation, a slight migration delay of the band corresponding to His-ERK2 is observed compared to that at the initial time. The band upper shift increases until the end of reaction. The amount of soluble His-ERK2 decreases with the incubation time due to precipitation. (B) SDS-PAGE analysis of Tau phosphorylation. About 1.2 μ g samples are loaded in 12% acrylamide gel. Compare to Tau control (see line1), ERK2-phosphorylated Tau has a lower mobility resulting in a shift of the band from 52 kDa to 60 kDa (line2) and phosphorylated Tau by rat brain extract a shift to 66 kDa (line3).

Figure 6: SDS-10% PAGE of the purification of GST-CBP[1202-1848] acetyltransferase on glutathione sepharose beads. Lane1: molecular weight markers; lane2: 5 μ l of the soluble bacterial extract; lane3: 7.5 μ l of the pooled flow through and first wash supernatant; lane4: 15 μ l of the final glutathione beads slurry.

Figure 7: Reverse-phase analysis on a C18 column of the acetylation reactions on a peptide substrate with recombinant GST-CBP[1202-1848]. Due to the presence of at least three acetylation sites, a complex pattern of elution was detected at 215 nm at both 20°C and 30°C. (A) Absorbance at 280 nm (red), 260 nm (blue) and 215 nm (green) of the acetylation reaction performed with 2 mM AcCoA at 30°C overnight. (B) Comparison of the absorbance detected at 215 nm of the acetylation reactions performed with (green) or without AcCoA (violet) at 30°C overnight or with AcCoA at 20°C overnight (blue). The linear gradient of buffer B (%B) is indicated by orange line. (C) MALDI-TOF mass spectra of the fractions 2, 3 and 4 of the analytical C18 chromatography (see fractions on panel A); m/z values of $[M+H]^+$ species are annotated. The 'M' character indicates the mass of the unmodified peptide.

Figure 8: Reverse-phase purification on a C8 column of the ^{15}N -Lys, ^{13}C -labeled Tau protein before and after acetylation reaction with recombinant GST-CBP[1202-1848]. (A) Chromatogram of the purification of control and acetylated ^{15}N -Lys, ^{13}C -labeled-Tau on a C8 column with a linear gradient of acetonitrile (orange line) as monitored by the absorbance at 215 nm for control ^{15}N -Lys, ^{13}C -Tau (red curve) and acetylated ^{15}N -Lys, ^{13}C -Tau (blue curve) and at 280 nm (green curve, control ^{15}N -Lys, ^{13}C -Tau). (B,C) 12% acrylamide SDS gel electrophoresis of the ^{15}N -Lys, ^{13}C -Tau protein before and after the acetylation reaction (B) Fractions of non-acetylated and acetylated ^{15}N -Lys, ^{13}C -Tau proteins purified by cation exchange chromatography. 2 μl of a 50 μM solution of protein were loaded on the gel. (C) Fractions of non-acetylated and acetylated ^{15}N -Lys, ^{13}C -Tau protein purified by reverse-phase chromatography. Only the fractions corresponding to the boxed region on the chromatograms in (A) are shown. 2.5 μl of the lyophilized fractions dissolved in 200 μl water are loaded on the gel.

Figure 9: Chromatogram of desalting in 50 mM ammonium bicarbonate of the ^{15}N -lysine, ^{13}C -Tau protein in its non-acetylated and acetylated forms from fractions of the purification step by C8 reverse-phase chromatography.

Figure 10: Overlaid 2D [^1H , ^{15}N] HSQC spectra of ^{15}N phosphorylated Tau in black with ^{15}N -Tau in red. HSQC spectrum records the J-coupling (through-bound magnetization transfer) correlation between ^1H and ^{15}N -nuclei. Each resonance thus corresponds to an amino acid of the protein backbone. The encircled multiple additional resonances in the black spectrum, compared to the red control spectrum of ^{15}N -Tau, correspond to phosphorylated residues of the Tau protein according to previous NMR studies of Tau protein (I. Landrieu et al. 2006) review in (Theillet et al. 2012).

Figure 11: Strategy of identification of 'X-pS/pT-P' motifs in Tau protein. Chemical shifts of CA and CB of 'i' and 'i-1' residues in [^1H , ^{15}N , ^{13}C] HNCACB 3D experiment and chemical shift of ^{15}N of the 'i-1'

residues in [^1H , ^{15}N , ^{15}N] HNCANN 3D experiment are used to assign a resonance in the [^1H , ^{15}N] 2D spectrum to a specific pS-P or pT-P motif in Tau sequence.

Figure 12: (A) [^1H , ^{13}C] 2D planes extracted from the [^1H , ^{15}N , ^{13}C] HNCACB 3D spectrum, at ^{15}N -values of 125.24 ppm (left) and 124.76 ppm (right). The ^{13}C -CA resonances (in black) in side chain of pT175 (left panel) and pT181 (right panel) are indicated. ^{13}C -CB resonances for these residues are outside the spectrum window (74 ppm). This combination of CA and CB chemical shift values is typical of a pT-P dipeptide. The weaker set of signals (indicated by arrows) corresponds to ^{13}C -CA (in black) and ^{13}C -CB resonances (in red) of the prior residue. Because for both pT-P dipeptide the *i*-1 residue shows chemical shift values typical of a lysine residue (CA is 55.8 ppm, CB is 33.3 ppm), these resonances cannot be uniquely identified among the 9 pT-P motifs of Tau. (B) [^1H , ^{15}N] 2D planes extracted from the [^1H , ^{15}N , ^{15}N] HNCANN 3D spectrum, at ^{15}N -values of 125.24 ppm (left) and 124.76 ppm (right). The ^{15}N -resonance in the third dimension represents the chemical shifts of the ^{15}N of the amide group of the K residue at position '*i*-1'. From the previously determined assignment of Tau (Lippens et al. 2004; Smet et al. 2004; M. D. Mukrasch et al. 2009), we could distinguished $\delta\text{N},i-1,\text{Lys}174=121.67\text{ppm}$ and $\delta\text{N},i-1,\text{K}180=122.47\text{ppm}$, which allow to discriminate the resonance of pT175 of pT181.

Figure 13: Comparison of the [^1H , ^{15}N] HSQC spectra of the non-acetylated (red) and acetylated (black) form of uniformly ^{15}N -labeled Tau (left spectra) and selectively ^{15}N -lysine labeled Tau (right spectra).

Figure 14: Strategy of acetylated lysine identification based on the $\text{H}\epsilon$ chemical shift of lysine side chain from the [^1H , ^{15}N] HSQC-TOCSY experiment acquired on ^{15}N -lysine, ^{13}C -labeled Tau protein.

Figure 15: Identification of lysine resonances using the [^1H , ^{15}N , ^{13}C] HN(CO)CACB experiment. (A) Zoom of the [^1H , ^{15}N] HSQC experiment acquired on selectively ^{15}N -lysine-labeled, acetylated Tau. (B) [^1H , ^{13}C] 2D planes extracted from the [^1H , ^{15}N , ^{13}C] HN(CO)CACB 3D spectrum, at ^{15}N -values of 126.25 ppm (left) and 124.85 ppm (right). The ^{13}C -CA (black) and ^{13}C -CB resonances (red) of '*i*-1' residue side

chain of K340 (left panel) and K257 (right panel) are indicated. This combination of CA and CB chemical shift values is typical of a Val residue. The unambiguous assignment of both Val-Lys dipeptide has been made with a non-acetylated Tau sample and uniform ^{15}N -labeling using the previously described $[^1\text{H},^{15}\text{N},^{13}\text{C}]$ HNCACB and $[^1\text{H},^{15}\text{N},^{15}\text{N}]$ HNCANN three-dimensional experiments (Method 3.15).

Figure 16: Increasing spectral complexity in the case of two close acetylation sites showing four resonances for the single Ile-Lys298 dipeptide (numbered from 1 to 4). (A) Zoom of the $[^1\text{H},^{15}\text{N}]$ HSQC experiment acquired on selectively ^{15}N -lysine-labeled, acetylated Tau (black). Sub-spectra of non-acetylated (red) and acetylated (blue) lysine (Method 3.16, 4) are overlaid and indicate that resonances 1 and 2 correspond to non-acetylated lysine while resonances 3 and 4 correspond to acetylated lysine. (B) $[^1\text{H},^{13}\text{C}]$ 2D planes extracted from the $[^1\text{H},^{15}\text{N},^{13}\text{C}]$ HN(CO)CACB 3D spectrum at ^{15}N -values of 125.07 ppm (for resonances 1 and 3) and 124.78 ppm (for resonances 2 and 4). According to the ^{13}C -CA (black) and ^{13}C -CB values (red) of the 'i-1' residue, resonances numbered 1 to 4 are all identified as Ile-Lys dipeptide which is represented by the sole Lys298 along the Tau sequence. Hence, the splitting of each of non-acetylated and acetylated K298 resonance is due to the proximity of another acetylation site in the Tau sequence which has been identified as the 'i-4' residue according to the same assignment strategy.

References

- Alonso, A.C., Zaidi, T., Grundke-Iqbal, I., and Iqbal, K. (1994). Role of abnormally phosphorylated tau in the breakdown of microtubules in Alzheimer disease. *Proc Natl Acad Sci U A* *91*, 5562–5566.
- Amniai, L., Barbier, P., Sillen, A., Wieruszeski, J.-M., Peyrot, V., Lippens, G., and Landrieu, I. (2009). Alzheimer disease specific phosphoepitopes of Tau interfere with assembly of tubulin but not binding to microtubules. *FASEB J* *23*, 1146–1152.
- Anderson, N.G., Maller, J.L., Tonks, N.K., and Sturgill, T.W. (1990). Requirement for integration of signals from two distinct phosphorylation pathways for activation of MAP kinase. *Nature* *343*, 651–653.
- Bienkiewicz, E.A., and Lumb, K.J. (1999). Random-coil chemical shifts of phosphorylated amino acids. *J Biomol NMR* *15*, 203–206.
- Biernat, J., Mandelkow, E.M., Schroter, C., Lichtenberg-Kraag, B., Steiner, B., Berling, B., Meyer, H., Mercken, M., Vandermeeren, A., Goedert, M., et al. (1992). The switch of tau protein to an Alzheimer-like state includes the phosphorylation of two serine-proline motifs upstream of the microtubule binding region. *EMBO J* *11*, 1593–1597.
- Boulton, T.G., Yancopoulos, G.D., Gregory, J.S., Slaughter, C., Moomaw, C., Hsu, J., and Cobb, M.H. (1990). An insulin-stimulated protein kinase similar to yeast kinases involved in cell cycle control. *Science* *249*, 64–67.
- Cohen, T.J., Guo, J.L., Hurtado, D.E., Kwong, L.K., Mills, I.P., Trojanowski, J.Q., and Lee, V.M. (2011). The acetylation of tau inhibits its function and promotes pathological tau aggregation. *Nat Commun* *2*, 252.
- Goedert, M., Jakes, R., Crowther, R.A., Six, J., Lubke, U., Vandermeeren, M., Cras, P., Trojanowski, J.Q., and Lee, V.M. (1993). The abnormal phosphorylation of tau protein at Ser-202 in Alzheimer disease recapitulates phosphorylation during development. *Proc Natl Acad Sci U A* *90*, 5066–5070.
- Hasegawa, M., Morishima-Kawashima, M., Takio, K., Suzuki, M., Titani, K., and Ihara, Y. (1992). Protein sequence and mass spectrometric analyses of tau in the Alzheimer's disease brain. *J Biol Chem* *267*, 17047–17054.
- Kamah, A., Huvent, I., Cantrelle, F.X., Qi, H., Lippens, G., Landrieu, I., and Smet-Nocca, C. (2014). Nuclear magnetic resonance analysis of the acetylation pattern of the neuronal Tau protein. *Biochemistry (Mosc.)* *53*, 3020–3032.
- Landrieu, I., Lacosse, L., Leroy, A., Wieruszeski, J.M., Trivelli, X., Sillen, A., Sibille, N., Schwalbe, H., Saxena, K., Langer, T., et al. (2006). NMR analysis of a Tau phosphorylation pattern. *J Am Chem Soc* *128*, 3575–3583.
- Lippens, G., Wieruszeski, J.M., Leroy, A., Smet, C., Sillen, A., Buee, L., and Landrieu, I. (2004). Proline-directed random-coil chemical shift values as a tool for the NMR assignment of the tau phosphorylation sites. *Chembiochem* *5*, 73–78.
- Mansour, S.J., Matten, W.T., Hermann, A.S., Candia, J.M., Rong, S., Fukasawa, K., Vande Woude, G.F., and Ahn, N.G. (1994). Transformation of mammalian cells by constitutively active MAP kinase kinase. *Science* *265*, 966–970.

- Martin, L., Latypova, X., Wilson, C.M., Magnaudeix, A., Perrin, M.L., Yardin, C., and Terro, F. (2013). Tau protein kinases: involvement in Alzheimer's disease. *Ageing Res Rev* 12, 289–309.
- Min, S.W., Cho, S.H., Zhou, Y., Schroeder, S., Haroutunian, V., Seeley, W.W., Huang, E.J., Shen, Y., Masliah, E., Mukherjee, C., et al. (2010). Acetylation of tau inhibits its degradation and contributes to tauopathy. *Neuron* 67, 953–966.
- Morishima-Kawashima, M., Hasegawa, M., Takio, K., Suzuki, M., Yoshida, H., Titani, K., and Ihara, Y. (1995). Proline-directed and non-proline-directed phosphorylation of PHF-tau. *J Biol Chem* 270, 823–829.
- Morris, M., Knudsen, G.M., Maeda, S., Trinidad, J.C., Ioanoviciu, A., Burlingame, A.L., and Mucke, L. (2015). Tau post-translational modifications in wild-type and human amyloid precursor protein transgenic mice. *Nat Neurosci* 18, 1183–1189.
- Mukrasch, M.D., Bibow, S., Korukottu, J., Jeganathan, S., Biernat, J., Griesinger, C., Mandelkow, E., and Zweckstetter, M. (2009). Structural polymorphism of 441-residue tau at single residue resolution. *PLoS Biol* 7, e34.
- Prabakaran, S., Everley, R.A., Landrieu, I., Wieruszeski, J.M., Lippens, G., Steen, H., and Gunawardena, J. (2011). Comparative analysis of Erk phosphorylation suggests a mixed strategy for measuring phospho-form distributions. *Mol Syst Biol* 7, 482.
- Qi, H., Cantrelle, F.-X., Benhelli-Mokrani, H., Smet-Nocca, C., Buée, L., Lippens, G., Bonnefoy, E., Galas, M.-C., and Landrieu, I. (2015). Nuclear magnetic resonance spectroscopy characterization of interaction of Tau with DNA and its regulation by phosphorylation. *Biochemistry (Mosc.)* 54, 1525–1533.
- Schleucher, J., Schwendinger, M., Sattler, M., Schmidt, P., Schedletzky, O., Glaser, S.J., Sorensen, O.W., and Griesinger, C. (1994). A general enhancement scheme in heteronuclear multidimensional NMR employing pulsed field gradients. *J Biomol NMR* 4, 301–306.
- Seger, R., Ahn, N.G., Boulton, T.G., Yancopoulos, G.D., Panayotatos, N., Radziejewska, E., Ericsson, L., Bratlien, R.L., Cobb, M.H., and Krebs, E.G. (1991). Microtubule-associated protein 2 kinases, ERK1 and ERK2, undergo autophosphorylation on both tyrosine and threonine residues: implications for their mechanism of activation. *Proc Natl Acad Sci U S A* 88, 6142–6146.
- Smet, C., Leroy, A., Sillen, A., Wieruszeski, J.M., Landrieu, I., and Lippens, G. (2004). Accepting its random coil nature allows a partial NMR assignment of the neuronal Tau protein. *Chembiochem* 5, 1639–1646.
- Smet-Nocca, C., Wieruszeski, J.M., Melnyk, O., and Benecke, A. (2010). NMR-based detection of acetylation sites in peptides. *J Pept Sci* 16, 414–423.
- Theillet, F.-X., Smet-Nocca, C., Liokatis, S., Thongwichian, R., Kosten, J., Yoon, M.-K., Kriwacki, R.W., Landrieu, I., Lippens, G., and Selenko, P. (2012). Cell signaling, post-translational protein modifications and NMR spectroscopy. *J. Biomol. NMR* 54, 217–236.
- Tini, M., Benecke, A., Um, S.J., Torchia, J., Evans, R.M., and Chambon, P. (2002). Association of CBP/p300 acetylase and thymine DNA glycosylase links DNA repair and transcription. *Mol Cell* 9, 265–277.

Weisemann, R., Ruterjans, H., and Bermel, W. (1993). 3D triple-resonance NMR techniques for the sequential assignment of NH and ^{15}N resonances in ^{15}N - and ^{13}C -labelled proteins. *J Biomol NMR* 3, 113–120.

Figure 1

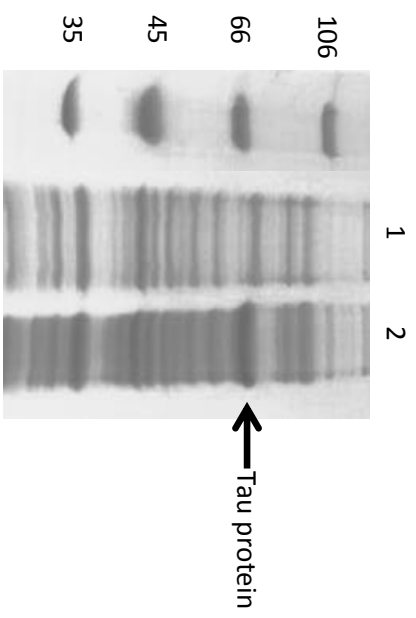


Figure 2

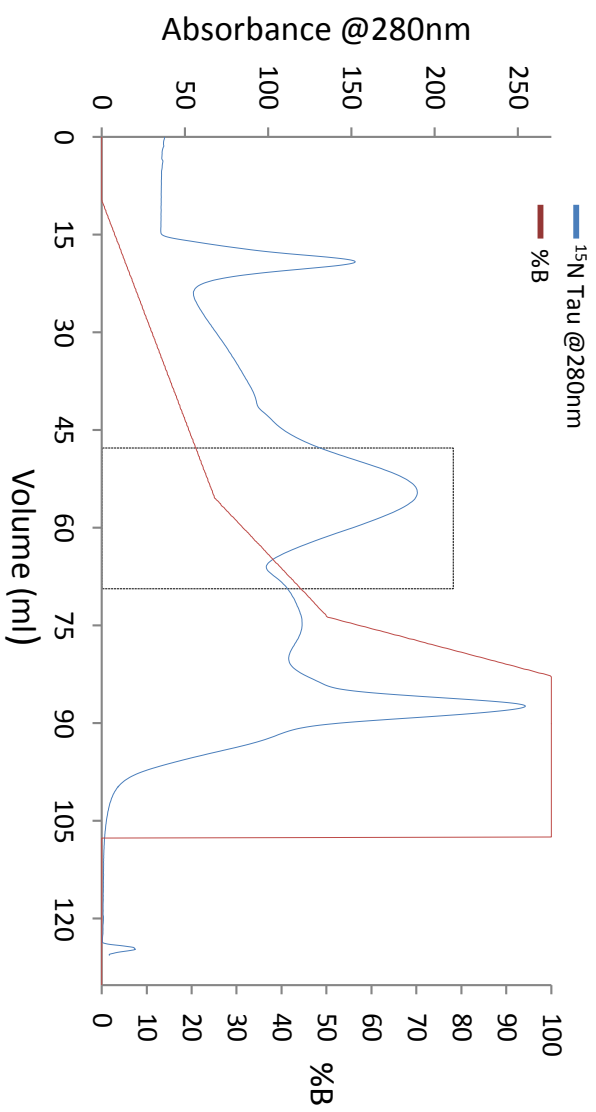


Figure 3

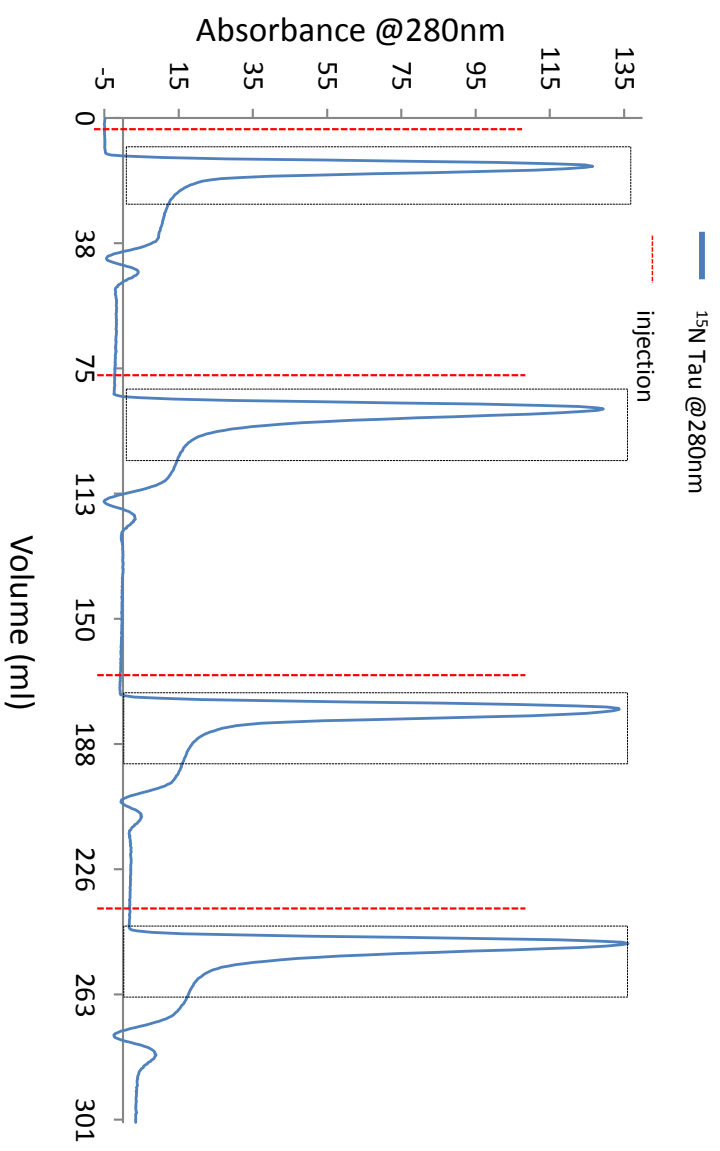
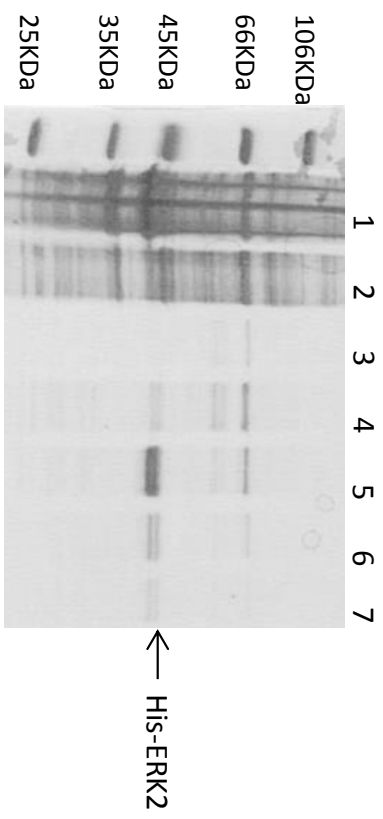
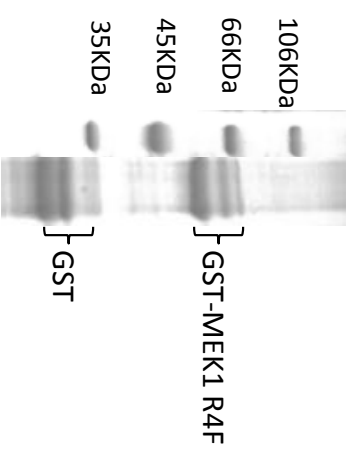


Figure 4:

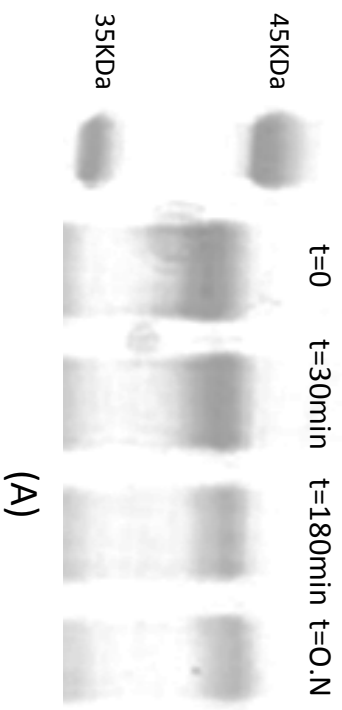


(A)

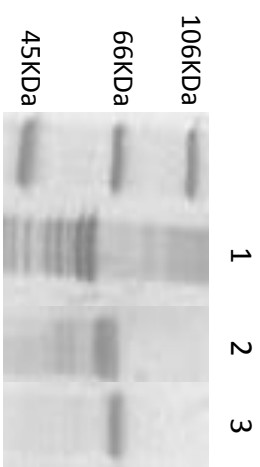


(B)

Figure 5:



(A)



(B)

1. Tau control
2. pTau by ERK2
3. pTau by rat brain extract

Figure 6:

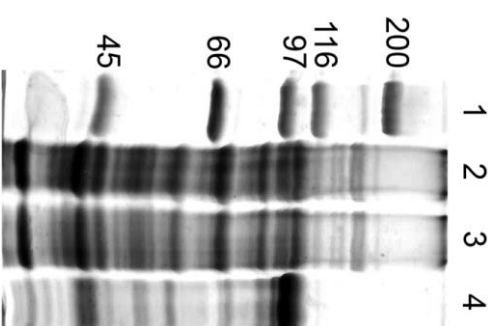


Figure 7:

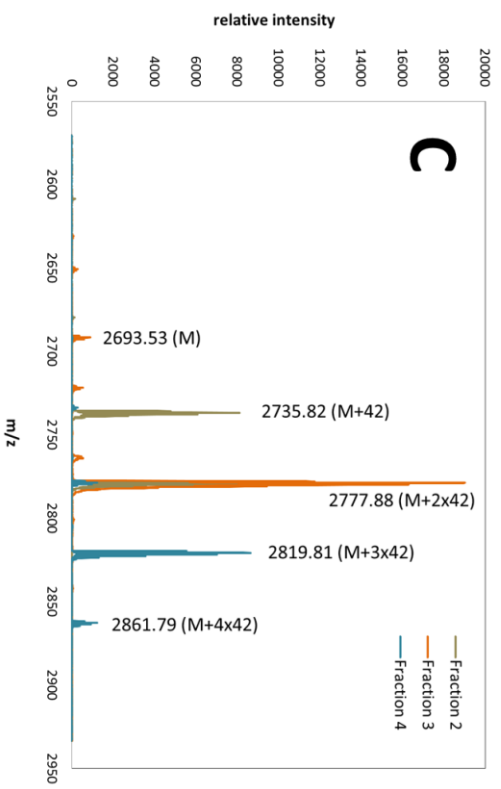
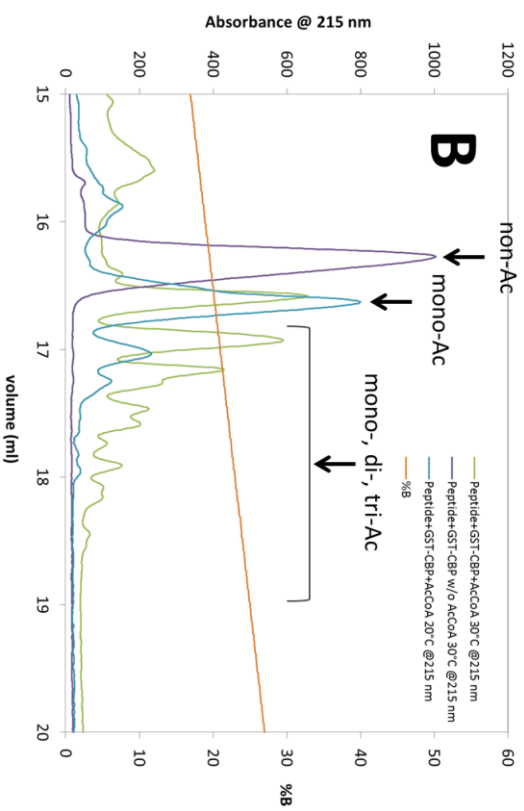
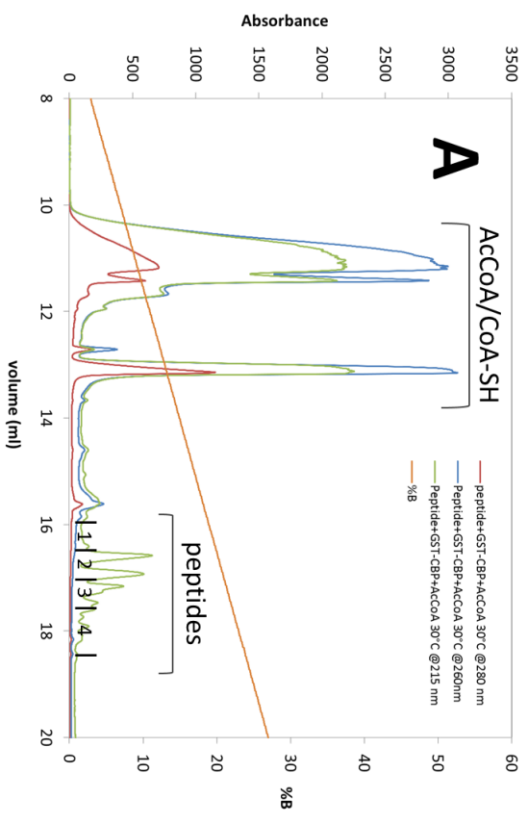


Figure 8:

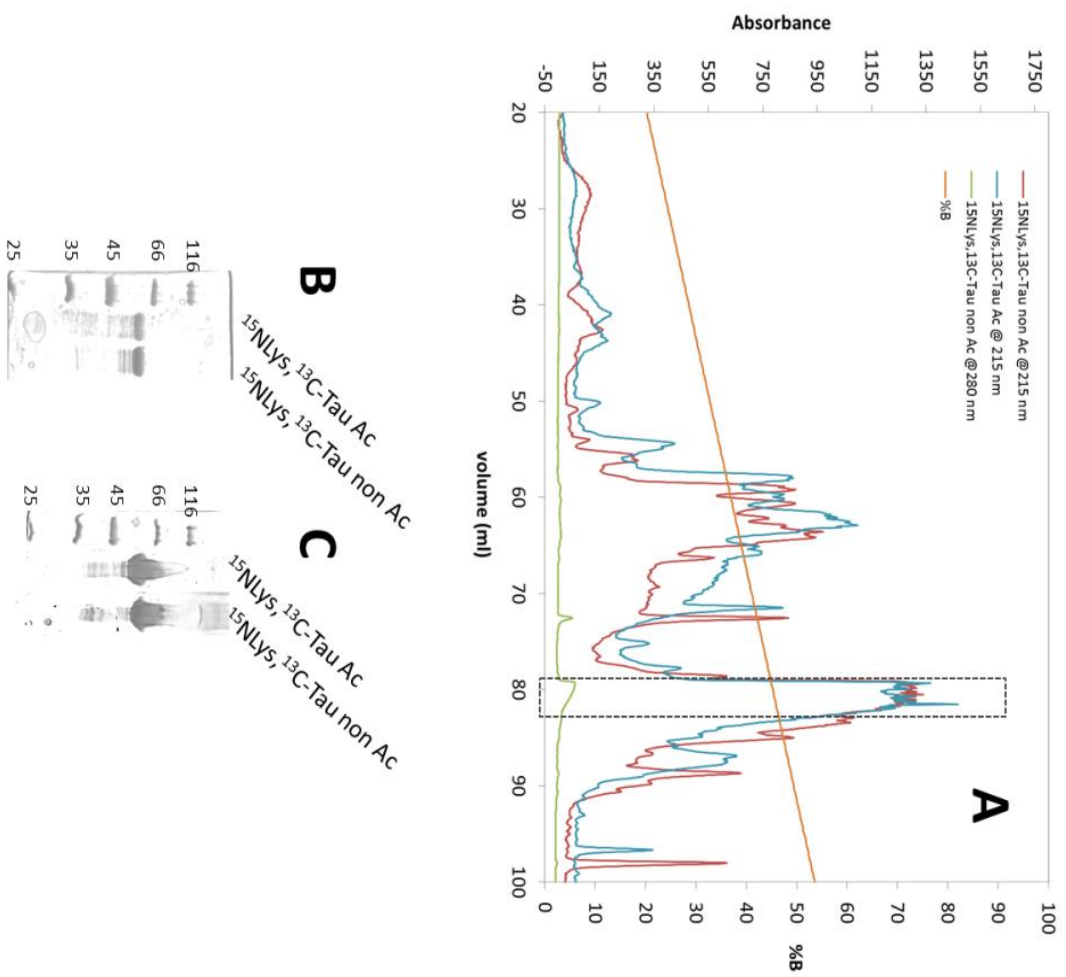


Figure 9:

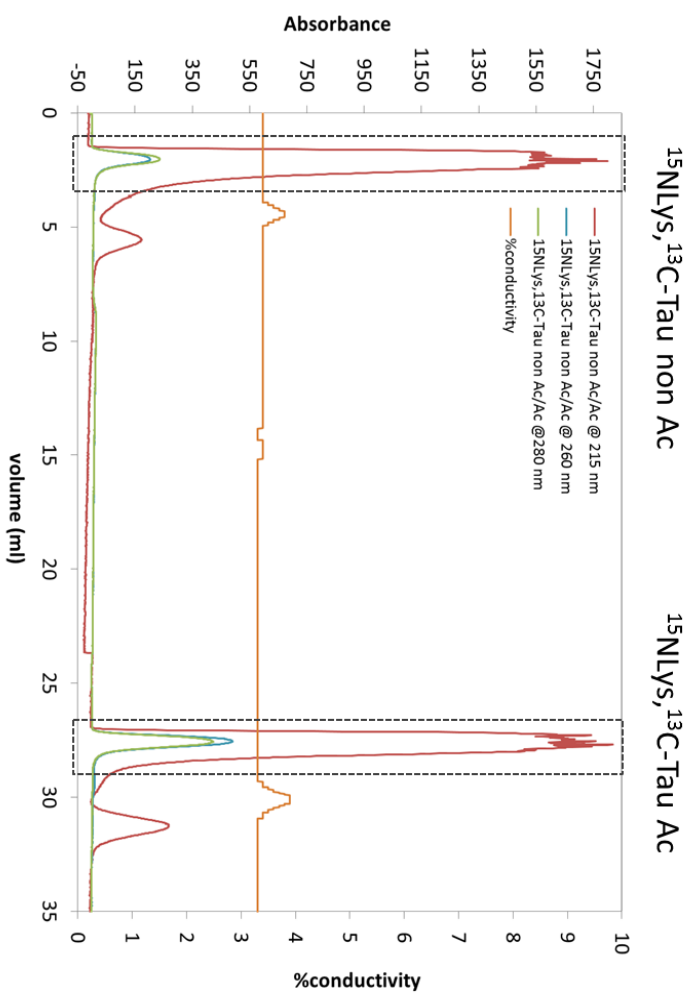


Figure 10:

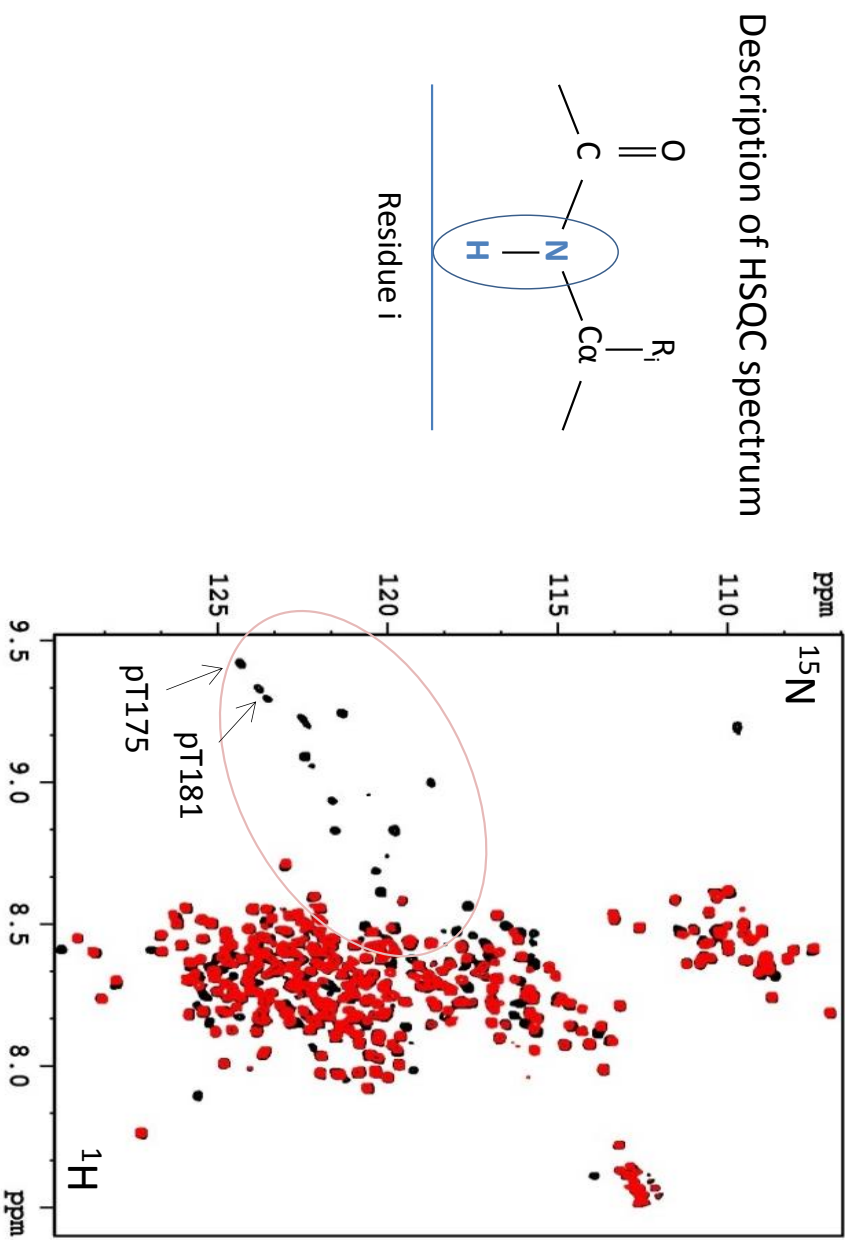


Figure 11:

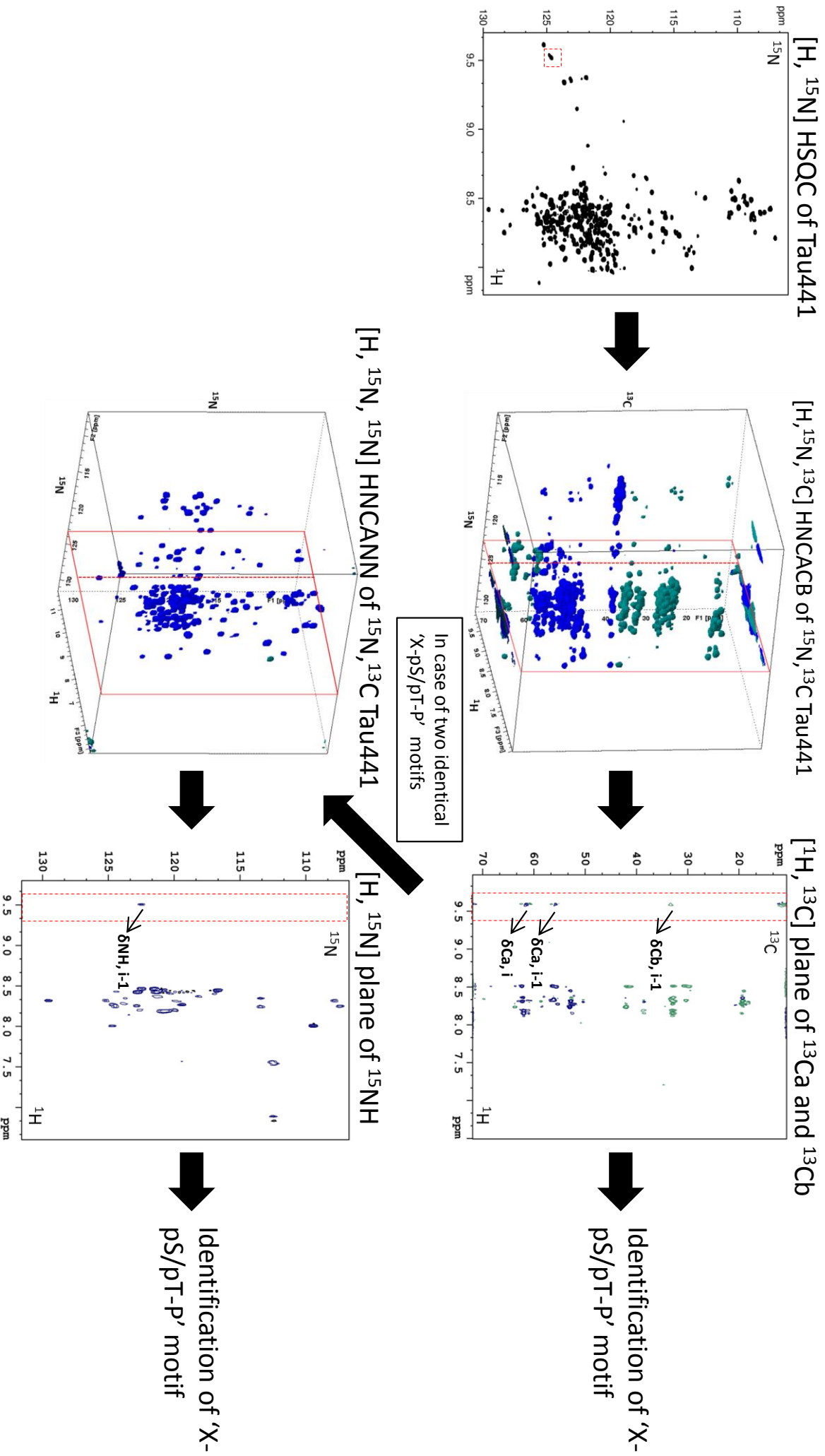
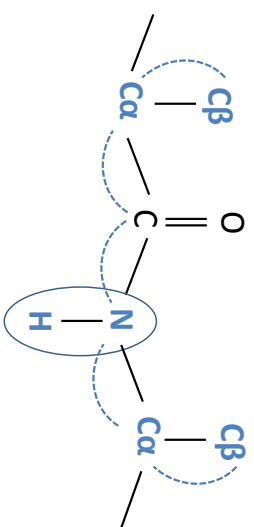


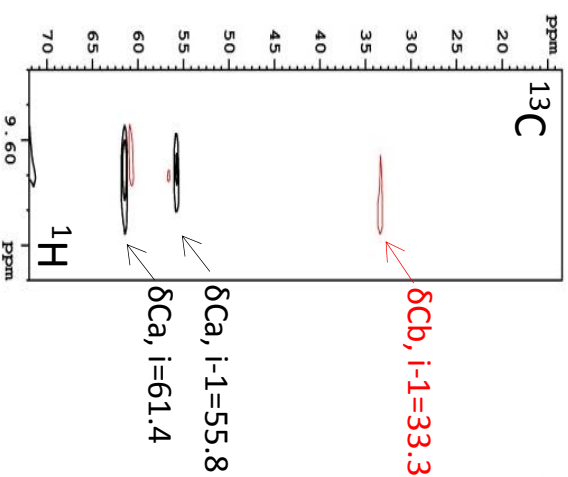
Figure 12:

Description of HNCACB spectrum



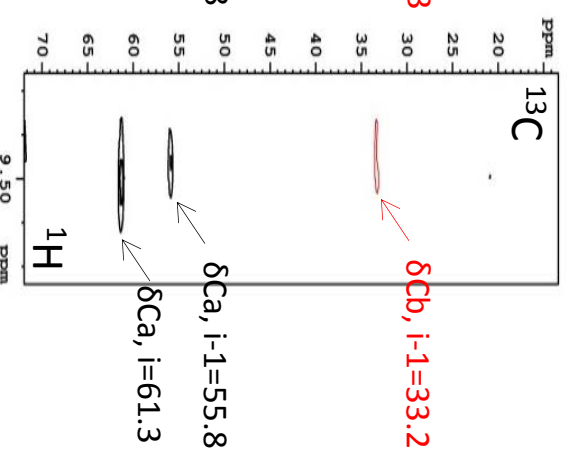
Residue i-1

Residue i



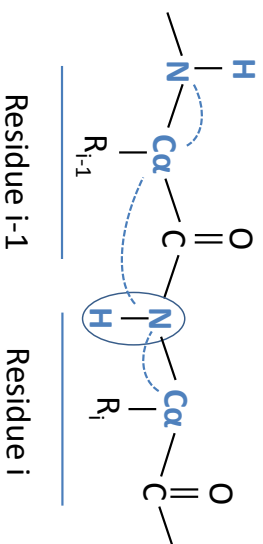
Lys-pThr175-Pro

(A)



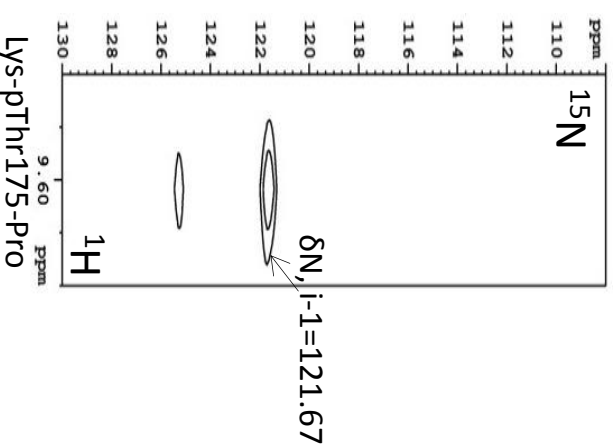
Lys-pThr181-Pro

Description of HNCANN spectrum



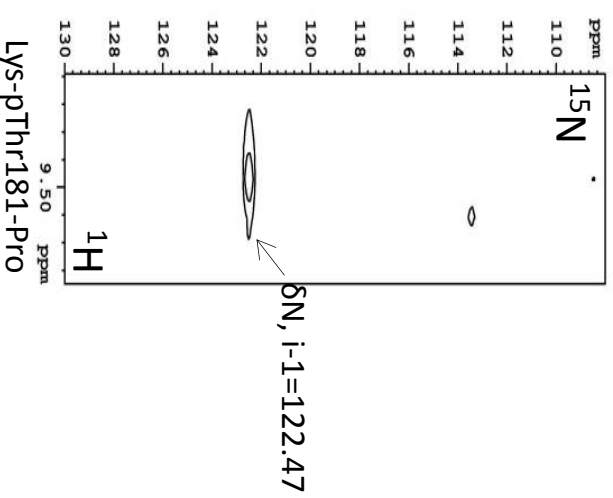
Residue i-1

Residue i



Lys-pThr175-Pro

(B)



Lys-pThr181-Pro

Figure 13:

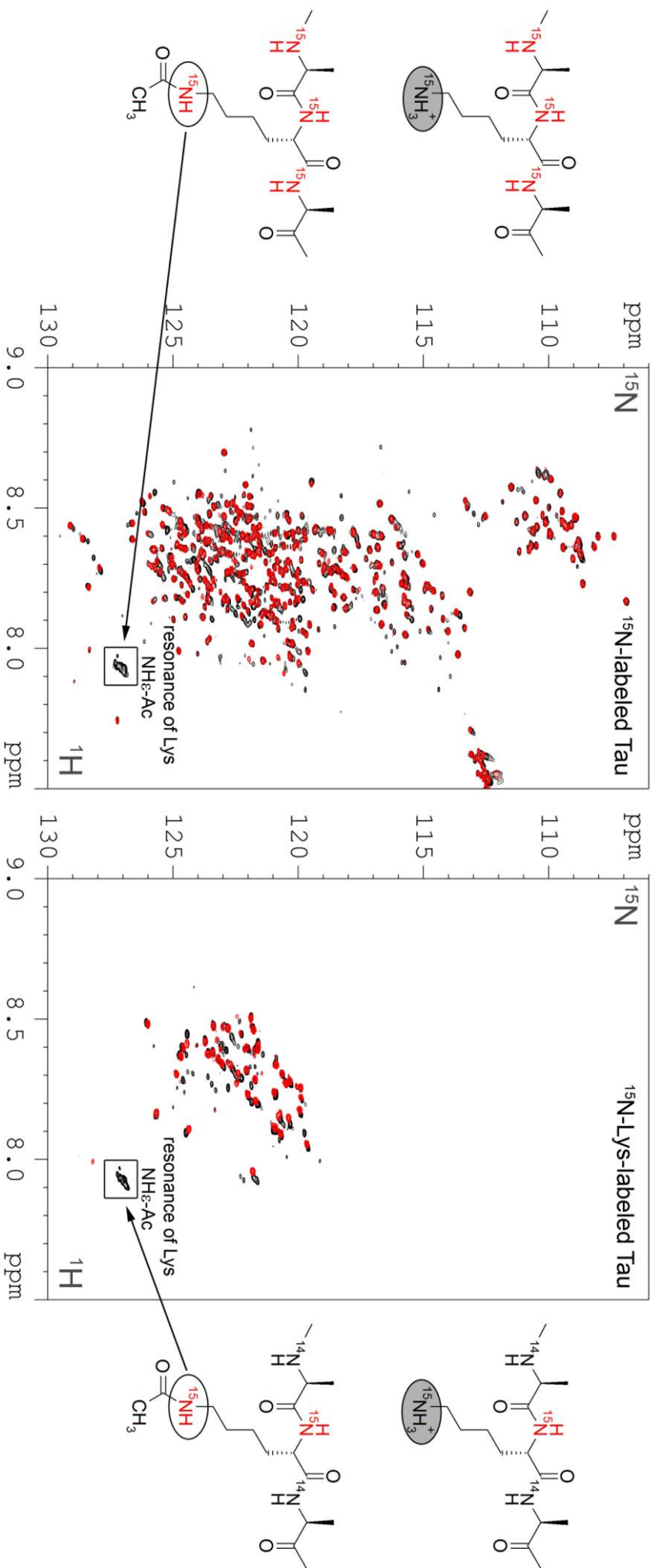


Figure 14:

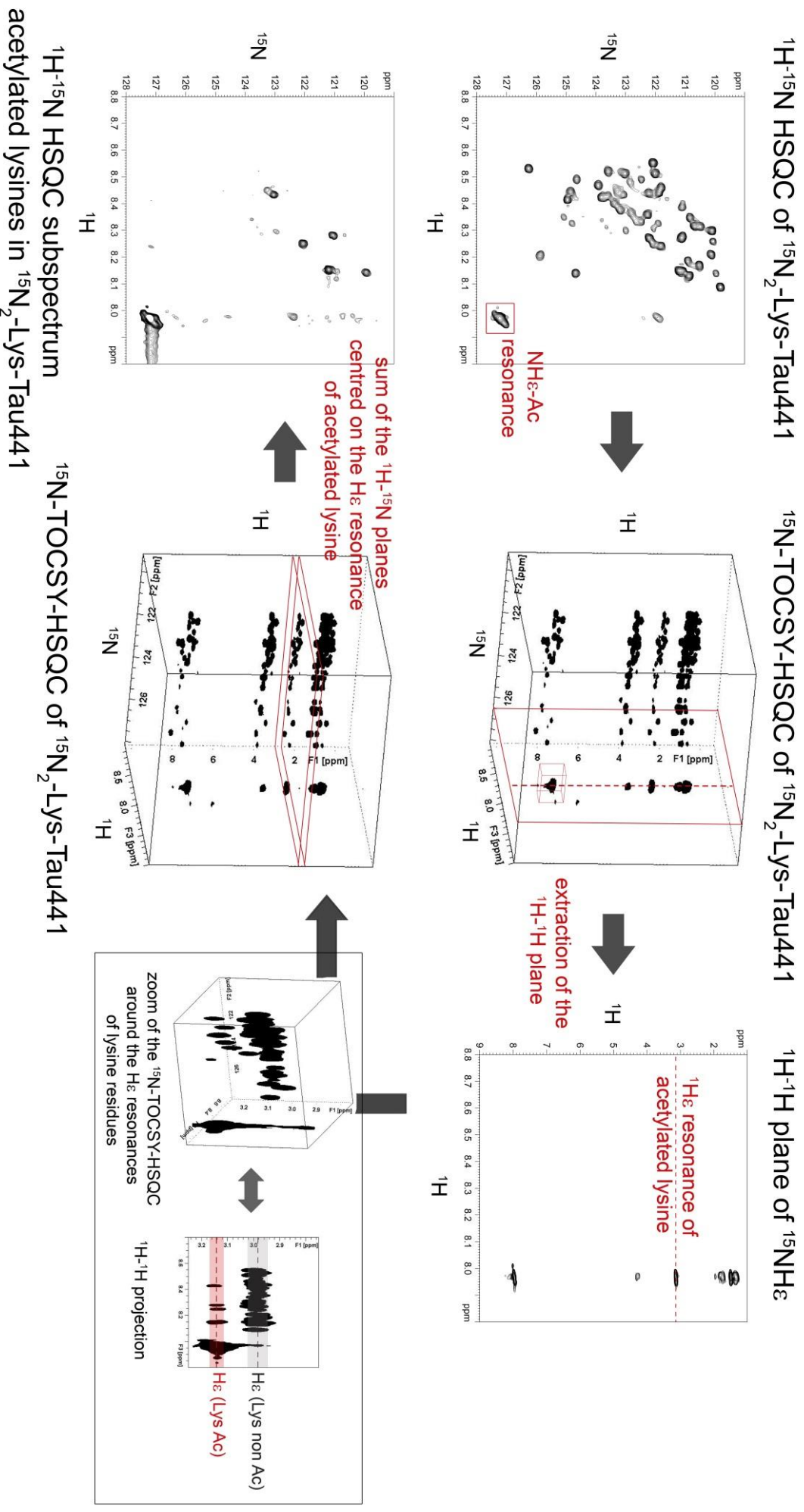
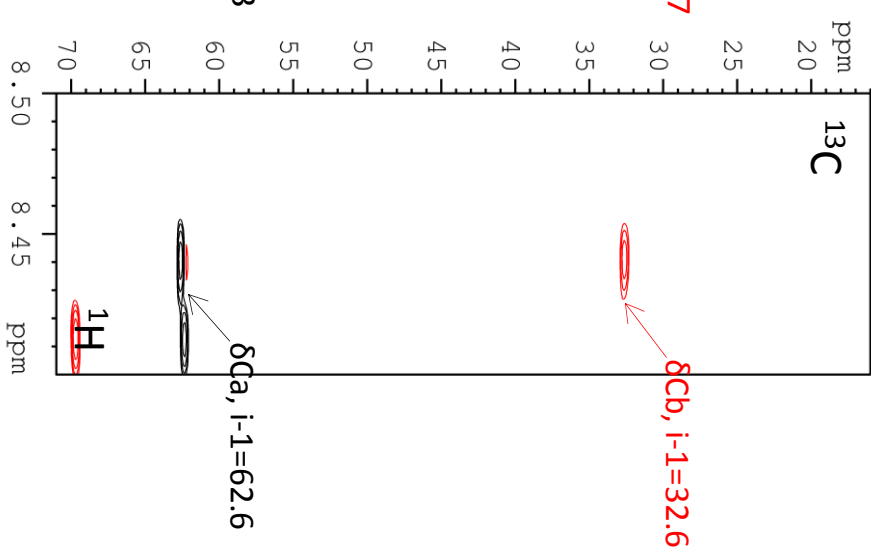
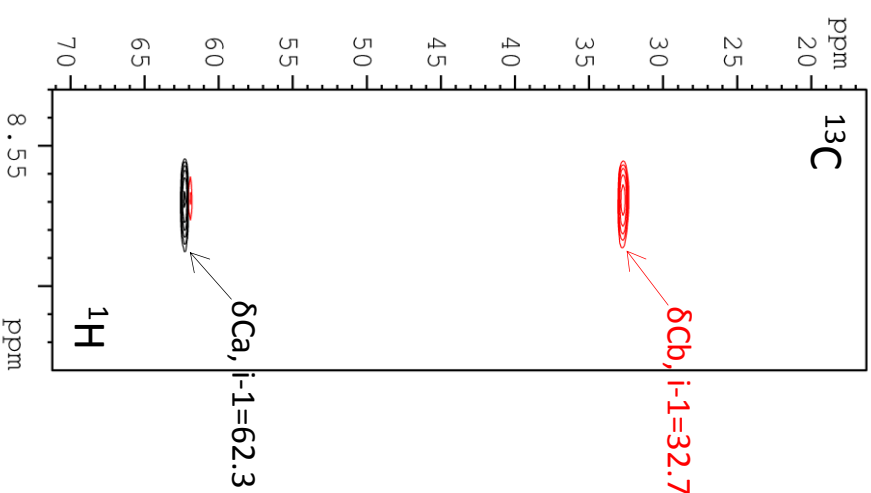
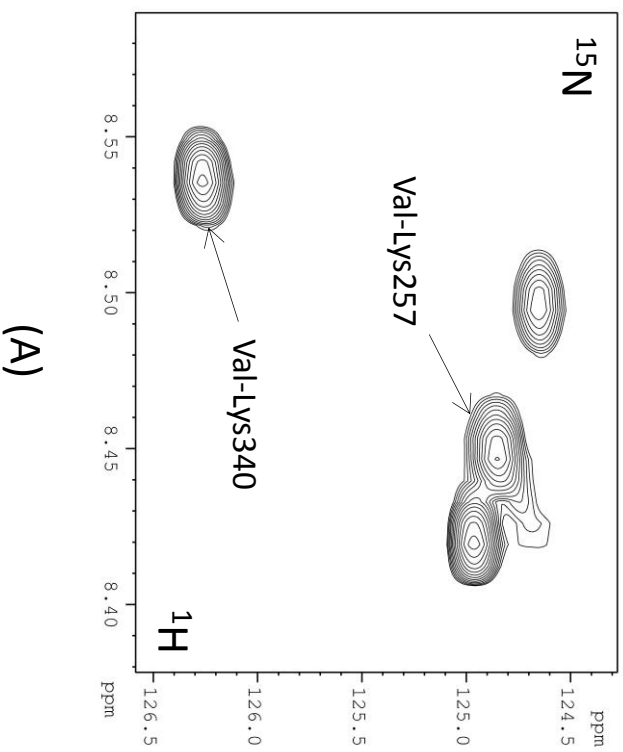
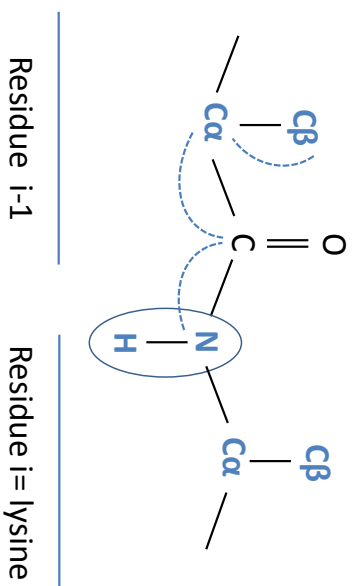


Figure 15:

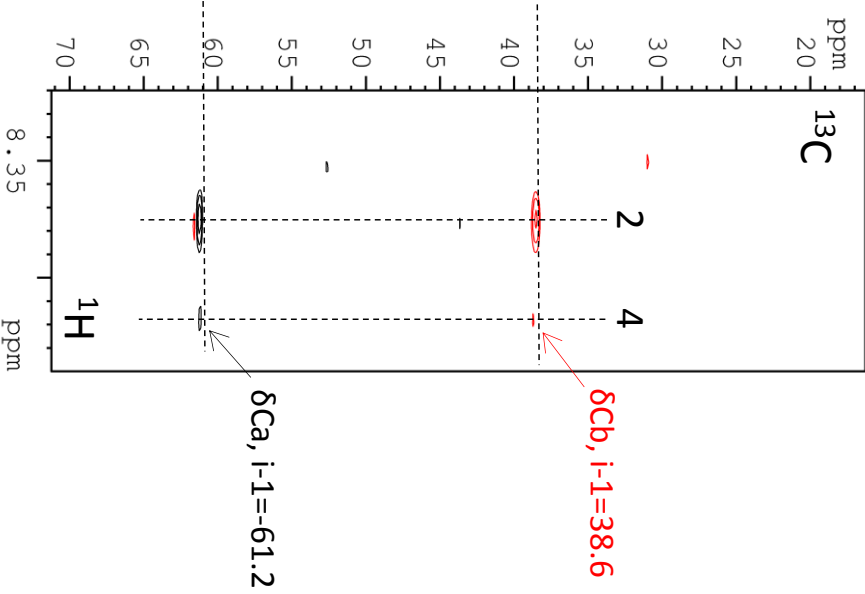
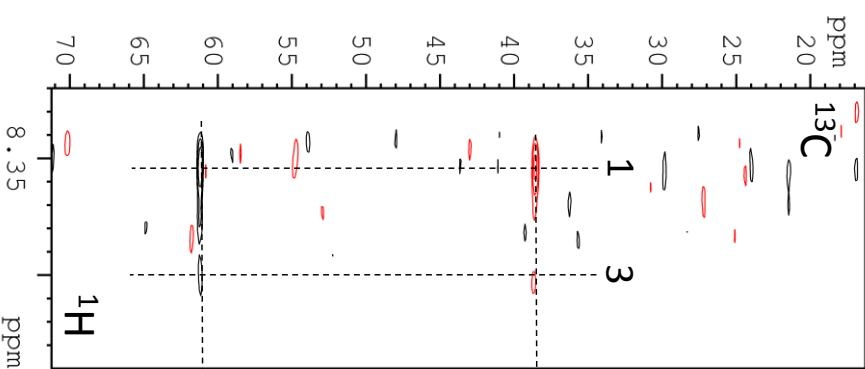
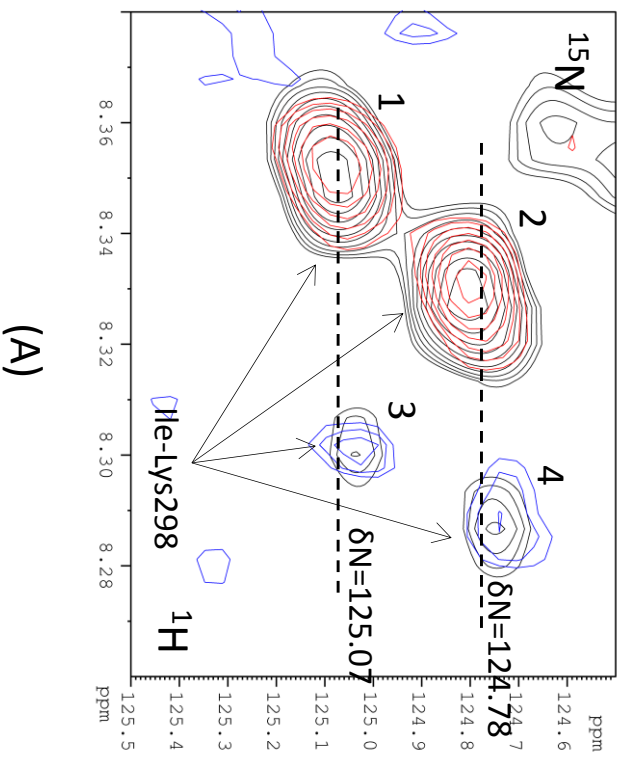
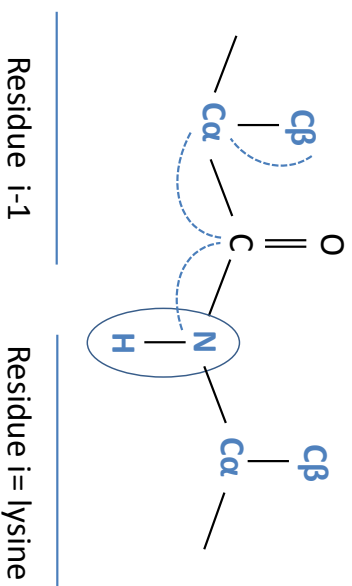
Description of HN(CO)CACB spectrum



(B)

Figure 16:

Description of HN(CO)CACB spectrum



(B)

References

- Abraha, A. et al., 2000. C-terminal inhibition of tau assembly in vitro and in Alzheimer's disease. *Journal of cell science*, 113(21), pp.3737–3745.
- Allen, B. et al., 2002. Abundant tau filaments and nonapoptotic neurodegeneration in transgenic mice expressing human P301S tau protein. *The Journal of neuroscience : the official journal of the Society for Neuroscience*, 22(21), pp.9340–9351.
- Alonso, a C. et al., 1994. Role of abnormally phosphorylated tau in the breakdown of microtubules in Alzheimer disease. *Proceedings of the National Academy of Sciences of the United States of America*, 91(12), pp.5562–5566.
- Alonso, A.D.C. et al., 2001. Hyperphosphorylation induces self-assembly of tau into tangles of paired helical filaments/straight filaments. *Proceedings of the National Academy of Sciences of the United States of America*, 98(12), pp.6923–8.
- Alonso, A.D.C. et al., 2004. Promotion of hyperphosphorylation by frontotemporal dementia tau mutations. *Journal of Biological Chemistry*, 279(33), pp.34873–34881.
- Alvarez, G. et al., 2012. Herpes simplex virus type 1 induces nuclear accumulation of hyperphosphorylated tau in neuronal cells. *J Neurosci Res*, 90(5), pp.1020–1029.
- Amniai, L. et al., 2009. Alzheimer disease specific phosphoepitopes of Tau interfere with assembly of tubulin but not binding to microtubules. *FASEB J*, 23, pp.1146–52.
- Amniai, L. et al., 2009. Alzheimer disease specific phosphoepitopes of Tau interfere with assembly of tubulin but not binding to microtubules. *The FASEB journal : official publication of the Federation of American Societies for Experimental Biology*, 23(4), pp.1146–1152.
- Anderson, N. et al., 1990. Requirement for integration of signals from two distinct phosphorylation pathways for activation of MAP kinase. *Letters To Nature*, 346, pp.183–187.
- Anderson, N.G. et al., 1990. Requirement for integration of signals from two distinct phosphorylation pathways for activation of MAP kinase. *Nature*, 343, pp.651–3.
- Andreadis, a, Broderick, J. a & Kosik, K.S., 1995. Relative exon affinities and suboptimal splice site signals lead to non-equivalence of two cassette exons. *Nucleic acids research*, 23(17), pp.3585–3593.
- Andreadis, a, Brown, W.M. & Kosik, K.S., 1992. Structure and novel exons of the human tau gene. *Biochemistry*, 31(43), pp.10626–10633.
- Aplin, a E. et al., 1996. In vitro phosphorylation of the cytoplasmic domain of the amyloid precursor protein by glycogen synthase kinase-3beta. *Journal of neurochemistry*, 67, pp.699–707.
- Arendt, T. et al., 1995. Increased expression and subcellular translocation of the mitogen activated protein kinase kinase and mitogen-activated protein kinase in Alzheimer's Disease. *Neuroscience*, 68(1), pp.5–18.
- Armstrong, R. a, 2009. The molecular biology of senile plaques and neurofibrillary tangles in Alzheimer's disease. *Folia neuropathologica / Association of Polish Neuropathologists and Medical Research Centre, Polish Academy of Sciences*, 47(4), pp.289–299.

- Arron, J.R. et al., 2006. NFAT dysregulation by increased dosage of DSCR1 and DYRK1A on chromosome 21. *Nature*, 441, pp.595–600.
- Augustinack, J.C. et al., 2002. Specific tau phosphorylation sites correlate with severity of neuronal cytopathology in Alzheimer's disease. *Acta neuropathologica*, 103(1), pp.26–35.
- Bagnoli, S. et al., 2004. Tau Gene delN296 Mutation , Parkinson ' s Disease. *Ann Neurol*, 55(3), p.448.
- Bandyopadhyay, B. et al., 2007. Tau aggregation and toxicity in a cell culture model of tauopathy. *Journal of Biological Chemistry*, 282(22), pp.16454–16464.
- Bardwell, a J., Frankson, E. & Bardwell, L., 2009. Selectivity of docking sites in MAPK kinases. *The Journal of biological chemistry*, 284(19), pp.13165–73.
- Bardwell, L. & Thorner, J., 1996. A conserved motif at the amino termini of MEKs might mediate high-affinity interaction with the cognate MAPKs. *Trends Biochem Sci*, 21(10), pp.373–374.
- Barghorn, S. et al., 2000. Structure, microtubule interactions, and paired helical filament aggregation by tau mutants of frontotemporal dementias. *Biochemistry*, 39, pp.11714–11721.
- Benneceb, M. et al., 2001. Inhibition of PP-2A upregulates CaMKII in rat forebrain and induces hyperphosphorylation of tau at Ser 262/356. *FEBS Letters*, 490, pp.15–22.
- Von Bergen, M. et al., 2000. Assembly of tau protein into Alzheimer paired helical filaments depends on a local sequence motif ((306)VQIVYK(311)) forming beta structure. *Proceedings of the National Academy of Sciences of the United States of America*, 97(10), pp.5129–5134.
- Von Bergen, M. et al., 2001. Mutations of Tau Protein in Frontotemporal Dementia Promote aggregation of paired helical filaments by enhancing local beta-structure. *Journal of Biological Chemistry*, 276, pp.48165–48174.
- Von Bergen, M. et al., 2006. Spectroscopic approaches to the conformation of tau protein in solution and in paired helical filaments . *Neurodegener Dis.*, 3(4-5), pp.197–206.
- Von Bergen, M. et al., 2005. Tau aggregation is driven by a transition from random coil to beta sheet structure. *Biochimica et Biophysica Acta - Molecular Basis of Disease*, 1739, pp.158–166.
- Berger, Z. et al., 2007. Accumulation of pathological tau species and memory loss in a conditional model of tauopathy. *The Journal of neuroscience : the official journal of the Society for Neuroscience*, 27(14), pp.3650–3662.
- Bhaskar, K., Yen, S.H. & Lee, G., 2005. Disease-related modifications in tau affect the interaction between Fyn and tau. *Journal of Biological Chemistry*, 280(42), pp.35119–35125.
- Bhat, R. V., Budd Haeberlein, S.L. & Avila, J., 2004. Glycogen synthase kinase 3: A drug target for CNS therapies. *Journal of Neurochemistry*, 89, pp.1313–1317.
- Bhattacharya, K. et al., 2001. Role of Cysteine-291 and Cysteine-322 in the Polymerization of Human Tau into Alzheimer-like Filaments. *Biochemical and Biophysical Research Communications*, 285, pp.20–26.

- Bhattacharyya, R.P. et al., 2006. Domains , Motifs , and Scaffolds : The Role of Modular Interactions in the Evolution and Wiring of Cell Signaling Circuits. *Annu. Rev. Biochem.*, 75, pp.655–80.
- Bibow, S. et al., 2014. Predictive Atomic Resolution Descriptions of Intrinsically Disordered hTau40 and a -Synuclein in Solution from NMR and Small Angle Scattering. *Cell*, 22, pp.238–249.
- Bibow, S. et al., 2011. Structural Impact of Proline-Directed Pseudophosphorylation at AT8, AT100, and PHF1 Epitopes on 441-Residue Tau. *Journal of the American Chemical Society*, 133(40), pp.15842–15845.
- Bienkiewicz, E. a & Lumb, K.J., 1999. Random-coil chemical shifts of phosphorylated amino acids. *Journal of biomolecular NMR*, 15(3), pp.203–206.
- Biernat, J. et al., 1992. The switch of tau protein to an Alzheimer-like state includes the phosphorylation of two serine-proline motifs upstream of the microtubule binding region. *The EMBO journal*, 11(4), pp.1593–7.
- Blair, L.J. et al., 2015. The emerging role of peptidyl-prolyl isomerase chaperones in tau oligomerization, amyloid processing, and Alzheimer's disease. *Journal of Neurochemistry*, 133, pp.1–13.
- Blanchard, B. et al., 1994. Hyperphosphorylation of Human TAU by Brain Kinase PK40erk beyond Phosphorylation by cAMP-dependent PKA: Relation to Alzheimer's Disease. *Biochemical and Biophysical Research Communications*, 200(1), pp.187–194.
- Boulton, T.G. et al., 1990. An insulin-stimulated protein kinase similar to yeast kinases involved in cell cycle control. *Science*, 249, pp.64–7.
- Braak, H. et al., 2006. Staging of Alzheimer disease-associated neurofibrillary pathology using paraffin sections and immunocytochemistry. *Acta Neuropathologica*, 112, pp.389–404.
- Braak, H., Braak, E. & Bohl, J., 1993. Staging of Alzheimer Related Cortical Destruction. *European Neurology*, 33(6), pp.403–408.
- Bramblett, G.T. et al., 1993. Abnormal tau phosphorylation at Ser396 in Alzheimer's disease recapitulates development and contributes to reduced microtubule binding. *Neuron*, 10(6), pp.1089–1099.
- Brion, J. et al., 1985. Neurofibrillary tangles of Alzheimer ' s disease : an immunohistochemical study . *J.submicrosc Cytol*, 17(1), pp.89–96.
- Brunet, a & Pouyssegur, J., 1996. Identification of MAP kinase domains by redirecting stress signals into growth factor responses. *Science (New York, N.Y.)*, 272(5268), pp.1652–1655.
- Buée, L. et al., 2000. Tau protein isoforms, phosphorylation and role in neurodegenerative disorders. *Brain Research Reviews*, 33(1), pp.95–130.
- Burns, A. & Liffie, S., 2009. Alzheimer ' s disease. *British Medical Journal*, 338, p.158.

- Caffrey, D.R., O'Neill, L. a & Shields, D.C., 1999. The evolution of the MAP kinase pathways: coduplication of interacting proteins leads to new signaling cascades. *Journal of molecular evolution*, 49(5), pp.567–582.
- Callaway, K. et al., 2007. The anti-apoptotic protein PEA-15 is a tight binding inhibitor of ERK1 and ERK2, which blocks docking interactions at the D-recruitment site. *Biochemistry*, 46(32), pp.9187–9198.
- Callaway, K., Rainey, M. a. & Dalby, K.N., 2005. Quantifying ERK2-protein interactions by fluorescence anisotropy: PEA-15 inhibits ERK2 by blocking the binding of DEJL domains. *Biochimica et Biophysica Acta - Proteins and Proteomics*, 1754(1-2), pp.316–323.
- Camero, S. et al., 2014. Thermodynamics of the interaction between Alzheimer's disease related tau protein and DNA. *PloS one*, 9(8), p.e104690.
- Camps, M. et al., 1998. Catalytic activation of the phosphatase MKP-3 by ERK2 mitogen-activated protein kinase. *Science (New York, N.Y.)*, 280, pp.1262–1265.
- Carlyle, B.C. et al., 2014. cAMP-PKA phosphorylation of tau confers risk for degeneration in aging association cortex. *Proceedings of the National Academy of Sciences of the United States of America*, 111(13), pp.5036–41.
- Cavallini, A. et al., 2013. An unbiased approach to identifying tau kinases that phosphorylate tau at sites associated with alzheimer disease. *Journal of Biological Chemistry*, 288(32), pp.23331–23347.
- Cha, H. & Shapiro, P., 2001. Tyrosine-Phosphorylated Extracellular Signal-Regulated Kinase Associates with the Golgi Complex during G2/M Phase of the Cell Cycle. *The Journal of cell biology*, 153(7), pp.1355–1368.
- Chambraud, B. et al., 2010. A role for FKBP52 in Tau protein function. *Proceedings of the National Academy of Sciences*, 107(6), pp.2658–2663.
- Chang, E. et al., 2012. pathogenic missense MAPT mutations differentially modulate tau aggregation propensity at nucleation and extension steps. *J Neurochem*, 29(4), pp.997–1003.
- Chen, J. et al., 1992. Projection domains of MAP2 and tau determine spacings between microtubules in dendrites and axons . *Nature*, 360(6405), pp.674–677.
- Chin, J. et al., 2005. Fyn kinase induces synaptic and cognitive impairments in a transgenic mouse model of Alzheimer's disease. *The Journal of neuroscience : the official journal of the Society for Neuroscience*, 25(42), pp.9694–9703.
- Chiti, F. & Dobson, C.M., 2006. Protein misfolding, functional amyloid, and human disease. *Annual review of biochemistry*, 75, pp.333–366.
- Chouraki, V. & Seshadri, S., 2014. Genetics of Alzheimer's Disease. *Advances in Genetics*, 87, pp.245–294.
- Chow, H.-M. et al., 2014. CDK5 activator protein p25 preferentially binds and activates GSK3β. *Proceedings of the National Academy of Sciences of the United States of America*, pp.1–9.

- Chris Gamblin, T. et al., 2000. In vitro polymerization of tau protein monitored by laser light scattering: Method and application to the study of FTDP-17 mutants. *Biochemistry*, 39, pp.6136–6144.
- Citron, M. et al., 1992. Mutation of the beta-amyloid precursor protein in familial Alzheimer's disease increases beta-protein production. *Nature*, 360(6405), pp.672–674.
- Clark, L.N. et al., 1998. Pathogenic implications of mutations in the tau gene in pallido-ponto-nigral degeneration and related neurodegenerative disorders linked to chromosome 17. *Proceedings of the National Academy of Sciences*, 95, pp.13103–13107.
- Clavaguera, F. et al., 2013. Brain homogenates from human tauopathies induce tau inclusions in mouse brain. *Proceedings of the National Academy of Sciences of the United States of America*, 110(23), pp.9535–40.
- Clavaguera, F., Grueninger, F. & Tolnay, M., 2014. Intercellular transfer of tau aggregates and spreading of tau pathology: Implications for therapeutic strategies. *Neuropharmacology*, 76, Part A, pp.9–15.
- Cohen, P., 1979. The hormonal control of glycogen metabolism in mammalian muscle by multivalent phosphorylation. *Biochemical Society transactions*, 7, pp.459–480.
- Cohen, P. & Goedert, M., 2004. GSK3 inhibitors: development and therapeutic potential. *Nature reviews. Drug discovery*, 3(6), pp.479–487.
- Cohen, T.J. et al., 2011. The acetylation of tau inhibits its function and promotes pathological tau aggregation. *Nat Commun*, 2, p.252.
- Cole, S.L. & Vassar, R., 2008. BACE1 structure and function in health and Alzheimer's disease. *Current Alzheimer research*, 5(2), pp.100–120.
- Cruchaga, C. et al., 2014. Rare coding variants in Phospholipase D3 (PLD3) confer risk for Alzheimer's disease. *Nature*, 505(7484), pp.550–554.
- Cuenda, A. & Rousseau, S., 2007. p38 MAP-kinases pathway regulation, function and role in human diseases. *Biochimica et biophysica acta*, 1773, pp.1358–1375.
- Daebel, V. et al., 2012. β - Sheet Core of Tau Paired Helical Filaments Revealed by Solid-State. *JACS*, 134, pp.13982–13989.
- Davis, R., 1993. The mitogen-activated protein kinase signal transduction pathway. *J. Biol. Chem.*, 268, pp.14553–14556.
- Dixit, R. et al., 2008. Differential regulation of dynein and kinesin motor proteins by tau. *Science*, 319(5866), pp.1086–1089.
- Drechsel, D.N. et al., 1992. Modulation of the Dynamic Instability of Tubulin Assembly by the Microtubule-Associated Protein Tau. *Molecular Biology of the Cell*, 3, pp.1141–1154.
- Drewes, G. et al., 1997. MARK, a novel family of protein kinases that phosphorylate microtubule-associated proteins and trigger microtubule disruption. *Cell*, 89, pp.297–308.

- Drewes, G. et al., 1992. Mitogen activated protein (MAP) kinase transforms tau protein into an Alzheimer-like state. *The EMBO journal*, 11(6), pp.2131–2138.
- Feldman, H.H. & Woodward, M., 2005. The staging and assessment of moderate to severe Alzheimer disease. *Neurology*, 65(Issue 6, Supplement 3), pp.S10–S17.
- Ferrer, I. et al., 2001. Phosphorylated map kinase (ERK1, ERK2) expression is associated with early tau deposition in neurones and glial cells, but not with increased nuclear DNA vulnerability and cell death, in Alzheimer disease, Pick's disease, progressive supranuclear palsy an. *Brain pathology (Zurich, Switzerland)*, 11(2), pp.144–158.
- Ferrer, I. et al., 2001. Phosphorylated mitogen - activated protein kinase (MAPK / ERK - P), protein kinase of 38 kDa (p38 - P), stress - activated protein kinase (SAPK / JNK - P), and calcium / calmodulin - dependent kinase II (CaM kinase II) are differentially expressed. *J Neural Transm*, 108(12), pp.1397–415.
- Fischer, D. et al., 2007. Structural and microtubule binding properties of tau mutants of frontotemporal dementias. *Biochemistry*, 46, pp.2574–2582.
- Fontaine, S.N. et al., 2015. Cellular factors modulating the mechanism of tau protein aggregation. *Cellular and Molecular Life Sciences*, 72(10), pp.1863–79.
- Formstecher, E. et al., 2001. PEA-15 Mediates Cytoplasmic Sequestration of ERK MAP Kinase. *Developmental Cell*, 1(2), pp.239–250.
- Frost, D. et al., 2011. β -Carboline Compounds, Including Harmine, Inhibit DYRK1A and Tau Phosphorylation at Multiple Alzheimer's Disease-Related Sites E. M. C. Skoulakis, ed. *PLoS ONE*, 6(5), p.e19264.
- Fukumoto, H. et al., 2004. Beta-secretase activity increases with aging in human, monkey, and mouse brain. *The American journal of pathology*, 164(2), pp.719–725.
- Fukumoto, H. et al., 2002. Beta-secretase protein and activity are increased in the neocortex in Alzheimer disease. *Archives of neurology*, 59(9), pp.1381–1389.
- Fulga, T. a et al., 2007. Abnormal bundling and accumulation of F-actin mediates tau-induced neuronal degeneration in vivo. *Nature cell biology*, 9(2), pp.139–148.
- Funk, K.E. et al., 2014. Lysine methylation is an endogenous post-translational modification of tau protein in human brain and a modulator of aggregation propensity. *Biochem J.*, 462(1), pp.77–88.
- Futran, A. et al., 2013. ERK as a model for systems biology of enzyme kinetics in cells. *Curr Biol*, 23(21), pp.R972–R979.
- Gamblin, T.C. et al., 2000. Oxidative regulation of fatty acid-induced tau polymerization. *Biochemistry*, 39, pp.14203–14210.
- Games, D. et al., 1995. Alzheimer-type neuropathology in transgenic mice overexpressing V717F beta-amyloid precursor protein. *Nature*, 373(6514), pp.523–527.

- Gandhi, N. et al., 2015. A Phosphorylation - Induced Turn Defines the Alzheimer ' s Disease AT8 Antibody Epitope on the Tau Protein . *Angew Chem Int Ed Engl.*, 54(23), pp.6819–23.
- Garai, Á. et al., 2013. Specificity of Linear Motifs That Bind to a Common Mitogen- Activated Protein Kinase Docking Groove. *Sci Signal*, 5(245), pp.1–28.
- Gilmore, E.C. et al., 1998. Cyclin-dependent kinase 5-deficient mice demonstrate novel developmental arrest in cerebral cortex. *The Journal of neuroscience : the official journal of the Society for Neuroscience*, 18(16), pp.6370–6377.
- Giustiniani, J. et al., 2014. Immunophilin FKBP52 induces Tau-P301L filamentous assembly in vitro and modulates its activity in a model of tauopathy. *Proceedings of the National Academy of Sciences of the United States of America*, 111, pp.4584–9.
- Goedert, M. et al., 1996. Assembly of microtubule-associated protein tau into Alzheimer-like filaments induced by sulphated glycosaminoglycans. *Nature*, 383(10), pp.550–553.
- Goedert, M. et al., 1989. Multiple Isoforms of Human Microtubule-Associated Protein Tau : Sequences and localization in Neurofibrillary Tangles of Alzheimer ' s Disease is found. *Neuron*, 3, pp.519–526.
- Goedert, M., 2005. Tau gene mutations and their effects. *Movement Disorders*, 20, pp.S45–S52.
- Goedert, M. et al., 1993. The abnormal phosphorylation of tau protein at Ser-202 in Alzheimer disease recapitulates phosphorylation during development. *Neurobiology*, 90, pp.5066–5070.
- Goedert, M. et al., 1993. The abnormal phosphorylation of tau protein at Ser-202 in Alzheimer disease recapitulates phosphorylation during development. *Proc Natl Acad Sci U S A*, 90, pp.5066–70.
- Goedert, M., Clavaguera, F. & Tolnay, M., 2010. The propagation of prion-like protein inclusions in neurodegenerative diseases. *Trends in Neurosciences*, 33(7), pp.317–325.
- Goedert, M. & Jakes, R., 1990. Expression of separate isoforms of human tau protein: correlation with the tau pattern in brain and effects on tubulin polymerization. *The EMBO journal*, 9(13), pp.4225–4230.
- Goldgaber, D. et al., 1987. Characterization and chromosomal localization of a cDNA encoding brain amyloid of Alzheimer's disease. *Science*, 235(4791), pp.877–880.
- Goode, B.L. & Feinstein, S.C., 1994. Identification of a novel microtubule binding and assembly domain in the developmentally regulated inter-repeat region of tau. *Journal of Cell Biology*, 124(5), pp.769–781.
- Grant, P., Sharma, P. & Pant, H.C., 2001. Cyclin-dependent protein kinase 5 (Cdk5) and the regulation of neurofilament metabolism. *European Journal of Biochemistry*, 268, pp.1534–1546.
- Grueninger, F. et al., 2011. Novel screening cascade identifies MKK4 as key kinase regulating Tau phosphorylation at Ser422. *Molecular and Cellular Biochemistry*, 357(1-2), pp.199–207.

- Grundke-Iqba, I. et al., 1986. Microtubule-associated protein tau. A component of Alzheimer paired helical filaments. *Journal of Biological Chemistry*, 261(13), pp.6084–6089.
- Grundke-Iqbal, I. et al., 1986. Abnormal phosphorylation of the microtubule-associated protein tau (tau) in Alzheimer cytoskeletal pathology. *Proceedings of the National Academy of Sciences of the United States of America*, 83, pp.4913–4917.
- Haass, C. & Mandelkow, E., 2010. Fyn-tau-amyloid: A toxic triad. *Cell*, 142(3), pp.356–358.
- Hahn, B. et al., 2013. Cellular ERK Phospho-Form Profiles with Conserved Preference for a Switch-Like Pattern. *Journal of proteome research*, 12, pp.637–646.
- Han, D. et al., 2009. Familial FTDP-17 missense mutations inhibit microtubule assembly-promoting activity of tau by increasing phosphorylation at Ser202 in vitro. *Journal of Biological Chemistry*, 284(20), pp.13422–13433.
- Hancock, C.N. et al., 2005. Identification of novel extracellular signal-regulated kinase docking domain inhibitors. *Journal of medicinal chemistry*, 48(14), pp.4586–95.
- Hanger, D.P. et al., 2002. New Phosphorylation Sites Identified in Hyperphosphorylated Tau (Paired Helical Filament-Tau) from Alzheimer's Disease Brain Using Nanoelectrospray Mass Spectrometry. *Journal of Neurochemistry*, 71(6), pp.2465–2476.
- Hardy, J. a & Higgins, G. a, 1992. Alzheimer's disease: the amyloid cascade hypothesis. *Science*, 256(5054), pp.184–185.
- Hardy, J. & Allsop, D., 1991. Amyloid Deposition As the Central Event in the Etiology of Alzheimers-Disease. *Trends in Pharmacological Sciences*, 12(10), pp.383–388.
- Hasegawa, M. et al., 1992. Protein sequence and mass spectrometric analyses of tau in the Alzheimer's disease brain. *The Journal of biological chemistry*, 267(24), pp.17047–17054.
- He, H.J. et al., 2009. The proline-rich domain of tau plays a role in interactions with actin. *BMC cell biology*, 10, p.81.
- Hibi, M. et al., 1993. Identification of an oncoprotein-responsive and UV-responsive protein-kinase that binds and potentiates the c-Jun activation domain. *Genes & Development*, 7, pp.2135–2148.
- Hirokawa, N., Shiomura, Y. & Okabe, S., 1988. Tau proteins: the molecular structure and mode of binding on microtubules. *Journal of Cell Biology*, 107, pp.1449–1459.
- Hogg, M. et al., 2003. The L266V tau mutation is associated with frontotemporal dementia and Pick-like 3R and 4R tauopathy. *Acta Neuropathologica*, 106, pp.323–336.
- Holland, P.M. & Cooper, J.A., 1999. Protein modification : Docking sites for kinases. *Current Biology*, 9, pp.329–331.
- Holmes, B.B. et al., 2013. Heparan sulfate proteoglycans mediate internalization and propagation of specific proteopathic seeds. *Proceedings of the National Academy of Sciences of the United States of America*, 110(33), pp.E3138–47.

- Holsinger, R.M.D. et al., 2002. Increased expression of the amyloid precursor B-secretase in Alzheimer's Disease. *Annals of Neurology*, 51(6), pp.783–6.
- Hong, M. et al., 1997. Lithium reduces tau phosphorylation by inhibition of glycogen synthase kinase-3. *Journal of Biological Chemistry*, 272(40), pp.25326–25332.
- Hong, M. et al., 1998. Mutation - specific functional impairments in distinct tau isoforms of hereditary FTDP -. *Science*, 282(5395), pp.1914–7.
- Hongtao, Y. et al., 1994. Structural basis for the binding of proline-rich peptides to SH3 domains. *Cell*, 76, pp.933–945.
- Huey, E. et al., 2006. Characteristics of Frontotemporal Dementia Patients with a Progranulin Mutation. *Ann Neurol*, 60(3), pp.374–380.
- Hunter, T., 2007. The Age of Crosstalk: Phosphorylation, Ubiquitination, and Beyond. *Molecular Cell*, 28, pp.730–738.
- Huvent, I. et al., 2014. A functional fragment of Tau forms fibers without the need for an intermolecular cysteine bridge. *Biochemical and Biophysical Research Communications*, 445(2), pp.299–303.
- Hwang, S.C. et al., 1996. Activation of phospholipase C-gamma by the concerted action of tau proteins and arachidonic acid. *The Journal of biological chemistry*, 271(31), pp.18342–18349.
- Hyman, B.T., 2014. Tau propagation, different tau phenotypes, and prion-like properties of tau. *Neuron*, 82(6), pp.1189–1190.
- Iba, M. et al., 2013. Synthetic Tau Fibrils Mediate Transmission of Neurofibrillary Tangles in a Transgenic Mouse Model of Alzheimer's-like Tauopathy. *The Journal of Neuroscience*, 33(3), pp.1024–1037.
- Illenberger, S. et al., 1996. Phosphorylation of Microtubule-associated Proteins MAP2 and MAP4 by the Protein Kinase p110 mark. *Journal of Biological Chemistry*, 271(18), pp.10834–10843.
- Iqbal, K. et al., 2009. Mechanisms of tau-induced neurodegeneration. *Acta Neuropathol*, 118(1), pp.53–69.
- Iqbal, K. et al., 2010. Tau in Alzheimer disease and related tauopathies. *Current Alzheimer research*, 7(8), pp.656–664.
- Iqbal, K., Gong, C.X. & Liu, F., 2013. Hyperphosphorylation-induced tau oligomers. *Frontiers in Neurology*, 4(112), pp.1–9.
- Ishiguro, K. et al., 1993. Glycogen synthase kinase 3 beta is identical to tau protein kinase I generating several epitopes of paired helical filaments. *FEBS letters*, 325(3), pp.167–172.
- Ittner, L.M. et al., 2010. Dendritic function of tau mediates amyloid- β toxicity in alzheimer's disease mouse models. *Cell*, 142(3), pp.387–397.

- Jacobs, D. et al., 1999. Multiple docking sites on substrate proteins form a modular system that mediates recognition by ERK MAP kinase. *Genes & Development*, 13(2), pp.163–175.
- Jaworski, T. et al., 2011. GSK-3 α/β kinases and amyloid production in vivo. *Nature*, 480(7376), pp.E4–E5.
- Jeffrey, P.D. et al., 1995. Mechanism of CDK activation revealed by the structure of a cyclinA-CDK2 complex. *Nature*, 376, pp.313–320.
- Jeganathan, S. et al., 2006. Global hairpin folding of tau in solution. *Biochemistry*, 45, pp.2283–2293.
- Jeganathan, S. et al., 2008. Proline-directed Pseudo-phosphorylation at AT8 and PHF1 Epitopes Induces a Compaction of the Paperclip Folding of Tau and Generates a Pathological (MC-1) Conformation. *Journal of Biological Chemistry*, 283(46), pp.32066–32076.
- Jicha, G.A. et al., 1997. Alz-50 and MC-1 , a New Monoclonal Antibody Raised to Paired Helical Filaments , Recognize Conformational Epitopes on Recombinant Tau. *Journal of neuroscience research*, 48, pp.128–132.
- Jin, S.C. et al., 2014. Coding variants in TREM2 increase risk for Alzheimer’s disease. *Human molecular genetics*, 23(21), pp.1–9.
- Johnson, G.L. & Nakamura, K., 2007. The c-jun kinase/stress-activated pathway: regulation, function and role in human disease. *Biochimica et biophysica acta*, 1773(8), pp.1341–1348.
- Johnson, G.V.W. & Stoothoff, W.H., 2004. Tau phosphorylation in neuronal cell function and dysfunction. *Journal of cell science*, 117, pp.5721–5729.
- Kallunki, T. et al., 1994. JNK2 contains a specificity-determining region responsible for efficient c-Jun binding and phosphorylation. *Genes and Development*, 8, pp.2996–3007.
- Kamah, A. et al., 2014. Nuclear magnetic resonance analysis of the acetylation pattern of the neuronal Tau protein. *Biochemistry*, 53, pp.3020–32.
- Kampers, T. et al., 1996. RNA stimulates aggregation of microtubule-associated protein tau into Alzheimer-like paired helical filaments. *FEBS Letters*, 399, pp.344–349.
- Kane, M.D. et al., 2000. Evidence for seeding of beta -amyloid by intracerebral infusion of Alzheimer brain extracts in beta -amyloid precursor protein-transgenic mice. *The Journal of neuroscience : the official journal of the Society for Neuroscience*, 20(10), pp.3606–3611.
- Kempf, M. et al., 1996. Tau binds to the distal axon early in development of polarity in a microtubule- and microfilament-dependent manner. *The Journal of neuroscience : the official journal of the Society for Neuroscience*, 16(18), pp.5583–5592.
- Keshet, Y. & Seger, R., 2010. The MAP Kinase Signaling Cascades: A System of Hundreds of Components Regulates a Diverse Array of Physiological Functions. *Methods in molecular biology Springer Science*, 661, pp.433–447.
- Kfoury, N. et al., 2012. Trans-cellular propagation of Tau aggregation by fibrillar species. *Journal of Biological Chemistry*, 287(23), pp.19440–19451.

- Kinoshita, T. et al., 2008. Crystal structure of human mono-phosphorylated ERK1 at Tyr204. *Biochemical and Biophysical Research Communications*, 377(4), pp.1123–1127.
- Kinoshita, T. et al., 2008. Crystal structure of human mono-phosphorylated ERK1 at Tyr204. *Biochemical and Biophysical Research Communications*, 377(4), pp.1123–1127.
- Kobayashi, T. et al., 2002. A Novel L266V Mutation of the Tau Gene Causes Frontotemporal Dementia with a Unique Tau Pathology. , pp.133–137.
- Kolarova, M. et al., 2012. Structure and Pathology of Tau Protein in Alzheimer Disease. *international Journal of Alzheimer's Disease*, 2012.
- Kopke, E. et al., 1993. Microtubule-associated protein tau. Abnormal phosphorylation of a non-paired helical filament pool in Alzheimer disease. *Journal of Biological Chemistry*, 268(18), pp.24374–24384.
- Kosik, K.S. et al., 1989. Developmentally regulated expression of specific tau sequences. *Neuron*, 2(4), pp.1389–1397.
- Kragelj, J. et al., 2015. Structure and dynamics of the MKK7–JNK signaling complex. *Proceedings of the National Academy of Sciences*, 112(11), pp.3409–3414.
- Kusakawa, G.I. et al., 2000. Calpain-dependent proteolytic cleavage of the p35 cyclin-dependent kinase 5 activator to p25. *Journal of Biological Chemistry*, 275(22), pp.17166–17172.
- Lalonde, R. et al., 2002. Spatial learning, exploration, anxiety, and motor coordination in female APP23 transgenic mice with the Swedish mutation. *Brain Research*, 956(1), pp.36–44.
- Landrieu, I. et al., 2011. Molecular implication of PP2A and Pin1 in the Alzheimer's disease specific hyperphosphorylation of Tau. *PloS one*, 6(6), p.e21521.
- Landrieu, I. et al., 2006. NMR analysis of a Tau phosphorylation pattern. *Journal of the American Chemical Society*, 128(11), pp.3575–3583.
- Landrieu, I. et al., 2006. NMR analysis of a Tau phosphorylation pattern. *J Am Chem Soc*, 128, pp.3575–83.
- Laurén, J. et al., 2009. Cellular prion protein mediates impairment of synaptic plasticity by amyloid-beta oligomers. *Nature*, 457(7233), pp.1128–1132.
- Lawrence, M.C. et al., 2008. The roles of MAPKs in disease. *Cell research*, 18(4), pp.436–442.
- Lee, G. et al., 2004. Phosphorylation of tau by fyn: implications for Alzheimer's disease. *The Journal of neuroscience : the official journal of the Society for Neuroscience*, 24(9), pp.2304–2312.
- Lee, G. et al., 1998. Tau interacts with src-family non-receptor tyrosine kinases. *Journal of cell science*, 111, pp.3167–3177.
- Lee, G., Cowan, N. & Kirschner, M., 1988. The primary structure and heterogeneity of tau protein from mouse brain. *Science (New York, N.Y.)*, 239(9), pp.285–288.

- Lee, M.S. et al., 2000. Neurotoxicity induces cleavage of p35 to p25 by calpain. *Nature*, 405, pp.360–364.
- Lee, T. et al., 2004. Docking motif interactions in Map kinases revealed by hydrogen exchange mass spectrometry. *Molecular Cell*, 14, pp.43–55.
- Lee, V.M. et al., 1991. A68: a major subunit of paired helical filaments and derivatized forms of normal Tau. *Science (New York, N.Y.)*, 251, pp.675–678.
- Lee, V.M., Goedert, M. & Trojanowski, J.Q., 2001. Neurodegenerative auopathies. *Annu. Rev. Neurosci*, 24, pp.1121–1159.
- Leroy, A. et al., 2010. Spectroscopic studies of GSK3{beta} phosphorylation of the neuronal tau protein and its interaction with the N-terminal domain of apolipoprotein E. *The Journal of biological chemistry*, 285(43), pp.33435–33444.
- Levy-Lahad, E. et al., 1995. A familial Alzheimer’s disease locus on chromosome 1. *Science*, 269(5226), pp.970–973.
- Lewis, J. et al., 2000. Neurofibrillary tangles, amyotrophy and progressive motor disturbance in mice expressing mutant (P301L) tau protein. *Nature genetics*, 25, pp.402–405.
- Lippens, G. et al., 2004. Proline-directed random-coil chemical shift values as a tool for the NMR assignment of the tau phosphorylation sites. *Chembiochem*, 5, pp.73–8.
- Liu, F. et al., 2005. Contributions of protein phosphatases PP1, PP2A, PP2B and PP5 to the regulation of tau phosphorylation. *European Journal of Neuroscience*, 22, pp.1942–1950.
- Liu, S. et al., 2006. Structural basis of docking interactions between ERK2 and MAP kinase phosphatase 3. *Proceedings of the National Academy of Sciences of the United States of America*, 103, pp.5326–5331.
- Lossos, A. et al., 2003. Frontotemporal dementia and parkinsonism with the P301S tau gene mutation in a Jewish family. *Journal of Neurology*, 250, pp.733–740.
- Lott, I.T. & Head, E., 2005. Alzheimer disease and Down syndrome: Factors in pathogenesis. *Neurobiology of Aging*, 26(3), pp.383–389.
- Louis, J. V et al., 2011. Mice lacking phosphatase PP2A subunit PR61/B’delta (Ppp2r5d) develop spatially restricted tauopathy by deregulation of CDK5 and GSK3beta. *Proceedings of the National Academy of Sciences of the United States of America*, 108(17), pp.6957–6962.
- Lovestone, S. et al., 1999. Lithium reduces tau phosphorylation: Effects in living cells and in neurons at therapeutic concentrations. *Biological Psychiatry*, 45, pp.995–1003.
- Lowe, E.D. et al., 2002. Specificity Determinants of Recruitment Peptides Bound to Phospho-CDK2 / Cyclin. *Biochemistry*, 41, pp.15625–15634.
- Lu, J. et al., 2013. Formaldehyde induces hyperphosphorylation and polymerization of Tau protein both in vitro and in vivo. *Biochimica et Biophysica Acta - General Subjects*, 1830(8), pp.4102–4116.

- Lu, Y. et al., 2013. Hyperphosphorylation results in tau dysfunction in DNA folding and protection. *Journal of Alzheimer's Disease*, 37(3), pp.551–563.
- Luna-Muñoz, J. et al., 2005. Regional conformational change involving phosphorylation of tau protein at the Thr231, precedes the structural change detected by Alz-50 antibody in Alzheimer's disease. *Journal of Alzheimer's disease : JAD*, 8, pp.29–41.
- Mace, P.D. et al., 2013. Structure of ERK2 bound to PEA-15 reveals a mechanism for rapid release of activated MAPK. *Nature communications*, 4(1681).
- Maeda, S. et al., 2007. Granular tau oligomers as intermediates of tau filaments. *Biochemistry*, 46(12), pp.3856–3861.
- Mandelkow, E.M. et al., 1995. Tau domains, phosphorylation, and interactions with microtubules. *Neurobiology of aging*, 16(3), pp.355–362.
- Mansour, S.J. et al., 1994. Transformation of mammalian cells by constitutively active MAP kinase kinase. *Science*, 265, pp.966–70.
- Martin, L. et al., 2013. Tau protein kinases: involvement in Alzheimer's disease. *Ageing Res Rev*, 12, pp.289–309.
- Matus, a., 1994. Stiff microtubules and neuronal morphology. *Trends in Neurosciences*, 17(1), pp.19–22.
- Mazanetz, M.P. & Fischer, P.M., 2007. Untangling tau hyperphosphorylation in drug design for neurodegenerative diseases. *Nature Reviews Drug Discovery*, 6(6), pp.464–479.
- Medina, M. & Avila, J., 2014. The role of extracellular Tau in the spreading of neurofibrillary pathology. *Frontiers in cellular neuroscience*, 8(113).
- Meyer-Luehmann, M. et al., 2006. Exogenous Induction of Cerebral β -Amyloidogenesis Is Governed by Agent and Host.pdf. *Science*, 313, pp.1781–1784.
- Mietelska-Porowska, A. et al., 2014. Tau protein modifications and interactions: Their role in function and dysfunction. *International Journal of Molecular Sciences*, 15(3), pp.4671–4713.
- Miller, W.T., 2003. Determinants of substrate recognition in nonreceptor tyrosine kinases. *Acc Chem Res.*, 36(6), pp.393–400.
- Min, S.W. et al., 2010. Acetylation of tau inhibits its degradation and contributes to tauopathy. *Neuron*, 67, pp.953–66.
- Morgan, D.O., 1997. CYCLIN-DEPENDENT KINASES : Engines , Clocks , and Microprocessors. *Annual review Cell Dev. Biol.*, 13, pp.261–91.
- Morishima, Y. et al., 2001. Beta-amyloid induces neuronal apoptosis via a mechanism that involves the c-Jun N-terminal kinase pathway and the induction of Fas ligand. *The Journal of neuroscience*, 21(19), pp.7551–7560.

- Morishima-Kawashima, M. et al., 1995. Hyperphosphorylation of Tau in PHF. *Neurobiology of Aging*, 16(3), pp.365–380.
- Morishima-Kawashima, M. et al., 1995. Proline-directed and non-proline-directed phosphorylation of PHF-tau. *J Biol Chem*, 270, pp.823–9.
- Morris, H.R. et al., 2001. Effect of ApoE and tau on age of onset of progressive supranuclear palsy and multiple system atrophy. *Neuroscience Letters*, 312, pp.118–120.
- Morris, M. et al., 2015. Tau post-translational modifications in wild-type and human amyloid precursor protein transgenic mice. *Nature Neuroscience*, 18(8), pp.1183–9.
- Morris, M. et al., 2015. Tau post-translational modifications in wild-type and human amyloid precursor protein transgenic mice. *Nat Neurosci*, 18, pp.1183–9.
- Morris, M. et al., 2011. The many faces of Tau. *Neuron*, 70(3), pp.410–426.
- Mukrasch, M.D. et al., 2009. Structural polymorphism of 441-residue Tau at single residue resolution. *PLoS Biology*, 7(2), pp.0399–0414.
- Mukrasch, M.D. et al., 2009. Structural polymorphism of 441-residue tau at single residue resolution. *PLoS Biol*, 7, p.e34.
- Munoz, L. & Ammit, A.J., 2010. Targeting p38 MAPK pathway for the treatment of Alzheimer's disease. *Neuropharmacology*, 58(3), pp.561–568.
- Nacharaju, P. et al., 1999. Accelerated filament formation from tau protein with specific FTDP-17 missense mutations. *FEBS Letters*, 447, pp.195–199.
- Neumann, M. et al., 2005. Novel G335V mutation in the tau gene associated with early onset familial frontotemporal dementia. *Neurogenetics*, 6, pp.91–95.
- Neve, R.L. et al., 1986. Identification of cDNA clones for the human microtubule-associated protein tau and chromosomal localization of the genes for tau and microtubule-associated protein 2. *Brain research*, 387(3), pp.271–280.
- Nisbet, R.M. et al., 2014. Tau aggregation and its interplay with amyloid- β . *Acta Neuropathologica*, 129(2), pp.207–220.
- Nistor, M. et al., 2007. Alpha- and beta-secretase activity as a function of age and beta-amyloid in Down syndrome and normal brain. *Neurobiol Aging*, 28(10), pp.1493–1506.
- Noble, W. et al., 2003. Cdk5 is a key factor in tau aggregation and tangle formation in vivo. *Neuron*, 38(4), pp.555–565.
- Noble, W. et al., 2013. The Importance of Tau Phosphorylation for Neurodegenerative Diseases. *Frontiers in neurology*, 4, p.83.
- Noël, A. et al., 2014. ERK/MAPK does not phosphorylate Tau under physiological conditions in vivo or in vitro. *Neurobiology of Aging*.

- Omalu, B. et al., 2011. Emerging histomorphologic phenotypes of chronic traumatic encephalopathy in american athletes. *Neurosurgery*, 69(1), pp.173–183.
- Panda, D. et al., 1995. Kinetic stabilization of microtubule dynamics at steady state by tau and microtubule-binding domains of tau. *Biochemistry*, 34(35), pp.11117–11127.
- Pearson G et al., 2001. Mitogen-activated protein(MAP) Kinase pathways: Regulation and Physiological Functions. *Endocrine Reviews*, 22(2), pp.153–183.
- Pei, J.-J. et al., 2002. Up-regulation of mitogen-activated protein kinases ERK1/2 and MEK1/2 is associated with the progression of neurofibrillary degeneration in Alzheimer's disease. *Molecular Brain Research*, 109(1–2), pp.45–55.
- Perez, M. et al., 2009. Tau - An inhibitor of deacetylase HDAC6 function. *Journal of Neurochemistry*, 109(6), pp.1756–1766.
- Pérez, M. et al., 2001. In vitro assembly of tau protein: Mapping the regions involved in filament formation. *Biochemistry*, 40, pp.5983–5991.
- Pérez, M. et al., 1996. Polymerization of tau into filaments in the presence of heparin: the minimal sequence required for tau-tau interaction. *Journal of neurochemistry*, 67, pp.1183–1190.
- Perry, G. et al., 1999. Activation of neuronal extracellular receptor kinase (ERK) in Alzheimer disease links oxidative stress to abnormal phosphorylation. *Neuroreport*, 10(11), pp.2411–2415.
- Peti, W. & Page, R., 2013. Molecular basis of MAP kinase regulation. *Protein science*, 22(12), pp.1698–710.
- Pooler, A.M. et al., 2013. Propagation of tau pathology in Alzheimer's disease: identification of novel therapeutic targets. *Alzheimer's research & therapy*, 5(5), p.49.
- Porzig, R., Singer, D. & Hoffmann, R., 2007. Epitope mapping of mAbs AT8 and Tau5 directed against hyperphosphorylated regions of the human tau protein. *Biochemical and Biophysical Research Communications*, 358, pp.644–649.
- Prabakaran, S. et al., 2011. Comparative analysis of Erk phosphorylation suggests a mixed strategy for measuring phospho-form distributions. *Molecular Systems Biology*, 7(482).
- Prabakaran, S. et al., 2011. Comparative analysis of Erk phosphorylation suggests a mixed strategy for measuring phospho-form distributions. *Mol Syst Biol*, 7, p.482.
- Qi, H. et al., 2015. Nuclear Magnetic Resonance Spectroscopy Characterization of Interaction of Tau with DNA and Its Regulation by Phosphorylation. *Biochemistry*, 54, pp.1525–1533.
- Qiang, L. et al., 2006. Tau protects microtubules in the axon from severing by katanin. *The Journal of neuroscience : the official journal of the Society for Neuroscience*, 26(12), pp.3120–3129.
- Qureshi, H. et al., 2013. Interaction of 14-3-3 ζ with Microtubule-Associated Protein Tau within Alzheimer ' s Disease Neuro fibrillary Tangles. *Biochemistry*, 52, pp.6445–6455.

- Rademakers, R., Cruts, M. & Van Broeckhoven, C., 2004. The role of tau (MAPT) in frontotemporal dementia and related tauopathies. *Human Mutation*, 24, pp.277–295.
- Rajput, a. et al., 2006. Parkinsonism, Lrrk2 G2019S, and tau neuropathology. *Neurology*, 67(8), pp.1506–1508.
- Rankin, C. a., Sun, Q. & Gamblin, T.C., 2005. Pseudo-phosphorylation of tau at Ser202 and Thr205 affects tau filament formation. *Molecular Brain Research*, 138, pp.84–93.
- Rankin, C., Sun, Q. & Gamblin, T., 2008. Pre-assembled tau filaments phosphorylated by GSK-3beta form large tangle-like structures. *Neurobiol Dis*, 31(3), pp.368–377.
- Ray, L.B. & Sturgill, W., 1988. Characterization of Insulin-stimulated Microtubule-associated Protein Kinase. , (25), pp.12721–12727.
- Remenyi, A., Good, M.C. & Lim, W.A., 2006. Docking interactions in protein kinase and phosphatase networks. *current opinion in structural biology*, 16, pp.676–685.
- Reynolds, C. et al., 1997. Stress-activated protein kinase/c-Jun N-terminal kinase phosphorylates t protein. *Journal of Neurochemistry*, 68, pp.1736–1744.
- Reynolds, C.H. et al., 2000. Phosphorylation sites on tau identified by nanoelectrospray mass spectrometry: Differences in vitro between the mitogen-activated protein kinases ERK2, c-Jun N-terminal kinase and P38, and glycogen synthase kinase- 3beta. *Journal of Neurochemistry*, 74(4), pp.1587–1595.
- Robinson, F.L. et al., 2002. Identification of novel point mutations in ERK2 that selectively disrupt binding to MEK1. *The Journal of biological chemistry*, 277(17), pp.14844–52.
- Rossi, G. et al., 2008. A new function of microtubule-associated protein tau: Involvement in chromosome stability. *Cell Cycle*, 7(12), pp.1788–1794.
- Ryder, J. et al., 2003. Divergent roles of GSK3 and CDK5 in APP processing. *Biochemical and Biophysical Research Communications*, 312, pp.922–929.
- Sahara, N. et al., 2002. Assembly of tau in transgenic animals expressing P301L tau: Alteration of phosphorylation and solubility. *Journal of Neurochemistry*, 83, pp.1498–1508.
- Sanders, D.W. et al., 2014. Distinct tau prion strains propagate in cells and mice and define different tauopathies. *Neuron*, 82(6), pp.1271–1288.
- Santpere, G. & Ferrer, I., 2009. LRRK2 and neurodegeneration. *Acta Neuropathologica*, 117(3), pp.227–246.
- Schleucher, J. et al., 1994. A general enhancement scheme in heteronuclear multidimensional NMR employing pulsed field gradients. *J Biomol NMR*, 4, pp.301–6.
- Schneider, a. et al., 1999. Phosphorylation that detaches tau protein from microtubules (Ser262, Ser214) also protects it against aggregation into Alzheimer paired helical filaments. *Biochemistry*, 38, pp.3549–3558.

- Schwalbe, M. et al., 2013. Phosphorylation of human tau protein by microtubule affinity-regulating kinase 2. *Biochemistry*, 52(50), pp.9068–9079.
- Schweers, O. et al., 1994. Structural studies of tau protein and Alzheimer paired helical filaments show no evidence for beta-structure. *The Journal of biological chemistry*, 269(39), pp.24290–24297.
- Schweers, O., Biernat, J. & Mandelkow, E., 1995. Oxidation of cysteine-322 in the repeat domain of microtubule-associated protein T controls the in vitro assembly of paired helical filaments. *Proceedings of the National Academy of Sciences*, 92, pp.8463–8467.
- Seger, R. et al., 1991. Microtubule-associated protein 2 kinases, ERK1 and ERK2, undergo autophosphorylation on both tyrosine and threonine residues: implications for their mechanism of activation. *Proc Natl Acad Sci U S A*, 88, pp.6142–6.
- Sengupta, A., Grundke-Iqbal, I. & Iqbal, K., 2006. Regulation of phosphorylation of tau by protein kinases in rat brain. *Neurochemical Research*, 31, pp.1473–1480.
- Sepulveda-Diaz, J.E. et al., 2015. HS3ST2 expression is critical for the abnormal phosphorylation of tau in Alzheimer's disease-related tau pathology. *Brain*, pp.1339–1354.
- Sharrocks, A.D., Yang, S.-H. & Galanis, A., 2000. Docking domains and substrate-specificity determination for MAP kinases. *Trends in Biochemical Sciences*, 25(9), pp.448–453.
- Sheridan, D.L. et al., 2008. Substrate Discrimination among Mitogen-activated Protein Kinases through Distinct Docking Sequence Motifs. *Journal of Biological Chemistry*, 283(28), pp.19511–19520.
- Sherrington, R. et al., 1995. Cloning of a gene bearing missense mutations in early-onset familial Alzheimer's disease. *Nature*, 375(6534), pp.754–760.
- Shi, J.L. et al., 2004. Tau becomes a more favorable substrate for GSK-3 when it is prephosphorylated by PKA in rat brain. *Journal of Biological Chemistry*, 279(48), pp.50078–50088.
- Shiurba, R. a. et al., 1996. Immunocytochemistry of tau phosphoserine 413 and tau protein kinase I in Alzheimer pathology. *Brain Research*, 737, pp.119–132.
- Sibille, N. et al., 2006. Structural impact of heparin binding to full-length Tau as studied by NMR spectroscopy. *Biochemistry*, 45(41), pp.12560–12572.
- Sillen, A. et al., 2007. NMR investigation of the interaction between the neuronal protein Tau and the microtubules. *Biochemistry*, 46(11), pp.3055–3064.
- Sironi, J.J. et al., 1998. Ser-262 in human recombinant tau protein is a markedly more favorable site for phosphorylation by CaMKII than PKA or PhK. *FEBS Letters*, 436(3), pp.471–475.
- Smet, C. et al., 2004. Accepting its random coil nature allows a partial NMR assignment of the neuronal Tau protein. *ChemBiochem*, 5, pp.1639–46.
- Smet-Nocca, C. et al., 2010. NMR-based detection of acetylation sites in peptides. *J Pept Sci*, 16, pp.414–23.

- Snow, A.D. et al., 1990. Early Accumulation of Heparan Sulfate in Neurons and in the Beta-amyloid Protein- containing Lesions of Alzheimer ' s Disease and Down ' s Syndrome. *American Journal of Pathology*, 137(5), pp.1253–1270.
- Songyang, Z. et al., 1996. A structural basis for substrate specificities of protein Ser/Thr kinases: primary sequence preference of casein kinases I and II, NIMA, phosphorylase kinase, calmodulin-dependent kinase II, CDK5, and Erk1. *Molecular and cellular biology*, 16(11), pp.6486–6493.
- Sontag, E. et al., 1999. Molecular Interactions among Protein Phosphatase 2A , Tau , and Microtubules. *The Journal of Biological Chemistry*, 274(36), pp.25490–25498.
- Sontag, J.M. et al., 2012. The protein phosphatase PP2A/B55 binds to the microtubule-associated proteins Tau and MAP2 at a motif also recognized by the kinase Fyn: Implications for tauopathies. *Journal of Biological Chemistry*, 287(18), pp.14984–14993.
- Sontag, J.-M. & Sontag, E., 2014. Protein phosphatase 2A dysfunction in Alzheimer's disease. *Frontiers in molecular neuroscience*, 7, p.16.
- Sturgill, T.W. et al., 1988. Insulin-stimulated MAP-2 kinase phosphorylates and activates ribosomal protein S6 kinase II. *Nature*, 334, pp.715–718.
- Stygelbout, V. et al., 2014. Inositol trisphosphate 3-kinase B is increased in human Alzheimer brain and exacerbates mouse Alzheimer pathology. *Brain*, 137(2), pp.537–552.
- Subramaniam, S. & Unsicker, K., 2010. ERK and cell death: ERK1/2 in neuronal death. *FEBS Journal*, 277(1), pp.22–29.
- Sugden, P.H. et al., 2010. Monophosphothreonyl extracellular signal-regulated kinases 1 and 2 (ERK1/2) are formed endogenously in intact cardiac myocytes and are enzymically active. *Cellular Signalling*, 32(2), pp.468–77.
- Sultan, A. et al., 2011. Nuclear Tau, a key player in neuronal DNA protection. *Journal of Biological Chemistry*, 286(6), pp.4566–4575.
- Sunbae, L. et al., 2012. Examining docking interactions on ERK2 with modular peptide substrates. *Biochemistry*, 50(44), pp.9500–9510.
- Tanoue, T. et al., 2000. A conserved docking motif in MAP kinases common to substrates , activators and regulators. *Nature cell biology*, 2, pp.110–116.
- Tepper, K. et al., 2014. Oligomer Formation of Tau Protein Hyperphosphorylated in Cells. *Journal of Biological Chemistry*, 289(49), pp.34389–34407.
- The Wellcome Trust Case Control Consortium, 2007. Genome-wide association study of 14 , 000 cases of seven common diseases and 3 , 000 shared controls. *Nature*, 447(7145), pp.661–678.
- Theillet, F.-X. et al., 2012. Cell signaling, post-translational protein modifications and NMR spectroscopy. *Journal of biomolecular NMR*, 54(3), pp.217–236.

- Tini, M. et al., 2002. Association of CBP/p300 acetylase and thymine DNA glycosylase links DNA repair and transcription. *Mol Cell*, 9, pp.265–77.
- Tokunaga, Y. et al., 2014. Allosteric enhancement of MAP kinase p38 α 's activity and substrate selectivity by docking interactions. *Nature structural & molecular biology*, 21(8), pp.704–711.
- Tsuboi, Y. et al., 2002. Clinical and genetic studies of families with the tau N279K mutation (FTDP-17). *Neurology*, 59, pp.1791–1793.
- Umahara, T. et al., 2004. 14-3-3 proteins and zeta isoform containing neurofibrillary tangles in patients with Alzheimer's disease. *Acta Neuropathologica*, 108, pp.279–286.
- Uversky, V.N., Gillespie, J.R. & Fink, a L., 2000. Why are “natively unfolded” proteins unstructured under physiologic conditions? *Proteins*, 41, pp.415–427.
- Violet, M. et al., 2014. A major role for Tau in neuronal DNA and RNA protection in vivo under physiological and hyperthermic conditions. *Frontiers in cellular neuroscience*, 8(84), pp.1–11.
- Vogelsberg-Ragaglia, V. et al., 2000. Distinct FTDP-17 missense mutations in tau produce tau aggregates and other pathological phenotypes in transfected CHO cells. *Molecular biology of the cell*, 11, pp.4093–4104.
- Vossel, K. a et al., 2010. Tau reduction prevents Abeta-induced defects in axonal transport. *Science*, 330(6001), pp.10–13.
- Wang, X., Destrumont, A. & Tournier, C., 2007. Physiological roles of MKK4 and MKK7: Insights from animal models. *Biochimica et Biophysica Acta - Molecular Cell Research*, 1773, pp.1349–1357.
- Weingarten, M.D. et al., 1975. A protein factor essential for microtubule assembly. *Proceedings of the National Academy of Sciences of the United States of America*, 72(5), pp.1858–62.
- Weisemann, R., Ruterjans, H. & Bermel, W., 1993. 3D triple-resonance NMR techniques for the sequential assignment of NH and 15N resonances in 15N- and 13C-labelled proteins. *J Biomol NMR*, 3, pp.113–20.
- Whisenant, T.C. et al., 2010. Computational prediction and experimental verification of new MAP kinase docking sites and substrates including Gli transcription factors. *PLoS Computational Biology*, 6(8).
- Whitehurst, A.W. et al., 2004. The Death Effector Domain Protein PEA-15 Prevents Nuclear Entry of ERK2 by Inhibiting Required Interactions. *Journal of Biological Chemistry*, 279(13), pp.12840–12847.
- Whittington, R.. et al., 2014. Anesthesia and Tau Pathology. *Prog Neuropsychopharmacol Biol Psychiatry*, 29(6), pp.997–1003.
- Wilson, D.M. & Binder, L.I., 1997. Free fatty acids stimulate the polymerization of tau and amyloid beta peptides. In vitro evidence for a common effector of pathogenesis in Alzheimer's disease. *The American journal of pathology*, 150(6), pp.2181–2195.

- Witman, G.B. et al., 1976. Tubulin requires tau for growth onto microtubule initiating sites. *Proceedings of the National Academy of Sciences of the United States of America*, 73(11), pp.4070–4074.
- Woods, Y.L. et al., 2001. The kinase DYRK phosphorylates protein-synthesis initiation factor eIF2Bepsilon at Ser539 and the microtubule-associated protein tau at Thr212: potential role for DYRK as a glycogen synthase kinase 3-priming kinase. *The Biochemical journal*, 355, pp.609–615.
- Xu, B.E. et al., 2001. Hydrophobic as well as Charged Residues in both MEK1 and ERK2 are Important for their Proper Docking. *Journal of Biological Chemistry*, 276(28), pp.26509–26515.
- Xu, Y. et al., 2008. Structure of a Protein Phosphatase 2A Holoenzyme: Insights into B55-Mediated Tau Dephosphorylation. *Molecular Cell*, 31(6), pp.873–885.
- Yamaguchi, H. et al., 1996. Preferential labeling of Alzheimer neurofibrillary tangles with antisera for tau protein kinase (TPK)I glycogen synthase kinase-3b and cyclin-dependent kinase 5, a component of TPK II. *Acta Neuropathol*, 92, pp.232–241.
- Yang, S. et al., 1998. Differential targeting of MAP kinases to the ETS-domain transcription factor Elk-1. *The EMBO Journal*, 17(6), pp.1740–1749.
- Yang, S. et al., 1998. The Elk-1 ETS-Domain Transcription Factor Contains a Mitogen-Activated Protein Kinase Targeting Motif. *Molecular and Cellular Biology*, 18(2), pp.710–720.
- Yoon, S. & Seger, R., 2006. The extracellular signal-regulated kinase: multiple substrates regulate diverse cellular functions. *Growth factors (Chur, Switzerland)*, 24(1), pp.21–44.
- Yu, D. et al., 2014. Tau proteins harboring neurodegeneration-linked mutations impair kinesin translocation in vitro. *Journal of Alzheimer's Disease*, 39, pp.301–314.
- Zhang, C., 2012. Natural compounds that modulate BACE1-processing of amyloid-beta precursor protein in Alzheimer's disease. *Discovery medicine*, 14(76), pp.189–97.
- Zhou, T. et al., 2006. Docking Interactions Induce Exposure of Activation Loop in the MAP Kinase ERK2. *Structure*, 14, pp.1011–1019.